Photocatalytic Degradation of Cyanobacteria and Cyanotoxins using Suspended and Immobilized TiO_2

A Dissertation to the UNIVERSITY OF PORTO

for Ph.D. degree in Chemical and Biological Engineering by

Lívia Xerez Pinho

Supervisor: Rui Alfredo da Rocha Boaventura, Ph.D.

Co-Supervisor: Vítor Manuel de Oliveira e Vasconcelos, Ph.D [FCUP]

Vítor Jorge Pais Vilar, Ph.D.

Associate Laboratory LSRE-LCM
Department of Chemical Engineering
Faculty of Engineering
University of Porto

April, 2014

Agradecimentos

Ao Professor Rui Boaventura, por ter aceitado ser meu orientador, pelos ensinamentos, pela atenção e dedicação a este trabalho e por ter feito todo o esforço necessário para realização desta tese. Ao Professor Vítor Vasconcelos, por ter aceitado me co-orientar, pelos ensinamentos e pelos recursos disponibilizados na área de cianobactérias e cianotoxinas. Ao Doutor Vítor Vilar, por ter aceitado me co-orientar, pelos ensinamentos, dedicação, disponibilidade e prontidão em ensinar e ajudar e por garantir as condições adequadas para realização deste trabalho.

Ao CNPQ – Centro Nacional de Desenvolvimento Científico e Tecnológico do Brasil, pelo financiamento de Doutorado Pleno no Exterior, processo GDE 200544/2010-1.

As unidades de investigação onde foram realizadas as experiências: Departamento de Engenharia Química; LSRE – Laboratório de Processos de Separação e Reação (Departamento de Engenharia química - FEUP) e ao LEGE – Laboratório de Ecotoxicologia, Genómica e Evolução (CIIMAR – Centro Interdisciplinar de Investigação Marinha e Ambiental FCUP).

Ao IBMC – Instituto de Biologia Molecular e Celular da Universidade do Porto – UP onde foram realizadas as análises de microscopia electrónica (TEM). A Ângela Brito e as Professoras Arlete Santos e Paula Tamagnini.

A Joana Ângelo e ao Professor Adélio Mendes pela colaboração com as tintas fotocatalíticas e a Sandra Miranda com os filmes de TiO_2.

A todos os colegas do LEGE que de alguma maneira contribuíram para realização deste trabalho, em especial a Joana Azevedo, Mafalda Baptista, Marisa Silva, Micaela Vale e Pedro Leão.

Aos colegas do laboratório 404a da FEUP que contribuíram de alguma maneira para o desenvolvimento deste trabalho: Lídia Salgado, Petrick Soares, Tânia Valente, André Monteiro, Carmen Deus e em especial ao João Pereira.

A Tatiana Pozdniakova, Bianca Souza, Eduardo Xerez, André Monteiro, Isabelli Dias, Ariana Pintor, João Pereira, Bruno Sousa, Evelyn Zuco, Petrick Soares, Sandra

Miranda, Andreia Reis, Fernanda Sousa e Fran Girardi, pelos momentos que partilhamos e pela amizade que foi fundamental durante os últimos quatro anos.

Aos Pastores Eduardo Silva e Sofia Costa, a todos os irmãos da Igreja Evangélica A Rocha e a Bianca Souza pelo carinho, ensinamentos, palavras de fé e principalmente por suas orações que me sustentaram durante o último ano.

A amiga Lorena Arcanjo porque mesmo à distância esteve sempre presente na minha vida durante o período do doutoramento. A Sandra Maria, por todo apoio que me deu desde a graduação e que foi fundamental para eu chegar aqui.

Aos meus irmãos Lana e Diego Pinho que sempre acreditaram em mim, me apoiaram e ajudaram a chegar até aqui.

Aos meus pais José e Mônica Pinho que nunca mediram esforços para investir na minha educação e formação, por terem acreditado e apoiado o meu sonho de fazer um doutoramento fora do meu País, por sempre me terem encorajado mesmo que a distância lhes tenha custado.

Ao Senhor toda honra e toda glória, porque dele, por ele e para ele, são todas as coisas.

A minha família

"Talvez não tenha conseguido fazer o melhor, mas lutei para que o melhor fosse feito. Não sou o que deveria ser, mas Graças a Deus, não sou o que era antes".

(Marthin Luther King)

Abstract

Blooms of cyanobacteria have been occurring largely due to the eutrophication of aquatic environments. These organisms produce a wide variety of toxins, and constitute a challenge for designers of water treatment systems, which largely depend on surface raw water quality. Although the presence of toxic cyanobacteria/cyanotoxins in water for human consumption, agricultural or recreational purposes poses a serious hazard to humans, this situation has been neglected or at most has been treated on a local level. Accumulation of cyanobacteria scum along the shores of ponds and lakes also present a hazard to wildlife and domestic animals. Currently, there is a greater concern for the protection of the environment and public health, which led to the need and obligation to control the presence of cyanotoxins in drinking water, which is now a global reality, firstly proposed by WHO by establishing a guideline value of 1 μg L^{-1} for MC-LR.

Photocatalytic processes, especially those driven by sunlight as a natural source of UV photons, have gained support in recent years, mainly in rural areas located in the sunniest regions in the world. Greater attention at this time should be focused on the development of photocatalysts with high oxidative power, inert, low cost and easily applicable. The proposed technology is based on the photocatalytic generation, by using sunlight, of reactive oxygen species, to disinfect/clean-up contaminated water with cyanobacteria and cyanobacterial toxins.

This thesis mainly aims i) to assess the efficiency of TiO_2 driven photocatalysis in the elimination of cyanobacteria *Microcystis aeruginosa,* and cyanotoxins microcystin-LR (MC-LR) and cylindrospermopsin (CYN) using a lab-scale tubular photoreactor equipped with compound parabolic collectors (CPCs), under simulated solar radiation; ii) to assess the efficiency of TiO_2 driven photocatalysis in the removal of cyanobacteria *Microcystis aeruginosa,* and cyanotoxin MC-LR using a pilot plant with CPCs, under natural radiation; iii) to compare the photocatalytic system efficiency using TiO_2 in suspension or immobilized on different types of supports; iv) to study the destruction pathways of the selected cyanobacteria and target cyanotoxins and identify the degradation by-products (DPs); v) to evaluate

the TiO_2 photocatalytic process in the treatment of natural water from a Portuguese river contaminated with cyanotoxins MC-LR and CYN.

Solar photolysis showed to be insufficient to *M. aeruginosa* inactivation and destruction of MC-LR and CYN. The experiments carried out with addition of TiO_2 in darkness showed negligible adsorption.

TiO_2 photocatalysis in a lab-scale photoreactor using artificial UV light and in a pilot-scale plant using natural solar radiation, as UV photon source, was employed to destroy *M. Aeruginosa* and MC-LR. The process showed to be effective in the destruction of *M. Aeruginosa* (~ 5-log order) and in the inactivation of MC-LR released into the aqueous solutions, in the reaction period between 5-15 min, even at extremely high toxin concentrations (1.87 μg mL^{-1}).

Transmission electron microcopy (TEM) showed that TiO_2 nanoparticles form a layer around the cells and, under UV irradiation, the mucilaginous external layer starts to be destroyed due to the attack of reactive species formed on the TiO_2 surface, which allows the penetration of TiO_2 nanoparticles to the inner parts of the cell, leading to cell deformation and destruction.

Inactivation of MC-LR (100 μg L^{-1}) spiked in distilled water was achieved by photocatalysis in the pilot plant using TiO_2 in suspension. Although the optimal catalyst concentration is 200 mg TiO_2 L^{-1}, similar profiles were obtained after 6 kJ_{UV} L^{-1} for the catalyst concentrations of 100 and 200 mg L^{-1}, leading to residual values lower than 20 μg L^{-1} , which corresponds to more than 80% MC-LR inactivation. To achieve a MC-LR concentration below the guideline for drinking water (< 1 μg L^{-1}) more than 12 kJ_{UV} L^{-1} (5 h exposure) is required. The photocatalytic oxidation of MC-LR in aqueous solutions is characterized by an initial fast reaction followed by a slow degradation stage, which was attributed to the competition for the hydroxyl radicals between the MC-LR molecules and degradation byproducts. LC-MS/MS analysis revealed the presence of two main MC-LR degradation byproducts (*m/z* 1029 and *m/z* 1011) during the initial part of the reaction.

Photocatalytic experiments using TiO_2 immobilized on different types of supports were carried out in a lab-scale tubular photoreactor with a compound parabolic

collector (CPC) using artificial and natural solar radiation to promote the inactivation of the cyanotoxins MC-LR and CYN in distilled and natural water. A catalytic bed of cellulose acetate transparent monoliths (CAM) coated with P25 or sol-gel TiO_2 film, or glass tube , PCV tube, glass spheres or polyethylene terephthalate transparent monoliths (PETM) with a photocatalytic 3D TiO_2-based exterior paint (PC500, VLP7000 and P25) was employed. The photocatalytic system P25-CAM/H_2O_2 can be considered the most viable process, considering the MC-LR inactivation efficiency (98 %), the cost and the simplicity of the catalyst preparation. CYN degradation was also achieved by the same system but a long exposure time was required. The oxidation of cyanotoxins was mainly attributed to hydroxyl radicals attack, but the role of other reactive species cannot be discarded. The presence of organic matter in natural water from Tâmega river impaired the MC-LR degradation rate. Oppositely, the CYN degradation rate using the same system was higher in natural water than in distilled water containing this toxin, which suggests that the presence of Fe in the river water promoted the photo-Fenton reaction.

TiO_2 photocatalysis using solar energy is a very efficient process to destroy cyanobacteria and cyanotoxins in a pilot plant treating a large volume of water intended for the abstraction of drinking water, allowing obtaining concentrations of toxins below the guideline value of 1 μg L^{-1}. This technology can be implemented in remote areas not reached by the drinking water network, and where qualified experts are not available, without any chemicals addition and using only the photocatalyst and sunlight.

Resumo

Florações de cianobactérias têm ocorrido em grande parte devido à eutrofização dos ambientes aquáticos. Estes organismos produzem uma grande variedade de toxinas denominadas cianotoxinas e representam um desafio para os projetistas de sistemas de tratamento de água que, em geral, dependem da qualidade das águas superficiais. Embora a presença de cianotoxinas na água para consumo humano, para fins agrícolas ou de lazer represente um risco grave para os seres humanos, esta situação tem sido negligenciada ou no máximo, tratada a nível local. A acumulação de escumas de cianobactérias ao longo das margens de rios e lagos também representa perigo para a vida selvagem e para animais domésticos. Atualmente há uma maior preocupação com a proteção do meio ambiente e da saúde pública, o que levou à necessidade e obrigatoriedade de controlar a presença de cianotoxinas na água potável, que já é uma realidade global, tenho sido a OMS a primeira instituição a propor esse controlo, estabelecendo um valor de referência de 1 μg L^{-1} para MC-LR.

A aplicação dos processos fotocatalíticos, especialmente aqueles que utilizam a luz solar como uma fonte natural de fotões UV, tem recebido bastante atenção nos últimos anos, principalmente em áreas rurais localizadas nas regiões mais ensolaradas do mundo. Atualmente a maior atenção deve estar voltada para o desenvolvimento de fotocatalisadores que apresentem um elevado poder oxidativo, sejam inertes, de baixo custo e de fácil aplicação. A tecnologia proposta é baseada na geração fotocatalítica de espécies reativas de oxigénio, utilizando luz solar para desinfeção/descontaminação de águas contaminadas com cianobactérias e cianotoxinas.

Esta tese teve como principais objetivos i) avaliar a eficiência da fotocatálise com TiO_2 aplicada na eliminação de cianobactérias *Microcystis aeruginosa* e cianotoxinas microcistina-LR (MC-LR) e cilindrospermopsina (CIN) usando um foto-reator tubular à escala laboratorial, equipado com coletores parabólicos compostos (CPCs), sob radiação solar simulada; ii) avaliar a eficiência da fotocatálise com TiO_2 na remoção de cianobactérias *Microcystis aeruginosa* e cianotoxina MC-LR utilizando uma instalação piloto com CPCs, sob radiação natural; iii) comparar a

eficiência do sistema fotocatalítico utilizando TiO_2 em suspensão ou imobilizado em diferentes tipos de suporte; iv) estudar as vias de destruição das cianobactérias e cianotoxinas e identificar subprodutos de degradação; v) avaliar o processo fotocatalítico com TiO_2 no tratamento de água natural proveniente de um rio Português contaminada com cianotoxinas MC-LR e CIN.

A fotólise solar mostrou-se insuficiente para a inativação de *M. aeruginosa* e inativação de MC-LR e CIN. As experiências realizadas com a adição de TiO_2, porém na ausência de UV, mostraram que a adsorção das cianotoxinas às partículas de TiO_2 é insignificante.

A fotocatálise com TiO_2 em foto-reator à escala laboratorial utilizando UV artificial e em instalação piloto utilizando a radiação solar natural como fonte de fotões UV, foi empregue para destruir *M. aeruginosa* e MC-LR. O processo mostrou-se eficaz na destruição de *M. aeruginosa* (~5-log) e na degradação de MC-LR libertada para a água, durante um período de 5-15 minutos de reação, mesmo em concentrações extremamente elevadas de toxina (1,87 mg mL^{-1}).

Imagens obtidas a partir de Microscopia Eletrónica de Transmissão (MET) revelaram que as nanopartículas de TiO_2 formam uma camada em torno das células e, sob irradiação UV, a camada externa das algas constituída por uma cápsula mucilaginosa começa a ser destruída, devido ao ataque de espécies reativas formadas na superfície do TiO_2, o que permitiu a penetração das nanopartículas de TiO_2 para o interior da célula, levando à sua deformação e consequente destruição.

A inativação de MC-LR (100 $\mu g\ L^{-1}$) adicionada a água destilada foi conseguida por fotocatálise em instalação piloto utilizando TiO_2 em suspensão. Embora a concentração do catalisador ótima seja de 200 mg L^{-1} de TiO_2, perfis semelhantes de degradação foram obtidos após 6 $kJ_{UV}\ L^{-1}$ utilizando concentrações de 100 e 200 mg L^{-1}, levando a valores residuais inferiores a 20 $\mu g\ L^{-1}$, o que corresponde a mais de 80 % de degradação de MC-LR. Para atingir uma concentração de MC-LR abaixo do limite estabelecido para a água potável (< 1 $\mu g\ L^{-1}$) é necessário um exposição a mais de 12 $kJ_{UV}\ L^{-1}$ (~ 5 h de exposição). A oxidação fotocatalítica de MC-LR em soluções aquosa é caracterizada por ser uma reação inicialmente rápida seguida por uma fase de degradação lenta, o que foi atribuído à concorrência entre as

moléculas de MC-LR e os subprodutos de degradação para os radicais de hidroxilo. Análises de LC-MS/MS revelaram a presença de dois principais subprodutos de degradação da MC-LR (m/z 1029 e m/z 1011) formados durante a fase inicial da reação.

Foram realizados experiências de fotocatálise utilizando TiO_2 imobilizado em diferentes tipos de suporte num foto-reator tubular à escala laboratorial com CPC, utilizando radiação solar artificial e natural, a fim de promover a inativação das cianotoxinas MC-LR e CIN em água destilada e água natural. Um leito catalítico de monólitos transparentes de acetato de celulose (MAC) revestidos com filmes de TiO_2 P25 ou sol-gel, ou monólitos transparentes de PET (MPET), tubo de PVC, tubo de vidro ou esferas de vidro revestidos com uma tinta fotocatalítica exterior 3D à base de TiO_2 (PC500, VLP7000 e P25) foi utilizado como catalisador. O sistema fotocatalítico P25-CAM/H_2O_2/UV foi considerado o mais viável, considerando a eficiência na inativação de MC-LR (98 %), o baixo custo e a simplicidade da preparação do catalisador. A inativação de CIN também foi conseguida pelo mesmo sistema, entretanto foi necessário um tempo de exposição mais longo. A oxidação de cianotoxinas foi principalmente atribuída ao ataque de radicais hidroxilo, porém a influência de outras espécies reativas não pode ser descartada. A presença de matéria orgânica na água natural do rio Tâmega prejudicou a velocidade de inativação de MC-LR. Contrariamente, a velocidade de inativação de CIN, usando o mesmo sistema, foi maior em água natural do que em água destilada, sugerindo que a presença de Fe na água do rio promoveu a reação de foto-Fenton.

A fotocatálise utilizando TiO_2 e energia solar numa instalação piloto é um processo bastante eficiente para destruir cianobactérias e cianotoxinas, bem como para tratar um grande volume de água destinada à produção de água potável, levando à obtenção de concentrações de toxinas abaixo do valor de referência de 1 $\mu g\ L^{-1}$. Esta tecnologia pode ser implementada em áreas remotas não alcançadas pela rede de água potável, e onde peritos qualificados não estão disponíveis, sem a necessidade de qualquer adição de produtos químicos e utilizando apenas o fotocatalisador e a luz solar.

Table of Contents

Page

Table of Figures

Page

Table of Tables

Page

List of abbreviations

ACH	Aluminium chlorohydrate
AOPs	Advanced Oxidation Processes
B	Brackish water
CAD	Collision gas
CAM	Cellulose Acetate Monolith
CPC(s)	Compound Parabolic Compound (s)
CYN	Cylindrospermopsin
CUR	Curtain gas
CXP	Cell exit potential
DPs	Degradation by-products
DSSR	Double skin sheet reactor
EC	Extracellular
EDX	Energy dispersive X-ray
ELISA	Enzyme Linked Immunosorbent Assay
EP	Entrance potential
F	Freshwater
GAC	Granular activated carbon
GC	Gas chromatography
GS	Glass spheres
GSM	Geosmin
HPLC-DAD	High performance liquid chromatography - Diode Array Detector
HPLC-PDA	High performance liquid chromatography- Photo-diode array
IC	Intracellular
LC-MS	Liquid chromatography - mass spectrometry
LP	Liquid phase
LPS	Lipopolysaccharides
M	Marine
MALDI-TOF-MS	Matrix Assisted Laser Desorption/ Ionization – Time of Flight – Mass Spectrometry
MC(s)	Microcystins
MP	Mobile phase

MS	Mass spectrometry
MRM	Multiple Reaction Monitoring
n.p.	Not provided
PAC	Powdered activated carbon
PTC	Parabolic trough concentrator
PTR	Parabolic trough reactor
PC	Parabolic trough concentrator
PETM	PET Monolith
PP	Particulate phase
PPIA	Protein phosphatase inhibition assay
PP1	Protein phosphatase type 1
Pnt	Paint
PSD	Post-Source-Decay
PT	Parabolic trough
SEM	Scanning electron microscopy
SPE	Solid phase extraction
SS	Stock solution
T	Terrestrial
TC	Tubular collector
TEM	Transmission electronic microcopy
TFA	Trifluoroacetic acid
TFFBR	Thin film fixed bed reactor
THMs	Trihalometanes
UF	Ultrafiltration
UV	Ultraviolet
VC	V-trough collector
WHO	World Health Organization

Notations

Q_{UV}	Accumulated UV energy per liter of solution ($kJ\ L^{-1}$)
T	Temperature (^{o}C)
t	Time (s / min / h)
Ar	Illuminated area (m^2)
$\overline{UV}_{G,n}$	average solar ultraviolet incident irradiance ($W_{UV}\ m^{-2}$)
V	volume
r_0	Initial reaction rate ($\mu g\ kJ^{-1}$)
k	kinetic rate ($L\ kJ^{-1}$)
Rt	Retention time (min)
TC-TOC-TN	Total carbon – Total organic carbon – Total nitrogen ($mg\ L^{-1}$)
DOC	Dissolved organic carbon ($mg\ L^{-1}$)
DO	Dissolved oxygen ($mg\ L^{-1}$)
TN	Total Nitrogen ($mg\ L^{-1}$)
TDC	Total Dissolved Carbon ($mg\ L^{-1}$)
DIC	Dissolved Inorganic Carbon ($mg\ L^{-1}$)

1 Introduction

This chapter contains a brief introduction to this thesis. The relevance and motivation of this study are highlighted and the objectives to be achieved are outlined. The thesis layout is also presented.

1.1 Relevance and Motivation

Blooms of cyanobacteria have being occurring largely due to the eutrophication of aquatic environments. Many rivers, lakes and reservoirs worldwide develop highly toxic cyanobacteria densities. This is especially common in the warmer months where they can appear as greenish suspensions in the water. These organisms produce a wide variety of toxins and other compounds with unknown toxic potential (e.g., microviridins, aeruginosins), and constitute a hard task for the designers of water treatment systems, which are dependent on surface raw water quality (Falconer and Humpage, 2005; Hoeger et al., 2005). Although the presence of toxic cyanobacteria/cyanotoxins in water for human consumption, agricultural or recreational purposes poses a serious hazard to humans, this situation has been neglected or at most has been treated on a local level. Accumulation of cyanobacteria scum along the shores of ponds and lakes also present a hazard to wildlife and domestic animals. Currently, there is a greater concern for the protection of the environment and public health which led to the need and obligation to control the presence of cyanotoxins in drinking water, which is now a global reality, firstly proposed by WHO by establishing a guideline value of 1 $\mu g\ L^{-1}$.

Due to the lack of on-site water treatment technologies in many rural areas, surface water or groundwater is not adequately treated and the risk of transmission of many diseases is very high and has been largely responsible for several large epidemics such as typhoid and cholera throughout the world. The most commonly used techniques for water disinfection are chlorination and ozonation. In spite of chlorine is widely used as main disinfectant, the overall water service coverage in rural areas is rather low, because of many factors (technological, cost, maintenance, social, cultural, logistics, education, etc.) responsible for the present situation. In addition, there is the risk caused by the chlorinated by-products such as trihalomethanes (THMs) and other organohalides resulting from the reaction of chlorine with organic matter. Other existing technologies, such as ozone and UV disinfection, are clearly of very difficult implementation in rural areas, often among the sunniest in the world. This is why photocatalytic processes, especially those driven by sunlight as a natural source of UV photons, have gained support in recent years, mainly in rural areas located in the sunniest regions in the world.

This technology can be used to promote disinfection/decontamination of water contaminated with cyanobacteria and cyanotoxins and can be implemented in remote areas not reached by the drinking water network, and where qualified experts are not available, without any

chemicals addition i.e. using only the photocatalyst and sunlight. Greater attention at this time should be focused on the development of photocatalysts with high oxidative power, inert, low cost and easily applicable. The proposed technology is based on the photocatalytic generation, by using sunlight, of reactive oxygen species, to disinfect/clean-up contaminated water with cyanobacteria and cyanobacterial toxins.

1.2 Thesis Objectives and Layout

i. To assess the efficiency of TiO_2 driven photocatalysis in the elimination of cyanobacteria *Microcystis aeruginosa*, and cyanotoxins microcystin-LR (MC-LR) and cylindrospermopsin (CYN) using a lab-scale tubular photoreactor equipped with compound parabolic collectors (CPCs), under simulated solar radiation;
ii. To assess the efficiency of TiO_2 driven photocatalysis in the elimination of cyanobacteria *Microcystis aeruginosa*, and cyanotoxin MC-LR using a pilot plant with CPCs, under natural radiation;
iii. To compare the photocatalytic system efficiency using TiO_2 in suspension or immobilized on different types of supports;
iv. To study the destruction pathways of the selected cyanobacteria and target cyanotoxins and identify the degradation by-products (DPs);
v. To evaluate and optimize the TiO_2 photocatalytic process in the treatment of natural water from a Portuguese river contaminated with cyanotoxins MC-LR and CYN.

This thesis has been organized into seven chapters. The bibliographic references are presented at the end of each chapter and are organized alphabetically by author and chronologically.

Chapter 1 refers to the present introduction, containing the relevance, motivation and objectives concerning this work.

Chapter 2 corresponds to the literature review about cyanobacteria and their physiological characteristics, the different kinds of toxins produced by several genera of cyanobacteria and the associated problems caused to water systems around the word. Some methods for cyanobacteria growth assessment, cell identification, and toxin identification/quantification are also described. Finally, procedures to eliminate cyanobacteria and toxins from water, such

as conventional methods and advanced oxidation processes (AOP), including photocatalysis with TiO_2, are presented.

Chapter 3 focuses on the description of the materials and methods employed to carry out the experimental work.

Chapter 4 refers to a study about the destruction of *M. aeruginosa* and the toxin microcystin-LR (MC-LR) by photolysis and TiO_2 photocatalysis in slurry conditions, comparing the efficiency of these processes using artificial UV light at lab-scale and solar radiation at pilot-scale, as UV photon source.

Chapter 5 deals with the treatment of water contaminated with *M. aeruginosa*, and also to observe the interaction of these cyanobacteria with the TiO_2 nanoparticles by TEM analysis. Natural water containing cyanobacterial blooms was also submitted to TiO_2 photocatalysis. The effect of the TiO_2 concentration on the photocatalytic process was evaluated for the inactivation of MC-LR from water. The degradation by-products were identified by LC-MS/MS. Finally, the best TiO_2 concentration was applied to inactivation of another cyanotoxin, cylindrospermopsin (CYN), previously purified from *C. raciborskii*.

Chapter 6 mainly reports the inactivation of MC-LR and CYN in natural and distilled water by photocatalysis employing artificial and solar UV energy in a tubular photoreactor packed with a catalytic bed of cellulose acetate transparent monoliths (CAM) coated with P25 or sol-gel TiO_2 films and with a photocatalytic 3D TiO_2-based exterior paint (PC500, VLP7000 and P25). The effect of the simultaneous addition of hydrogen peroxide is also reported. Other kind of supports, such as PVC or glass tubes and glass spheres were coated with the photocatalytic 3D TiO_2-based exterior paint. The experiments were carried out in a lab scale photoreactor prototype (SUNTEST).

Finally, the general conclusions and suggestions for future work are outlined in Chapter 7.

2 Literature Review

This chapter contains a brief review concerning cyanobacteria and their physiological characteristics, their main habitats around the world, growth conditions and occurrence of blooms. The different kinds of toxins produced by several genera of cyanobacteria are also described, namely microcystin and cylindrospermopsin, which have an important impact on the environment and human health, whenever present in water. Some methods for cyanobacteria growth assessment, cell identification, and toxin identification/quantification are also summarized. Finally, procedures to eliminate cyanobacteria and toxins from water, such as conventional methods and advanced oxidation processes (AOP), including photocatalysis, are focused in this chapter.

2.1 Cyanobacteria

Cyanobacteria are a group of Gram-negative prokaryotes that possess chlorophyll and perform oxygenic photosynthesis associated with photosystems I and II and synthesize organic compounds. The basic morphology comprises unicellular, colonial and multicellular filamentous forms. Unicellular forms have spherical, ovoid or cylindrical cells. The multicellular structure consisting of a chain of cells is called a trichome. The trichome may be straight or coiled. Cell size and shape show great variability among the filamentous cyanobacteria (Chorus and Bartram, 1999; Martins et al., 2010). According to the current taxonomy, 150 genera from 2000 species have been identified, and at least 40 are known to be toxigenic. Additionally, cyanobacteria produce lipopolysaccharides (LPS) as well as secondary metabolites that have potential pharmacological application (Hitzfeld et al., 2000a).

As the human population density rises, the inflow of nutrients into water bodies, mainly due to fertilizer use and urban run-off and sewage discharges, increases, leading to eutrophication, which is observed worldwide. The increasing incidence of blooms of algae and cyanobacteria (Figure 2.1) has occurred largely due to the eutrophication of the aquatic environments. Many rivers, lakes and reservoirs develop high cyanobacteria cell concentrations, especially in the summer months, which appear as greenish suspensions in the water. Some species float to the surface under warm, still conditions, forming scums with cell concentrations above 1×10^{6} cells mL^{-1}. Dried scums often appear blue-green or red through the liberation of phycocyanin pigment, leading to the previous common name of these organisms: blue-green algae (Falconer and Humpage, 2005).

Figure 2.1 Bloom of cyanobacteria in Marco de Canaveses, Tâmega River – Portugal (September 2012).

2.1.1 Occurrence of cyanobacteria

Cyanobacteria are found throughout the world under different weather situations, for example, some species were observed on the glacier surface colonizing snow and ice at high altitudes in Alaska. Cyanobacteria are most commonly found in waters with neutral or slightly alkaline pH, in a great range of salinity and temperature, and they occasionally occur in the soil, including rocks and their fissures (Svrcek and Smith, 2004; Takeuchi, 2001). Table 2.1 reports toxic cyanobacterial blooms, scums, or mats in different regions of the world.

They occur both in freshwater and marine environments (Hitzfeld et al., 2000a). The blooms of cyanobacteria are usually found in lakes and reservoirs, but rivers with slower water flow have also been affected (Lawton and Robertson, 1999).

Wind, light intensity and temperature are some of the local climatological factors that influence and modify the phytoplankton structure. The biomass and composition of phytoplankton are also influenced by the stability of the water column (Bouvy et al., 2000).

Cyanobacterial blooms are often preceded by nutrient enrichment and some climatological factors, which play a role in the global climate (Bouvy et al., 1999). The El Niño phenomenon, for example in north-east Brazil, in 1997, created excellent conditions of temperature and irradiation for the dominance of *Cylindrospermopsis* sp. cyanobacteria in many water reservoirs. This fact is attributed to the reduction of water volume, stability of water column and long water retention time, allowing the adaption of their physiological capacities to compete with other phytoplanktonic species, and they seem less edible for zooplankton and fish than non-blooming algae (Bouvy et al., 2000).

The incidence of toxic cyanobacteria is also increasingly common in drinking water reservoirs. Populations of the toxic *Cylindrospermopsins raciborskii* were observed in three of the main water reservoirs supplying Brisbane city (Australia). These cyanobacteria form dense layers 5-10 m below the surface, so that the first indication of the proliferation of the organism may be the blocking of filters in the drinking water treatment plant (Falconer and Humpage, 2005).

Table 2.1 Reports on the occurrence of toxic cyanobacterial blooms, scums or mats.

Continent/Region	Country	Place	Reference
America	Argentina, Bermuda, Chile, Mexico, Uruguay		Codd et al. (2005),Vasconcelos et al. (2010b).
	Canada	Alberta, British Columbia, Manitoba, Ontario, Saskatchewan	Svrcek and Smith (2004)
	EUA	California, Colorado, Florida, Hawaii (marine only), Idaho, Illinois, Iowa, Michigan, Minnesota, Mississippi, Montana, Nebraska, Nevada, New Hampshire, New Mexico, New York, North Dakota, Ohio, Oklahoma, Oregon, Pennsylvania, South Dakota, Texas, Washington, Wisconsin, Wyoming.	Svrcek and Smith (2004)
	Brazil	Pernambuco, São Paulo, Rio Grande do Sul, Paraná, Rio de Janeiro, Mato Grosso do Sul (Pantanal), Distrito Federal, Minas Gerais	Agujaro and Lima Isaac (2003), Bouvy et al. (1999), Castro et al. (1990), Damazio and Silva (2006), Dörr et al. (2010), Fonseca and Rodrigues (2005), Matthiensen et al. (1999), Santos and Sant'Anna (2010).
Europe	Belgium, Czech Republic, Denmark, Estonia, Finland, France, Germany, Greece, Hungary, Ireland, Italy, Latvia, Netherlands, Norway, Poland, Portugal, Russia, Slovakia, Slovenia, Spain, Sweden, Switzerland, Ukraine, United Kingdom		Albay et al. (2003), Codd et al. (2005), Hoeger et al. (2005), Jurczak et al. (2005), Rivasseau et al. (1999), Rodríguez et al. (2007), Svrcek and Smith (2004), Vasconcelos and Pereira (2001).
Africa	Botswana, Tunisia Egypt, Ethiopia, Kenya, Morocco, South Africa, Zimbabwe		Codd et al. (2005), Fathalli et al. (2011), Krienitz et al. (2002), Mhlanga et al. (2006), Oudra et al. (2001).
Oceania	Australia	New South Wales, Queensland, South Australia, Tasmania, Victoria, Western Australia	Baker et al. (2001a), Baker et al. (2001b), Bourne et al. (2006), Chow et al. (1999), Ho et al. (2011), Wang et al. (2007b), Orr et al. (2004).
	New Zealand, New Caledonia		
Middle East and Asia	Bangladesh, India, Israel, Japan, Jordan, Malaysia, Nepal, Peoples' Republic of China, Philippines, Saudi Arabia, Sri Lanka, South Korea, Thailand, Turkey, Vietnam		Albay et al. (2003), Codd et al. (2005), Cuvin-Aralar et al. (2002), Hummert et al. (2001), Ratnayake et al. (2012).
Antarctica			Hitzfeld et al. (2000b)
Oceans and Seas	Atlantic Ocean, Baltic Sea, Caribbean Sea, Indian Ocean		Codd et al. (2005)

Heavy blooms of the toxic *M. aeruginosa* appeared in the main drinking water supply reservoirs of Sao Paulo (Brazil) and Lodz (Poland) cities during summer (Falconer and Humpage, 2005). Several eutrophic water bodies of Central Mexico revealed the presence of high levels of microcystin (MC) in sites used for drinking water production, agriculture irrigation and/or recreation, highlighting the potential risk for human health (Vasconcelos et al., 2010b).

High concentrations of *C. raciborskii*, a cylindrospermopsin producing species, and other codominant cyanobacteria, the most notable being of the genus Aphanizomenon, Merismopedia and Oscillatoriales, were detected in Portuguese freshwaters from three reservoirs and one river in the south of Portugal, during the warmer months in 1999 (Saker et al., 2003). Freitas (2009) also reported the presence of a wide variety of cyanobacteria in two ponds of the central coast of Portugal, Lakes of Mira and Vela, prevailing the Oscillatoriales and Nostocaceae families, respectively. The author attributed the proliferation of the cyanobacteria to the high density of farmlands, which promoted the nutrients enrichment of the water through leaching from soils and water stagnation.

The presence of other organisms, for example, heterotrophic bacteria, can be an important biotic factor that leads to cyanobacteria blooms during warm periods of the year, as it was found in studies about ponds in Marrakech, which has an arid Mediterranean climate. The interaction between algae and bacteria has also an important ecological effect and appears to play a key role in the process of self-purification. It was showed that cyanobacteria *Synechocystis sp*. and *Pseudanabaena sp*. stimulated the growth and survival of heterotrophic bacteria and non-O1 *V. cholerae* and reduced the survival of *E. coli* and Salmonella (Oufdou et al., 2000).

2.1.2 Cyanotoxins

Cyanobacteria produce a variety of toxins called cyanotoxins, classified according to their mechanism of toxicity to humans as hepatotoxins, neurotoxins or dermatotoxins. Table 2.2 summarizes toxic effects from cyanotoxins, producer genera and chemical structure.

Table 2.2 Cyanotoxins, effects, producer organisms and structure adapted from Carmichael (2001), Codd (2000), Codd et al. (2005), Hitzfeld et al. (2000a) and Svrcek and Smith (2004).

Cyanotoxins	Toxic effect	LD_{50} (i.p. mouse, μg kg^{-1} body wt)	Producer cyanobacteria genera	Habitat	Chemical structure
Microcystins	Hepatotoxic	25 to ~ 1000	Microcystis, Oscillatoria, Anabaena, Nostoc, Haphalosiphon, Anabaenopsis, others	F, B F, B T F, M	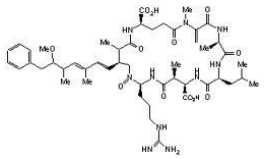
Nodularins	Hepatotoxic	30 – 50	Nodularia	F, B	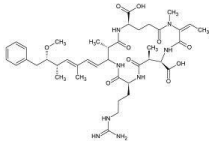
Anatoxin-a	Neurotoxic	250	Anabaena, Oscillatoria, Aphanizomenon,	F, B F, B	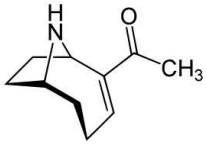
Anatoxin-a(S)	Neurotoxic	40	Anabaena, Oscillatoria	F, B	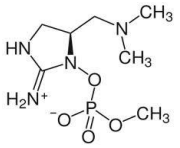
Saxitoxins	Neurotoxic	10 – 30	Anabaena, Aphanizomenon, Cylindrospermopsis, Lyngbya	F F, B F F	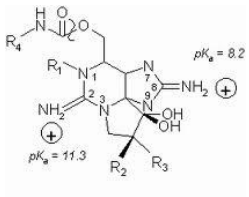

Table 2.2 Cyanotoxins, effects, producer organisms and structure adapted from Carmichael (2001), Codd (2000), Codd et al. (2005), Hitzfeld et al. (2000a) and Svrcek and Smith (2004) (cont.).

Cyanotoxins	Toxic effect	LD_{50} (i.p. mouse, μg kg^{-1} body wt)	Producer cyanobacteria genera	Habitat	Chemical structure
Cylindrospermopsin	Cytotoxic, hepatotoxic, neurotoxic, genotoxic	200 – 2100	Anabaena, Aphanizomenon, Cylindrospermopsis, Umezakia	F F, B F	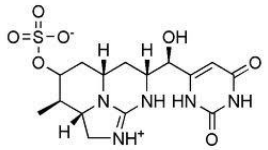
Aplysiatoxin	Dermatotoxic	–	Lyngbya, Schizothrix, Oscillatoria	M F, B	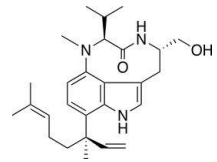
Debromoaplysiatoxin	Dermatotoxic	–	Lyngbya, Schizothrix, Oscillatoria	M M	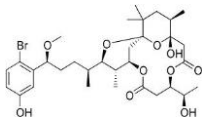
Lyngbyatoxin-a	Dermatotoxic, oral and gastrointestinal inflammation	–	Lyngbya	M	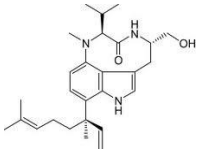

F: freshwater; B: brackish water; M: marine; T: terrestrial

Each type of toxin is described below:

- Dermatotoxins

  Swimming in water contaminated with cyanobacteria may exposure the swimmers to cyanotoxins and dermal contact may cause eye, ear and skin irritation and gastrointestinal symptoms (Msagati et al., 2006).

- Neurotoxins

  Neurotoxins are produced by several genera and constitute the majority of cyanobacterial toxins, although hepatotoxins are more common (Herrero et al., 2008). However, neurotoxins have been reported far less in the literature on cyanotoxin occurrence than peptide hepatotoxins (Ibelings and Chorus, 2007).

  Neurotoxins poison acts rapidly and has been reported most frequently in North America, Europe and Australia (Herrero et al., 2008). Anatoxin-a, for example, has been implicated in the death of waterfowl (Ibelings and Chorus, 2007).

  Neurotoxins also may play a simultaneous role and have additive or synergistic effects with others toxins, as it was the case of the death of the flamingos in Africa's Rift valley lakes by intoxication with neurotoxin and hepatotoxins (Ibelings and Chorus, 2007).

- Hepatotoxins – microcystins (MCs)

  The most common toxins found in water are the hepatotoxins microcystins (MCs), corresponding to a group of at least 70 peptides produced primarily by freshwater cyanobacteria belonging to the genera *Microcystis, Anabaena, Nostoc and Oscillatoria/Plankthotrix* (Lawton et al., 2003). The MC-LR is a cyclic heptapeptide 3-amino-9-methoxy-2,6,8-trimethyl-10-phenyldeca-4,6-dienoicacid (ADDA), containing in the variable positions 2 and 4 leucine (L) e arginine (R) (Lee et al., 2004b). It acts by inhibiting protein phosphatase which leads to hyperphosphorylation of cellular proteins such as cytokeratin 8 and 18 (Hitzfeld et al., 2000b). All protein phosphatase inhibitors are harmful to humans or warm-blooded animals (Dahlmann et al., 2001).

  Microcystins are produced and retained within healthy cyanobacterial cells and are only released into the surrounding water after cells death and breakdown. They can, therefore, enter in the water treatment plant either as dissolved compounds in the raw water or within the cells, which represents a significant challenge to water treatment process. Removal of toxin containing cells at the early stages of treatment can be a

relatively straightforward way of greatly reducing the microcystin burden. Although, great care must be taken to prevent cell lyse, otherwise toxin will move into the water phase and the benefit is null. In contrast, it may be more desirable to release microcystins into the liquid phase where they can be removed along the treatment process (Lawton and Robertson, 1999).

MCs are known to be relatively stable compounds, possibly as a result of their cyclic structure. They have been reported to withstand many hours of boiling and may persist for many years when dry stored at room temperature. Therefore MCs are not really removed from drinking water by conventional treatment methods (Lawton and Robertson, 1999).

The ingestion of contaminated water with MC-LR has caused death of animals and negative effects on human health and a long-term exposure to sublethal levels of microcystins may promote primary liver cancer by disruption of protein phosphates 1 and 2A (Lee et al., 2004b).

Episodes of intoxications of humans occurred in some places, for example in Rudyard Reservoir, U.K. (1989), Nandong District, Jiangsu Province, Nanhui/Shanghai, Fusui, China (1994-1995), Caruaru, Brazil (1996), and also involving fish deaths in Loch Leven, Scotland, U.K. (1994) (Hitzfeld et al., 2000a). The most dramatic case occurred in Caruaru, Brazil, in February of 1996, where 101 of 124 patients (81 %) who underwent dialysis had acute liver injury, and 50 died, due to the contaminated water by cyanobacteria used for hemodialysis (Jochimsen et al., 1998).

Because of the severity of the poisoning, a thorough investigation was carried out, which showed up major defects in the operation of the water treatment unit at the clinic. Exposure to toxins through renal dialysis is a particularly potent route of poisoning, equivalent to an intravenous injection in the case of water soluble toxins. The volume of water used in perfusion is large, about 120 L, so that the total amount of toxin to which a dialysis patient is exposed is much greater than possible through drinking water (Falconer and Humpage, 2005).

Carcinogenicity of these toxins is not yet established, though both microcystins and cylindrospermopsin have caused excess tumors in experiments with rodents. With the increased eutrophication of water supplies and global warming, cyanobacterial populations and hence toxic risks are likely to rise in the immediate future (Falconer and Humpage, 2005).

Lun et al. (2002) correlated the presence of MC in drinking water with the incidence of colorectal cancer (408 cases of colon and rectum carcinomas diagnosed from 1977 to 1996) in eight townships or towns in Haining City of Zhejiang Province, China. In order to determine the causes, a survey on the types of drinking water consumed by these patients was performed. Samples from different water sources (well, tap, river and pond) were collected and MC concentrations were determined. The concentration of MC in river and pond water was significantly higher than that in well and tap water. The incidence rate of colorectal cancer was significantly higher in population who drank river and pond water than those who drank well and tap water.

- Cytotoxins – cylindrospermopsins (CYN) – hepatotoxins and cytotoxins

  Cylindrospermopsins (CYN) is an alkaloid structure of sulphated and methylated tricyclic guanidine joined via a hydroxylated single carbon bridge to uracil, and contains a uracil moiety attached to a sulphated guanidine moiety, suggesting that it may have carcinogenic activity (Hummert et al., 2001). In contrast to microcystin, where the toxin releases from the cells after their rupture, the higher concentrations of CYN can be found in the aqueous media toward the end of the bloom, when the cell is still viable (Song et al., 2012).

  Over the past decade, species of cyanobacteria other than *C. raciborskii* have been shown to produce CYN, including *Umezakia natans*, *Raphidiopsis curvata*, *Anabaena bergii*, *Aphanizomenon ovalisporum*, *Aphanizomenon flos-aquae*, *Anabaena lapponica* and *Lyngbya wollei* (YIlmaz et al., 2008).

  The cyanobacteria that produce this toxin may flourish in tropical and sub-tropical regions around the word, mainly in fresh water and constitutes an important potential contaminant of water supplies (Codd, 2000; Humpage and Falconer, 2003; Shalev-Alon et al., 2002). Saker et al. (2003) detected high concentration of *C. raciborskii* and codominant species, including other cyanobacteria in smaller concentration, *as Aphanizomenon, Merismopedia and Oscillatoriales*, in Portuguese freshwaters, however only during the warmer months.

  Preußel et al. (2006) reported the first poisoning incident originated by cyanobacteria *C. raciborskii* in 1979 at Palm Island (Australia), where 148 aborigines, mainly children, fell ill with gastroenteritis symptoms.

  This toxin has been associated with liver damage in mouse bioassays, with symptoms that clearly can be distinguished from those caused by other cyanobacterial hepatotoxins including MCs. CYN also has been implicated in outbreaks of human

sickness and cattle mortality (Saker et al., 2003). Toxicological studies have demonstrated an inhibitory effect on protein synthesis, which may result from the binding of an activated metabolite of CYN to DNA (Bernard et al., 2003). According to Humpage et al. (2000) it was proven in vitro that CYN can induce the mutagenicity by DNA strand breaking chromosome loss during cell division.

Falconer (2001) treated 53 mice orally up to three times with *C. raciborskii* extract with CYN. After 30 weeks, five tumours were found in all cylindrospermopsin-treated mice. For the author, the calculated relative risk indicates a potential biological and public health significance requiring more investigation.

Humpage and Falconer (2003) performed experiments to determine a no-observed-adverse-effect level (NOAEL) for CYN in Male Swiss Albino Mice, leading to a guideline for a safe drinking water level for this toxin of 1 µg L^{-1} CYN, based on a NOAEL of 30 µg kg^{-1} day^{-1}.

2.1.3 Culture of cyanobacteria and cyanotoxins isolation

Studies of cyanobacteria can be performed with environmental samples and laboratory-grown. Laboratory media and various culture conditions can be used to grow cyanobacteria, as ZEHNDER medium (Pietsch et al., 2002), Z8 medium (Saker et al., 2003), (Martins et al., 2009), Z8 medium supplemented with NaCl (Martins et al., 2005), BG11 (Hoeger et al., 2002), BG110 medium (+2 mM $NaNO_3$)(Robillot et al., 2000), WC (Pires et al., 2004), and ASM-1 (Soares et al., 2004). In addition to the appropriate culture medium is also necessary to control the lighting and aeration. Table 2.3 summarizes medium compositions and conditions used by different authors to grow cyanobacteria.

Sample from natural waters are normally collected at points where the accumulation of cyanobacteria is likely to affect humans and livestock, or at drinking water reservoirs (Msagati et al., 2006).

The sample can be stored in plastic containers (Bouvy et al., 1999; Shaw et al., 1999), or in glass bottles (Hoeger et al., 2005). The sample volume depends on the sensitivity of the toxins detection methods that will be adopted; if the method requires sample pre-concentration, a high sample volume is often necessary.

A portion of each sample must be immediately preserved in formol for phytoplankton/cyanobacteria identification and a lugol solution is added to better quantify the

cyanobacteria (Hoeger et al., 2005; Shaw et al., 1999; Vasconcelos et al., 2010a). The sample intended to cyanotoxins analysis can be frozen or concentrated depending on the analytical method (Vasconcelos et al., 2010a).

Different methods, types of microscope and counting chambers are used for quantification and measurement of cells. The ideal chamber should be selected according to cell size and density of the culture: i) for size of 50 - 500 µm and a density of 30 - 104 cell mL^{-1} the chamber appropriate is the Sedgwick-Rafter; ii) for 5 - 150 µm and 102 - 105 cell mL^{-1} can be used the Palmer-Maloney counting chamber; for size of 5 - 75 µm and 104 - 106 cell mL^{-1} we have two options, Speirs-Levy or Hemacytometer chambers, the second can be also used for count cells of 2 - 30 µm and 104 - 107 cell mL^{-1}; iv) to size less than 1 - 5 µm and 106 – 108 cell mL^{-1} the Petroff-Hausser chamber is a good option (Andersen, 2005).

Table 2.3 Different media and conditions used to grow cyanobacteria.

Cyanobacteria	Medium	Medium composition	Conditions	Reference
Synechocystis sp Oscillatoria sp *C. stanieri* *C. raciborskii* IZANCYA 2	Z8 medium	$NaNO_3$; $Ca(NO_3)_2.4H_2O$; $MgSO_4.7H_2O$, K_2HPO_4; Na_2CO_3, Fe-EDTA, micronutrient solution	25 ºC, light intensity 10 µmol photons s-1 m^{-2}, with a light/dark cycle of 14 h/10 h	Kotai (1972), Martins et al. (2009), Martins et al. (2005), Saker et al. (2003).
M. aeruginosa (PCC 7813)	BG11 medium	BG11 medium contains $NaNO_3$, $K_2HPO_4{\cdot}3H_2O$, $MgSO_4{\cdot}7H_2O$, $CaCl_2{\cdot}2H_2O$, citric acid, ferric ammonium citrate, EDTA (dinatrium-salt), Na_2CO_3 and micronutrient solution	26 ºC, 0.003% CO_2 and 24 h light 25±0.5 ºC with incandescent light of 2000 lx (12 h dark, 12 h light)	Hoeger et al. (2002), Msagati et al. (2006), Zhang et al. (2006).
M. aeruginosa (PCC 7813)	BG110 medium (+2 mM $NaNO_3$)	BG11 medium contains $NaNO_3$, $K_2HPO_4{\cdot}3H_2O$, $MgSO_4{\cdot}7H_2O$, $CaCl_2{\cdot}2H_2O$, citric acid, ferric ammonium citrate, EDTA (dinatrium-salt), Na_2CO_3 and micronutrient	25 ºC under white light (1900 lux, LD 18-8 h)	Msagati et al. (2006), Robillot et al. (2000).
M. aeruginosa (NIVA-CYA 140)	WC medium	$CaCl_2{\cdot}2H_2O$, $MgSO_4{\cdot}7H_2O$, $NaHCO_3$, $K_2HPO_4{\cdot}3H_2O$, $NaNO_3$, $Na_2SiO_3{\cdot}5H_2O$, micronutrient solution, vitamin solution of thiamin HCl and biotin	20±1 °C, light intensity 7 µmol photons s^{-1} m^{-2}	Msagati et al. (2006), Pires et al. (2004).
M. aeruginosa (NPLJ-4)	ASM-1	$MgSO_4{\cdot}7H_2O$, KCl, $NaNO_3$, $CaCl_2{\cdot}2H_2O$, KH_2O_4, vitamins B1 and B12 and trace elements	23±2 °C, light intensity 22 µE s^{-1} m^{-2} photoperiod of 12 h/d pH = 8.0	Msagati et al. (2006), Soares et al. (2004).
M. aeruginosa (B.14.85)	Zehnder medium	$NaNO_3$, $Ca(NO_3)_2{\cdot}4H_2O$, K_2HPO_4, $MgSO_4{\cdot}4H_2O$, Na_2CO_3, Fe-EDTA complex micronutrient solution and distilled water	21-23 °C under continuous stirring, photoperiod of 12 h/d (ca. 80 µmol m^{-2} photons, day-night-change)	Msagati et al. (2006), Pietsch et al. (2002).
C. raci	Jaworski's medium (JM)	$Ca(NO_3)_2{\cdot}4H_2O$, KH_2PO_4, $MgSO_4{\cdot}7H_2O$, $NaHCO_3$, EDTAFeNa, Na_2EDTA, H_3BO_3, $MnCl_2{\cdot}4H_2O$, $(NH_4)6Mo_7O_{24}{\cdot}4H_2O$, Cyanocobalamin, Thiamine HCl, Biotin, $NaNO_3$, $NaH_2PO_4{\cdot}12H_2O$,	27-30 ºC with aeration, light intensity 43 µE $m^{-1}s^{-1}$	Norris et al. (2001)
N. spumigena	f/2 nutrient medium	$NaNO_3$, $NaH_2PO_4{\cdot}H_2O$, $Na_2SiO_3{\cdot}9H_2O$, trace metal solution, vitamin solution	16 ºC and photoperiod 12 h	Dahlmann et al. (2001), Guillard (1975).

The analysis of cyanotoxins can be performed not only in water samples, but also in organisms from aquatic environments, like snails, bivalves (Gérard et al., 2009; Puerto et al., 2011), fish (da Silva et al., 2011; Karim et al., 2011), crabs (Garcia et al., 2010), shrimp (Zimba et al., 2006), or others crustaceans as well as in vertebrates samples, from humans and rats (Msagati et al., 2006).

Fish may be exposed to marine toxins during the different stages, as adults during sexual maturation, as eggs and as larvae. In all phases of their reproduction, the impact of a single toxin is different because of the levels of exposure and the way the toxin may find their target is also different. The contact with the toxins may be direct, via food or during collapse of phytoplankton blooms when the toxins are dissolved in the aquatic environment. Studies on the effects of the marine toxins on egg hatching and embryo development are very difficult due to the fact that several model fish species are used such as Danio rerio and Oryzias latipes and different routes of administration, microinjection of pure toxin, exposure to pure toxin or to raw extracts, can be considered (Vasconcelos et al., 2010b).

2.1.4 Extraction of toxin from water sample

In water samples, the toxin may be intra and extracellular. To determine the total level of toxins, first the cells must be lysed to liberate toxins, usually by freeze-thawing, with a probe sonicator or ultrasonication bath; however some studies suggested that probe sonicator is more effective. In raw water samples, the toxins release is a necessity; in a filtered water sample, such as at outlet of a water treatment plant, all toxins will likely be in solution and total concentration will be determined by analyzing the total dissolved toxins (Svrcek and Smith, 2004). Figure 2.2 displays the flowchart of the steps normally used for extraction and determination of toxins according to Sangolkar et al. (2006).

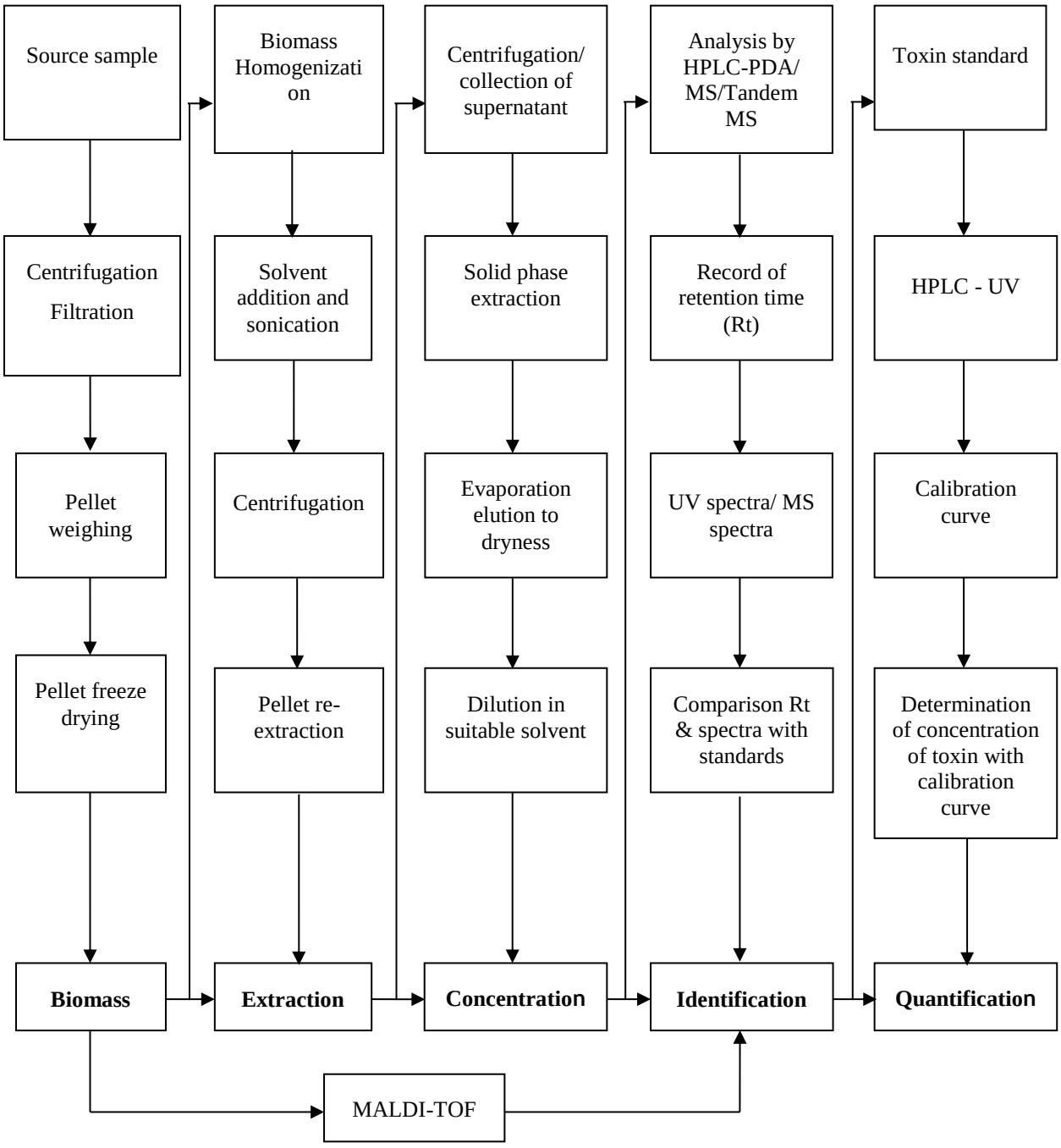

Figure 2.2 Toxin extraction, pre-concentration/clean-up, and quantification.

If the cyanotoxins concentration in water sample is low, a pre-concentration is often necessary (Sangolkar et al., 2006; Yen et al., 2011). Table 2.4 shows the detection limit of different methods used for cyanotoxins quantification.

Table 2.4 Detection limit of different methods used for MC-LR quantification (adapted from Svrcek and Smith (2004)).

Method	Detection limit or range
Mouse bioassay	1 to 200 µg
HPLC separation – UV, PDA, MS detection	0.02 µg L^{-1}, dependent on concentration factor
HPLC separation – fluorescence detection	34 µg L^{-1}, no preconcentration
Chromatography	0.01 µg L^{-1}, qualitative
GC/MS	1 µg L^{-1}
LC/MS/MS	1 µg L^{-1}, no extraction or preconcentration step
MMPB method (GC method)	0.43 ng microcystin, dependent on concentration factor
ELISA	0.05 µg L^{-1}, no preconcentration, depends on antibodies
PPIA, colourimetric	0.3 µg L^{-1}, no preconcentration
PPIA, radiolabelled	Sub-picogram

HPLC, high performance liquid chromatography; GC, gas chromatography; MS, mass spectrometry; UV, ultraviolet; PDA, photo-diode array; MMPB method, 3-methoxy-2-methyl-4-phenylbutryric acid method

There are several concentration methods, including liquid-liquid extraction, solid-phase micro-extraction, freeze-drying and solid-phase extraction (SPE) (El Herry et al., 2008; Poon et al., 2001; Yen et al., 2011). Thus SPE can be used not only to concentrate toxins but also to perform a cleanup by allowing removal of co-extracted material which may interfere in the analysis (Nicholson et al., 2001). SPE often is performed with a C18 cartridge, a vacuum manifold and a vacuum pump. The sample is passed directly through the cartridge, which must be preconditioned using an organic solvent such as methanol and further with Milli-Q water, and the toxin is retained in the solid phase. The toxin is eluted using again the organic solvent. Solvent extracts may be reduced in volume by evaporation resulting in increased toxin concentration (Lawton et al., 1994; Magalhães et al., 2003; Msagati et al., 2006). Several organic solvents have been used in several steps for extraction, concentration/clean-up and detection of cyanotoxins (see Table 2.5).

Table 2.5 Extraction solvents usually used for cyanotoxins.

Solvents	Methods	Reference
Methanol Dichloromethane	C18 SPE Cartridges for CYN	Norris et al. (2001)
Methanol Ammonium acetate	HPLC-MS/MS analysis for CYN	Shaw et al. (1999)
Methanol 20 %	HPLC analysis for MC-LR	Hoeger et al. (2005)
Methanol, TFA, Ammonium acetate	HPLC analysis for MC and NOD	Spoof et al. (2001)
Acetonitrile, methanol, TFA	HPLC analysis for MC	Lawton et al. (1994)
Acetic acid and methanol/ chloroform	HPLC-UV analysis for MC-LR	Moreno et al. (2004)
Acetic acid (5 %), methanol	HPLC and LC-ESI-MS analysis for MC-LR	Harada et al. (2004)
Acetic acid/ water or alcohol/ water	HPLC analysis for MC	Harada et al. (1997)
Acetonitrile, water and formic acid	LC-MS and MS-MS analysis for CYN	Dell'Aversano et al. (2004)

TFA Trifluoroacetic acid

2.1.5 Analytical methods for cyanotoxins detection

Until recently, the identification of cyanobacteria followed taxonomic methods, generally based on morphological characteristics. However, several problems may occur when trying to identify and distinguish the cyanobacterial strains (Baker et al., 2001a):

i. Identification of a cyanobacteria genus morphology by microscopy does not indicate the potential for toxin production;
ii. A single genus can contain toxic and nontoxic species, or may be able to produce one of several different types of toxins;
iii. Some species, for example those belonging to the genus Anabaena, can produce microcystins, anatoxin-a, anatoxin-s or a particular toxin that has been identified as causing paralyzing effect on mollusks.

The detection of cyanotoxins can be performed by using different chemical and biological methods (El Semary, 2010). Each test has advantages and disadvantages depending on the

aim of the user and the analytical problem. The “best” method for cyanobacterial toxins analysis depends on the goal of the sampling program (Dahlmann et al., 2001; Svrcek and Smith, 2004). Table 2.6 shows a summary of different analytical methods used for cyanotoxins quantification.

The different chemical properties and structure of each toxin may difficult their simultaneous detection; for example microcystin and nodularin are polycyclopeptides, while ATX and CYN are alkaloids (Yen et al., 2011).

Table 2.6 Identification/quantification of cyanobacterial toxins at several places around the word using different analytical methods.

Location	Sampling sites	Organisms found	Toxin	Method of detection	Toxin quantification/ identification	Additional information	Reference
McMurdo Ice Shelf-Antarctica	Meltwater ponds	*Oscillatoriales*, *Nostoc* sp., *Nodularia* sp., *A. antarctica*	MC-LR	HPLC, PPIA	≥ 0.15 µM	–	Hitzfeld et al. (2000b)
German	Lakes Melangsee and Heiliger See	*C. raciborskii* *Aphanizomenon flos-aquae*	CYN	LC-MS/MS	6.6 mg g^{-1}	–	Preußel et al. (2006)
Australia	Palm Lakes and ocean Park lakes in Queensland	*A. ovalisporum*	CYN	HPLC-MS/MS,	4-120 µg L^{-1}	Concentration in water and algae, and filtered water	Shaw et al. (1999)
						Dose of 110 – 2450 mg FDA kg^{-1} (0.06 – 1.3 mg CYN kg^{-1})	
			Toxicity of Bloom samples	Animal bioassays	Survival time of less than lethal dose – 24 h		
					Survival time of approx. 2 h	1 mL of 100-fold concentration of water	
Israel	Lake Kinnert	*A. ovalisporum*	CYN	Animal bioassays	Lethal dose of 800 mg d.w. of *A. ovalisporum* kg^{-1} mouse within 24 h	–	Banker et al. (1997)
Tunisia	Seven different Tunisian reservoirs	*C. raciborskii* *M. aeruginosa* *Plantonthrix agardhii* *Anabaena circulars* *Limnothrix* sp. *Leptolyngbya* sp. *Limnothrix redekei*	MC-LR, MC-FR, MC-RR, MC-YR AND MC-WR	MALDI-TOF-MS	MC- LR was found to be produced by all strains. Other variants were only produced by some of them	–	(Fathalli et al., 2011)

Table 2.6 Identification/quantification of cyanobacterial toxins at several places around the word using different analytical methods (cont.).

Location	Sampling sites	Organisms found	Toxin	Method of detection	Toxin quantification/ identification	Additional information	Reference
Central Mexico	Nine different eutrophic water bodies	*M. aeruginosa, M. panniforms, M. protocystis, P. agardhii, Merismopedia* sp. and *Pseudanabaena mucicola*	MC-LR	ELISA analysis for MC MALDI-TOF-MS	Detected MC-LR in five samples, varied from 4.9 – 78 μg L^{-1} MC-LR and MC-RR	Were analyzed seven places for ELISA, presence and type of MC was confirmed by MALDI-TOF MS Blooms 1.6×10^{3} – 7.5×10^{6} cell mL^{-1} in seven location sample	Vasconcelos et al. (2010b)
Morocco	Lalla Takerkoust lake-reservoir	*M. aeruginosa,* *P. mucicola*	Microcystins Microcystins	ELISA	0.60-0.71 μg mg^{-1} 0.02 μg mg^{-1}	–	Oudra et al. (2001)
Portugal	Northern border (Minho) and southern coast	*Synecocystis* sp, *Oscillatoria* sp, *Cyanobecterium stanieri, Synechococcus* sp	Toxicity samples Microcystin PST (saxitoxin family)	Mouse bioassays ELISA MALDI-TOF MS HPLC-FLD	Death between 28 and 48 h or pathological effects 0.0042-0.048 μg g^{-1} (detected in seven of 22 strains) None toxin was detected Provided no evidence of the PST-paralytic shellfish toxin	Concentration of 2000 mg kg^{-1}	Martins et al. (2005)
China	Meiliang Bay (Lake Taihu)		Microcystins	ELISA HPLC	24.53 – 97.32 μg g^{-1} MC-LR was detected Retention time of 9.7 min	–	Shen et al. (2003)

2.1.5.1 Mouse bioassay

Mouse bioassay is a non-selective method for toxins identification via symptoms (Svrcek and Smith, 2004), which can be applied to all toxic substances, as a screening method in the whole range of toxins, but do not have enough sensitivity to be applied to water samples without impractical levels of pre-concentration. Generally is necessary a long-term exposition, so, specific, straightforward, and rapid procedures are required for the detection, identification and quantification of the toxin (Dahlmann et al., 2001). Nowadays, legal and ethical issues limit the use of mouse bioassays for toxicological purposes.

2.1.5.2 Protein phosphatase inhibition assay (PPIA)

Serine and threonine phosphatase enzymes are responsible for the dephosphorylation of intracellular phosphoprotein. The two enzymes are classified as Type 1 (PP1) and Type 2 (PP2) (Msagati et al., 2006). Protein phosphatase PP1 and PP2A are specifically inhibited by naturally occurring toxins such as okadaic acid (a fatty acid derivative) or microcystins (Garcia et al., 2003); the PP1 is the most inhibited by cyclic peptide heptatoxin (Msagati et al., 2006).

One of the methods used for detection of microcystin is the protein phosphatase inhibition assay, which is based on the degradation of p-nitrophenyl phosphate (uncoloured) into p-nitrophenol (yellow). Antibody cross-reactivity of microcystin and nodularin are compared with their ability to inhibit protein phosphatase type 1 (PP1). Inhibition rate is directly related to the absorbance at 405 nm. Microcystin concentration is obtained by reporting the inhibition rate on a standard MC-LR calibration curve (Robillot et al., 2000).

The detection of MC by the phosphatase inhibition method is based on toxic effects. The PP2A activity inhibition test is important since it gives a measure of the whole toxinogenic potential of the sample. However, in case of positive, the accurate determination and identification of the toxin requires the use of complementary analytical techniques, such as, LC-UV or LC-MS (Rivasseau et al., 1999).

According to Robillot et al. (2000) the PP2A assay is performed as a screening technique followed by HPLC as a confirmation method. This strategy appears to be very efficient for the environmental monitoring of microcystins.

Dahlmann et al. (2001) showed that PP1 test is more selective towards nodularin and microcystin and the detection limit is 100 and 500 times higher than LC-MS and HPLC-UV methods. The main advantage of PP1 test is the high sensitivity, which allows to detect trace toxin concentrations.

2.1.5.3 High Performance Liquid Chromatography (HPLC) and Liquid Chromatography – Mass Spectrometry (LC-MS)

High Performance Liquid Chromatography (HPLC) is the standard method used for quantification of hepatotoxins microcystins and nodularins, although UV/Vis absorbance and PDA are the mostly used detectors (Ibelings and Chorus, 2007).

Different HPLC methods for the determination of microcystins were established during the last 15 years. HPLC methods and especially LC with mass spectrometry detection (MS) are sensitive, selective and provide highly reliable quantitative results. However, for samples with a complex composition and when it is necessary to know qualitatively and quantitatively which toxins are present in the phytoplankton sample, HPLC-UV is a good compromise between the biological test and the expensive LC-MS technology (Dahlmann et al., 2001).

HPLC can be a powerful tool for the identification of microcystins, and is capable of providing both quantitative and qualitative data. However, the method is both technically demanding and expensive, and its strength often depends on the availability of a range of toxin standards. HPLC detection of the toxins in natural samples also relies on on-site sampling followed by sample processing and analysis in the laboratory, which can consume much time (McElhiney and Lawton, 2005).

Quantitative analysis of trace microcystins by HPLC-UV is performed using external standardization or a calibration curve, which can also be used to indicate, to some extent, the identity of the toxin present, i.e., by matching the retention time of a peak in a sample chromatogram with that of an authentic standard. Only few microcystins are commercially available, namely MC-LR, which contains leucine and arginine, MC-YR, substituted with tyrosine and arginine and MC-RR, containing two arginines (Msagati et al., 2006; Rivasseau et al., 1999). Microcystins show two typical spectra. Most of them show UV absorption at 238 nm, however a few microcystins that contain tryptophan give an absorption maximum at 222 nm (Lawton et al., 1994).

A further difficulty affecting HPLC, ELISA (cf. section 2.1.5.5) and PP1A methods is the need for extensive sample handling and lengthy analysis times (Howard and Boyer, 2007). However LC-MS with various interface and ionization configurations have been reported as a good option for the detection of cyanotoxins with detection limits of ~ 0.02 µg L^{-1} (Msagati et al., 2006). Mass spectrometry (MS) is an excellent technology for molecular imaging because of its high data dimensionality. MS can monitor thousands of individual molecular data channels measured as mass-to-charge (m/z) (Burnum et al., 2008).

Detection limits less than 1 µg L^{-1} for microcystin are normally attainable after concentration and clean-up of the sample (Msagati et al., 2006). LC-MS is used also to detect other types of cyanotoxins, for example Krüger et al. (2010) applied LC–MS/MS method to detect BMAA and DAB resulting in high reproducibility and stability of the chromatographic retention time for different sample matrices.

2.1.5.4 MALDI-TOF-MS

Mass measurement of peptides can be fast and sensitive by Matrix Assisted Laser Desorption/ Ionization – Time of Flight – Mass Spectrometry (MALDI-TOF-MS), which is based on the desorption and ionization of proteins with a laser beam associated with a matrix (MALDI) that analyzes the time dispersion of ions (TOF) (Mann and Talbo, 1996). Ions produced by the ionization source are separated in the mass analyzer according to the ratio mass/charge (*m/z*) and data are recorded as a spectrum (intensity vs *m/z*). The matrix is used to protect the biomolecule from being destroyed by direct laser beam and to facilitate vaporization and ionization (Freitas, 2009).

Different matrix substances and application methods are used depending on the nature of the compound to be analyzed and type of measurement used in MALDI-TOF MS (Howard and Boyer, 2007). Cyanobacterial toxins (MCs) were analyzed using as normal matrix the α-cyano-4-hydroxycinnamic acid (CHCA) and as an alternative MALDI matrix, CHCA + cell component (CHCAcell). Other researchers (Vasconcelos et al., 2010b) used as matrix a solution with 2,5-dihydroxybenzoic acid in water:acetonitrile:ethanol (1:1:1 + 1 % TFA).

MALDI-TOF-MS is an advantageous method for cyanotoxins detection because it is extremely rapid, of high-resolution, requires little sample handling, is tolerant to contaminants, requires low sample volumes, and allows identification of toxin congeners (Howard and Boyer, 2007).

This technique provides accurate molecular weights of cyanobacterial polypeptides from intact cells in minutes. The cyanotoxins can be identified by comparison with standards, but also can be detected new polypeptides that may be later characterized by the same analysis technique by Post-Source-Decay (PSD). Contrasting with the techniques of HPLC, MALDI-TOF-MS requires no sample preparation and a single cell may be sufficient for the characterization of its polypeptide profile (da Silva Fernandes, 2008).

2.1.5.5 ELISA

Environmental monitoring of water samples requires rapid determination methods, principally when blooms occur. The bioassay Enzyme Linked Immunosorbent Assay (ELISA) is well adapted to that aim. However, such methods have only been evaluated using laboratory-synthesized antibodies or laboratory-isolated enzymes (Rivasseau et al., 1999).

ELISA is an immunoassay used for quantitative analysis of microcystins and nodularins in water samples with a high sensitivity of 0.1 ng mL^{-1} (Ibelings and Chorus, 2007). It is based on the recognition of microcystins, nodularins and their congeneres by a monoclonal antibody. When these toxins are present in a sample, and a microcystins-horseradish peroxidase (HRP) analogue compete for the binding sites of anti-microcystins antibodies in solution, microcystins antibodies are bound by a second antibody (goat anti-mouse) immobilized in the plate. Quantitative analysis of the trace microcystins by ELISA method is performed using a calibration curve prepared with standard solutions of microcystins and a colorimetric antibody/antigen (da Silva Fernandes, 2008).

Although ELISA does not detect all variants of microcystin, is a rapid method for routine monitoring. The sensitivity and selectivity offered by ELISA can provide a reasonably accurate estimation of MCs with minimum sample processing (sample pre-concentration is not required), good cross-reactivity across microcystin variants and correlation with PP1 and HPLC for quantification of total microcystins (El Semary, 2010; McElhiney and Lawton, 2005; Rogalus and Watzin, 2008).

However, the commercially expensive kits available have shown variable cross-reactivity, and in the absence of standards, they are only capable of determining toxicity in terms of microcystin-LR equivalence (McElhiney and Lawton, 2005). So, as some false positives can occur, positive samples can be confirmed by HPLC, protein phosphatase assay or other conventional methods (El Semary, 2010).

2.2 Styles water treatment processes for the removal of cyanobacteria and cyanotoxins from water

Cyanobacteria produce a wide variety of toxins, and additionally molecules with unknown toxic potential (microviridins and aeruginosins) and cause, therefore, incalculable difficulties in water treatment works, which are dependent on raw surface water (Hoeger et al., 2005). The presence of toxic cyanobacteria in water intended for human consumption or recreational purposes poses a serious hazard to humans but has for too long been neglected or at most has been treated on a local level. Accumulation of cyanobacteria scum along the shores of ponds and lakes also present a hazard to wild and domestic animals. Providing the human population with safe drinking water is one of the most important issues in public health and will have more importance in the coming millennium (Hitzfeld et al., 2000a).

Bacterial biodegradation, ozonation, photodegradation by UV exposure or adsorption using traditional adsorbents, are some treatment processes that can be used for cyanobacteria elimination (El Semary, 2010). According to Antoniou et al. (2005), each different technology has advantages and limitations and the most efficient, safest and cost-effective should be selected on a case-per-case basis. Table 2.7 compares the efficiency of different water treatment technologies to eliminate cyanotoxins.

Table 2.7 Efficiency of different water treatment processes to eliminate cyanotoxins.

Removal process technology	Concentration/ additional information	Toxin	Initial toxin concentration	Detection method	Time	Process efficiency	References
ACH GAC + ACH UF (PVDF membranes)	23 % 20 mg L^{-1} 0.02 µm	Saxitoxins Microcystins	3.9 µg L^{-1} (IC) 1.2 µg L^{-1} (EC) 5.9 µg L^{-1}	ELISA HPLC	Flux decline: 0-90 min, 90-110 (ACH), 110-140 (AGH + GAC)	IC: 87 %, 46 % (ACH), 74% (AGH + GAC) Total removal: 70 %, 6 6 % (ACH), 35 % (AGH + GAC)	Dixon et al. (2011a)
GAC		Microcystins	5.0 µg L^{-1}	HPLC	225 days	100 % from 38 days	Wang et al. (2007a)
GAC	5, 10, 25, 50 and 100 mg L^{-1}	Microcystin-LR Cylindros permopsin	10 µg L^{-1} 20 µg L^{-1}	HPLC	30, 45 and 60 min (time did not influence)	Highest removal with GAC 50 mg L^{-1}, MC-LR <1 µg L^{-1}	Ho et al. (2011)
GAC/dark GAC/UV GAC+TiO_2/UV	GAC 1 g L^{-1} TiO_2 0.6 % wt. 4 W UV black light lamp, 370 nm	Microcystin-LR	200 µg mL^{-1}	HPLC	30 min 30 min 20 min	50 % 50 % 100 %	Lee et al. (2004a)
TiO_2 TiO_2/ H_2O_2	1 % (w/v) TiO_2 0.1 % (w/v) H_2O_2 480 W UV lamp, 330-450 nm	Microcystin-LR	1006 µM 1000 µM	PPIA	10 min	92.6 %	Liu et al. (2002)
TiO_2 film	6.7 µm film	Microcystin-LR	4.14 µM	PPIA	120 min	>50 %	Antoniou et al. (2009)
TiO_2 immobilized	5 g L^{-1} TiO_2 Film (layer thickness: 150 µm) 15 W UV lamp, 243.7 nm	Microcystin-LR Microcystin-RR	55 ng mL^{-1} 60 ng mL^{-1}	HPLC	MC-LR 2.7 min and MC-RR 3.5 min	100 %	Shephard et al. (2002)

ACH Aluminium chlorohydrate; GAC Granular activated carbon; UF Ultrafiltration; IC Intracellular; EC Extracellular

Table 2.7 Efficiency of different water treatment processes to eliminate cyanotoxins (cont.).

Removal process technology	Concentration/ additional information	Toxin	Initial toxin concentration	Detection method	Time	Process efficiency	References
Fenton, Fe^{2+}/H_2O_2	2.5 mM Fe^{2+} 5 mM H_2O_2	Microcystin-LR	3 µM	HPLC	180 min	61 %	Bandala et al. (2004b)
Photo-Fenton, Fe^{2+}/ H_2O_2/UV	0.25 mM Fe^{2+} 0.1-0.5 mM H_2O_2 36 W UV lamp, 365 nm	Microcystin-LR	8 µM		35 - 40 min	100 %	Bandala et al. (2004b)
Fenton, Fe/ H_2O_2	1.5 mM Fe^{2+} /15 mM H_2O_2 1.5 mM Fe^{3+} /15 mM H_2O_2 0.5 mM Fe^{2+} /5 mM H_2O_2	Microcystin-LR	300 µM	HPLC	30 min	100 % ~ 47 % ~ 13 %	Gajdek et al. (2001)
Ozone	1.12 mg L^{-1}	Microcystin-LR	116 µg L^{-1}	HPLC	4 min	>99 %	Rositano et al. (1998)
N-F-codoped TiO_2/Visible light	15 W fluorescent lamps, > 420 nm Nanoparticles surface area: 141 m^2/g	Microcystin-LR	1 mg L^{-1}	HPLC	300 min	100 %	Pelaez et al. (2009)
Ultrasonic	640 kHz	Microcystin-LR	2.7 µM	HPLC	6 min	85 %	Song et al. (2005)
Radiolysis/gamma irradiation	0.2-8 kGy	Microcystin-LR	0.8 mg L^{-1}	HPLC	-	98.8 %	Zhang et al. (2007)

ACH Aluminium chlorohydrate; GAC Granular activated carbon; UF Ultrafiltration; IC Intracellular; EC Extracellular

2.2.1 Conventional methods

Wastewater treatment usually involves three stages: preliminary treatment that mainly involves the settling and the removal of solids; secondary treatment including biological removal of organic matter and sludge clarification; tertiary treatment that mainly includes processes for phosphorus and nitrogen removal and pathogenic bacteria inactivation by UV light. Most of the secondary treatment configurations are open structures, which contain microbial communities that contribute to the partial removal of organic substances and nutrients before the discharge in receiving waters. In this way, secondary treatment systems may offer the ideal habitat for the development of cyanobacteria, and several studies have documented the presence of these organisms in these systems (Hitzfeld et al., 2000a; Martins et al., 2010).

When the toxin-producing cyanobacteria lyse either due to water/wastewater treatments or natural cause, most of the cellular microcystin is released into water thus causing a toxic hazard, therefore lysing cyanobacterial cells by traditional chemical treatments of water does not solve the problem of toxin but rather exacerbate it (El Semary, 2010).

Chemical coagulation, flocculation and sand filtration are conventional water treatment methods, but are poor as regards the removal of low concentrations of cyanotoxins. Chlorination requires high doses and long contact times, and may generate toxic byproducts such as trihalomethanes (Feitz et al., 1999).

2.2.2 Microbial degradation

When cyanobacterial bloom material collapses and the toxins are released into the water phase together with other lysate, it quickly stimulates the growth of bacterial strains capable of degrading the dissolved substrates (Christoffersen et al., 2002). For example microcystins can be a rich source of amino acids for the microorganisms. However they have a cyclic structure, which makes them resistant to common bacterial proteases, then it is necessary to have more specific enzymes for biodegradation (Valeria et al., 2006).

Bourne et al. (1996) used *Sphingomonas sp* to degrade MC-LR and observed that the concentration of toxin decreased proportionally with the increase of cell extract of these bacteria. Over degradation, two non-toxic byproducts were generated, named by the author as A and B. Three enzymes were involved in the degradation process, the first is the responsible

for the breakdown of the MC-LR cyclic structure and converts the MC-LR into byproduct A, the second enzyme converts A into B and the third catalyzes the breakdown of product B.

El Semary (2010) reported a natural breakdown of MC by bacteria belonging to a novel genus *Sphingosinicella, Microcystinivorans* and *Burkholderia sp*. from a Brazilian lagoon. Rapala et al. (2005) also revealed a novel genus of bacteria capable of degrading microcystins and nodularins. Okano et al. (2009) isolated *Sphingospyxis* sp. able to degrade MC under alkaline conditions, which corresponds to the same conditions for cyanobacterial bloom growth. Other authors (Christoffersen et al., 2002; Hyenstrand et al., 2003) reported the degradation of MC by the bacterial community in surface water from a eutrophic lake; the microcystin-LR concentration decreased to an undetectable level after 4-5 days.

Wu et al. (2010) used periphyton (assemblage of organisms growing upon free surfaces submerged in water, and covering them with a slimy coat (Sládečková (1962)) to degrade MC-RR. The periphyton community was composed primarily by bacteria, mainly bacilli and cocci, and diatoms such as *Melosira varians Ag., Gomphonema parvulum Kütz., Synedra ulna Kütz., Nitzschia amphibian Grun., and Fragilaria vaucheriae Kütz.* The maximum removal (86.5 % of MC-RR) was obtained in the first day through adsorption and biodegradation.

Valeria et al. (2006) performed a study to analyze the capacity of the bacteria isolated from an Argentinian reservoir to degrade MC-RR, which revealed that only one of the three isolated bacteria was efficient, the genus *Sphingomonas sp*.

Although several studies indicate cyanotoxins as biodegradable compounds, Wormer et al. (2008) revealed that CYN produced by *Aphanizomenon ovalisporum* was not degraded after 40 days exposure to bacterial communities. Ho et al. (2012b) studied the biodegradation of CYN (10 µg L^{-1}) in a natural water body at temperatures of 14 and 24 ºC; no degradation was observed under 14 ºC, while the concentration decreased 0.6 µg L^{-1} per day at 24 ºC, which means that the biodegradation of the metabolites is affected by the seasonal variation of temperature. However in another reservoir the authors did not observe degradation of saxitoxins, suggesting that this result was due to the lack of organism ability to degrade the saxitoxins, because these organisms were low in abundance or were inhibited by some environmental factor.

Microbial biodegradation of cyanobacteria toxins may take a long time because in some cases microorganisms naturally present in the environment may not be very efficient. In this way the use of selected strains and / or combination with other processes is often required.

Bourne et al. (2006) used biologically active slow sand filters and concluded that the addition of bacteria previously known as degrading cyanotoxins may have an activity combined with endemic bacteria, which facilitates the degradation of toxins and shortens the acclimatization. This process offers also a cost-effective water treatment. The presence of easily degradable carbon source also shortens or eliminates the lag phase, because the degradation rate of cyanotoxins also depends on the presence and composition of dissolved organic matter (Klitzke et al., 2010).

2.2.3 Activated carbon

The removal of taste and odor were one of the initial applications of activated carbon in the water industry, but its use was expanded to a wide range of contaminants (Lawton et al., 1999).

A problem caused by cyanobacteria is the occurrence of taste and odor episodes during the summer months due to the production of substances that are released to the water after the breakdown of the cells. The most common and problematic substances are alicyclic sesquiterpenoids, geosmin E-1,10-dimethyl-E-9-decanol (GSM) and 2-methyl-isoborneol (MIB), which are generally associated with poor water quality, affecting the palatability of water and leading to public complaints. Likewise in aquaculture, accumulation of these compounds in fish meat leads to quality problems (Scharf et al., 2010; Song and O'Shea, 2007).

The presence of cyanobacteria in water treatment plants can originate several operating problems, such as additional demands of chemicals and reduced filter run-times (Ho et al., 2012a). According to Scharf et al. (2010) if the granular activated carbon (GAC) is used with a film of bacteria, the bed life of GAC filter may be extended by biological degradation of GSM.

When using activated carbon it must be taken into account the concentration of toxins and their derivatives and solubility's and the origin of the activated carbon. In addition, the pore size distribution of the activated carbon plays an important role in microcystin-LR adsorption.

Microcystin has a diameter of approximately 3 nm, so it is too large to be adsorbed in micropores (diameter less than 2.0 nm), but can be fully adsorbed in mesopores (diameter between 2 and 50 nm) (Antoniou et al., 2005; Lee and Walker, 2006).

Ho et al. (2011) performed experiments using two commercial types of GAC and some differences were observed between them, which suggested that the selection of the most appropriate GAC is crucial to achieve optimum cyanotoxins removal. The authors also concluded that adsorption by GAC could be an effective treatment for the removal of CYN and MCs (LR, RR, YR and LA).

Lee and Walker (2006) compared the efficiency of two GAC, wood-based and coconut-based activated carbons. The first adsorbed approximately 80 % of MC-LR due to its greater mesopore volume, while the coconut-based GAC only adsorbed 20 % of MC-LR.

Although powdered activated carbon (PAC) and GAC have proven to be effective, the adsorption process might become expensive due to the necessity of frequent replacement or regeneration of the activated carbon (Lee et al., 2004a). According to Lee et al. (2004a), the adsorption of MC-LR on GAC may require a long time exposure (12 h) for the complete removal, which indicates that the adsorption on the surface is hindered by diffusion limitation.

A most effective way to remove cyanobacteria and metabolites may be the use of an integrated membrane system with activated carbon (Dixon et al., 2011b).

Ultrafiltration may be efficient to remove cyanobacteria cells under different growth ages, although it occurs more readily in older cells. However the procedure causes cell lysis and the release of toxins that may not be completely removed, requiring an additional treatment (Campinas and Rosa, 2010). The same result was obtained by Lee and Walker (2006) when using ultrafiltration on cellulose acetate membrane (pore 20 kDa). The membrane did not reject or adsorb microcystin-LR but when used in combination with wood-based GAC, 70 % toxin removal was achieved.

Ratnayake et al. (2012) also tested different treatment strategies in a water treatment plant: (i) pre-chlorination with powdered activated carbon; (ii) no pre-chlorination, with and without powdered activated carbon; (iii) coagulation/flocculation/dissolved air flotation, filtration, disinfection, and post lime addition for stabilization. The results showed that PAC was effective in reducing the microcystins concentration. However, since the chlorine and PAC

were both added at the same location of the treatment plant, the pre-chlorination may affect the performance of adsorption. Post-chlorination after PAC addition seems to be the best option to remove any remaining microcystins.

A good result was obtained by the combination of adsorption by activated carbon with photocatalysis (UV radiation at 370 nm) using GAC and TiO_2 completely dispersed in an aqueous phase containing MC-LR (Lee et al., 2004b). MC-LR disappeared in approximately 20 min, although in the absence of radiation, the MC-LR concentration remained constant.

2.2.4 Advanced oxidation processes

Advanced Oxidation Processes (AOPs) may be used for decontamination of water containing organic pollutants, classified as bio-recalcitrant, and/ or for destruction of current and emerging pathogens, instead of a simple and more common phase transfer (Andreozzi et al., 1999). These processes rely on the formation of highly reactive chemical species which degrade even the most recalcitrant molecules into more biodegradable compounds. Those reactive chemical species, such as hydroxyl radicals ($HO^{\bullet}$), are able to oxidize and mineralize almost any organic molecule, yielding CO_2, H_2O and inorganic ions. Kinetic constants (k_{OH}, $r = k_{OH}[HO^{\bullet}]$ C) for most reactions involving the attack of organic molecules by hydroxyl radicals in aqueous solution are usually in the order of 10^6 to 10^9 M^{-1} s^{-1}. They are also characterized by their little selective attack, which is a useful attribute for wastewater treatment and solution for many pollution problems (Malato et al., 2002; Malato et al., 2009).

2.2.4.1 Ozonation

Ozone has been used in Europe and North America for disinfection or color and/or odor removal. In recent years, many water treatment plants included two stage ozonation treatment steps, either pre- and interozonation, inter- and postozonation, or pre- and postozonation (Hitzfeld et al., 2000a). Activated carbon can eliminate the surplus ozone, adsorbs hydrophobic compounds, and acts as substrate for bacteria, which mineralize most of the organic by-products (ketones, aldehydes and acids) produced by ozonation (Hoeger et al., 2005).

Ozonation of drinking water is often considered to be an advanced treatment process, because of the inherent complexity of operation (Svrcek and Smith, 2004). Reactions with ozone can take place directly through oxidation of dissolved compounds with molecular ozone, or

indirectly through oxidation with hydroxyl free radicals (*HO•*) that originate from the decomposition of ozone. Hydroxyl radical oxidation is quite non-selective, reacting rapidly with a broad range of species. Ozone combined with UV light has proved to be an effective system in destroying a wide range of organics (Lawton and Robertson, 1999).

Ozone is one of the most powerful oxidizing agents, and its potential to destroy cyanobacteria is used in water treatment by dispersing the gas in the aqueous medium. It is widely used for treating drinking water but it is an expensive and sometimes unpredictable reagent (El Semary, 2010). Other disadvantages include the rapid depletion of ozone, due to the competition between the toxins and organic material in the raw water, resulting in incomplete oxidation of the toxin. In this situation, single ozonation, sometimes may not be enough and an additional treatment is required (Hoeger et al., 2002).

High doses of ozone are required to destroy the cyanobacteria and toxins. So, the best treatment option is the preliminary physical cells elimination via dissolved-air-flotation or coagulation and filtration and then use ozonation only to inactivate the extracellular toxins (Onstad et al., 2007).

Miao and Tao (2009) applied an ozonation process in the treatment of water contaminated with *M. aeruginosa* cells. The authors observed an impact on cellular morphology and the increment of ozone dosage (1 – 5 mg L^{-1}) resulted in cell wall modification and cellular cytoplasm release from the cells, which caused an increment in DOC, which reduced significantly the MCs degradation.

The same authors also studied the effect of ozonation in two different types of MC and found that under the same conditions of degradation, pre-ozonation showed to be significantly more efficient for MC-LR degradation (95.7 and 92.1 %, respectively) than for MC-RR degradation (82.4 and 89.3 %, respectively). According to Miao et al. (2010) MC-LR and MC-RR had Adda moyet, the Adda conjugated position showing similar sensibility to ozonation in both toxins, although MC-RR has a larger Arg group, which hinders the O_3 attack and reduces the reactivity (Miao et al., 2010; Miao and Tao, 2009).

Different ozone doses were applied to microcystin-spiked drinking water samples from two lakes using a batch ozonation method. In both types of water, complete removal of MC-LR and MC-LA was achieved, only at the doses where significant residual ozone was still present after 5 min of exposure. The authors also concluded that the typical ozonation regimes used in

water treatment (ozone oxidation following conventional flocculation, sedimentation and filtration) are adequate to remove dissolved microcystins, and most of them are already removed in the coagulation process prior to ozonation (Brooke et al., 2006). However, if the toxin load is low, preozonation may be sufficient to oxidize the toxins completely (Onstad et al., 2007).

When the oxidation is applied to degrade dissolved toxins, the treatment can be efficient mainly if the water has been previously treated. The ozonation efficiency can be reduced by the presence of cyanobacterial cells, because ozone can cause lysis of the cells and the toxins are released into the water. Then the oxidant available can be insufficient to react with the toxins released and with other organic and inorganic matter (Hall et al., 2000).

2.2.4.2 Ultrasonic irradiation

Ultrasonic irradiation does not require addition of chemicals, and can be used for the treatment of turbid waters. It can remove surface contamination and biofilms, enhance soil washing, remove chemical and biological contamination from water (Hu et al., 2011; Song et al., 2005). When applied to water, ultrasound power leads to acoustic cavitation, in which bubbles collapse rapidly to reach temperature in excess of 5000 K, called 'hot spot' (Wu et al., 2011; Zhang et al., 2006). The pyrolysis of water produces H^+ and $HO^{\bullet}$ and the reaction pathways for ultrasonic irradiation are similar to those observed for other $HO^{\bullet}$ generating techniques (Song et al., 2005).

Gas vesicles inside algae cells control the floating of the cells (Zhang et al., 2006). According to studies about cyanobacteria bloom control (Lee T.-J., 2002), ultrasounds effectively reduce the grow rate, destruct the gas vacuoles by cavitation and promote close contact between cyanobacteria leading to immediate and accelerated destruction of the cells.

The effect of ultrasounds on cyanobacteria and toxins degradation depends on the frequency, intensity and sonication time (Wu et al., 2011). Ultrasonic irradiation may also cause undesirable effects such as the cell lysis and the release of intracellular material into the water. According to Zhang et al. (2006) ultrasounds at lower frequencies of 20, 80 or 150 kHz can destroy *M. aeruginosa*, but increase the extracellular MC-LR concentration from 0.87 to 3.1 μg L^{-1} due to the rupture of the cells.

Song et al. (2005) reported that high frequency ultrasounds, per example 640 kHz, destroy 85 % of MC-LR in 6 min. Although higher ultrasound power causes more violent cavitation and accelerates reactions, higher energy costs are associated and this is not always desirable (Zhang et al., 2006). Another option to cyanobacterial bloom removal is the rapid catalytic microwave method after $FeCl_3$/ Activated carbon (AC) addition. The addition of $FeCl_3$/AC firstly makes the cells gradually aggregate, and after the microwave irradiation was turned on, only 2 min was enough to cause the cells damage. The authors suggest that $FeCl_3$ could induce flocculation of *M. aeruginosa*, while activated carbon could enhance this flocculation under microwave irradiation in such a way that only $FeCl_3$/AC could effectively induce the *M. aeruginosa* damage under microwave MW irradiation (Li et al., 2011).

Ultrasonic irradiation at 640 kHz also promotes a rapid degradation of MIB and GSM. Radical-generating processes generally dominate during the ultrasonic-induced degradation. However pyrolysis also appears to be responsible for a significant fraction of the degradation (Song and O'Shea, 2007). Song et al. (2006) found a rapid degradation (80-90 % destruction after 105 min) of MC-LR and MC-RR by ultrasonic irradiation at 640 kHz.

2.2.4.3 Fenton oxidation

For more than a century the catalytic oxidation of tartaric acid in the presence of ferrous salts and hydrogen peroxide was reported by Fenton. Forty years after the first observation of what is called "Fenton reaction", it was proposed that the hydroxyl radical is the oxidant species in this system, capable of oxidizing various classes of organic or inorganic compounds by an spontaneous reaction that occurs in the dark (Nogueira et al., 2007; Pignatello et al., 2006), according to the following reactions (Gajdek et al., 2001):

$$Fe^{2+} + H_2O_2 \rightarrow Fe^{3+} + HO^{\bullet} + HO^{-} \quad \text{(Eq. 2.01)}$$

$$Fe^{3+} + H_2O_2 \rightarrow Fe^{2+} + HO_2^{\bullet} + H^{+} \quad \text{(Eq. 2.02)}$$

$$Fe^{2+} + HO^{\bullet} \rightarrow Fe^{3+} + HO^{-} \quad \text{(Eq. 2.03)}$$

$$Fe^{3+} + HO_2^{\bullet} \rightarrow Fe^{2+} + O_2 + H^{+} \quad \text{(Eq. 2.04)}$$

$$H_2O_2 + HO^{\bullet} \rightarrow H_2O + HO_2^{\bullet} \quad \text{(Eq. 2.05)}$$

The hydroxyl radical $HO^{\bullet}$ and the superoxide radical $HO_2^{\bullet}$ convert the substrate into the form of radical which subsequently undergoes oxidation, dimerizes, or is reduced (Gajdek et al., 2001).

The radical $HO^{\bullet}$ is produced according to equation (2.01) leading to a stoichiometric production of Fe^{3+}, forming precipitates that increase as the pH approaches neutrality. This phenomenon is technologically undesirable and can be minimized by reducing the pH of the water to be treated to a value between 2.5 and 3.0 (Pignatello et al., 2006).

The Fenton reactions are viewed as potentially convenient and economical ways to generate oxidizing species for treating chemical wastes. Compared to other bulk oxidants, hydrogen peroxide is inexpensive, safe, and easy to handle, and poses no lasting environmental threat since it readily decomposes to water and oxygen (Pignatello et al., 2006).

Fenton reagent (Fe^{2+} + H_2O_2) has been tested and demonstrated to be a promising alternative for the degradation of MC-LR (Gajdek et al., 2001).

2.2.4.4 Photo-Fenton oxidation

The presence of irradiation source is responsible for an increase in the degradation rate of the pollutants by the Fenton process. It occurs due to the photoreduction of Fe^{3+} to Fe^{2+} ions, where new $HO^{\bullet}$ radicals are formed, and regenerate Fe^{2+} ions that can further react with more H_2O_2 molecules. The photoreduction of Fe^{3+} follows the Eq. 2.07 (Torrades et al., 2003):

$$Fe^{2+} + H_2O_2 \rightarrow Fe^{3+} + HO^{\bullet} + HO^{-} \quad \text{(Eq. 2.06)}$$

$$Fe(OH)^{2+} + h\upsilon \rightarrow Fe^{2+} + HO^{\bullet} \quad \text{(Eq. 2.07)}$$

$Fe(OH)^{2+}$ is the dominant Fe^{3+} species in solution at pH 2–3, which requires an initial acidification. The irradiation of Fe^{3+} and H_2O_2, enhances the rate of oxidant production, through the involvement of high valence Fe intermediates responsible for the direct attack to organic matter (Bossmann et al., 1998; Pignatello et al., 2006).

The photoexcitation of the complexes formed between Fe^{3+} and organic matter, mainly carboxylic acids, is another way for the regeneration of Fe^{2+} from Fe^{3+}. The molar absorption coefficients of such complexes and the quantum yields of their reaction of photolysis are even

larger (Bossmann et al., 1998; Torrades et al., 2003). They also make it possible to work in the near neutral pH range (Pignatello et al., 2006).

One of the major difficulties in using Fenton and photo-Fenton processes is the need to remove the iron at the end of the reaction. The method commonly used for this purpose is alkaline precipitation. However if the effluent to be treated has a high organic load, a high amount of catalyst may be required, leading to increased generation of ferric hydroxide sludge, which would hinder the removal process (Navarro et al., 2010).

The photo-Fenton process (Fenton oxidation complemented with UV-visible radiation) exhibits enhanced reaction rates for the degradation of organic pollutants. Photo-Fenton is also effective for the degradation of MC (Bandala et al., 2004b). The source of UV radiation used in photo-Fenton reaction can be natural or artificial, but the use of sunlight would lower the cost of the process and facilitates the industrial application (Malato et al., 2002).

According to (Bandala et al., 2004b), photo-Fenton and Fenton processes may effectively degrade MC-LR, especially photo-Fenton. The authors tested both technologies and observed that 100 % of toxin was removed by the photo-Fenton process in around 35-40 min of irradiation, while in the Fenton experiment the amount of MC-LR only decreased by about 60 % in approximately 180 min. In general, results from this work agree with those of several previous reports dealing with the degradation of this toxin by other advanced oxidation technologies. In particular, photo-Fenton oxidation can be an attractive technology since it can be easily scaled-up and has 'green features'. For example, it includes UV-visible radiation and environmentally friendly chemicals such as iron and hydrogen peroxide. Photo-Fenton reaction could be comparable (i.e. at least from a feasibility prospective) to other hydroxyl-radical based technologies, such TiO_2 photocatalysis, which is the most widely AOP that has been investigated for the destruction of cyanobacterial toxins.

According to Zhong et al. (2009) not only the pH but also the initial concentration of H_2O_2 plays an important role. The same authors promoted the destruction of MC-RR by photo-Fenton reaction using different concentrations of H_2O_2 and noted that the optimum concentration of peroxide was 1.5 mmol L^{-1} and at low H_2O_2 doses (0.5-1.5 mM) the destruction of MC-RR increased with increasing H_2O_2. The authors explain that H_2O_2 acts as a promoter and a scavenger of $HO^{\bullet}$ and H_2O_2 also reacts with $HO^{\bullet}$ to produce $HO_2^{\bullet}$ which is also an oxidizing agent, however with less oxidation capacity than the $HO^{\bullet}$. Moreover, high

H_2O_2 concentrations exhibited a cleansing effect that inhibits the spread of $HO^{\bullet}$, to some extent, so the oxidation capacity is also reduced. For this experiment the optimal conditions were 1.5 mmol L^{-1} H_2O_2, 0.10 mmol L^{-1} Fe^{2+}, T ± 25 ºC, pH 3-4 and 30 min reaction time to destroy 96 % of MC-RR.

2.2.4.5 Heterogeneous photocatalysis

Photocatalysis consists in the combination of photochemistry with catalysis, requiring the presence of light and an active photocatalyst to produce a photochemical change of some chemical species as the result of radiation absorption by the photosensitive catalyst, as for example, TiO_2, ZnO, CeO_2, CdS, ZnS, and others (Mills and Hunte, 1997). In a simple way, photocatalysis is a redox process that uses a catalyst activated by photonic energy (Águia et al., 2010).

For a heterogeneous solar photocatalytic detoxification process the near-ultraviolet (UV) band of the solar spectrum (wavelength shorter than 400 nm), can be used to photo-excite a semiconductor catalyst in contact with water and in the presence of oxygen. The most important features of this process, making it applicable to the treatment of contaminated aqueous solutions, are (Malato et al., 2009):

i. It takes place at ambient temperature and without overpressure.
ii. Oxidation of organics into CO_2 and other inorganic species is complete.
iii. The oxygen necessary for the reaction can be directly obtained from atmosphere.
iv. The catalyst is cheap, innocuous and can be reused.
v. The catalyst can be attached to different types of inert matrices.
vi. The energy for photo-exciting the catalyst can be obtained from the sun.

The photocatalysis for water treatment can be accomplished by using solar or artificial UV-light, both processes can be operated at ambient temperature and destroy a large variety of chemicals and microbiological pollutants. The equipment required for the process is of easy access and simple and may be used in regions without electricity.

- ✓ ***Titanium dioxide (TiO_2)***

In recent years the use of TiO_2 as photocatalyst for water treatment has been widely reported (Chong et al., 2010). Irradiating the semi-conductor TiO_2 in suspension or fixed to various

supports in aqueous solutions containing organic pollutants, creates a redox environment able to destroy these pollutants (Robert and Malato, 2002). When TiO_2 is exposed to radiation of wavelength below 380 nm, highly reactive species, such as $HO^{\bullet}$ are generated. It has been demonstrated that these species have the ability to mineralize a variety of aromatic and aliphatic organic compounds, including dyes, pesticides and herbicides (Robertson et al., 2005).

Titanium dioxide is particularly appropriate as a photocatalyst for water treatment in comparison with other semiconductors (Robertson et al., 2005), because it is relatively inexpensive, highly chemically stable, the photo-generated holes are highly oxidizing, and the photo-generated electrons are reducing enough to produce superoxide from dioxygen (Fujishima et al., 2000). When compared with some substances that are usually used to promote water treatment, the hydroxyl radical produced by TiO_2 is more oxidizing, with oxidation potential of 2.8 V, compared to 2.07 V for ozone, 1.78 V for H_2O_2, 1.49 V for hypochlorous acid and 1.36 V for chlorine (Robertson, 1996).

Monteiro et al. (2014) described the mechanism of TiO_2 photocatalysis, as follows (adapted Augugliaro et al. (1999) and Peral and Ollis (1992)):

$$TiO_2 + h\upsilon \longrightarrow e^-_{cb}(TiO_2) + h^+_{vb}(TiO_2) \quad \text{(Eq. 2.08)}$$

$$h^+_{vb}(TiO_2) + H_2O \longrightarrow HO^{\bullet} + H^+ \quad \text{(Eq. 2.09)}$$

$$h^+_{vb}(TiO_2) + HO^- \longrightarrow HO^{\bullet} \quad \text{(Eq. 2.10)}$$

$$e^-_{cb}(TiO_2) + O_2 \longrightarrow O_2^{\bullet -} \quad \text{(Eq. 2.11)}$$

$$HO^{\bullet} + RH \longrightarrow RH^{\bullet +} \longrightarrow R^{\bullet} + H^+ \quad \text{(Eq. 2.12)}$$

$$h^+_{vb}(TiO_2) + RH \longrightarrow RH^{\bullet +} \longrightarrow R^{\bullet} + H^+ \quad \text{(Eq. 2.13)}$$

$$O_2^{\bullet -} + H^+ \longrightarrow HOO^{\bullet} \quad \text{(Eq. 2.14)}$$

$$O_2^{\bullet -} + HOO^{\bullet} + H^+ \longrightarrow H_2O_2 + O_2 \quad \text{(Eq. 2.15)}$$

Conduction-band electrons $e^-_{cb}(TiO_2)$ and valence-band holes $h^+_{vb}(TiO_2)$, i.e. electron-hole pairs, are generated when photons of energy $h\upsilon$ matching or exceeding the semiconductor band-gap energy are absorbed (Eq. 2.08). Once at the surface of the semiconductor, and on

the absence of any suitable acceptor (for e_{cb}^{-}) and donor (for h_{vb}^{+}) recombination will occur in a matter of nanoseconds; therefore no reaction occurs (Furube et al., 2001; Linsebigler et al., 1995). Hydroxyl anions and water molecules adsorbed on TiO_2 surface, act as electron donors, while molecular oxygen acts as electron acceptor, leading to the formation of hydroxyl ($HO^{\bullet}$) and superoxide ($O_2^{\bullet -}$) radicals (Augugliaro et al., 1999; Pelizzetti and Minero, 1993; Peral and Ollis, 1992) (see Eq. 2.09-11). When an organic molecule (RH) is adsorbed onto the semiconductor surface, the reaction with hydroxyl radical occurs, followed by structural breakdown into several intermediates until, eventually, total mineralization (Hoffmann et al., 1995; Kolen'ko et al., 2005) (see Eq. 2.12). The photogenerated holes due to the high oxidation potential can also participate in the direct oxidation of the organic pollutants (Eq. 2.13) (Benoit-Marquié et al., 2000; Cermenati et al., 1997). Peroxide radical ($HOO^{\bullet}$) can also be generated from the protonation of $O_2^{\bullet -}$ radical and subsequently forms hydrogen peroxide (see Eq. 2.14 and 15).

According to Davor (2005) TiO_2 could be separated and reused after treatment with an average loss of 2 % after filtration by 0.45 mm cellulose nitrate membranes.

Gogate and Pandit (2004a) and Gogate and Pandit (2004b) listed some others advantages of the use of TiO_2 photocatalytic oxidation:

- Can work at conditions of room temperature and pressure;
- Uses natural resources, i.e. sunlight;
- Chemical stability of TiO_2 in aqueous media and in larger range of pH ($0 \leq pH \leq 14$);
- Low cost of TiO_2;
- System applicable at low concentrations and no additives are required;
- Great deposition capacity for noble metal recovery;
- Total mineralization achieved for many organic pollutants;
- Efficiency of photocatalysis as regards halogenated compounds, sometimes very toxic for bacteria in biological water treatment.

Photocatalysis using TiO_2 is considered an emerging technology for the destruction of cyanotoxins, and has been previously shown to effectively destroy MC-LR and related toxins in aqueous solutions even at extremely high concentrations (Antoniou et al., 2005; Liu et al., 2009). Despite Microcystins are very stable compounds under natural sunlight (Hitzfeld et al., 2000a), they can be rapidly decomposed in a photocatalytic reactor and the use of the

semiconductor catalyst leads to faster reaction rates than UV radiation alone (photolysis) (Shephard et al., 1998). Not only does the process rapidly remove the toxin but also the by-products appear to be non-toxic (Liu et al., 2002). Figure 2.3 shows an increase of the scientific publications concerning the destruction of cyanobacteria in water treatment and the removal of cyanotoxins by TiO_2 photocatalysis, in the last 18 years.

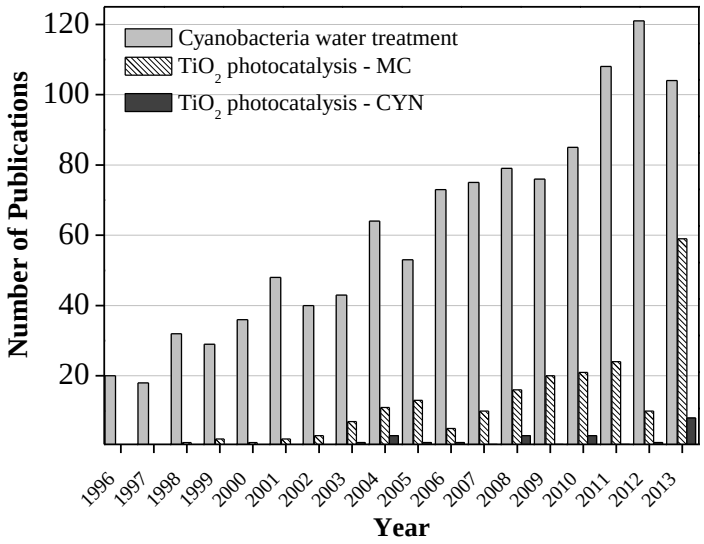

Figure 2.3 Publications about water treatment to destroy cyanobacteria, and TiO_2 photocatalysis to remove MC and CYN (source: http://www.scopus.com, 2014, search terms "Cyanobacteria water treatment", "TiO_2 photocatalysis microcystin" and "TiO_2 photocatalysis cylindrospermopsin").

In recent years, the use of titanium dioxide (TiO_2) as photocatalyst for water treatment has been widely reported, either as a powder in suspension or fixed to various supports (Robert and Malato, 2002). The photocatalytic reaction involving the irradiation of TiO_2 can only occur by using UV light, which corresponds to 4 - 5 % of solar light spectrum, because of the wide band gap of approximately 3.2 eV for anatase and 3.0 eV for rutile (Han et al., 2011; Pelaez et al., 2009; Yang et al., 2009). This method is mainly based on the generation of electron/hole pairs and highly oxidizing hydroxyl radicals, leading to mineralization of different organic pollutants (Robert and Malato, 2002; Robertson et al., 2005; Triantis et al., 2012), including cyanotoxins (Pinho et al., 2012).

Most water treatment studies concerning TiO_2 photocatalytic processes uses slurry suspensions of the semiconductor, showing a high efficiency in the pollutants degradation and mineralization, since the contact of the photocatalyst with the pollutants is promoted and the mass transfer limitations are avoided. However, heterogeneous photocatalytic processes are an interesting approach for water decontamination since a post-filtration step to retain the

photocatalyst is unnecessary, contrarily to what happens when slurry suspensions are used. Since mass transfer is usually the rate-limiting step in these processes applied to liquid or gas phases, the photocatalytic reaction rate can be enhanced by incrementing the catalyst surface (Águia et al., 2011b; Gumy et al., 2006; Robert et al., 1999; van Grieken et al., 2009b).

Chemical vapor deposition, physical vapor deposition, sputtering and dip-coating are some examples of methods employed to obtain TiO_2 films supported in inert surfaces (Cardona et al., 2004). Dip coating is a good option because it is simple and the equipment required is not expensive. TiO_2 concentration in the film must be taken into account and adjusted to avoid loss of the catalyst by erosion (Ávila et al., 2002). Another advantage of the application of immobilized catalyst is the fact that it can be re-used for several treatment cycles while maintaining its stability (Garcia et al., 2010; van Grieken et al., 2009b).

Mendes and co-workers (Águia et al., 2010, 2011a, b) developed a coating for immobilizing photocatalysts based on a commercial paint, which is porous (pigment volume concentration slightly above the critical value) and very resistant to photodegradation induced by the presence of the photocatalyst. The photocatalyst is incorporated in the paint by substituting the pigmentary TiO_2, allowing a large illuminated contact area, more than 100 μm optical thickness (3D structure). The main results reported by the same authors showed that the highest yields towards NO_x photocatalytic oxidation were obtained when incorporating in paint formulations the photocatalysts PC500 (Millennium), PC105 (Millennium), and UV100 (Sachtleben).

The type of material to be used as support is an important factor to be considered, because it directly affects activity, homogeneity, and adhesion of TiO_2 to the surface. Materials like ceramics tiles, paper, glass, fiberglass, and stainless steel have been employed (Cardona et al., 2004; Shephard et al., 2002). Borosilicate glass or quartz (Choi et al., 2006), quartz wool (Vella et al., 2010), glass reactor walls or glass flat plates, Raschig rings, glass tubes, glass cylinders (Hernández-Alonso et al., 2006; Pablos et al., 2012; Sordo et al., 2010; van Grieken et al., 2009a; van Grieken et al., 2009b), pumice stone (Subrahmanyam et al., 2008), monolithic structures (honeycomb) of ceramic (Avila et al., 1998) or metallic materials (Choi et al., 2006) have been studied as support. The thin-walled monoliths structures of polyethylene terephthalate (PET) and cellulose acetate (CA) are promising alternatives because these are inexpensive, lightweight, easily shaped polymeric materials and UV-transparent (Portela et al., 2007).

Several commercial TiO_2 semiconductors are available in the market, showing different photocatalytic activity depending on the particle size, crystalline form and surface area, as also according to the structure of pollutants to be degraded (Gumy et al., 2006). The advances on this type of nanomaterial, which has been regarded as innovative and very efficient, can contribute to the development of insightful and proper design of nanotechnology-based photo-reactors using sunlight as a source of energy for the treatment of water contaminated with cyanobacteria toxins and other emerging contaminants (Pelaez et al., 2012).

The addition of H_2O_2 to titanium dioxide have a positive effect in the prevention of the electron-hole recombination by accepting photogenerated electron from the conduction band (Eq. 10) and production of additional $OH^{\bullet}$ radicals through reactions (2.16) and (2.17) (Rodríguez et al., 1996).

$$H_2O_2 + e_{CB}^{-} \longrightarrow OH^{\bullet} + OH^{-} \qquad \text{(Eq. 2.16)}$$

$$H_2O_2 + O_2^{\bullet -} \longrightarrow OH^{\bullet} + OH^{-} + O_2 \qquad \text{(Eq. 2.17)}$$

Cornish et al. (2000) proved that another way to potentiate the reaction is the addition of H_2O_2 to the photocatalytic system, not only to remove cyanotoxin from water more quickly, but also many of the observable by-products appear to be destroyed.

Based on the analysis of the existing literature on the photocatalytic oxidation of the MC-LR some of the illustrative works are depicted in Table 2.8, with TiO_2 immobilized and sometimes doped with other material, at different pH values, and using different kinds of light source.

Table 2.8 Degradation of MC-LR using supported TiO_2 materials.

Catalyst	Degradation method	Reaction time	Initial MC-LR concentration	Efficiency	Reference
- Reference TiO_2-Sol-gel - Sulfur doped TiO_2 film Thickness: 1.02µm Total mass: 4.51 mg In borosilicate glass (10 cm^2)	pH 5.8 Two 15 W fluorescent lamp-UV-vis 9.05×10^{-5} W cm^{-2} > 420 nm	300 min	500 µg L^{-1}	- Reference: No significant degradation - Sulfur doped TiO_2 film: Until 60 %	Han et al. (2011)
- Reference.: TiO_2 film - C-N-codoped TiO_2 film. In borosilicate glass (10 cm^2)	pH 3.0 Two 15 W fluorescent lamp-UV-vis 9.05×10^{-5} W cm^{-2}	300 min	500 µg L^{-1}	- Reference: ~ 30 % - C-N-codop ed Until ~70-80%	Liu et al. (2013)
TiO_2 nanotubes anodized at: - 5 V - 10 V - 20 V - 30 V	pH no adjusted 100 W high-pressure mercury lamp 17.20 mW cm^{-2}	120 min	5000 µg L^{-1}	Increased with nanotubes anodized from 5 to 20 V, reaching 84.6 % at 20 V	Su et al. (2013)
P25 falling film in a sheet of fiberglass: 40 cm wide × 110 cm high TiO_2 mass:7.5g	pH 3, 8 and 11; 15 W low pressure Mercury germicidal UV lamp 253.7 nm 204.5 W m^{-2}	20 min	55 ng mL^{-1}	k_{obs} (min^{-1}) - pH: 80.12 ± 0.01 - pH 3 (HCl) 0.13 ± 0.01 - pH 11 0.095 ± 0.008 - pH 3(H_2SO_4) 0.093 ± 0.011	Shephard et al. (2002)
- NF-TiO_2 only - NF-TiO_2 + 5 g L^{-1} P25 - NF-TiO_2 + 15 g L^{-1} P25 Borosilicate glass (10 cm^2)	pH 3 Two 15 W fluorescent lamp-UV-vis 9.52×10^{-5} W cm^{-2}	180 min	0.5 µM	Almost similar r_0 ~ 2.5×10^{-3} µM min^{-1}	Pelaez et al. (2012)

- ***Photoreactors***

Gogate and Pandit (2004b) listed a number of important operating parameters that affect the overall pollutants destruction efficiency of the photocatalytic oxidation process such as: amount and type of the catalyst, reactor design, radiation wavelength, initial concentration of the pollutant, temperature, radiation flux, pH, aeration and presence of ionic species.

The reactor design should ensure that uniform irradiation of the entire catalyst surface is achieved. Near complete elimination of mass transfer resistances is another important point. In case of the use of immobilized catalyst, to obtain an efficient degradation, the reactor must be packed with a great amount of the activated catalyst close to the illuminated surface and must have a high density of active catalyst in contact with the liquid (Gogate and Pandit, 2004a).

The catalyst used in the photoreactor can be employed in different ways, i.e. immobilized on an inert support or as slurry (Robert and Malato, 2002). Different types of photocatalytic reactors operating with TiO_2 in these conditions have been used: annular reactor (Doll and Frimmel, 2005); annular hexagonal (Gogate et al., 2002); tubular (Esplugas et al., 2002); tubular spiral (Chen et al., 2001); tubular loop (Melo et al., 2001); multi tubular (Ray and Beenackers, 1998a); corrugated board (Zhang et al., 2004); falling film (Shephard et al., 2002); channel and lamp in U (Ray and Beenackers, 1998b); collectors (Bandala et al., 2004a); double-cylindrical-shell photoreactor (Li et al., 2014); maze (Mozia et al., 2005); rotating disc (Dionysiou et al., 2000); step reactor (Guillard et al., 2003) and many others.

During the last years some solar photocatalytic treatment plants have been constructed, mainly based in non-concentrating collectors (Blanco-Galvez et al., 2007). Table 2.9 shows some solar reactor designs based on concentrated and non-concentrated light: Parabolic trough reactor (PT); thin film fixed bed reactor (TFFB); double skin sheet reactor (DSS) and compound parabolic collecting reactor (CPC).

Table 2.9 Examples of solar reactor designs

Reactor design	Considerations
Parabolic trough reactor (PTR)  (Nogueira et al., 2007)	PTR are light-concentrating systems. The structure supports a reflective parabolic surface. They make efficient use of direct solar radiation, and have as main disadvantage the use direct radiation only, are expensive and have low optical and quantum efficiencies (Malato et al., 2009).
Thin film fixed bed reactor (TFFBR) 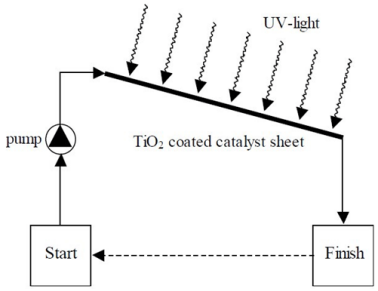 http://www.thenbs.com/topics/constructionproducts/articles/photocatalystsInConstruction.asp	Thin-film-fixed-bed reactor (TFFBR) is one of the first solar reactors not applying a light-concentrating system and thus being able to utilize the diffuse as well as the direct portion of the solar UV-A radiation for the photocatalytic process. (Bahnemann, 2004).
Double skin sheet reactor (DSSR) 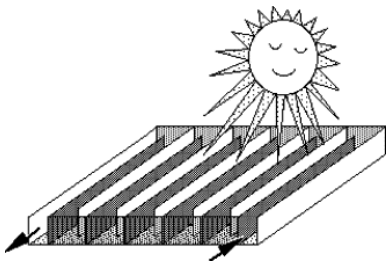 (van Well et al., 1997)	DSSR consists of a flat and transparent structured box. The suspension containing the pollutant and the photocatalyst is pumped through these channels. This type of reactor can utilize both the direct and the diffuse portion of the solar radiation in analogy to the CPC. After the degradation process, the photocatalyst has to be removed from the suspension either by filtering or by sedimentation (Bahnemann, 2004).
Compound parabolic collecting reactor (CPC) 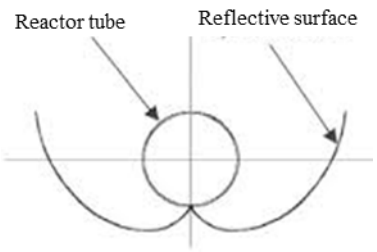 (Nogueira et al., 2007)	CPC is more efficient than the concentrator-based system due to the use of both direct and diffuse UV and its simplicity (Robert and Malato, 2002).

Compound parabolic collectors (CPCs) are the best option for solar photochemical applications. The use of CPCs has some advantages as turbulent flow conditions, no evaporation of volatile components, no search system for direct and diffuse solar radiation, resistance to adverse weather, high optical efficiency and high quantum yield (Blanco-Galvez et al., 2007).

The light reflected by the CPC is distributed around the back of the tubular photo reactor illuminating the entire reactor tube circumference. Due to the ratio of CPC aperture to tube diameter, the incident light on the reactor is very similar to that of non-concentrating or "one-sun" photo reactor. As in a parabolic trough reactor, the water is more easily piped and distributed than in many non-concentrating designs (Robert and Malato, 2002).

Bandala et al. (2004a) compared the photocatalytic degradation of oxalic acid in water (solar energy, TiO_2 catalyst and heterogeneous phase), using four different solar photoreactors (Figure 2.4: (i) a parabolic trough concentrator (PC) consisting of a single glass tube of 2.54 cm diameter, mounted on the focal axis of a parabolic trough for a concentration ratio of 13 suns, and an aluminium sheet curved to a parabolic shape over a rigid steel structure as reflector; (ii) a tubular collector (TC) consisting of a row of 14 parallel glass tubes without any kind of reflectors; (iii) a compound parabolic collector (CPC), and (iv) a V-trough collector (VC). Both the CPC and the VC consisted of a parallel row of eight glass tubes of 3 cm diameter, each tube had a back reflector to enhance solar incidence, the reflectors were shaped from aluminium sheets as CPC and V troughs, respectively, with a concentration ratio of one sun. They are therefore, non-concentrating reflectors whose only function is to improve the distribution of solar irradiation around the tube walls. The authors found differences in the degradation rates depending on the collector geometry. The CPC showed the best overall performance in terms of accumulated energy, followed closely by the VC. However the incidence angle affects the total amount of energy collected, but does not reduce very much the efficiency of the reactors.

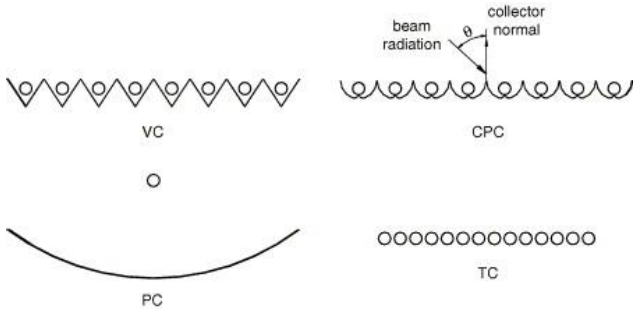

Figure 2.4 Four solar photoreactors configurations (VC, CPC, PC and TC) used by Bandala et al. (2004a) for oxalic acid photocatalytic degradation in water.

The lab-scale reactors can be engineered into flow-through reactors representing a feasible option for solar-driven water treatment technologies or for the remediation of contaminated water with cyanobacterial toxins or other emerging contaminants of concern, using visible light-activated TiO_2 photocatalyst under solar irradiation (Pelaez et al., 2009). Table 2.10 shows some examples of reactors used in experiments to destroy cyanotoxins in water.

Table 2.10 Example of photoreactors used by different authors to destroy cyanotoxins.

Photoreactor	Description
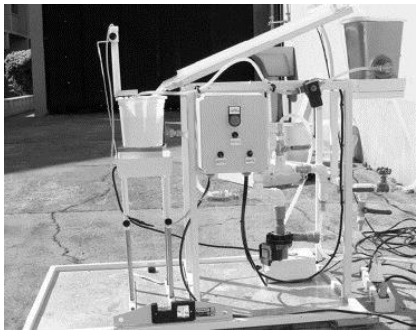	Solar photocatalytic reactor with an inclination angle of 22º, operated in bath mode with recycle, containing 1.6 L of solution under continuous agitation. The solution was pumped at a fixed flow rate, with the help of a peristaltic pump, to the top of the reactor and flowed to the bottom by gravity while illuminated. The irradiance and the solar spectrum during the experiments were measured with the aid of a spectroradiometer StellarNet. It was used TiO_2 immobilized in a sandblasted (Vilela et al., 2012).
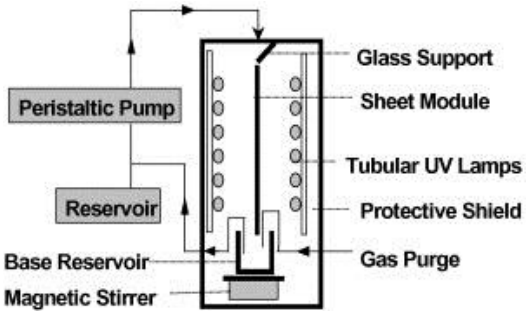	Diagram of experimental 'falling film' lab-scale reactor containing fiberglass sheet with immobilized TiO_2 catalyst, surrounded on each side by a set of six 15 W low pressure mercury germicidal UV lamps and UV radiance within the reactor of 204.5 W m^{-2} (Shephard et al., 2002).
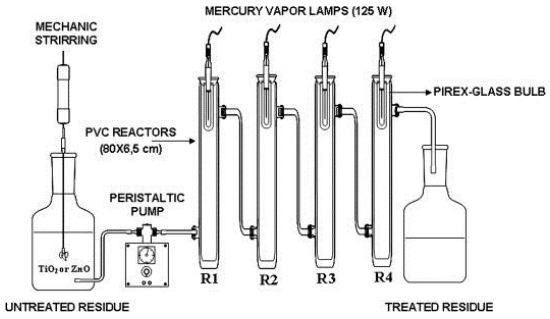	Continuous photochemical reactor, irradiated by a 125 W mercury vapour lamp inserted in the solution through a quartz (UV-C) or Pyrex (UV-A) bulb. TiO_2 in suspension was used as catalyst (Jacobs et al., 2013).
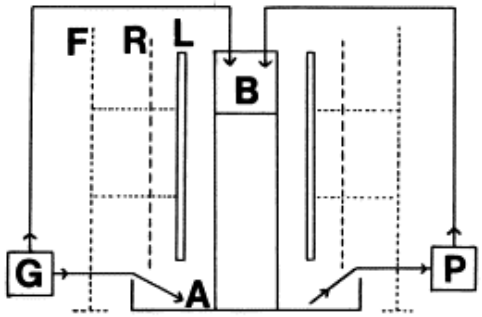	Falling film lab-scale reactor, consisting of a glass tube equipped at the top with a cup, surrounded by a set of eight 30 W low pressure mercury germicidal UV lamps (90 cm long; emitting wavelength 254 nm). Operated in a circular "closed-loop" mode. The polluted water contains TiO_2 in suspension (Shephard et al., 1998).

(A) Reservoir; (B) Glass tube with cup; (F) External frame;
(G) Gas supply; (L) UV lamps; (P) Pump; (R) Reflector.

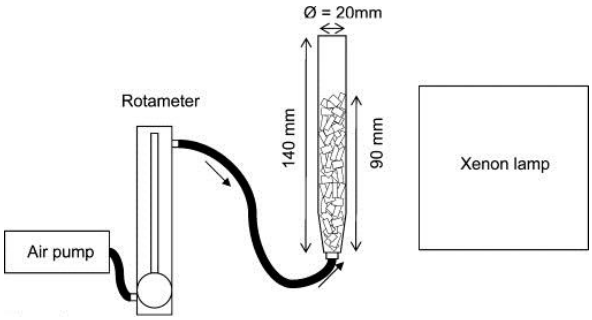

The main body of the reactor was constructed from glass and all tubing was Teflon. Illuminated in the presence of air with a xenon UV lamp (400 W; spectral output 330–500 nm). Reactions were carried out in a glass batch reactor with a constant air flow (30 mL min^{-1} ± 5 %) via the bottom of the reactor (Robertson et al., 2011).

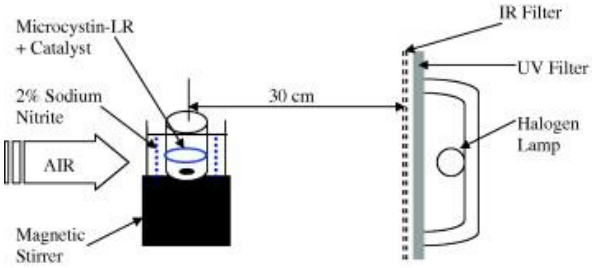

Slurry TiO_2 driven photocatalysis experiments were performed in 20 mL glass vials under constant stirring at a distance of 30 cm from the front of the light source (500 W Halogen, irradiation 393 μM^{-1}, T = 33–36 °C) (Graham et al., 2010).

2.3 References

Águia, C., Ângelo, J., Madeira, L.M., Mendes, A., 2010. Influence of photocatalytic paint components on the photoactivity of P25 towards NO abatement. Catalysis Today 151, 77-83.

Águia, C., Ângelo, J., Madeira, L.M., Mendes, A., 2011a. Influence of paint components on photoactivity of P25 titania toward NO abatement. Polymer Degradation and Stability 96, 898-906.

Águia, C., Ângelo, J., Madeira, L.M., Mendes, A., 2011b. Photo-oxidation of NO using an exterior paint – Screening of various commercial titania in powder pressed and paint films. Journal of Environmental Management 92, 1724-1732.

Agujaro, L.F., Lima Isaac, R., 2003. Floraçôes de cianobacterias potencialmente tóxicas nas bacias dos rios Piracicaba, Capivari e Jundiai, estado do Sâo Paulo-Brasil e avaliaçâo dos manaciais em relaçâo a eutrofiçâo. ABES, pp. 1-20.

Albay, M., Akcaalan, R., Aykulu, G., Tufekci, H., Beattie, K.A., Codd, G.A., 2003. Occurrence of toxic cyanobacteria before and after copper sulphate treatment in a water reservoir, Istanbul, Turkey. Algological Studies 109, 67-78.

Andersen, R.A., 2005. *Algal culturing techniques*. Academic Press.

Andreozzi, R., Caprio, V., Insola, A., Marotta, R., 1999. Advanced oxidation processes (AOP) for water purification and recovery. Catalysis Today 53, 51-59.

Antoniou, M.G., Armah, A., Dionysiou, D.D., 2005. Cyanotoxins: New generation of water contaminants. Journal of Environmental Engineering 131, 1239.

Antoniou, M.G., Nicolaou, P.A., Shoemaker, J.A., de la Cruz, A.A., Dionysiou, D.D., 2009. Impact of the morphological properties of thin TiO_2 photocatalytic films on the detoxification of water contaminated with the cyanotoxin, microcystin-LR. Applied Catalysis B: Environmental 91, 165-173.

Augugliaro, V., Coluccia, S., Loddo, V., Marchese, L., Martra, G., Palmisano, L., Schiavello, M., 1999. Photocatalytic oxidation of gaseous toluene on anatase TiO_2 catalyst: Mechanistic aspects and FT-IR investigation. Applied Catalysis B: Environmental 20, 15-27.

Avila, P., Bahamonde, A., Blanco, J., Sánchez, B., Cardona, A.I., Romero, M., 1998. Gas-phase photo-assisted mineralization of volatile organic compounds by monolithic titania catalysts. Applied Catalysis B: Environmental 17, 75-88.

Ávila, P., Sánchez, B., Cardona, A.I., Rebollar, M., Candal, R., 2002. Influence of the methods of TiO_2 incorporation in monolithic catalysts for the photocatalytic destruction of chlorinated hydrocarbons in gas phase. Catalysis Today 76, 271-278.

Bahnemann, D., 2004. Photocatalytic water treatment: solar energy applications. Solar Energy 77, 445-459.

Baker, J.A., Neilan, B.A., Entsch, B., Mckay, D.B., 2001a. Identification of cyanobacteria and their toxigenicity in environmental samples by rapid molecular analysis. Environmental toxicology 16, 472-482.

Baker, P.D., Steffensen, D.A., Humpage, A.R., Nicholson, B.C., Falconer, I.R., Lanthois, B., Fergusson, K.M., Saint, C.P., 2001b. Preliminary evidence of toxicity associated with the benthic cyanobacterium Phormidium in South Australia. Environmental toxicology 16, 506-511.

Bandala, E.R., Arancibia-Bulnes, C.A., Orozco, S.L., Estrada, C.A., 2004a. Solar photoreactors comparison based on oxalic acid photocatalytic degradation. Solar Energy 77, 503-512.

Bandala, E.R., Martínez, D., Martínez, E., Dionysiou, D.D., 2004b. Degradation of microcystin-LR toxin by Fenton and Photo-Fenton processes. Toxicon 43, 829-832.

Banker, R., Carmeli, S., Hadas, O., Teltsch, B., Porat, R., Sukenik, A., 1997. Identification of cylindrospermopsin in Aphanizomenon ovalisporum (Cyanophyceae) isolated from Lake kinneret, Israel 1, Journal of Phycology. Wiley Online Library, pp. 613-616.

Benoit-Marquié, F., Wilkenhöner, U., Simon, V., Braun, A.M., Oliveros, E., Maurette, M.T., 2000. VOC photodegradation at the gas-solid interface of a TiO_2 photocatalyst: Part I: 1-butanol and 1-butylamine. Journal of Photochemistry and Photobiology A: Chemistry 132, 225-232.

Bernard, C., Harvey, M., Briand, J., Biré, R., Krys, S., Fontaine, J., 2003. Toxicological comparison of diverse Cylindrospermopsis raciborskii strains: Evidence of liver damage caused by a French C. raciborskii strain. Environmental toxicology 18, 176-186.

Blanco-Galvez, J., Fernández-Ibáñez, P., Malato-Rodríguez, S., 2007. Solar photocatalytic detoxification and disinfection of water: recent overview. Journal of solar energy engineering 129, 4.

Bossmann, S.H., Oliveros, E., Göb, S., Siegwart, S., Dahlen, E.P., Payawan, L., Straub, M., Wörner, M., Braun, A.M., 1998. New Evidence against Hydroxyl Radicals as Reactive Intermediates in the Thermal and Photochemically Enhanced Fenton Reactions. The Journal of Physical Chemistry A 102, 5542-5550.

Bourne, D.G., Blakeley, R.L., Riddles, P., Jones, G.J., 2006. Biodegradation of the cyanobacterial toxin microcystin LR in natural water and biologically active slow sand filters. Water Research 40, 1294-1302.

Bourne, D.G., Jones, G.J., Blakeley, R.L., Jones, A., Negri, A.P., Riddles, P., 1996. Enzymatic pathway for the bacterial degradation of the cyanobacterial cyclic peptide toxin microcystin LR. Applied and environmental microbiology 62, 4086-4094.

Bouvy, M., Falcão, D., Marinho, M., Pagano, M., Moura, A., 2000. Occurrence of Cylindrospermopsis (Cyanobacteria) in 39 Brazilian tropical reservoirs during the 1998 drought. Aquatic Microbial Ecology 23, 13-27.

Bouvy, M., Molica, R., De Oliveira, S., Marinho, M., Beker, B., 1999. Dynamics of a toxic cyanobacterial bloom (Cylindrospermopsis raciborskii) in a shallow reservoir in the semi-arid region of northeast Brazil. Aquatic Microbial Ecology 20, 285-297.

Brooke, S., Newcombe, G., Nicholson, B., Klass, G., 2006. Decrease in toxicity of microcystins LA and LR in drinking water by ozonation. Toxicon 48, 1054-1059.

Burnum, K.E., Frappier, S.L., Caprioli, R.M., 2008. Matrix-assisted laser desorption/ionization imaging mass spectrometry for the investigation of proteins and peptides. Annu. Rev. Anal. Chem. 1, 689-705.

Campinas, M., Rosa, M.J., 2010. Evaluation of cyanobacterial cells removal and lysis by ultrafiltration. Separation and Purification Technology 70, 345-353.

Cardona, A.I., Candal, R., Sánchez, B., Ávila, P., Rebollar, M., 2004. TiO_2 on magnesium silicate monolith: effects of different preparation techniques on the photocatalytic oxidation of chlorinated hydrocarbons. Energy 29, 845-852.

Carmichael, W., 2001. Health effects of toxin-producing cyanobacteria:"The cyanoHABs". Human and Ecological Risk Assessment: An International Journal 7, 1393-1407.

Castro, M.E.B., Scorpione, R.C., Sihler, W., Lima, V., 1990. Isolamento e cultivo de cianobacterias causadoras de floracao em lagos e identificacao de patogenos com agentes de controle na Regiao do Distrito Federal. In: Simposio de Controle Biológico, 2.

Cermenati, L., Pichat, P., Guillard, C., Albini, A., 1997. Probing the TiO_2 photocatalytic mechanisms in water purification by use of quinoline, photo-fenton generated OH. radicals and superoxide dismutase. Journal of Physical Chemistry B 101, 2650-2658.

Chen, A., Lu, G., Tao, Y., Dai, Z., Gu, H., 2001. Novel photocatalyst immobilized on springs and packed photoreactor. Materials Physics and Mechanics 4, 121-124.

Choi, H., Stathatos, E., Dionysiou, D.D., 2006. Sol–gel preparation of mesoporous photocatalytic TiO_2 films and $TiO_2/Al2O_3$ composite membranes for environmental applications. Applied Catalysis B: Environmental 63, 60-67.

Chong, M.N., Jin, B., Chow, C.W.K., Saint, C., 2010. Recent developments in photocatalytic water treatment technology: A review. Water Research 44, 2997-3027.

Chorus, I., Bartram, J., 1999. Toxic cyanobacteria in water: a guide to their public health consequences, monitoring, and management. Taylor & Francis.

Chow, C.W.K., Drikas, M., House, J., Burch, M.D., Velzeboer, R.M.A., 1999. The impact of conventional water treatment processes on cells of the cyanobacterium Microcystis aeruginosa. Water Research 33, 3253-3262.

Christoffersen, K., Lyck, S., Winding, A., 2002. Microbial activity and bacterial community structure during degradation of microcystins. Aquatic Microbial Ecology 27, 125-136.

Codd, G.A., 2000. Cyanobacterial toxins, the perception of water quality, and the prioritisation of eutrophication control. Ecological Engineering 16, 51-60.

Codd, G.A., Morrison, L.F., Metcalf, J.S., 2005. Cyanobacterial toxins: risk management for health protection. Toxicology and Applied Pharmacology 203, 264-272.

Cornish, B., Lawton, L., Robertson, P., 2000. Hydrogen peroxide enhanced photocatalytic oxidation of microcystin-LR using titanium dioxide. Applied Catalysis B, Environmental 25, 59-67.

Cuvin-Aralar, M.L., Fastner, J., Focken, U., Becker, K., Aralar, E.V., 2002. Microcystins in Natural Blooms and Laboratory Cultured Microcystis aeruginosa from Laguna de Bay, Philippines. Systematic and Applied Microbiology 25, 179-182.

da Silva, C.A., Oba, E.T., Ramsdorf, W.A., Magalhães, V.F., Cestari, M.M., Oliveira Ribeiro, C.A., Silva de Assis, H.C., 2011. First report about saxitoxins in freshwater fish Hoplias malabaricus through trophic exposure. Toxicon 57, 141-147.

da Silva Fernandes, S., 2008. Biodisponibilidade de Cianotoxinas em Bivalves, Faculdade de Ciência. Universidade do Porto, Porto.

Dahlmann, J., Rühl, A., Hummert, C., Liebezeit, G., Carlsson, P., Graneli, E., 2001. Different methods for toxin analysis in the cyanobacterium Nodularia spumigena (Cyanophyceae). Toxicon 39, 1183-1190.

Damazio, C.M., Silva, L.H.S.E., 2006. Cianobactérias em Esteiras Microbianas Coloformes da Lagoa Pitanguinha, Rio de Janeiro, Brasil. Revista Brasileira de Paleontologia 9, 165-170.

Davor, L., 2005. Solar photocatalysis—a possible step in drinking water treatment. Energy 30, 1699-1710.

Dell'Aversano, C., Eaglesham, G.K., Quilliam, M.A., 2004. Analysis of cyanobacterial toxins by hydrophilic interaction liquid chromatography-mass spectrometry. Journal of Chromatography A 1028, 155-164.

Dionysiou, D.D., Balasubramanian, G., Suidan, M.T., Khodadoust, A.P., Baudin, I., Laîné, J.-M., 2000. Rotating disk photocatalytic reactor: development, characterization, and evaluation for the destruction of organic pollutants in water. Water Research 34, 2927-2940.

Dixon, M.B., Richard, Y., Ho, L., Chow, C.W.K., O'Neill, B.K., Newcombe, G., 2011a. A coagulation-powdered activated carbon-ultrafiltration - Multiple barrier approach for removing toxins from two Australian cyanobacterial blooms. Journal of Hazardous Materials 186, 1553-1559.

Dixon, M.B., Richard, Y., Ho, L., Chow, C.W.K., O'Neill, B.K., Newcombe, G., 2011b. Integrated membrane systems incorporating coagulation, activated carbon and ultrafiltration for the removal of toxic cyanobacterial metabolites from Anabaena circinalis. Water Science and Technology 63, 1405-1411.

Doll, T.E., Frimmel, F.H., 2005. Cross-flow microfiltration with periodical back-washing for photocatalytic degradation of pharmaceutical and diagnostic residues–evaluation of the long-term stability of the photocatalytic activity of TiO_2. Water Research 39, 847-854.

Dörr, F.A., Pinto, E., Soares, R.M., Feliciano de Oliveira e Azevedo, S.M., 2010. Microcystins in South American aquatic ecosystems: Occurrence, toxicity and toxicological assays. Toxicon 56, 1247-1256.

El Herry, S., Fathalli, A., Rejeb, A.J.-B., Bouaïcha, N., 2008. Seasonal occurrence and toxicity of Microcystis spp. and Oscillatoria tenuis in the Lebna Dam, Tunisia. Water Research 42, 1263-1273.

El Semary, N., 2010. Modern Methods for Detection and Elimination of Microcystins Toxins Produced by Cyanobacteria: Mini-review. Journal of Applied Sciences 10, 1662-1666.

Esplugas, S., Giménez, J., Contreras, S., Pascual, E., Rodríguez, M., 2002. Comparison of different advanced oxidation processes for phenol degradation. Water Research 36, 1034-1042.

Falconer, I.R., Humpage, A.R., 2005. Health Risk Assessment of Cyanobacterial(Blue-green Algal) Toxins in Drinking Water. International Journal of Environmental Research and Public Health 2, 43-50.

Falconer, I.R., Humpage, A.R., 2001. Preliminary evidence for in vivo tumour initiation by oral administration of extracts of the blue-green alga cylindrospermopsis raciborskii containing the toxin cylindrospermopsin. Environmental Toxicology 16, 192-195.

Fathalli, A., Ben Rejeb Jenhani, A., Moreira, C., Welker, M., Romdhane, M., Antunes, A., Vasconcelos, V., 2011. Molecular and phylogenetic characterization of potentially toxic cyanobacteria in Tunisian freshwaters. Systematic and Applied Microbiology 34, 303-310.

Feitz, A., Waite, T., Jones, G., Boyden, B., Orr, P., 1999. Photocatalytic degradation of the blue green algal toxin microcystin-LR in a natural organic-aqueous matrix. Environ. Sci. Technol 33, 243-249.

Fonseca, I.A., Rodrigues, L., 2005. Cianobactérias perifíticas em dois ambientes lênticos da planície de inundação do alto Rio Paraná, PR, Brasil. Revista Brasil. Bot 28, 821-834.

Freitas, M.A.M., 2009. Monitorização de cianobactérias e cianotoxinas nas lagoas portuguesas de Mira e Vela comparando métodos moleculares, imunológicos e volumes de amostragem, Faculdade de Ciência. Universidade do Porto, Porto, p. 118.

Fujishima, A., Rao, T.N., Tryk, D.A., 2000. Titanium dioxide photocatalysis. Journal of Photochemistry and Photobiology C: Photochemistry Reviews 1, 1-21.

Furube, A., Asahi, T., Masuhara, H., Yamashita, H., Anpo, M., 2001. Direct observation of a picosecond charge separation process in photoexcited platinum-loaded TiO_2 particles by femtosecond diffuse reflectance spectroscopy. Chemical Physics Letters 336, 424-430.

Gajdek, P., Lechowski, Z., Bochnia, T., Kpczyski, M., 2001. Decomposition of microcystin-LR by Fenton oxidation. Toxicon 39, 1575-1578.

Garcia, A., Cayla, X., Guergnon, J., Dessauge, F., Hospital, V., Rebollo, M.P., Fleischer, A., Rebollo, A., 2003. Serine/threonine protein phosphatases PP1 and PP2A are key players in apoptosis. Biochimie 85, 721-726.

Garcia, A.C., Bargu, S., Dash, P., Rabalais, N.N., Sutor, M., Morrison, W., Walker, N.D., 2010. Evaluating the potential risk of microcystins to blue crab (Callinectes sapidus) fisheries and human health in a eutrophic estuary. Harmful Algae 9, 134-143.

Gérard, C., Poullain, V., Lance, E., Acou, A., Brient, L., Carpentier, A., 2009. Influence of toxic cyanobacteria on community structure and microcystin accumulation of freshwater molluscs. Environmental Pollution 157, 609-617.

Gogate, P.R., Mujumdar, S., Pandit, A.B., 2002. A Sonophotochemical Reactor for the Removal of Formic Acid from Wastewater. Industrial & Engineering Chemistry Research 41, 3370-3378.

Gogate, P.R., Pandit, A.B., 2004a. A review of imperative technologies for wastewater treatment I: oxidation technologies at ambient conditions. Advances in Environmental Research 8, 501-551.

Gogate, P.R., Pandit, A.B., 2004b. A review of imperative technologies for wastewater treatment II: hybrid methods. Advances in Environmental Research 8, 553-597.

Graham, D., Kisch, H., Lawton, L.A., Robertson, P.K.J., 2010. The degradation of microcystin-LR using doped visible light absorbing photocatalysts. Chemosphere 78, 1182-1185.

Guillard, C., Disdier, J., Monnet, C., Dussaud, J., Malato, S., Blanco, J., Maldonado, M.I., Herrmann, J.-M., 2003. Solar efficiency of a new deposited titania photocatalyst: chlorophenol, pesticide and dye removal applications. Applied Catalysis B: Environmental 46, 319-332.

Guillard, R.R.L., 1975. Culture of phytoplankton for feeding marine invertebrates, in: Smith, W.L., Chanley, M.H. (Ed.), Culture of Marine Invertebrate Animals. Plenum Press, New York, pp. 26-60.

Gumy, D., Rincon, A.G., Hajdu, R., Pulgarin, C., 2006. Solar photocatalysis for detoxification and disinfection of water: Different types of suspended and fixed TiO_2 catalysts study. Solar Energy 80, 1376-1381.

Hall, T., Hart, J., Croll, B., Gregory, R., 2000. Laboratory-Scale Investigations of Algal Toxin Removal by Water Treatment. Water and Environment Journal 14, 143-149.

Han, C., Pelaez, M., Likodimos, V., Kontos, A.G., Falaras, P., O'Shea, K., Dionysiou, D.D., 2011. Innovative visible light-activated sulfur doped TiO_2 films for water treatment. Applied Catalysis B: Environmental 107, 77-87.

Harada, K.-i., Nakano, T., Fujii, K., Shirai, M., 2004. Comprehensive analysis system using liquid chromatography-mass spectrometry for the biosynthetic study of peptides produced by cyanobacteria. Journal of Chromatography 1033, 107-113.

Harada, K., Oshikata, M., Shimada, T., Nagata, A., Ishikawa, N., Suzuki, M., Kondo, F., Shimizu, M., Yamada, S., 1997. High performance liquid chromatographic separation of microcystins derivatized with a highly fluorescent dienophile. Natural Toxins 5, 201-207.

Hernández-Alonso, M.D., Tejedor-Tejedor, I., Coronado, J.M., Soria, J., Anderson, M.A., 2006. Sol–gel preparation of TiO_2–ZrO_2 thin films supported on glass rings: Influence of phase composition on photocatalytic activity. Thin Solid Films 502, 125-131.

Herrero, A., Flores, E., Flores, F.G., 2008. The cyanobacteria: molecular biology, genomics, and evolution. Caister Academic Pr.

Hitzfeld, B., Höger, S., Dietrich, D., 2000a. Cyanobacterial toxins: removal during drinking water treatment, and human risk assessment. Environmental health perspectives 108, 113.

Hitzfeld, B.C., Lampert, C.S., Spaeth, N., Mountfort, D., Kaspar, H., Dietrich, D.R., 2000b. Toxin production in cyanobacterial mats from ponds on the McMurdo Ice Shelf, Antarctica. Toxicon 38, 1731-1748.

Ho, L., Dreyfus, J., Boyer, J., Lowe, T., Bustamante, H., Duker, P., Meli, T., Newcombe, G., 2012a. Fate of cyanobacteria and their metabolites during water treatment sludge management processes. Science of The Total Environment 424, 232-238.

Ho, L., Lambling, P., Bustamante, H., Duker, P., Newcombe, G., 2011. Application of powdered activated carbon for the adsorption of cylindrospermopsin and microcystin toxins from drinking water supplies. Water Research 45, 2954-2964.

Ho, L., Tang, T., Monis, P.T., Hoefel, D., 2012b. Biodegradation of multiple cyanobacterial metabolites in drinking water supplies. Chemosphere 87, 1149-1154.

Hoeger, S.J., Dietrich, D.R., Hitzfeld, B.C., 2002. Effect of ozonation on the removal of cyanobacterial toxins during drinking water treatment. Environmental health perspectives 110, 1127.

Hoeger, S.J., Hitzfeld, B.C., Dietrich, D.R., 2005. Occurrence and elimination of cyanobacterial toxins in drinking water treatment plants. Toxicology and Applied Pharmacology 203, 231-242.

Hoffmann, M.R., Martin, S.T., Choi, W., Bahnemann, D.W., 1995. Environmental applications of semiconductor photocatalysis. Chemical Reviews 95, 69-96.

Howard, K.L., Boyer, G.L., 2007. Quantitative analysis of cyanobacterial toxins by matrix-assisted laser desorption ionization mass spectrometry. Analytical chemistry 79, 5980-5986.

Hu, Y., Li, D., Zheng, Y., Chen, W., He, Y., Shao, Y., Fu, X., Xiao, G., 2011. $BiVO4/TiO_2$ nanocrystalline heterostructure: A wide spectrum responsive photocatalyst towards the highly efficient decomposition of gaseous benzene. Applied Catalysis B: Environmental 104, 30-36.

Hummert, C., Dahlmann, J., Reinhardt, K., Dang, H., Dang, D., Luckas, B., 2001. Liquid chromatography-mass spectrometry identification of microcystins inMicrocystis aeruginosa strain from lake Thanh Cong, Hanoi, Vietnam. Chromatographia 54, 569-575.

Humpage, A., Falconer, I., 2003. Oral toxicity of the cyanobacterial toxin cylindrospermopsin in male Swiss albino mice: Determination of no observed adverse effect level for deriving a drinking water guideline value. Environmental toxicology 18, 94-103.

Humpage, A., Fenech, M., Thomas, P., Falconer, I., 2000. Micronucleus induction and chromosome loss in transformed human white cells indicate clastogenic and aneugenic action of the cyanobacterial toxin, cylindrospermopsin. Mutation Research/Genetic Toxicology and Environmental Mutagenesis 472, 155-161.

Hyenstrand, P., Rohrlack, T., Beattie, K.A., Metcalf, J.S., Codd, G.A., Christoffersen, K., 2003. Laboratory studies of dissolved radiolabelled microcystin-LR in lake water. Water Research 37, 3299-3306.

Ibelings, B.W., Chorus, I., 2007. Accumulation of cyanobacterial toxins in freshwater "seafood" and its consequences for public health: A review. Environmental Pollution 150, 177-192.

Jacobs, L.C.V., Peralta-Zamora, P., Campos, F.R., Pontarolo, R., 2013. Photocatalytic degradation of microcystin-LR in aqueous solutions. Chemosphere 90, 1552-1557.

Jochimsen, E., Carmichael, W., An, J., Cardo, D., Cookson, S., Holmes, C., Antunes, M., de Melo Filho, D., Lyra, T., Barreto, V., 1998. Liver failure and death after exposure to microcystins at a hemodialysis center in Brazil. New England Journal of Medicine 338, 873.

Jurczak, T., Tarczynska, M., Izydorczyk, K., Mankiewicz, J., Zalewski, M., Meriluoto, J., 2005. Elimination of microcystins by water treatment processes—examples from Sulejow Reservoir, Poland. Water Research 39, 2394-2406.

Karim, M., Puiseux-Dao, S., Edery, M., 2011. Toxins and stress in fish: Proteomic analyses and response network. Toxicon 57, 959-969.

Klitzke, S., Apelt, S., Weiler, C., Fastner, J., Chorus, I., 2010. Retention and degradation of the cyanobacterial toxin cylindrospermopsin in sediments - The role of sediment preconditioning and DOM composition. Toxicon 55, 999-1007.

Kolen'ko, Y.V., Kovnir, K.A., Gavrilov, A.I., Garshev, A.V., Meskin, P.E., Churagulov, B.R., Bouchard, M., Colbeau-Justin, C., Lebedev, O.I., Van Tendeloo, G., Yoshimura, M., 2005. Structural, textural, and electronic properties of a nanosized mesoporous ZnxTi1-xO2-x solid solution prepared by a supercritical drying route. Journal of Physical Chemistry B 109, 20303-20309.

Kotai, J., 1972. Instructions for preparation of modified nutrient solution Z8 for algae. Norwegian Institute for Water Research 11, 5.

Krienitz, L., Ballot, A., Wiegand, C., Kotut, K., Codd, G., Pflugmacher, S., 2002. Cyanotoxin-producing bloom of Anabaena flos-aquae, Anabaena discoidea and Microcystis aeruginosa (Cyanobacteria) in Nyanza Gulf of Lake Victoria, Kenya. Journal of applied botany 76, 179-183.

Krüger, T., Mönch, B., Oppenhäuser, S., Luckas, B., 2010. LC-MS/MS determination of the isomeric neurotoxins BMAA ([beta]-N-methylamino-l-alanine) and DAB (2,4-diaminobutyric acid) in cyanobacteria and seeds of Cycas revoluta and Lathyrus latifolius. Toxicon 55, 547-557.

Lawton, L., Robertson, P., 1999. Physico-chemical treatment methods for the removal of microcystins (cyanobacterial hepatotoxins) from potable waters. Chemical Society Reviews 28, 217-224.

Lawton, L., Robertson, P., Cornish, B., Jaspars, M., 1999. Detoxification of microcystins (cyanobacterial hepatotoxins) using TiO_2 photocatalytic oxidation. Environ. Sci. Technol 33, 771-775.

Lawton, L., Robertson, P., Cornish, B., Marr, I., Jaspars, M., 2003. Processes influencing surface interaction and photocatalytic destruction of microcystins on titanium dioxide photocatalysts. Journal of Catalysis 213, 109-113.

Lawton, L.A., Edwards, C., Codd, G.A., 1994. Extraction and high-performance liquid chromatographic method for the determination of microcystins in raw and treated waters. Analyst 119, 1525-1530.

Lee, D.-K., Kim, S.-C., Kim, S.-J., Chung, I.-S., Kim, S.-W., 2004a. Photocatalytic oxidation of microcystin-LR with TiO_2-coated activated carbon. Chemical Engineering Journal 102, 93-98.

Lee, D., Kim, S., Cho, I., Kim, S., Kim, S., 2004b. Photocatalytic oxidation of microcystin-LR in a fluidized bed reactor having TiO_2-coated activated carbon. Separation and Purification Technology 34, 59-66.

Lee, J., Walker, H.W., 2006. Effect of Process Variables and Natural Organic Matter on Removal of Microcystin-LR by PAC−UF†. Environmental Science & Technology 40, 7336-7342.

Lee T.-J., N.K., Matsumura M. , 2002. A novel strategy for cyanobacterial bloom control by ultrasonic irradiation. Water Science & Technology 46, 207-215.

Li, D., Zheng, H., Wang, Q., Wang, X., Jiang, W., Zhang, Z., Yang, Y., 2014. A novel double-cylindrical-shell photoreactor immobilized with monolayer TiO_2-coated silica gel beads for photocatalytic degradation of Rhodamine B and Methyl Orange in aqueous solution. Separation and Purification Technology 123, 130-138.

Li, P., Zhang, L., Wang, W., Su, J., Feng, L., 2011. Rapid catalytic microwave method to damage microcystis aeruginosa with FeCl3-loaded active carbon. Environmental Science and Technology 45, 4521-4526.

Linsebigler, A.L., Lu, G., Yates Jr, J.T., 1995. Photocatalysis on TiO_2 surfaces: Principles, mechanisms, and selected results. Chemical Reviews 95, 735-758.

Liu, G., Han, C., Pelaez, M., Zhu, D., Liao, S., Likodimos, V., Kontos, A.G., Falaras, P., Dionysiou, D.D., 2013. Enhanced visible light photocatalytic activity of CN-codoped TiO 2 films for the degradation of microcystin-LR. Journal of Molecular Catalysis A: Chemical 372, 58-65.

Liu, I., Lawton, L.A., Bahnemann, D.W., Liu, L., Proft, B., Robertson, P.K.J., 2009. The photocatalytic decomposition of microcystin-LR using selected titanium dioxide materials. Chemosphere 76, 549-553.

Liu, I., Lawton, L.A., Cornish, B., Robertson, P.K.J., 2002. Mechanistic and toxicity studies of the photocatalytic oxidation of microcystin-LR. Journal of Photochemistry and Photobiology A: Chemistry 148, 349-354.

Lun, Z., Hai, Y., Kun, C., 2002. Relationship between microcystin in drinking water and colorectal cancer. Biomedical and environmental sciences 15.

Magalhães, V.F., Marinho, M.M., Domingos, P., Oliveira, A.C., Costa, S.M., Azevedo, L.O., Azevedo, S.M.F.O., 2003. Microcystins (cyanobacteria hepatotoxins) bioaccumulation in fish and crustaceans from Sepetiba Bay (Brasil, RJ). Toxicon 42, 289-295.

Malato, S., Blanco, J., Vidal, A., Richter, C., 2002. Photocatalysis with solar energy at a pilot-plant scale: an overview. Applied Catalysis B: Environmental 37, 1-15.

Malato, S., Fernández-Ibáñez, P., Maldonado, M.I., Blanco, J., Gernjak, W., 2009. Decontamination and disinfection of water by solar photocatalysis: Recent overview and trends. Catalysis Today 147, 1-59.

Mann, M., Talbo, G., 1996. Developments in matrix-assisted laser desorption/ionization peptide mass spectrometry. Current Opinion in Biotechnology 7, 11-19.

Martins, J., Peixe, L., Vasconcelos, V., 2010. Cyanobacteria and bacteria co-occurrence in a wastewater treatment plant: absence of allelopathic effects. Water science and technology: a journal of the International Association on Water Pollution Research 62, 1954.

Martins, J.C., Leão, P.N., Vasconcelos, V., 2009. Differential protein expression in Corbicula fluminea upon exposure to a Microcystis aeruginosa toxic strain. Toxicon 53, 409-416.

Martins, R., Pereira, P., Welker, M., Fastner, J., Vasconcelos, V.M., 2005. Toxicity of culturable cyanobacteria strains isolated from the Portuguese coast. Toxicon 46, 454-464.

Matthiensen, A., Yunes, J., Codd, G., 1999. Ocorrência, distribuição e toxicidade de cianobactérias no estuário da Lagoa dos Patos, RS. Revista Brasileira de Biologia 59, 361-376.

McElhiney, J., Lawton, L.A., 2005. Detection of the cyanobacterial hepatotoxins microcystins. Toxicology and Applied Pharmacology 203, 219-230.

Melo, P.a.A., Pinto, J.C., Biscaia Jr, E.C., 2001. Characterization of the residence time distribution in loop reactors. Chemical Engineering Science 56, 2703-2713.

Mhlanga, L., Day, J., Cronberg, G., Chimbari, M., Siziba, N., Annadotter, H., 2006. Cyanobacteria and cyanotoxins in the source water from Lake Chivero, Harare, Zimbabwe, and the presence of cyanotoxins in drinking water. African Journal of Aquatic Science 31, 165-173.

Miao, H.-F., Qin, F., Tao, G.-J., Tao, W.-Y., Ruan, W.-Q., 2010. Detoxification and degradation of microcystin-LR and -RR by ozonation. Chemosphere 79, 355-361.

Miao, H., Tao, W., 2009. The mechanisms of ozonation on cyanobacteria and its toxins removal. Separation and Purification Technology 66, 187-193.

Mills, A., Hunte, S.L., 1997. An overview of semiconductor photocatalysis. Journal of Photochemistry and Photobiology-Chemistry Section 108, 1-36.

Monteiro, R.A.R., Lopes, F.V.S., Silva, A.M.T., Ângelo, J., Silva, G.V., Mendes, A.M., Boaventura, R.A.R., Vilar, V.J.P., 2014. Are TiO_2-based exterior paints useful catalysts for gas-phase photooxidation processes? A case study on n-decane abatement for air detoxification. Applied Catalysis B: Environmental 147, 988-999.

Moreno, I.M., Pereira, P., Franca, S., Camean, A., 2004. Toxic cyanobacteria strains isolated from blooms in the Guadiana River (southwestern Spain). Biological Research 37, 405-418.

Mozia, S., Tomaszewska, M., Morawski, A.W., 2005. A new photocatalytic membrane reactor (PMR) for removal of azo-dye Acid Red 18 from water. Applied Catalysis B: Environmental 59, 131-137.

Msagati, T.A.M., Siame, B.A., Shushu, D.D., 2006. Evaluation of methods for the isolation, detection and quantification of cyanobacterial hepatotoxins. Aquatic Toxicology 78, 382-397.

Navarro, R.R., Ichikawa, H., Tatsumi, K., 2010. Ferrite formation from photo-Fenton treated wastewater. Chemosphere 80, 404-409.

Nicholson, B.C., Burch, M.D., Health, N., Council, M.R., 2001. Evaluation of analytical methods for detection and quantification of cyanotoxins in relation to Australian drinking water guidelines. National Health and Medical Research Council of Australia.

Nogueira, R.F.P., Trovó, A.G., Silva, M.R.A.d., Villa, R.D., Oliveira, M.C.d., 2007. Fundamentos e aplicações ambientais dos processos fenton e foto-fenton. Química Nova 30, 400-408.

Norris, R., Eaglesham, G., Shaw, G., Senogles, P., Chiswell, R., Smith, M., Davis, B., Seawright, A., Moore, M., 2001. Extraction and purification of the zwitterions cylindrospermopsin and deoxycylindrospermopsin from Cylindrospermopsis raciborskii. Environmental toxicology 16, 391-396.

Okano, K., Shimizu, K., Kawauchi, Y., Maseda, H., Utsumi, M., Zhang, Z., Neilan, B., Sugiura, N., 2009. Characteristics of a Microcystin-Degrading Bacterium under Alkaline Environmental Conditions. Journal of toxicology 2009.

Onstad, G.D., Strauch, S., Meriluoto, J., Codd, G.A., von Gunten, U., 2007. Selective oxidation of key functional groups in cyanotoxins during drinking water ozonation. Environmental Science & Technology 41, 4397-4404.

Orr, P.T., Jones, G.J., Hamilton, G.R., 2004. Removal of saxitoxins from drinking water by granular activated carbon, ozone and hydrogen peroxide--implications for compliance with the Australian drinking water guidelines. Water Research 38, 4455-4461.

Oudra, B., Loudiki, M., Sbiyyaa, B., Martins, R., Vasconcelos, V., Namikoshi, N., 2001. Isolation, characterization and quantification of microcystins (heptapeptides hepatotoxins) in Microcystis aeruginosa dominated bloom of Lalla Takerkoust lake-reservoir (Morocco). Toxicon 39, 1375-1381.

Oufdou, K., Mezrioul, N., Oudra, B., Barakate, M., Loudiki, M., AIT ALLA, A., 2000. Relationships between bacteria and cyanobacteria in the Marrakech waste stabilisation ponds. Water science and technology, 171-178.

Pablos, C., Van Grieken, R., Marugań, J., Muñoz, A., 2012. Simultaneous photocatalytic oxidation of pharmaceuticals and inactivation of Escherichia coli in wastewater treatment plant effluents with suspended and immobilised TiO_2. Water Science and Technology 65, 2016-2023.

Pelaez, M., de la Cruz, A.A., Stathatos, E., Falaras, P., Dionysiou, D.D., 2009. Visible light-activated N-F-codoped TiO_2 nanoparticles for the photocatalytic degradation of microcystin-LR in water. Catalysis Today 144, 19-25.

Pelaez, M., Falaras, P., Kontos, A.G., de la Cruz, A.A., O'Shea, K., Dunlop, P.S.M., Byrne, J.A., Dionysiou, D.D., 2012. A comparative study on the removal of cylindrospermopsin and microcystins from water with NF-TiO_2-P25 composite films with visible and UV–vis light photocatalytic activity. Applied Catalysis B: Environmental 121–122, 30-39.

Pelizzetti, E., Minero, C., 1993. Mechanism of the photo-oxidative degradation of organic pollutants over TiO_2 particles. Electrochim. Acta 38, 47-55.

Peral, J., Ollis, D.F., 1992. Heterogeneous photocatalytic oxidation of gas-phase organics for air purification: Acetone, 1-butanol, butyraldehyde, formaldehyde, and m-xylene oxidation. Journal of Catalysis 136, 554-565.

Pietsch, J., Bornmann, K., Schmidt, W., 2002. Relevance of Intra and Extracellular Cyanotoxins for Drinking Water Treatment. Acta hydrochimica et hydrobiologica 30, 7-15.

Pignatello, J.J., Oliveros, E., MacKay, A., 2006. Advanced oxidation processes for organic contaminant destruction based on the Fenton reaction and related chemistry. Critical Reviews in Environmental Science and Technology 36, 1-84.

Pinho, L.X., Azevedo, J., Vasconcelos, V.M., Vilar, V.J.P., Boaventura, R.A.R., 2012. Decomposition of Microcystis aeruginosa and Microcystin-LR by TiO_2 Oxidation Using Artificial UV Light or Natural Sunlight. Journal of Advanced Oxidation Technologies 15, 98-106.

Pires, L.M.D., Karlsson, K.M., Meriluoto, J.A.O., Kardinaal, E., Visser, P.M., Siewertsen, K., Donk, E.V., Ibelings, B.W., 2004. Assimilation and depuration of microcystin-LR by the zebra mussel, Dreissena polymorpha. Aquatic Toxicology 69, 385-396.

Poon, K.F., Lam, M.H., Lam, P.K.S., Wong, B.S.F., 2001. Determination of microcystins in cyanobacterial blooms by solid phase microextraction high performance liquid chromatography. Environmental toxicology and chemistry 20, 1648-1655.

Portela, R., Sánchez, B., Coronado, J.M., Candal, R., Suárez, S., 2007. Selection of TiO_2-support: UV-transparent alternatives and long-term use limitations for H2S removal. Catalysis Today 129, 223-230.

Preußel, K., Stüken, A., Wiedner, C., Chorus, I., Fastner, J., 2006. First report on cylindrospermopsin producing Aphanizomenon flos-aquae (Cyanobacteria) isolated from two German lakes. Toxicon 47, 156-162.

Puerto, M., Campos, A., Prieto, A., Cameán, A., Almeida, A.M.d., Coelho, A.V., Vasconcelos, V., 2011. Differential protein expression in two bivalve species; Mytilus galloprovincialis and Corbicula fluminea; exposed to Cylindrospermopsis raciborskii cells. Aquatic Toxicology 101, 109-116.

Rapala, J., Berg, K.A., Lyra, C., Niemi, R.M., Manz, W., Suomalainen, S., Paulin, L., Lahti, K., 2005. Paucibacter toxinivorans gen. nov., sp. nov., a bacterium that degrades cyclic cyanobacterial hepatotoxins microcystins and nodularin. International Journal of Systematic and Evolutionary Microbiology 55, 1563-1568.

Ratnayake, N., Manatunge, J., Hapuarachchi, D.P., 2012. Dealing with Algal Toxins and Dissolved Organics in Drinking Water. Journal of Hazardous, Toxic, and Radioactive Waste 16, 118-124.

Ray, A.K., Beenackers, A.A., 1998a. Novel photocatalytic reactor for water purification. AIChE Journal 44, 477-483.

Ray, A.K., Beenackers, A.A.C.M., 1998b. Development of a new photocatalytic reactor for water purification. Catalysis Today 40, 73-83.

Rivasseau, C., Racaud, P., Deguin, A., Hennion, M., 1999. Development of a bioanalytical phosphatase inhibition test for the monitoring of microcystins in environmental water samples. Analytica Chimica Acta 394, 243-257.

Robert, D., Malato, S., 2002. Solar photocatalysis: a clean process for water detoxification. The Science of The Total Environment 291, 85-97.

Robert, D., Piscopo, A., Heintz, O., Weber, J.V., 1999. Photocatalytic detoxification with TiO_2 supported on glass-fibre by using artificial and natural light. Catalysis Today 54, 291-296.

Robertson, J.M.C., J. Robertson, P.K., Lawton, L.A., 2005. A comparison of the effectiveness of TiO_2 photocatalysis and UVA photolysis for the destruction of three pathogenic micro-organisms. Journal of Photochemistry and Photobiology A: Chemistry 175, 51-56.

Robertson, P.K.J., 1996. Semiconductor photocatalysis: an environmentally acceptable alternative production technique and effluent treatment process. Journal of Cleaner Production 4, 203-212.

Robertson, P.K.J., Bahnemann, D.W., Lawton, L.A., Bellu, E., 2011. A study of the kinetic solvent isotope effect on the destruction of microcystin-LR and geosmin using TiO_2 photocatalysis. Applied Catalysis B: Environmental 108–109, 1-5.

Robillot, C., Vinh, J., Puiseux-Dao, S., Hennion, M.C., 2000. Hepatotoxin production kinetics of the cyanobacterium Microcystis aeruginosa PCC 7820, as determined by HPLC-mass spectrometry and protein phosphatase bioassay. Environmental science & technology 34, 3372-3378.

Rodríguez, E., Majado, M.E., Meriluoto, J., Acero, J.L., 2007. Oxidation of microcystins by permanganate: Reaction kinetics and implications for water treatment. Water Research 41, 102-110.

Rodríguez, S.M., Richter, C., Gálvez, J.B., Vincent, M., 1996. Photocatalytic degradation of industrial residual waters. Solar Energy 56, 401-410.

Rogalus, M.K., Watzin, M.C., 2008. Evaluation of sampling and screening techniques for tiered monitoring of toxic cyanobacteria in lakes. Harmful Algae 7, 504-514.

Rositano, J., Nicholson, B., Pieronne, P., 1998. Destruction of cyanobacterial toxins by ozone. Ozone: science & engineering 20, 223-238.

Saker, M., Nogueira, I., Vasconcelos, V., Neilan, B., Eaglesham, G., Pereira, P., 2003. First report and toxicological assessment of the cyanobacterium Cylindrospermopsis raciborskii from Portuguese freshwaters. Ecotoxicology and Environmental Safety 55, 243-250.

Sangolkar, L., Maske, S., Chakrabarti, T., 2006. Methods for determining microcystins (peptide hepatotoxins) and microcystin-producing cyanobacteria. Water Research 40, 3485-3496.

Santos, K., Sant'Anna, C.L., 2010. Cianobactérias de diferentes tipos de lagoas ("salina","salitrada" e "baía") representativas do Pantanal da Nhecolândia, MS, Brasil. Revista Brasileira de Botânica 33, 61-83.

Scharf, R.G., Johnston, R.W., Semmens, M.J., Hozalski, R.M., 2010. Comparison of batch sorption tests, pilot studies, and modeling for estimating GAC bed life. Water Research 44, 769-780.

Shalev-Alon, G., Sukenik, A., Livnah, O., Schwarz, R., Kaplan, A., 2002. A novel gene encoding amidinotransferase in the cylindrospermopsin producing cyanobacterium Aphanizomenon ovalisporum. FEMS Microbiology Letters 209, 87-91.

Shaw, G., Sukenik, A., Livne, A., Chiswell, R., Smith, M., Seawright, A., Norris, R., Eaglesham, G., Moore, M., 1999. Blooms of the cylindrospermopsin containing cyanobacterium, Aphanizomenon ovalisporum (Forti), in newly constructed lakes, Queensland, Australia. Environmental toxicology 14, 167-177.

Shen, P.P., Shi, Q., Hua, Z.C., Kong, F.X., Wang, Z.G., Zhuang, S.X., Chen, D.C., 2003. Analysis of microcystins in cyanobacteria blooms and surface water samples from Meiliang Bay, Taihu Lake, China. Environment International 29, 641-647.

Shephard, G., Stockenström, S., De Villiers, D., Engelbrecht, W., Sydenham, E., Wessels, G., 1998. Photocatalytic degradation of cyanobacterial microcystin toxins in water. Toxicon 36, 1895-1901.

Shephard, G.S., Stockenström, S., de Villiers, D., Engelbrecht, W.J., Wessels, G.F.S., 2002. Degradation of microcystin toxins in a falling film photocatalytic reactor with immobilized titanium dioxide catalyst. Water Research 36, 140-146.

Sládečková, A., 1962. Limnological investigation methods for the periphyton ("Aufwuchs") community. The Botanical Review 28, 286-350.

Soares, R.M., Magalhães, V.F., Azevedo, S.M.F.O., 2004. Accumulation and depuration of microcystins (cyanobacteria hepatotoxins) in Tilapia rendalli (Cichlidae) under laboratory conditions. Aquatic Toxicology 70, 1-10.

Song, W., Armah, A., Rein, K., O'Shea, K.E., 2006. Ultrasonically induced degradation of microcystin-LR and-RR: Identification of products, effect of pH, formation and destruction of peroxides. Environmental Science & Technology 40, 3941-3946.

Song, W., O'Shea, K.E., 2007. Ultrasonically induced degradation of 2-methylisoborneol and geosmin. Water Research 41, 2672-2678.

Song, W., Teshiba, T., Rein, K., Kevin, E.O.S., 2005. Ultrasonically induced degradation and detoxification of microcystin-LR (cyanobacterial toxin). Environmental science & technology 39, 6300-6305.

Song, W., Yan, S., Cooper, W.J., Dionysiou, D.D., O'Shea, K.E., 2012. Hydroxyl radical oxidation of cylindrospermopsin (cyanobacterial toxin) and its role in the photochemical transformation. Environmental Science & Technology 46, 12608-12615.

Sordo, C., Van Grieken, R., Marugán, J., Fernández-Ibáñez, P., 2010. Solar photocatalytic disinfection with immobilised TiO_2 at pilot-plant scale. Warter Science & Technology 61, 507-512.

Spoof, L., Karlsson, K., Meriluoto, J., 2001. High-performance liquid chromatographic separation of microcystins and nodularin, cyanobacterial peptide toxins, on C18 and amide C16 sorbents. Journal of Chromatography A 909, 225-236.

Su, Y., Deng, Y., Du, Y., 2013. Alternative pathways for photocatalytic degradation of microcystin-LR revealed by TiO_2 nanotubes. Journal of Molecular Catalysis A: Chemical 373, 18-24.

Subrahmanyam, M., Boule, P., Durga Kumari, V., Naveen Kumar, D., Sancelme, M., Rachel, A., 2008. Pumice stone supported titanium dioxide for removal of pathogen in drinking water and recalcitrant in wastewater. Solar Energy 82, 1099-1106.

Svrcek, C., Smith, D.W., 2004. Cyanobacteria toxins and the current state of knowledge on water treatment options: a review. Journal of Environmental Engineering & Science 3, 155-185.

Takeuchi, N., 2001. The altitudinal distribution of snow algae on an Alaska glacier (Gulkana Glacier in the Alaska Range). Hydrological Processes 15, 3447-3459.

Torrades, F., Pérez, M., Mansilla, H.D., Peral, J., 2003. Experimental design of Fenton and photo-Fenton reactions for the treatment of cellulose bleaching effluents. Chemosphere 53, 1211-1220.

Triantis, T.M., Fotiou, T., Kaloudis, T., Kontos, A.G., Falaras, P., Dionysiou, D.D., Pelaez, M., Hiskia, A., 2012. Photocatalytic degradation and mineralization of microcystin-LR under UV-A, solar and visible light using nanostructured nitrogen doped TiO_2. Journal of Hazardous Materials 211–212, 196-202.

Valeria, A., Ricardo, E., Stephan, P., Alberto, W., 2006. Degradation of Microcystin-RR by Sphingomonas sp. CBA4 isolated from San Roque reservoir (Córdoba – Argentina). Biodegradation 17, 447-455.

van Grieken, R., Marugán, J., Sordo, C., Martínez, P., Pablos, C., 2009a. Photocatalytic inactivation of bacteria in water using suspended and immobilized silver-TiO_2. Applied Catalysis B: Environmental 93, 112-118.

van Grieken, R., Marugán, J., Sordo, C., Pablos, C., 2009b. Comparison of the photocatalytic disinfection of E. coli suspensions in slurry, wall and fixed-bed reactors. Catalysis Today 144, 48-54.

van Well, M., Benz, V., Mueller, M., Dillert, R., Bahnemann, D., 1997. A novel nonconcentrating reactor for solar water detoxification. Journal of solar energy engineering 119, 114-119.

Vasconcelos, V., Azevedo, J., Silva, M., Ramos, V., 2010a. Effects of Marine Toxins on the Reproduction and Early Stages Development of Aquatic Organisms. Marine Drugs 8, 59-79.

Vasconcelos, V., Martins, A., Vale, M., Antunes, A., Azevedo, J., Welker, M., Lopez, O., Montejano, G., 2010b. First report on the occurrence of microcystins in planktonic cyanobacteria from Central Mexico. Toxicon 56, 425-431.

Vasconcelos, V., Pereira, E., 2001. Cyanobacteria diversity and toxicity in a wastewater treatment plant (Portugal). Water Research 35, 1354-1357.

Vella, G., Imoberdorf, G.E., Sclafani, A., Cassano, A.E., Alfano, O.M., Rizzuti, L., 2010. Modeling of a TiO_2-coated quartz wool packed bed photocatalytic reactor. Applied Catalysis B: Environmental 96, 399-407.

Vilela, W.F.D., Minillo, A., Rocha, O., Vieira, E.M., Azevedo, E.B., 2012. Degradation of [D-Leu]-Microcystin-LR by solar heterogeneous photocatalysis (TiO_2). Solar Energy 86, 2746-2752.

Wang, H., Ho, L., Lewis, D.M., Brookes, J.D., Newcombe, G., 2007a. Discriminating and assessing adsorption and biodegradation removal mechanisms during granular activated carbon filtration of microcystin toxins. Water Research 41, 4262-4270.

Wang, S., Ang, H.M., Tade, M.O., 2007b. Volatile organic compounds in indoor environment and photocatalytic oxidation: State of the art. Environment International 33, 694-705.

Wormer, L., Cirés, S., Carrasco, D., Quesada, A., 2008. Cylindrospermopsin is not degraded by co-occurring natural bacterial communities during a 40-day study. Harmful Algae 7, 206-213.

Wu, X., Joyce, E.M., Mason, T.J., 2011. The effects of ultrasound on cyanobacteria. Harmful Algae.

Wu, Y., He, J., Yang, L., 2010. Evaluating adsorption and biodegradation mechanisms during the removal of microcystin-RR by periphyton. Environmental Science and Technology 44, 6319-6324.

Yang, X., Cao, C., Erickson, L., Hohn, K., Maghirang, R., Klabunde, K., 2009. Photo-catalytic degradation of Rhodamine B on C-, S-, N-, and Fe-doped TiO_2 under visible-light irradiation. Applied Catalysis B: Environmental 91, 657-662.

Yen, H.-K., Lin, T.-F., Liao, P.-C., 2011. Simultaneous detection of nine cyanotoxins in drinking water using dual solid-phase extraction and liquid chromatography-mass spectrometry. Toxicon 58, 209-218.

YIlmaz, M., Phlips, E., Szabo, N., Badylak, S., 2008. A comparative study of Florida strains of Cylindrospermopsis and Aphanizomenon for cylindrospermopsin production. Toxicon 51, 130-139.

Zhang, G., Zhang, P., Wang, B., Liu, H., 2006. Ultrasonic frequency effects on the removal of Microcystis aeruginosa. Ultrasonics Sonochemistry 13, 446-450.

Zhang, J.B., Zheng, Z., Yang, G.J., Zhao, Y.F., 2007. Degradation of microcystin by gamma irradiation. Nuclear Instruments and Methods in Physics Research Section A: Accelerators, Spectrometers, Detectors and Associated Equipment 580, 687-689.

Zhang, Z., Anderson, W.A., Moo-Young, M., 2004. Experimental analysis of a corrugated plate photocatalytic reactor. Chemical Engineering Journal 99, 145-152.

Zhong, Y., Jin, X., Qiao, R., Qi, X., Zhuang, Y., 2009. Destruction of microcystin-RR by Fenton oxidation. Journal of Hazardous Materials 167, 1114-1118.

Zimba, P.V., Camus, A., Allen, E.H., Burkholder, J.M., 2006. Co-occurrence of white shrimp, Litopenaeus vannamei, mortalities and microcystin toxin in a southeastern USA shrimp facility. Aquaculture 261, 1048-1055.

3 Material and methods

This chapter refers to all the chemical reagents, analytical methods and cyanobacteria cultivation and cyanotoxins purification methods used in this thesis. A detailed description of the photocatalysts preparation procedure and respective characterization techniques, photoreactors used in the experiments, as well as the corresponding experimental procedures, is also given.

3.1 Chemicals and reagents

All solvents used in HPLC-DAD and LC-MS analyses were high-purity chromatography grade (LiChrosolv, Merck). Aqueous solutions were prepared with ultrapure water supplied from a Millipore water purification system (0.0054 µS cm^{-1}). Reagents used in the culture medium were analytical grade. Formic acid and trifluoroacetic acid (TFA) were 99% spectrophotometric grade. MC-LR was used as the reference standard (lot nº MC-LR-a080227, >95% purity, Cyano Biotech GmbH) to quantify the LEGE in-house MC-LR standard (data unpublished) isolated from *M. aeruginosa* (>94% purity). Standard CYN was supplied by NCR CRM-Cyn (Lot nº 200505310197, 12.6 ppm).

The reagents used for Light and Transmission Electron Microcopy were Glutaraldehyde (Merck, KGaA, Germany), sodium cacodylate (Electron Microscopy Sciences, Hatfield, PA) and EPON (EMBed-812 - Electron Microscopy Sciences, Hatfield, PA).

Heterogeneous photocatalytic experiments used suspensions of TiO_2 Degussa P25. The paint films incorporated TiO_2 P25 (Degussa), VLP 7000 (Kronos) and PC500 (Millennium).

Nitric acid (HNO_3; 65%, Merck S.A.), titanium (IV) isopropoxide (TIP: $Ti(iOPr)_4$; 97%, Sigma–Aldrich Co. LLC.), and TritonTM X-100 (t-Oct-C_6H_4-(OCH_2CH_2)nOH, n = 9–10, Sigma–Aldrich Co. LLC.) were used in the preparation of titanium dioxide (TiO_2) sol-gel.

Ultrapure and deionized water necessary for analysis and preparation of cyanotoxins solutions were obtained from a Milli-Q water (18.2 MΩ cm at 25 ºC) Direct-Q model and a reverse osmosis system (Panice®), respectively.

Pure or diluted solutions of sulfuric acid (Pronalab, 96%, 1.84 g cm^{-3}) and sodium hydroxide (Merck) were used for pH adjustment.

Hydrogen peroxide (Quimitécnica, S.A., 50% (w/v), 1.10 g cm^{-3}), D-Mannitol and NaN_3 were all analytical grade.

3.2 Cyanobacteria cultivation

In general cyanobacteria and cyanotoxins represent a significant health hazard, therefore they must be handled very carefully. The toxic solution should not be inhaled, ingested or come in contact with skin (Antoniou et al., 2008).

The *M. Aeruginosa* strain LEGE 91094 (IZANCYA2) and *C. raciborskii* LEGE 97047 were cultivated at the Laboratory of Ecotoxicology, Genomics and Evolution - LEGE of the Interdisciplinary Centre

of Marine and Environmental Research – CIIMAR (see Fig.3.1). The cyanobacteria were cultivated separately in Z8 growth medium, under sterile conditions. The culture was kept at 25 ± 1 ºC under light intensity of 25 µmol m^{-2} s^{-1} with a 14/10h light/dark cycle, for approximately 30 - 45 days (Kotai, 1972).

Figure 3.1 Cyanobacteria culture room

3.3 *M. Aeruginosa* identification and counting

A Neubauer chamber was used for the counting of *M. Aeruginosa* cells preserved in lugol; this chamber is the most suitable for the detection of cells with size of 7-75 µm (Guillard and Sieracki, 2005). *M. aeruginosa* live cells were identified by their spherical morphology and green colour, characteristic of the presence of chlorophyll. A Nikon stereomicroscope was used with a total amplification of 400x.

3.4 Microcystin-LR extraction, purification and quantification by HPLC-PDA

The toxin MC-LR was extracted and purified from the culture of *M. aeruginosa*, according to the flowchart presented in the Figure 3.2. The *M. aeruginosa* cell crude extract was prepared according to (Ramanan et al., 2000), introducing some modifications.

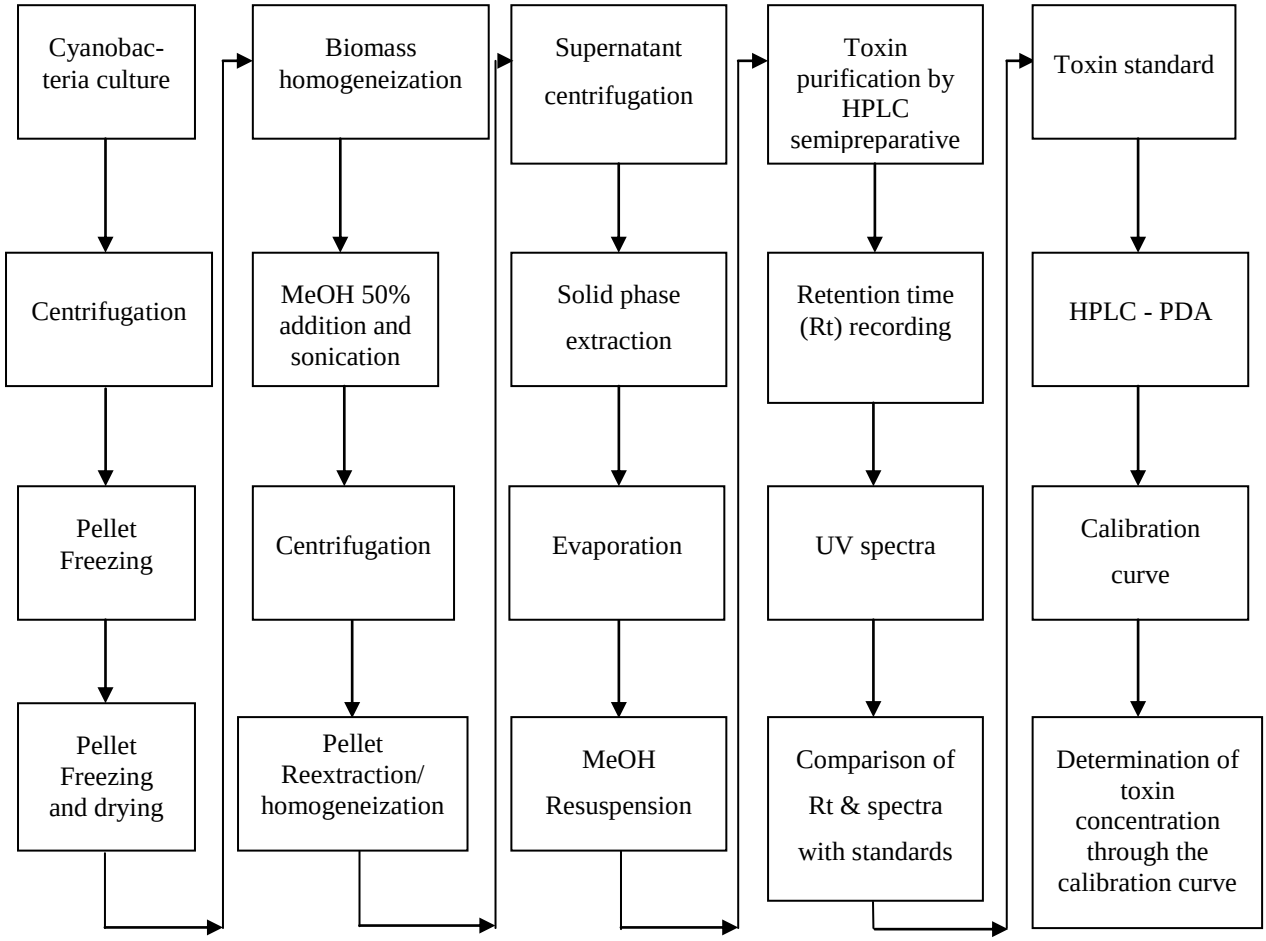

Figure 3.2 Toxin purification flow chart adapted from Sangolkar et al. (2006).

i. *Microcistis aeruginosa cultivation*

M.aeruginosa was cultivated according to the procedure described in topic 3.1, for a growth period of approximately 30-60 days.

ii. *Centrifugation*

The cyanobacteria culture was centrifuged at a Sorvall Legend RT Centrifuge (Thermo Electron Corporation), for 20 min at 4995 *g* and 4 ºC.

iii. *Pellet freezing and drying*

After centrifugation the pellet was collected and frozen at -80 ºC, and then freeze dried in a Telstar – LyoQuest during approximately three days.

iv. *MeOH addition and sonication*

Briefly, the lyophilized *M. aeruginosa* biomass was extracted with MeOH 75% (v/v) by continuous stirring for 20 min at room temperature. The sample was then ultrasonicated on ice bath at 60 Hz for 5×1 min (VibraCell 50-sonics & Material Inc. Danbury, CT, USA). The homogenate was centrifuged at 4995 *g* for 15 min to remove cell debris. The resulting supernatant was then collected and stored at 4ºC.

v. *Solid phase extraction - SPE*

The pellet was re-extracted with an equal volume of solvent. The supernatants resulting from both steps of extraction were combined and passed through a solid-phase extraction (SPE) cartridge (Water Sep-Pak® Vac 6 mL C18 cartridge) at 1 mL min^{-1}, which had been preconditioned with MeOH 100% and distilled water. The loaded column was washed with MeOH 20% (v/v) and then the toxin MC-LR was eluted using MeOH 80% (v/v).

vi. Evaporation

The MC-LR fraction was evaporated in a rotary evaporator BÜCHI - RE111, water bath BÜCHI - 461, Huberminichiller and vacuum pump BÜCHI - V-700, at 35ºC to remove the entire MeOH portion.

vii. MC-LR purification

The concentrated MC-LR extract was thereafter purified and quantified by HPLC-PDA. The MC-LR semi-preparative assay was performed using a reversed phase column (Phenomenex Luna RP-18 (25 cm × 10 mm, 10 µm) kept at 40ºC. The eluent was methanol + water, both acidified with 0.1 % TFA, delivered at a flow rate of 2.5 mL min^{-1}. The injected volume was 500 to 1000 µL. The amount of purified MC-LR was calculated at 214 nm and 238 nm. The fraction with purified MC-LR was then evaporated by speedvac until removing all the solvent. The residue was resuspended in distilled water to the desired concentration. Chromatographic purity of MC-LR was of 97%.

viii. MC-LR quantification

The MC-LR purified fractions were then quantified in the same HPLC system using a Merck Lichrospher RP-18 endcapped column (250 mm x 4.6 mm i.d., 5 µm) equipped with a guard column (4 × 4 mm, 5 µm) both kept at 45ºC. The PDA range was 210-400 nm with a fixed wavelength of 238 nm. The linear gradient elution ((eluents MeOH + 0.1% trifluoroacetic acid (A) and (B) H_2O + 0.1% TFA (B)) consisted of 55% A and 45% B at 0 min, 65% A and 35% B at 5 min, 80% A and 20% B at 10 min, 100% A at 15 min, 55% A and 45% B between 15.1 and 20 min, at a flow rate of 0.9 mLmin^{-1}. The injected volume was 20 µL. The MC-LR was identified by comparison of spectra and retention time with a standard of MC-LR (batch nº MCLR-110, 11.028 µg mL^{-1} in MeOH, 95% purity, DHI). The system was calibrated by using a set of 7 dilutions of MC-LR standard (0.3 to 11.028 µg mL^{-1}) in MeOH 50%. Each vial was injected in duplicate and every HPLC run series of ten samples included a blank and two standards. Empower 2 Chromatography Data Software was used for calculation and reporting peak information. The MC-LR detection limit was 0.2 µg mL^{-1}, based on a signal-to-noise ratio of 3. The retention time of the MC-LR peak was approximately 9.5 min. The validation of the analytical method followed the ICH (*International Conference on Harmonization*) guidelines. Validation demonstrated the selectivity for microcystin-LR: the dynamic interval for MC-LR was linear ($R^2 \geq 0{,}996$) between 0.3 and 11 µg mL^{-1}; the limit of detection was 0.17 µg mL^{-1} and the limit of quantification was 0.58 µg mL^{-1}, for the biomass extract

samples. The method showed to be precise (Repeatability < 1.4%; Reproducibility < 2%) and accurate (R.S.D. < 2%, $n = 3$) for the biomass extract samples.

3.5 Cylindrospermopsin extraction, purification and quantification by HPLC-PDA

Cylindrospermopsin (CYN) was extracted from the cyanobacteria *A. ovalisporum* following a modified version of the method described by Welker et al. (2002).

The steps (*i*) to (*iii*) were the same used for MC-LR purification.

iv. *Solvent addition and sonication*

Briefly, freeze dried cells (0.7 g) were first sonicated in bath for 15 min in 5mL 0.1%, v/v trifluoracetic acid (TFA) of spectrophotometric grade, followed by a second treatment with at 60 HZ at 5 cycles of 1 min. The homogenate was stirred for 1 hour at room temperature, centrifuged (20000*g*, 4ºC, 20 min) and the supernatant collected. A second extraction on the cell pellet was performed. Finally, supernatants were pooled together and stored at -20 ºC.

v. *Evaporation*

See session 3.3 (*vi*).

vi. *CYN purification*

CYN was thereafter purified by HPLC system coupled with a PDA on a semi-preparative Gemini C18 column (250 mm x 10 mm i.d., 5 µm) from Phenomenex kept at 40ºC. The isocratic elution was done with 5% MeOH solution containing 0.1%, v/v TFA at a flow rate of 2.5 mL min^{-1}. The injection volume was 1000 µL. Chromatographic purity of CYN was of 98%.

vii. The CYN purified fractions were then quantified in the same HPLC system using a Lichrospher 100 RP-18 column (250 mm x 4.6 mm i.d., 5 µm) from Merk kept at 40 ºC. The PDA range was 210-400 nm with a fixed wavelength of 262 nm. The isocratic elution was done with 5% MeOH solution containing 0.1%, v/v TFA at a flow of 0.9 mL min^{-1}. The injection volume was10 µL. Working solutions of CYN (0.1-12.6 µg mL^{-1}) were prepared in Milli-Q water. Standard CYN was supplied by NCR CRM-Cyn (Lot nº 200505310197, 12.6 ppm). Each vial was injected in duplicate and every HPLC run series of ten samples comprised a blank and two standards. Empower 2 Chromatography Data Software was used for calculation and reporting peak information. The CYN detection limit was 0.3 µg mL^{-1} based on a signal-to-noise ratio of 3. The retention time of the CYN peak was approximately 5.9 min. The validation of the analytical method followed the ICH (*International Conference on Harmonization*) guidelines. Validation demonstrated the selectivity for cylindrospermopsin. The dynamic interval for CYN was linear ($R^2 \geq 0{,}999$) between 0.1 and 12 µg mL^{-1}; limit of detection was 0.3 µg mL^{-1} and the limit of quantification was 0.5 µg mL^{-}

[1], for the biomass extract samples. The method showed to be precise (Repeatability < 1%; Reproducibility < 2%) and accurate (R.S.D. < 2%, n = 3) for the biomass extract samples.

3.6 Photocatalyst

Photocatalytic experiments were carried out by using suspended or immobilized TiO_2. Degussa P25, supplied by Degussa Portuguesa, was used in the experiments under slurry conditions in different concentrations (20, 30, 50, 100 and 200 mg L^{-1}).

Several types of photocatalytic paints and films were formulated with TiO_2 and immobilized in different kinds of inert supports. Briefly, before painting or coating, all the substrate samples were soaked for 1 h in distilled water and alkaline detergent (Derquim LM 01, PanreacQuímica, S.A.U.), subsequently washed exhaustively with Milli Q water (18.2 MΩ cm at 25 ºC), and heated up to 50 ºC to dry.

3.6.1 Paint films formulation

In the present work, TiO_2 P25, VLP 7000, PC500 were used to prepare the paint films formulations (Table 3.1). The paint formulation was based on commercial water-based vinyl paint (Águia et al., 2011b), modified by total or partial replacement of the pigmentary TiO_2 by 9 or 12 wt.% of photo-TiO_2 commercial P25, VLP7000 or PC500, as reported by Águia et al. (2010) (Table 3.2).

Table 3.1 Properties of the TiO_2 used for the paint formulations, and base paint components (Águia et al., 2011a, b).

TiO_2	**Crystal structure**	**Crystal size (nm)**	**Surface area $A_{photo\text{-}TiO_2}$($m^2\ g^{-1}$)**	**Particle size (μm)**
P25	80 % Anatase 20 % Rutile	25	50	n.p.
VLP7000	Anatase	~ 15	> 250	n.p.
PC500	> 99 %	5 – 10	345	1.2 – 1.7

Paint component (wt.%)	**Pigmentary TiO_2**	**Water**	**Extenders ($CaCO_3$ and silicates)**	**Polymer extender slurry**	**Binder slurry**	**Additive* slurry**
	18	30	18	8	20	6

n.p.: not provided; *dispersing agents, coalescent, thickeners and other additives

Table 3.2 Formulations, characteristics of the TiO_2 in the formulations, material used as support and type of MC-LR stock solution.

Catalytic-bed	TiO_2 type	$[TiO_2]$ (% / mg L^{-1})	Pigmentary TiO_2 Replacement	Support type	Area (m^2)	MC-LR SS
Pnt(1)	P25	9 / 75	Half	G. tube	0.013	MeOH
Pnt(2)	VLP7000	9 / 75	Half	G. tube	0.013	MeOH
Pnt(3)	PC500	9 / 75	Total	G. tube	0.013	MeOH
Pnt(4)-PVCT(M)	PC500	12 / 100	Total	PVCT	0.015	MeOH
Pnt(4)-PVCT(W)	PC500	12 / 100	Total	PVCT	0.015	Water
Pnt(4)-PETM	PC500	12 / 200	Total	PETM	0.10	Water
Pnt(4)-GS	PC500	12 / 600	Total	G.S.	0.083	MeOH
P25-CAM	P25 paste	30 mg L^{-1}	-	CAM	0.10	Water
TiO_2-CAM	Sol Gel	55 mg L^{-1}	-	CAM	0.10	Water
Photolysis(Pnt)		Photolysis with paint*		PVCT	0.015	MeOH
Photolysis		Photolysis		-	-	MeOH

Pnt: Paint; PVCT: PVC tube; PETM: PET Monolith; CAM: Cellulose Acetate Monolith; *without TiO_2; G.: glass GS: glass spheres; SS: stock solution; M: stock solution in MeOH:water (50:50%); W: stock solution in water.

A glass tube (0.013 m^2), PCV tube (0.015 m^2), and glass spheres (1 cm diameter) were painted with TiO_2-based paints in two layers with a brush (Figure 3.3). Polyethylene terephthalate transparent monoliths (PETM) (type: WaveCore PET150-9/S–width100 mm, hole diameter 9 mm, thickness tolerance 0.2 mm; Wacosystems), were coated with a thin film of the photocatalytic paint Pnt(4) by using the dip-coating method (Dip-Coater RDC21-K, BungardElektronik GmbH & Co. KG.). Each layer of the photocatalyst was deposited at a withdrawal rate of 0.8 mm s^{-1}, allowing the formation of a thin and uniform film on the support surface. After depositing each layer, PETM samples were dried at 323 K for 1 h. Finally, the supports were packed into a tubular photocatalytic reactor for the study of MC-LR inactivation.

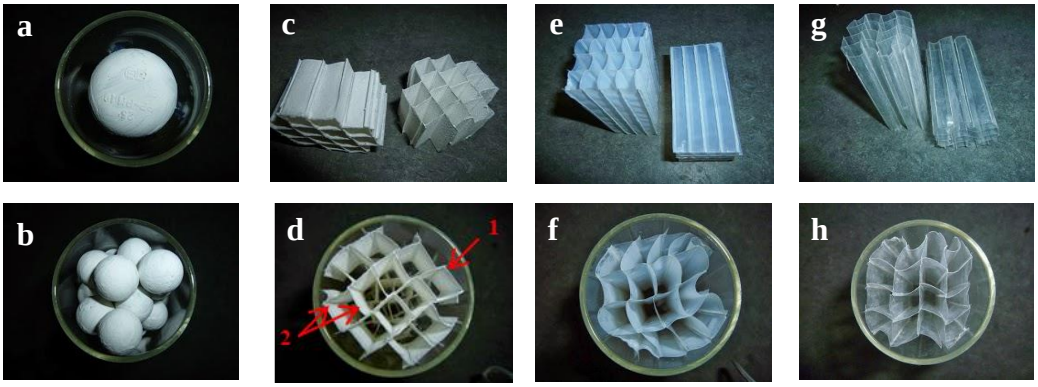

Figure 3.3 a) Catalytic-bed Pnt(4)-PVCT packed into borosilicate tube; b) Catalytic-bed Pnt(4)-GS packed into borosilicate tube; c) Catalytic-bed Pnt(4)-PETM; d) Catalytic-bed Pnt(4)-PETM packed into borosilicate tube, 1: one sheet, 2: two sheets; e) Catalytic-bed P25-CAM; f) Catalytic-bed P25-CAM packed into borosilicate tube; g) Catalytic-bed TiO_2-CAM and h) TiO_2-CAM packed into borosilicate tube.

3.6.2 TiO_2 thin-films

When preparing titanium dioxide (TiO_2) sol-gel, a cellulose membrane (Spectra/Por® Dialysis Membrane 3500 MWCO, Spectrum Laboratories, Inc.) was employed in the final sol-gel dialysis. Cellulose acetate monoliths – CAM (named C: TIMax CA50-9/S – width 80 mm, hole diameter 9 mm, thickness tolerance 0.1 mm; Wacotech GmbH & Co. KG.) were used as support of the catalytic film.

TiO_2 thin-films were prepared on CAM samples by combining sol-gel and dip-coating methods (Anderson et al., 2001), resulting in TiO_2-supported cellulose acetate monoliths (TiO_2-CAM). TIP was employed as precursor and it was added to an aqueous solution of nitric acid (74:900:6.5, v/v/v of TIP, H_2O, and HNO_3); this solution was stirred at ~25 ºC until complete peptization. The final sol-gel was dialyzed in a cellulose membrane until pH 3.0. All preparation steps were performed at room temperature (~25 ºC). Nine layers were deposited by dip-coating at a withdrawal rate of 0.8 mm s^{-1}.

P25 paste thin-films (P25-CAM) were prepared on CAM samples according to the method adapted from Quici et al. (2010). P25 in suspension (2% wt.), previously submitted to sonication (1 cycle of 10 min under 50 kHz), was used for the deposition of nine layers by dip-coating at a withdrawal rate of 0.8 mm s^{-1}.

After applying each layer, the monoliths (TiO_2-CAM and P25-CAM) were dried at 50 ºC for 1 h, finally the materials were rinsed three times with Milli-Q water (18.2 MΩ cm at 25 ºC) and dried at 50 ºC for 2 h (Lopes et al., 2013).

It is also important to mention that before dip-coating CAM, 10 drops of Triton™ X-100 were added per liter of TiO_2 suspension as surfactant, aiming at improving the adherence of the catalyst layers to

the support.

The number of layers was defined having into account a previous work with SG-CAM (Lopes et al., 2013), where a superior efficiency of the photocatalytic processes to degrade perchloroethylene was confirmed in CAM samples (sol gel-TiO_2 consisting of 51%, 45% and 4% of anatase, brookite and rutile crystalline phases, respectively, as determined by X-ray diffraction) similar to those used in this work.

3.6.3 Photocatalytic films surface characterization

UV transmittance spectra of PET and CAM monoliths without film and samples Pnt(4)-PETM, P25-CAM and TiO_2-CAM, with one and two sheets (Figure 3.3), were obtained by spectrometry (VWR UV-6300 PC Double Beam Spectrophotometer).

Scanning electron microscopy (SEM) coupled with energy dispersive X-ray (EDX) analyses were performed in a FEI Quanta 400 FEG ESEM / EDAX Genesis X4M apparatus equipped with a Schottky field emission gun (for optimal spatial resolution) to obtain the surface morphology of fresh and used (after experiments) Pnt(4)-PETM, Pnt(4)-GS, P25-CAM and TiO_2-CAM, as well as their chemical composition by EDX. Each sample was mounted on a double-sided adhesive tape made of carbon for observation of the surface at different magnifications; the cross-section of the sample was also measured by this technique. These SEM/EDX analyses were made at CEMUP (Centro de Materiais da Universidade do Porto).

3.7 Photoreactors design

Different photoreactors were used in this work: lab-scale glass immersion photoreactor, lab scale photoreactor prototype and pilot scale solar photoreactor. The experimental procedures concerning the operation of the reactors are described in Chapters 4, 5 and 6.

3.7.1 Lab-scale glass immersion photoreactor

Photolytic and TiO_2-photocatalytic experiments were first conducted in a glass immersion photochemical reactor (water column of 8 cm diameter and 16 cm height), see Figure 3.4. The reactor can be loaded with 850 mL of solution (photolysis)/suspension (photocatalysis), with constant stirring for the total reaction period. It is equipped with a medium pressure mercury lamp Heraeus TQ 150 W (dominant emission line at 366 nm), placed axially and held in a quartz immersion tube with a surface contact area of ~233 cm^2. The system is refrigerated by a continuous tap water flow, which allows the temperature to be maintained below 35 °C.

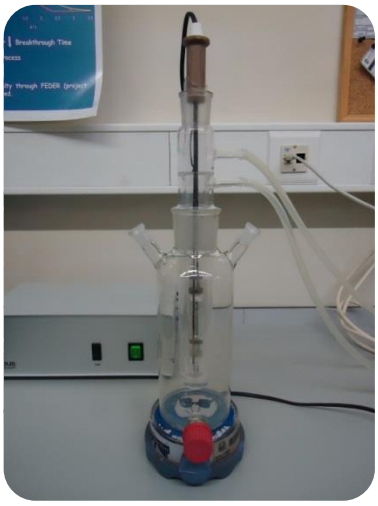

Figure 3.4 Lab-scale glass immersion photoreactor.

3.7.2 Lab scale photoreactor prototype – SUNTEST

The oxidation experiments were carried out in a lab-scale photoreactor (Figure 3.5) equipped with: i) a solar radiation simulator (ATLAS, model SUNTEST XLS) with 1100 cm^2 of exposition area, a 1700 Watt air-cooled xenon arc lamp, a daylight filter and quartz filter with IR coating; ii) a compound parabolic collector (CPC) with 0.026 m^2 of illuminated area with anodized aluminium reflectors and borosilicate tube (Schott-Duran type 3.3, Germany, cut-off at 280 nm, internal diameter 46.4 mm, length 161 mm and thickness 1.8 mm); iii) one acrylic vessel (capacity of 2.5 L) with a cooling jacket coupled to a refrigerated thermostatic bath (Lab. Companion, model RW-0525G) to ensure a constant temperature during the experiment; iv) a magnetic stirrer (VelpScientifica, model ARE) to ensure complete homogenization of the solution inside the acrylic vessel; v) one peristaltic pump (Ismatec, model Ecoline VC-380 II, 0.65 L min^{-1}) to promote the water recirculation between the CPC and the acrylic vessel; vi) pH and temperature meter (VWR symphony - SB90M5). Both inlet and outlet polypropylene caps of the tubular photoreactor have four equidistant inlets to ensure a better distribution of the feed solution into the reactor. The inlets and outlets are made of Teflon, which minimizes the adsorption of organic compounds. The intensity of the UV radiation was measured by a broadband UV radiometer (Kipp&Zonen B.V., model CUV5), which was placed inside the sunlight simulator at the same level than the photoreactor center. The radiometer was plugged into a handheld display unit (Kipp&Zonen B.V., model Meteon) to record the incident irradiance (W m^{-2}), measured in the wavelength range 280 - 400 nm. The following equation allows to obtain the accumulated UV energy ($Q_{UV,n}$ J L^{-1}) received on any surface, per unit of volume of water inside the reactor, in the time interval Δt (Malato et al., 2002):

$$Q_{UV,n} = Q_{UV,n-1} + \Delta t_n \overline{UV}_{G,n} \frac{A_r}{V_t}; \quad \Delta t_n = t_n - t_{n-1} \qquad \text{(Eq.3.01)}$$

where t_n is the time corresponding to the n-water sample (s), V_t the total reactor volume (L), A_r the

illuminated collector surface area (m^2) and $\overline{UV}_{G,n}$ the average solar ultraviolet incident irradiance (W_{UV} m^{-2}) measured during the period Δt_n (s).

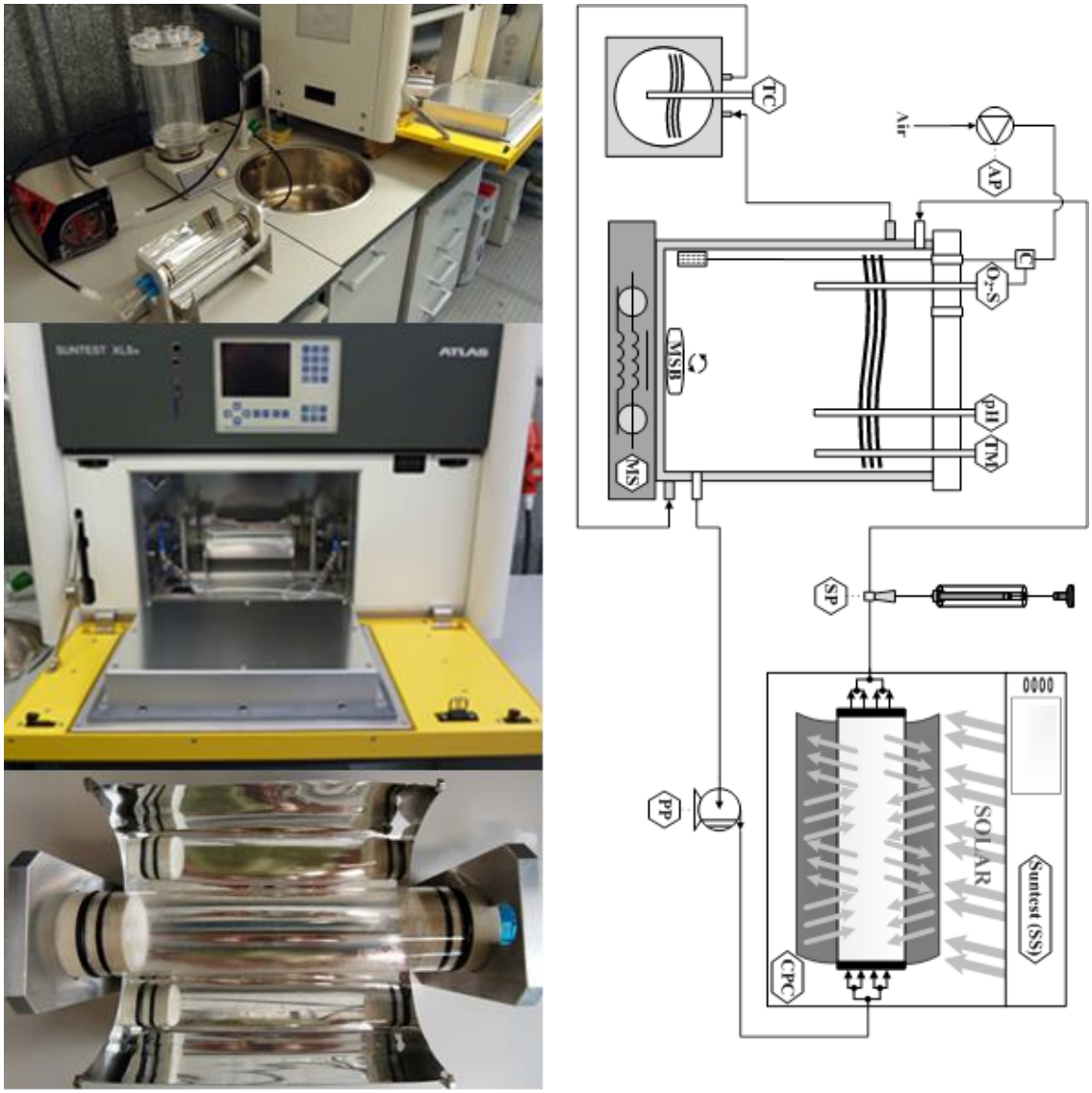

(a) **(b)**

Figure 3.5 (a) Photograph and (b) scheme of the lab-scale photocatalytic system.TC – temperature controller; PP – peristaltic pump; AP – air pump; C – controller; O_2-S – dissolved oxygen sensor; pH – pH meter; TM – temperature meter; MSB – magnetic bar; MS – magnetic stirrer; CPC – Compound Parabolic Collector; SS – SUNTEST System; SP – sampling point. Reprinted (adapted) with permission from Soares et al. (2013). Copyright © 2013, Springer-Verlag Berlin Heidelberg, License Number: 3190821060851.

3.7.3 Pilot scale solar photoreactor

The solar photocatalytic experiments were carried out in a CPC pilot plant (Figure 3.6) installed at the roof of the Chemical Engineering Department of the Faculty of Engineering, University of Porto (FEUP), Portugal. The solar collector consists of one CPC unit (0.91 m^2) of four borosilicate tubes (Schott-Duran type 3.3, Germany, cut-off at 280 nm, internal diameter 50 mm, length 1500 mm and width 1.8 mm) connected in series by polypropylene junctions with CPC anodized aluminum mirrors. The pilot plant has also two recirculation tanks (10 L and 20 L), two recirculation pumps (maximum 20 L min^{-1}), two flow rate meters, five polypropylene valves and an electric board for process control (Fig. 5b and c). The pilot plant can be operated in two ways: using the total CPCs area (0.91 m^2) or 0.455 m^2 of CPCs area individually, giving the possibility of performing two different experiments at the same time and at the same solar radiation conditions. The intensity of solar UV radiation was measured by a global UV radiometer (ACADUS 85-PLS) mounted on the pilot plant at the same inclination, which provides data in terms of incident W_{UV} m^{-2}.

(a) (b)

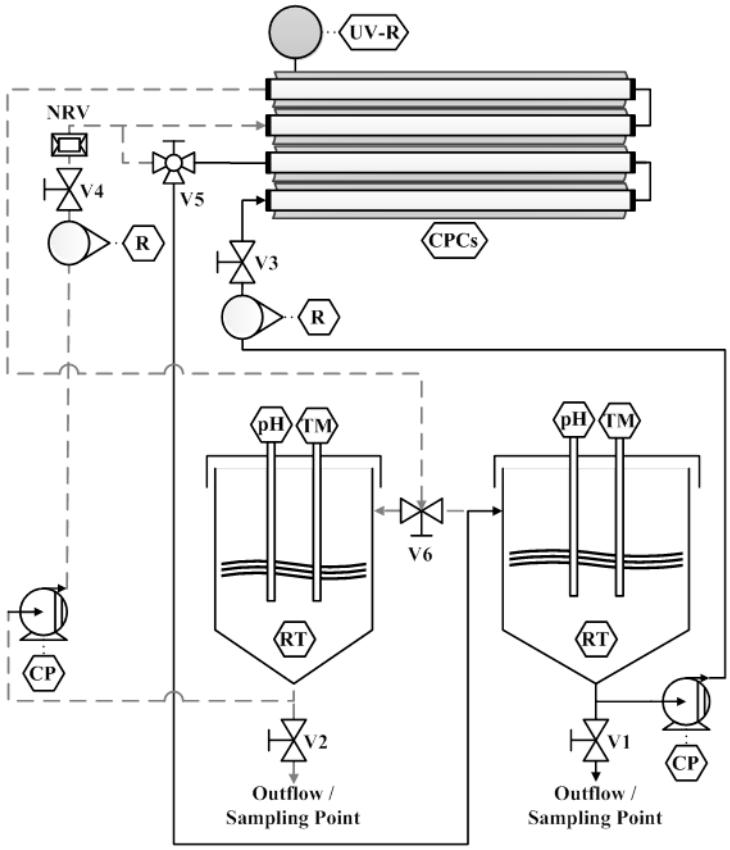

(c)

Figure 3.6 (a) Frontal view and (c) back view of the solar pilot plant with CPCs.(c) Plant scheme: TM – Temperature meter; pH – pH-meter; CPCs – Compound Parabolic Collectors; UV-R – UV radiometer; RT - Recirculation tank; CP – Centrifugal pump; R – Rotameter; V1 and V2 – Recirculation / Discharge valves; V3, V4– Flow rate control valves; V5 – CPCs mode valve; V6 – RTs feeding valve; ── Main path; --- - Alternative path; NRV – Non-return valve. Reprinted (adapted) with permission from Pereira et al. (2013). Copyright © 2013, Springer-Verlag Berlin Heidelberg, License Number: 3219390117722.

3.8 Analytical methods

3.8.1 Light and Transmission Electron Microscopy – TEM

Visual cyanobacteria analysis was performed by means of Light and Transmission Electron Microscopy – TEM - in the Institute for Molecular and Cell Biology (IBMC) at the University of Porto. Collected cyanobacteria samples were immediately centrifuged and fixed with 2% glutaraldehyde in 50 mM sodium cacodylate buffer (pH 7.2) for 2 h, washed three times in double-strength buffer, post fixed with 2% osmium tetroxide in 50 mM sodium cacodylate buffer (pH 7.2) for 2 h, and washed again in double-strength buffer. The dehydration was firstly performed using an ethanol series (25–100%; v/v), and secondly with propylene oxide. Samples were then embedded in mixtures of propylene oxide and Epon resin, followed by Epon resin only for at least 24 h, before being placed in embedding moulds with Epon, and allowed to polymerize at 55 ± 1 ºC. Thin sections were cut with a Leica Reichert Supernova Ultramicrotome and mounted in copper grids. The sections were contrasted before being visualized using an electron microscope TEM Jeol JEM-1400 operating at 80 kV (Seabra et al., 2009).

3.8.2 UV spectra and photometric measurements

The UV spectra of MC-LR solutions at pH 1.0, 3.0, 7.0 and 12.0, and of CYN solutions at pH 3.0, 7.0, 9.0 and 12, as also of the natural water and natural water spiked with MC-LR or CYN were obtained by a VWR UV-6300 PC Double Beam Spectrophotometer.

3.8.3 MC-LR analysis

3.8.3.1 Sample clean up and concentration - liquid phase preparation

The procedure to sample clean up and concentration was described in section 3.3 (v), but a Strata C18-E (55um, 70A) 500 mg/ 6 mL or a Phenomenex Sep-Pak® Vac 60 mL C18–10 g cartridge, depending of the initial MC-LR concentration, were used.

To determine MC-LR in the filtrate (liquid phase), each sample was applied directly to the cartridge, which had been preconditioned using 100% MeOH and distilled water. The cartridge was then washed with 20% MeOH and the toxin was eluted with 80% MeOH. The MC containing fraction was evaporated in speed vacuum constituted by one CentriVap concentrator (from LABCONCO), a CentriVap cold trap (-50 ºC) (from LABCONCO) and a vacuum pump (from ILMVAC) until complete removal of the methanol. The residue was suspended in 300 µL of 50% aqueous methanol and analyzed by HPLC-PDA.

3.8.3.2 Particulate phase preparation

When working with live cells, it was also necessary to analyze the MC-LR remaining inside the cell. The sample was filtered using glass microfibers filter with pore diameter of 1.5 µm (GF/C) from VWR. The filter containing the particulate phase was washed with 30 mL of 50% aqueous methanol. The resulting washing solution was sonicated (60 Hz, 5 min) and centrifuged (4495 g, 15 min, 4 ºC). The supernatant was evaporated and the residue was resuspended in 1.5 mL of 50% aqueous methanol and finally quantified by HPLC-PDA.

3.8.3.3 Microcystin-LR identification by HPLC-PDA

The chromatographic system consisted of a Waters Alliance 2695 HPLC equipped with a photodiode array detector 2998. The MC-LR analytical assay was performed using a reversed phase endcapped column from Merck (Lichrospher RP-18, 25 cm × 4.6 mm, 5 µm) coupled to a guard column (Merck Lichrospher RP-18 endcapped, 4 × 4 mm, 5 µm), both kept at 40 ºC. The eluents were methanol and water both acidified with 0.1% TFA, fed to the chromatograph at a flow rate of 0.9 mL min^{-1}. A linear gradient elution in three steps was adopted: 55–65% methanol acidified with 0.1% TFA in 5 min, increasing to 80% and 100% also in intervals of 5 min. An equilibration step to the initial organic percentage was applied over 10 min. The injected volume was 50 µL. The PDA range was 210–400 nm, with a fixed wavelength at 238 nm, according to Lawton and Edwards (2001).

3.8.3.4 Microcystin-LR quantification and degradation by-products identification by LC-MS/MS

The identification of MC-LR and degradation by-products was performed by LC-MS/MS system (LCQ Fleet ion trap MSn, ThermoScientific, USA) with an electrospray (ESI) interface, including a Surveyor LC pump, a Surveyor autosampler and a Surveyor photoelectric diode array (PDA) detector. Separation was achieved on a C18 Hypersil Gold column (100 × 4.6 mm I.D., 5 µm, ThermoScientific, USA) kept at 25 ºC. The injected volume was 25 µL. The equipment was operated in gradient mode at a flow rate of 0.8 mL min^{-1}. The mobile phase MeOH (A), and water (B), both acidified with 0.1% formic acid. Mobile phase A was linearly increased from 55% to 90% in 12 min, then increased to 100% in 0.5 min, held for 2.5 min, and finally brought back to 55% and held for 10 min until the next injection. The retention time of MC-LR was 31.5 min. The mass spectrometer was operated in a multiple-reaction monitoring mode (MRM) with collision energy of 35 eV. The capillary voltage and tube lens were maintained at 22 and 120 V, respectively. Nitrogen was used as the sheath and auxiliary gas. Helium was used as the collision gas in the ion trap. The sheath gas flow rate was set at 80 (arb units), and the capillary temperature was held at 350 ºC. Samples were analyzed using the mass-to-charge ratio (m/z) transition of 995 > 599 at 23 V collision energy. The MC-LR transition was monitored over one micro-scan.

3.8.4 CYN analysis

Quantification of CYN in the aqueous samples was performed in the Biotechnology Innovation Center (BIOCANT), on an Ultimate™3000 LC system (LC Packings, Dionex) coupled to an ESI Turbo V ion source and an hybrid triple quadrupole/linear ion-trap 4000 QTrap mass spectrometer operated by Analyst 1.6.1 (AB Sciex). The chromatographic separation was performed in a 3 μm Luna NH_2 column (150 × 2.0 mm, 100 Å, Phenomenex) with a 4 × 2.0 mm NH_2 guard-column (Phenomenex). The flow rate was set to 150 μL min^{-1} and mobile phase A (MP A) and B (MP B) were 0.1% formic acid in water and 0.1% formic acid in acetonitrile, respectively. The LC program started with a linear gradient from 50% to 5% of B (0 - 0.5 min) and it was maintained at 5% of B for 6 min. After each sample analysis, a 6 min run was performed in isocratic mode with 50% of B for column equilibration. The ionization source was operated in the positive mode set to an ion spray voltage of 5500 V, 30 psi for nebulizer gas 1 (GS1), 2 atm for the nebulizer gas 2 (GS2), 1.36 atm for the curtain gas (CUR) and the temperature was 450 °C.

Cylindrospermopsin was quantified by Multiple Reaction Monitoring (MRM) triple quadrupole scan mode, at unit resolution both in Q1 and Q3 and the MRM transitions were 416.4/194.3 (used for quantification), 416.4/176.1 and 416.4/336.5 (both used for compound confirmation). The MRM parameters used were 10 eV for the entrance potential (EP), 15 eV for the collision cell exit potential (CXP), 100 V for the declustering potential (DP) and the collision gas (CAD) was set to 0.54 atm. The dwell time was set to 100 ms and the collision energies were 50 eV for transition 416.4/176.1, 60 eV for transition 416.4/176.1 and 32 eV for transition 416.4/336.5. Peak areas were integrated by MultiQuant software (version 2.1, AB Sciex). The calibration curve used for the quantification was constructed by injecting 10μL of seven different known concentrations of the pure standard (2.6 – 166 ng mL^{-1}) and analyzing by LC-MS/MS.

3.8.5 Dissolved organic carbon (DOC)/Dissolved nitrogen

Dissolved organic carbon (DOC) was determined in a TC-TOC-TN analyzer equipped with an ASI-V autosampler (Shimadzu, model TOC-VCSN) and provided with a NDIR detector, calibrated with standard solutions of potassium hydrogen phthalate (total carbon) and a mixture of sodium hydrogen carbonate/carbonate (inorganic carbon). Dissolved nitrogen was measured in the same TC-TOC-TN analyser coupled with a TNM unit (Shimadzu, model TOC-VCSN) calibrated with standard solutions of potassium nitrate, through thermal decomposition and NO detection by chemiluminescence methods.

3.8.6 Inorganic ions

Anions and cations (sulfate, chloride, nitrite, nitrate, phosphate, ammonium, sodium, potassium, calcium and magnesium) were measured by ion chromatography (Dionex ICS-2100 and Dionex DX-120 for anions and cations, respectively), using DionexIonpac AS9-HC/CS12A 4 mm × 250 mm columns and ASRS®300/CSRS®300 4 mm suppressors, respectively for anions and cations. The programme for anions/cations determination comprises a 12 min run with 30 mM NaOH or 20 mM methanesulfonic acid at a flow rate of 1.5 or 1.0 mL min^{-1}, respectively.

3.8.7 H_2O_2 and dissolved iron

The evaluation of H_2O_2 concentration during the experiments was performed by the metavanadate method, based on the reaction of H_2O_2 with ammonium metavanadate in acidic medium, which results in the formation of a red-orange color peroxovanadium cation, with maximum absorbance at 450 nm (Nogueira et al., 2005).

Iron concentration was determined by colorimetry with 1,10-phenantroline according to ISO-6332 (1988). The absorbance measurements to determine the concentration of dissolved iron and H_2O_2 were performed in a Spectroquant® Pharo 100 (Merck) spectrophotometer.

3.9 References

Águia, C., Ângelo, J., Madeira, L.M., Mendes, A., 2010. Influence of photocatalytic paint components on the photoactivity of P25 towards NO abatement. Catalysis Today 151, 77-83.

Águia, C., Ângelo, J., Madeira, L.M., Mendes, A., 2011a. Influence of paint components on photoactivity of P25 titania toward NO abatement. Polymer Degradation and Stability 96, 898-906.

Águia, C., Ângelo, J., Madeira, L.M., Mendes, A., 2011b. Photo-oxidation of NO using an exterior paint – Screening of various commercial titania in powder pressed and paint films. Journal of Environmental Management 92, 1724-1732.

Anderson, M.A., Miller, L.W., Tejedor-Anderson, Isabel, M., 2001. A waveguide comprising a transparent substrate and a metal oxide coating having the disclosed properties on the substrate can propagate light in an attenuated total reflection mode. , United States Patent

Antoniou, M.G., Shoemaker, J.A., de la Cruz, A.A., Dionysiou, D.D., 2008. LC/MS/MS structure elucidation of reaction intermediates formed during the TiO2 photocatalysis of microcystin-LR. Toxicon 51, 1103-1118.

Guillard, R.R.L., Sieracki, M.S., 2005. Algal culturing techniques, in: Andersen, R.A. (Ed.), Algal culturing techniques. Elsevier Academic Press, Oxford, pp. 253-268.

ISO-6332, 1988. Water Quality – Determination of iron – Spectrometric Method Using 1,10-Phenanthroline.

Kotai, J., 1972. Instructions for preparation of modified nutrient solution Z8 for algae. Norwegian Institute for Water Research 11, 5.

Lopes, F.V.S., Miranda, S.M., Monteiro, R.A.R., Martins, S.D.S., Silva, A.M.T., Faria, J.L., Boaventura, R.A.R., Vilar, V.J.P., 2013. Perchloroethylene gas-phase degradation over titania-coated transparent monoliths. Applied Catalysis B: Environmental 140-141, 444-456.

Malato, S., Blanco, J., Vidal, A., Richter, C., 2002. Photocatalysis with solar energy at a pilot-plant scale: an overview. Applied Catalysis B: Environmental 37, 1-15.

Pereira, J.O.S., Reis, A., Nunes, O., Borges, M., Vilar, V.P., Boaventura, R.R., 2013. Assessment of solar driven TiO2-assisted photocatalysis efficiency on amoxicillin degradation. Environmental Science and Pollution Research, 1-12.

Quici, N., Vera, M.L., Choi, H., Puma, G.L., Dionysiou, D.D., Litter, M.I., Destaillats, H., 2010. Effect of key parameters on the photocatalytic oxidation of toluene at low concentrations in air under 254 + 185 nm UV irradiation. Applied Catalysis B: Environmental 95, 312-319.

Ramanan, S., Tang, J., Velayudhan, A., 2000. Isolation and preparative purification of microcystin variants. Journal of Chromatography A 883, 103-112.

Seabra, R., Santos, A., Pereira, S., Moradas-Ferreira, P., Tamagnini, P., 2009. Immunolocalization of the uptake hydrogenase in the marine cyanobacterium Lyngbya majuscula CCAP 1446/4 and two Nostoc strains. FEMS Microbiology Letters 292, 57-62.

Soares, P., Silva, T.C.V., Manenti, D., Souza, S.A.G.U., Boaventura, R.R., Vilar, V.P., 2013. Insights into real cotton-textile dyeing wastewater treatment using solar advanced oxidation processes. Environmental Science and Pollution Research in press, 1-14.

Welker, M., Bickel, H., Fastner, J., 2002. HPLC-PDA detection of cylindrospermopsin--opportunities and limits. Water Research 36, 4659-4663.

4 Decomposition of *Microcystis aeruginosa* and Microcystin-LR by TiO_2 Oxidation Using Artificial UV Light or Natural Sunlight

In this chapter, it is reported the destruction of M. aeruginosa and the toxin microcystin-LR (MC-LR) by photolysis and TiO_2 photocatalysis in a lab-scale photoreactor prototype using artificial UV light and in a pilot-scale plant using natural solar radiation, as UV photon source. TiO_2 photocatalysis showed to be effective in the destruction of M. Aeruginosa (~ 5-log order) and in the inactivation of MC-LR released into the aqueous solutions, in the reaction period between 5-15 min, even at extremely high concentrations (1.87 µg mL^{-1}). The photocatalytic process can be considered as a viable alternative for disinfection of contaminated water by cyanobacteria, especially in countries with high solar insolation. Oppositely, UV light or sunlight alone is not sufficient to achieve complete elimination of cells and inactivation of MC-LR in full-scale water treatment.

This Chapter is based on the research article "Pinho, L.X., Azevedo, J., Vasconcelos, V.M., Vilar, V.J.P., Boaventura, R.A.R., 2012. Decomposition of Microcystis aeruginosa and Microcystin-LR by TiO_2 Oxidation Using Artificial UV Light or Natural Sunlight. Journal of Advanced Oxidation Technologies 15,98-106".

4.1 Introduction

Cyanobacteria produce different types of toxins (cyanotoxins) that are classified as hepatotoxins, neurotoxins or dermatotoxins according to their mechanism of toxicity in humans (Chorus and Bartram, 1999). The most common cyanotoxins found in water are the hepatotoxic microcystin (MC), which represents a group of at least 70 peptides produced primarily by freshwater cyanobacteria belonging to the genera *Microcystis, Anabaena, Nostoc* and *Oscillatoria* (Lawton et al., 2003).

MC-LR is a cyclic heptapeptide containing the unusual amino acid 3-amino-9-methoxy-2,6,8-trimethyl-10-phenyldeca-4,6-dienoicacid (ADDA), and also leucine (L) and arginine (R) in the variable positions. MC-LR has caused the death of animals and acute intoxication in humans as a result of ingestion of contaminated water. It is also reported that long-term exposure to sublethal levels of microcystin may promote primary liver cancer by disruption of protein phosphates 1 and 2A (Lee et al., 2004). MC is known to be stable compounds, possibly as a result of their cyclic structure, withstanding many hours of boiling and may persist for many years when dry stored at room temperature. Therefore MC is not removed from drinking water by conventional treatment methods (Lawton and Robertson, 1999).

MC is produced and retained inside healthy cyanobacterial cells and is only released into the surrounding water when cells die. They can, therefore, enter in the water treatment plant either as dissolved compounds in the raw water or within cells. Partitioning of this nature presents a unique challenge to water treatment process. Removal of toxin containing cells at the early stages of treatment can be a relatively straightforward way of reducing the microcystin burden. Great care must be taken to prevent cell lyses otherwise the toxin will move into the water phase and the benefit is negated (Lawton and Robertson, 1999).

Traditional water treatment methods such as chemical coagulation, flocculation, and sand filtration are often completely ineffective in cyanobacterial toxins removal. Treatment by chlorination requires high doses and long contact times, and there is the possibility of generating toxic by-products such as trihalomethanes (Feitz et al., 1999).

Advanced Oxidation Processes (AOPs) may be used for decontamination of water containing organic pollutants classified as bio-recalcitrant, and/ or for disinfection of current and emerging pathogens. These methods rely on the formation of highly reactive chemical species which degrade even the most recalcitrant molecules into biodegradable compounds or achieve complete mineralization into CO_2, H_2O and mineral acids. Although there are different reacting systems, many of them are characterized by the same chemical feature, production of hydroxyl radicals ($HO^{\bullet}$), which are able to oxidize and mineralize almost any organic molecule. Constant rates (k_{OH}, $r = k_{OH}\,[HO^{\bullet}]\,C$) for most reactions

involving hydroxyl radicals in aqueous solution are usually on the order of 10^6 to10^9 M^{-1} s^{-1}. They are also characterized by their non-selective attack, which is a useful attribute when dealing with complex mixtures of pollutants (Malato et al., 2009).

The photocatalysis is an efficient AOP in which free hydroxyl radicals $OH^{\bullet}$ are generated by irradiating semiconductors in water with artificial or natural radiation. The MC can be rapidly decomposed in a photocatalytic reactor and the use of the semiconductor catalyst leads to faster reaction rates than UV radiation alone (photolysis) (Shephard et al., 1998). These materials can be engineered into flow-through reactors representing a feasible option for solar-driven water treatment technologies or for the remediation of contaminated water with cyanobacterial toxins or other emerging contaminants of concern using visible light-activated TiO_2 photocatalyst under solar irradiation (Antoniou et al., 2008).

TiO_2 photocatalysis has been previously shown to effectively destroy MC-LR and related toxins in aqueous solutions even at extremely high concentrations using UV lamps (Liu et al., 2009; Robertson et al., 1997). In most of the studies, the aqueous solutions of MC-LR containing TiO_2 were irradiated with a UV lamp. A new perspective is to study the effects of using UV photons from solar light for destruction of these contaminants.

In this study we report the destruction of *M. aeruginosa* and the toxin MC-LR by photolysis and TiO_2 photocatalysis in a lab-scale photoreactor prototype using artificial UV radiation and in a pilot-scale plant with CPCs using natural solar radiation, as UV photon source.

4.2 Material and methods and experimental procedure

The material and methods employed for the development of this work are described in Chapter 3 (sections: 3.1 – 3.3/ 3.6.1/ 3.6.3/ 3.7.3.1 – 3.7.3.3).

4.2.1 Experimental procedure

4.2.1.1 Lab-scale glass immersion photoreactor

The reactor was loaded with 850 mL of solution with constant stirring for a total reaction period of 40 min. A first control sample was taken for further characterization. Tap water was used, because the use of distilled water can cause cell lysis by osmotic pressure between the cells and the water. The water was dechlorinated in a glass bottle with mechanical agitation for 24 hours before starting the experiments. The total and residual chlorine was analyzed according to Standard Methods (Eaton, 2005) and the content was < 0.002 mg Cl_2 L^{-1}. Normally, chlorination treatments require higher doses of chlorine and longer contact times (Feitz et al., 1999). The residual chlorine present in water used

for our studies has a negligible influence in the destruction of *M. aeruginosa* and MC-LR. Temperature and pH were measured using a pH meter HANNA HI8424. The solution pH was adjusted between 7.7 and 8.0, similar to the growth medium of cyanobacteria. Temperature was controlled below 35 °C.

A control experiment in the absence of artificial UV radiation was conducted to identify possible losses of cells. A solution of 850 mL of water and *M. aeruginosa* inoculum was used with an initial concentration of 2.8×10^5 cell mL^{-1}.

100 mL of *M. aeruginosa* inoculum with a density of 1×10^7 cell mL^{-1} and 1.4×10^7 cell mL^{-1}, respectively for the photolysis and photocatalytic experiments, were diluted with dechlorinated water in order to get a final solution volume of 850 mL. In the case of the photocatalytic experiments, 200 mg TiO_2 L^{-1} were added to the cyanobacteria suspension. For TiO_2/UV tests, a second sample was collected just before uncovering the CPC units, in order to evaluate the cells adsorption onto the catalyst surface.

It should also be underlined that catalyst concentration (200 mg TiO_2 L^{-1}) is the optimum concentration for the photoreactors used in this work, with an internal diameter of 46.4 mm,(Malato Rodríguez et al., 2004; Vilar et al., 2009) which has recently been supported by accurate modeling of radiation field in a CPC solar photoreactor by a six-flux absorption scattering model (SFM), showing that TiO_2 in the concentration of 200 mg L^{-1} is able to absorb 100 % of the solar UV photons (Colina-Márquez et al., 2010).

For the UV test, no TiO_2 addition was performed. In all cases, samples were taken at successive time intervals to evaluate the progress of the oxidation.

4.2.1.2 Pilot scale solar photoreactor

Each recirculation tank was filled with 20 L of tap water. The tap water was pumped between the recirculation tank and the CPC tubes to dechlorination during 24 hours before starting the experiment (the content of residual and total chlorine was < 0.002 mg Cl_2 L^{-1} (Eaton, 2005)). The pH was adjusted with NaOH (w/v= 50 %) between 7.7 and 8.0.

In the next day the cyanobacteria suspension was added and mixed during 10 min in order to obtain a perfectly homogeneous suspension. A control sample was taken to determine the initial concentration of the contaminant in both tanks. In the case of the photocatalytic experiments, after taking the control sample, TiO_2 particles were added to the recirculation tank ([TiO_2] = 30 and 50 mg L^{-1}), and samples were taken at pre-defined times to evaluate the degradation process.

It should be underlined that the catalyst concentration (200 mg TiO_2 L^{-1}) is the optimum concentration for the solar photoreactors used in this work (Malato Rodríguez et al., 2004). However, for the evaluation of toxin inactivation it was used lower doses of TiO_2, since the sample filtration step necessary for the quantification of MC-LR was much simpler, and reported results by Antoniou et al. (2008) showed that TiO_2 concentrations of 50 mg L^{-1} are the optimum range for these kinds of applications.

Photocatalytic and photolysis experiments were performed at the same time, in the same weather conditions, using each one two CPC borosilicate tubes (Table 1). The experimental conditions for Experiment 1 were: initial concentration of 5.3×10^6 cell mL^{-1}, 6.5 h of treatment for photolysis and photocatalysis (50 mg L^{-1} TiO_2); and for experiment 2 were: initial concentration of 6.6×10^6 cell mL^{-1}, a total treatment time of 2.0 h (photocatalysis with 30 mg TiO_2 L^{-1}) and 6 h (photolysis).

Control experiments in the absence of solar UV radiation were conducted to identify possible losses of cells for a period of 60 min using ([TiO_2] = 30 and 50 mg L^{-1}) and initial *M. aeruginosa* concentration of 3.6×10^5 cell mL^{-1} and 4.35×10^5 cell mL^{-1} respectively.

In all cases, samples were taken at successive time intervals to evaluate the progress of the oxidation systems, considering the cell concentration and, eventually intracellular and extracellular cyanotoxin MC-LR concentration. The analysis of intracellular and extracellular cyanotoxin concentration carried out according to described on section 3.8.3.1 – 3.8.3.3.

4.3 Results and discussion

4.3.1 Removal of *M. aeruginosa* in the laboratory-scale photocatalytic reactor

The concentration of *M. aeruginosa* remaining in the solution over time in the absence of UV radiation, only decreased from 2.8×10^5 cell mL^{-1} to 2.0×10^5 cell mL^{-1} (29 %) after 40 min of exposure.

The effects of photocatalysis with 200 mg TiO_2 L^{-1} and photolysis on the removal of *M. aeruginosa* in the presence of artificial UV radiation are shown in Figure 4.1. *M. aeruginosa* cell density under photolysis conditions remained approximately constant throughout the experiment (40 min of irradiation).

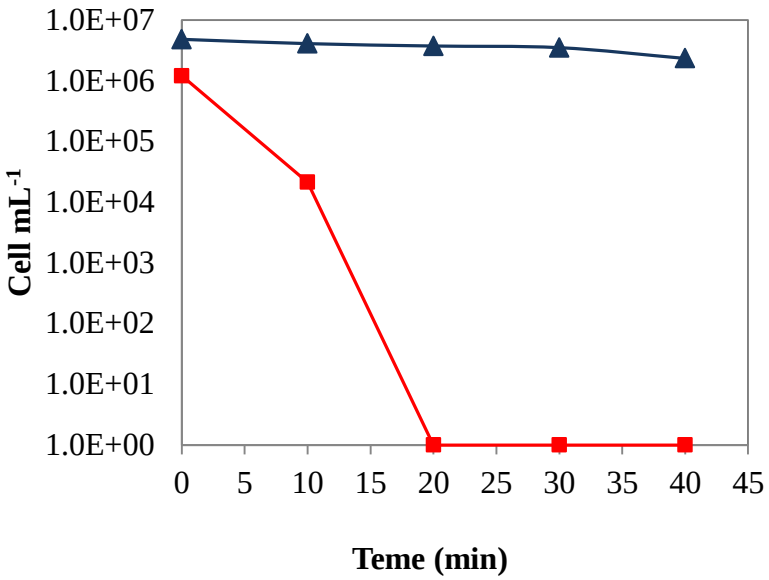

Figure 4.1 *M. aeruginosa* removal in the lab-scale photocatalytic reactor: ▲ photolysis and ■ photocatalysis with 200 mg L^{-1} of TiO_2.

The same irradiation source in the presence of 200 mg L^{-1} of TiO_2 led to a complete decontamination after 20 min of artificial irradiation, which is equivalent to 2.6 kJ of accumulated UV energy per liter of water. The results support the hypothesis that an adsorption process by TiO_2 in dark experiment and the photolysis, contributes only for a low concentration reduction of *M. aeruginosa*, comparing with the photocatalytic process that is much more efficient.

4.3.2 Removal of *M. aeruginosa* in the CPC photoreactor

The results from the inactivation of *M. aeruginosa* in water by photolysis and photocatalysis under natural solar radiation, presented in Figure 4.2, are in accordance with those obtained with artificial UV radiation. The decrease in the concentration of *M. aeruginosa* by solar photocatalysis was approximately 5-log (complete disappearance), when using [TiO_2] = 50 mg L^{-1} and only 1-log by photolysis. Less than 1.3 kJ of accumulated UV energy per liter of water (30 min at ~ 32 W_{UV} m^{-2}) was needed to have a complete disappearance of *M. aeruginosa* using 50 mg L^{-1} of TiO_2. Solution temperature during experiment ranged from 20.1 ºC to 27.5 ºC, which is not enough to destroy the MC-LR, since reported results showed that they can withstand many hours of boiling (Lawton and Robertson, 1999).

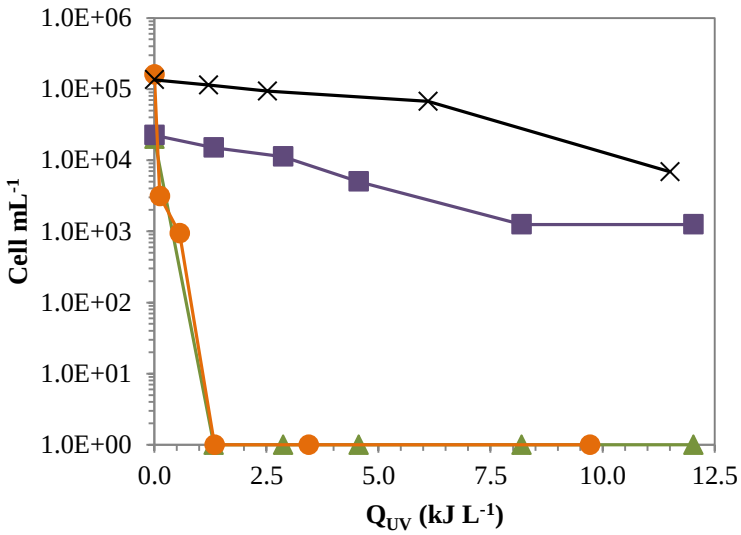

Figure 4.2 *M. aeruginosa* degradation with and without TiO_2 in the CPC photoreactor (experiment 1: ▲ [TiO_2] = 50 mg L^{-1}; ■ photolysis) and (experiment 2: ● [TiO_2] = 30 mg L^{-1}; × photolysis).

The same behaviour was observed in experiment 2, using a lower concentration of TiO_2 (30 mg L^{-1}), even for a higher initial concentration of *M. aeruginosa* (Figure 4.2). Solution temperature ranged from 24.3 ºC to 30.1 ºC. Photolysis showed that even after 360 min of solar exposition (25.6 kJ_{UV} L^{-1} at an average solar radiation of 28 W_{UV} m^{-2}), only a decrease on *M. aeruginosa* concentration of 1-log was observed.

In the absence of solar UV radiation there was a decrease of around 50 % after 20 min, however no difference was observed between 20 and 60 min of exposure for both experiments, with 30 mg L^{-1} and 50 mg L^{-1}. Higher removal efficiencies were obtained at pilot scale than using a laboratory-scale photoreactor (200 mg L^{-1} of TiO_2) (Figure 4.3), probably associated to the recirculation system which may have caused some cell rupture.

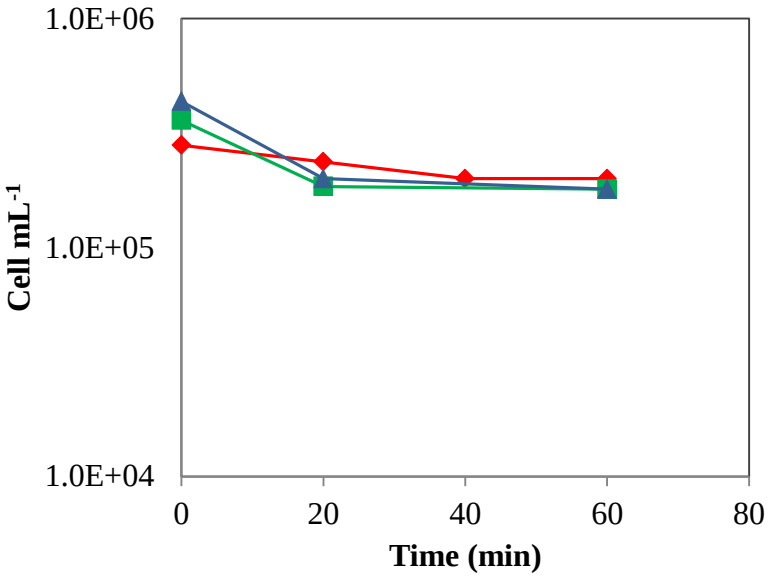

Figure 4.3 *M. aeruginosa* disappearance in the presence of TiO_2 and in the absence of UV light, using a lab and pilot scale photoreactors. CPC: ▲ 50 mg L^{-1}, ■ 30 mg L^{-1}; Lab-scale: ● 200 mg L^{-1}.

Table 4.1 summarizes different methodologies used for the inactivation of cyanobacteria, according to the work conditions, as treatment time, initial cellular concentration and genera. Ozonation and slow filtration achieved 100 % of cells destruction (Humbert et al., 2000), which can be comparable to the present work, which had a complete and fast destruction of *M. aeruginosa*.

Table 4.1 Removal of cyanobacteria by different methods.

Organism	Disinfection method	Reaction time	Initial concentration Cell mL^{-1}	Efficiency	Reference
O. tenuisa	$ZnO/\gamma\text{-}Al_2O_3$ 130-525 mg L^{-1} solar lamp	25 h	1.5×10^5	92 %	(Huang et al., 2011)
M. aeruginosa	Ultrasonic 25kHz, 0.32W/mL	5 min	10^{11}	10.8 %	(Zhang et al., 2006)
A. circinalis	Ultrafiltration	120 min	5×10^5	100 %	(Dixon et al., 2011)
	ACH (4.4 mg Al^{3+} L^{-1})	70 min	3.8×10^5	74 %	
	ACH (4.4 mg Al^{3+} L^{-1})/ GAC (20 mg L^{-1})	80 min	3.6×10^5	87 %	
M. flos-aquae	ACH (4.4 mg L^{-1} Al^{3+})	20 min	1.3×10^7	73 %	(Dixon et al., 2011)
	ACH (4.4 mg L^{-1} Al^{3+})/ GAC (20 mg L^{-1})	30 min	1.5×10^8	73 %	
P. rubescens	Preozonation (1 mg L^{-1}) Preozonation (1 mg L^{-1}) /Rapid filtration (pumice/quartz sand)	After two treatment steps of five in treatment plant	3×10^4	20 %	(Hoeger et al., 2005)
Microcystis, Anabaena	FLSE/GAC/SF/CHL	Drinking water reservoir	$< 2.2 \times 10^6$	99 %	(NH et al.)
P. rubescens	Ozonation/SF	Drinking water reservoir	$< 1.2 \times 10^4$	100 %	(Humbert et al., 2000)
		Present work			
M. aeruginosa	TiO_2 200 mg L^{-1}/ UV lamp	20 min	10^6	100 %	
M. aeruginosa	TiO_2 50 mg L^{-1}/UV solar	1.3 kJ_{UV} L^{-1} (30 min)	5.3×10^6	100 %	
M. aeruginosa	TiO_2 30 mg L^{-1}/ UV solar	1.3 kJ_{UV} L^{-1} (30 min)	6.6×10^6	100 %	

ACH - aluminum chlorohydrate (coagulant), CHL - Chlorination, GAC - granular activated carbon, FLSE - flocculation/sedimentation, SF - slow filtration.

4.3.3 Photocatalytic inactivation of MC-LR using the CPC photoreactor

The photocatalytic destruction of MC due to cell lysis was investigated in the samples from the experiment 2 performed in the CPC photoreactor. Table 4.2 shows respectively the evolution of MC-LR concentration in both dissolved and particulate phases, for the systems with sunlight plus TiO_2 and

only sunlight. In the initial control samples, the presence of toxins was only detected in the particulate phase, for both processes, which means that up to this moment the cells were intact.

Table 4.2 Evolution of Microcystin-LR (MC-LR) concentration in the water (liquid phase) and in the filter (particulate phase) for the photocatalytic and photolysis processes.

Photocatalytic process					**Photolysis process**				
Time min	Q_{UV} $kJ_{UV}\ L^{-1}$	MC-LR $\mu g\ mL^{-1}$ LP	MC-LR $\mu g\ mL^{-1}$ PP	Cell mL^{-1}	Time min	Q_{UV} $kJ_{UV}\ L^{-1}$	MC-LR $\mu g\ mL^{-1}$ LP	MC-LR $\mu g\ mL^{-1}$ PP	Cell mL^{-1}
0	0.00	0.0	1.87	1.6×10^{5}	0	0.00	0.0	1.55	1.4×10^{5}
5	0.12	0.45	0.0	3.1×10^{3}	30	1.21	0.0	1.45	1.1×10^{5}
15	0.57	0.0	0.0	9.4×10^{2}	60	2.52	0.0	1.36	9.4×10^{4}
30	1.34	0.0	0.0	0.0	120	6.11	0.95	0.43	6.7×10^{4}
60	3.43	0.0	0.0	0.0	180	11.43	0.49	0.0	6.9×10^{3}
120	9.72	0.0	0.0	0.0	360	25.60	0.52	0.0	5.0×10^{3}

During the photocatalytic reaction, and consequently hydroxyl radical formation and interaction with the cells, a release of MC-LR to the liquid phase was observed. However, after 5 minutes of photocatalytic reaction, no MC-LR was detected in the liquid and particulate phase, although total inactivation of cells occurs only after 30 minutes. This suggests a rapid inactivation of MC-LR toxin once released into water by cell lysis, which is in agreement with the results obtained by different authors (Lawton and Robertson, 1999; Lawton et al., 2003; Robertson et al., 1997; Shephard et al., 1998).

Feitz et al. (1999) reported a rapid inactivation of MC-LR combining UV light (280 W spectral output 330 - 450 nm) with TiO_2, with little toxin detectable by HPLC after 20 min. This destruction was not observed when MC-LR was illuminated in the absence of TiO_2 (Lawton and Robertson, 1999). In the same work, following the complete disappearance of MC-LR, the catalyst was subjected to solvent extraction to determine if residual toxin was adsorbed to the surface, but no residual toxin was detected on the TiO_2 surface. The same result was observed in aqueous solutions of MC (LR, RR, LW and LF) irradiated in the presence of TiO_2 by an UV lamp (480 W with spectral output 330-450 nm) (Lawton et al., 2003), even for high concentrations of toxin, which were completely undetectable after 10-40 min, depending on the initial concentration in the range of 50-200 μM (Robertson et al., 1997).

Liu et al. (2009) using different TiO_2 powders (P25, PC50, PC100, PC500 and UV100) and illuminated with a 480 W Xenon lamp (spectral output 250-600 nm) observed a fast and complete degradation of MC after 100 min irradiation. TiO_2, P25 from Degussa, the same used in present work,

appeared to be the most effective catalyst, with efficiency higher than 90 % for the toxin destruction within 20 min irradiation.

TiO_2 photocatalytic activity can be also efficient when combined with GAC (Liu et al., 2002) and H_2O_2 (Table 4.3) (Lee et al., 2004). Lee et al. (2004) showed that the combination of granular activated carbon with TiO_2 (GAC/TiO_2/UV), completely dispersed in an aqueous phase with MC-LR, led to toxin disappearance in approximately 20 min, although in the absence of radiation the MC-LR concentration remained constant. The experiment with only GAC/UV destroyed 50 % of the toxin after 30 min, which is substantially lower that the efficiency obtained in this work with the TiO_2/UV system.

The results of this work were also better than those obtained by Pelaez et al. (2009) using visible light and N-F-codoped TiO_2 to destroy MC-LR, because they required a longer exposure time for a complete destruction.

Table 4.3 Inactivation of microcystin by different methods.

Inactivation method	Reaction condition	Reaction time (min)	Initial concentration	Efficiency	Analytical method	Reference
TiO_2/UV UV only	280 W 330-450 nm	20	200 µg mL^{-1}	Little toxin detectable No destruction	HPLC	(Lawton et al., 1999)
TiO_2/UV	480 W 330-450nm	10-40	50-200 µM	100 %	HPLC	(Robertson et al., 1997)
TiO_2/UV	480 W 330-450nm	30	100-200 µg mL^{-1}	100 %	HPLC	(Lawton et al., 2003)
TiO_2/H_2O_2/UV	480 W 330-450nm	5 10	1000 µg mL^{-1}	99.6 % 100 %	HPLC	(Liu et al., 2002)
GAC/TiO_2/UV GAC/TiO_2 GAC/UV	4 W 370 nm	20 20 30	200 µg mL^{-1}	100 % 0 % 50 %	HPLC	(Lee et al., 2004)
N-F-codoped TiO_2/Visible light	15 W	300	1 mg L^{-1}	100 %	HPLC	(Pelaez et al., 2009)
Ozonation	1.12 mg O_3 L^{-1}	4	116 µg L^{-1}	> 99 %		(Rositano et al., 1998)
Photo-Fenton Fe^{2+}/H_2O_2/UV	Fe^{2+} 0.25 mM/ H_2O_2 0.1-0.5 mM 36 W UV lamp, 365nm	35-40	8 µM	100 %	HPLC	(Bandala et al., 2004)
Fenton Fe^{2+}/H_2O_2	Fe^{2+} 2.5 mM/ H_2O_2 5 mM	180	3 µM	61 %	HPLC	(Bandala et al., 2004)
Ultrafiltration	PVDF membranes		5.9 µg L^{-1}	70 %	HPLC	(Dixon et al., 2011)
Ultrasonic	640 kHz	6	2.7 µM	85 %	HPLC	(Song et al., 2005)
Radiolysis/gamma irradiation	0.2-8 kGy	-	0.8 mg L^{-1}	98.8 %	HPLC	(Zhang et al., 2007)

GAC - granular activated carbon, PVDF - polyvinylidene fluoride

The results reported in the present work are comparable to other technologies, like ozonation (Rositano et al., 1998) and photo-Fenton (Bandala et al., 2004), radiolysis (Zhang et al., 2007), and

better than ultrafiltration, which seems a good method for cyanobacterial cells removal (Humbert et al., 2000), although only presents 70 % cyanotoxin removal (Dixon et al., 2011).

Others AOPs can also be efficient, such as radiolysis (Zhang et al., 2007) and ultrasonically in high frequency. For example, Song et al. (2005) reported that ultrasonically in 640 kHz destroy 85 % of MC-LR in 6 min. Although higher ultrasound power causes more violent cavitation and accelerates reactions, higher costs should be avoided (Zhang et al., 2006). According to Zhang et al. (2006), lower frequencies of 20, 80 or 150 kHz can only destroy *M. aeuginosa* and increase the extracellular MC-LR concentration of 0.87 to 3.1 μg L^{-1} due to the rupture of the cells.

In the present work, sunlight alone (photolysis) led to a very slow destruction of the cells, and consequently to a slow release of toxins to the water (Table 4.2). The MC-LR concentration in the particulate phase decreased slowly during the photolysis and was only detected in the liquid phase after 120 minutes. Even after 360 minutes of solar exposure, a continuously release of toxins to water was detected which is a consequence of the presence of life cells until the end of the experiment. Tsuji et al. (1995) reported that the toxins are easily decomposed by UV radiation (photolysis) at wavelengths around maximum absorption of the toxins, depending on the radiation intensity. Much of the work on photolysis is inapplicable to the removal of MC from potable supplies since very long reaction times would be required (Lawton and Robertson, 1999).

4.4 Conclusions

TiO_2 photocatalysis using solar radiation appears to be a highly effective method for the treatment of cyanobacteria contaminated waters. *M. aeruginosa* is rapidly decomposed by the photocatalytic process, leading to the release of toxins, which rapidly disappear from solution. The initial cellular density in water used in this work was very high ($5.3\text{-}6.6\times10^6$ cell mL^{-1}) but comparable to dense cyanobacterial blooms. This process can be more efficient in the treatment of water containing lower cell densitie. The use of UV radiation or sunlight alone, and reaction with TiO_2 in absence of UV light are insufficient to achieve the complete elimination of cells and inactivation of toxins in a full-scale water treatment system. Therefore, the photocatalytic process can be considered as a viable alternative for disinfection of contaminated water by cyanobacteria, especially in countries with high insolation levels.

4.5 References

Antoniou, M.G., Shoemaker, J.A., de la Cruz, A.A., Dionysiou, D.D., 2008. LC/MS/MS structure elucidation of reaction intermediates formed during the TiO_2 photocatalysis of microcystin-LR. Toxicon 51, 1103-1118.

Bandala, E.R., Martínez, D., Martínez, E., Dionysiou, D.D., 2004. Degradation of microcystin-LR toxin by Fenton and Photo-Fenton processes. Toxicon 43, 829-832.

Chorus, I., Bartram, J., 1999. Toxic cyanobacteria in water: a guide to their public health consequences, monitoring, and management. Taylor & Francis.

Colina-Márquez, J., Machuca-Martínez, F., Puma, G.L., 2010. Radiation absorption and optimization of solar photocatalytic reactors for environmental applications. Environmental Science & Technology 44, 5112-5120.

Dixon, M.B., Richard, Y., Ho, L., Chow, C.W.K., O'Neill, B.K., Newcombe, G., 2011. A coagulation-powdered activated carbon-ultrafiltration - Multiple barrier approach for removing toxins from two Australian cyanobacterial blooms. Journal of Hazardous Materials 186, 1553-1559.

Eaton, A.D., L.S. Clesceri, E.W. Rice, A.E. Greenberg, M.A.H. Franson, 2005. Standard Methods for the Examination of Water and Wastewater American Public Health Association., Washington, D.C.

Feitz, A., Waite, T., Jones, G., Boyden, B., Orr, P., 1999. Photocatalytic degradation of the blue green algal toxin microcystin-LR in a natural organic-aqueous matrix. Environ. Sci. Technol 33, 243-249.

Hoeger, S.J., Hitzfeld, B.C., Dietrich, D.R., 2005. Occurrence and elimination of cyanobacterial toxins in drinking water treatment plants. Toxicology and Applied Pharmacology 203, 231-242.

Huang, W.-J., Lin, T.-P., Chen, J.-S., Shih, F.-H., 2011. Photocatalytic inactivation of cyanobacteria with ZnO/γ-Al 2 O 3 composite under solar light. Journal of Environmental Biology 32.

Humbert, J.-F., Paolini, G., Le Berre, B., 2000. Monitoring a toxic cyanobacterial bloom in Lake Bourget (France) and its consequences for water quality, Proceedings of the 9th International Conference on Harmful Algal Blooms. Hobart, Australia, pp. 496-499.

Lawton, L., Robertson, P., 1999. Physico-chemical treatment methods for the removal of microcystins (cyanobacterial hepatotoxins) from potable waters. Chemical Society Reviews 28, 217-224.

Lawton, L., Robertson, P., Cornish, B., Jaspars, M., 1999. Detoxification of microcystins (cyanobacterial hepatotoxins) using TiO_2 photocatalytic oxidation. Environ. Sci. Technol 33, 771-775.

Lawton, L., Robertson, P., Cornish, B., Marr, I., Jaspars, M., 2003. Processes influencing surface interaction and photocatalytic destruction of microcystins on titanium dioxide photocatalysts. Journal of Catalysis 213, 109-113.

Lee, D., Kim, S., Cho, I., Kim, S., Kim, S., 2004. Photocatalytic oxidation of microcystin-LR in a fluidized bed reactor having TiO_2-coated activated carbon. Separation and Purification Technology 34, 59-66.

Liu, I., Lawton, L.A., Bahnemann, D.W., Liu, L., Proft, B., Robertson, P.K.J., 2009. The photocatalytic decomposition of microcystin-LR using selected titanium dioxide materials. Chemosphere 76, 549-553.

Liu, I., Lawton, L.A., Cornish, B., Robertson, P.K.J., 2002. Mechanistic and toxicity studies of the photocatalytic oxidation of microcystin-LR. Journal of Photochemistry and Photobiology A: Chemistry 148, 349-354.

Malato Rodríguez, S., Blanco Gálvez, J., Maldonado Rubio, M.I., Fernández Ibáñez, P., Alarcón Padilla, D., Collares Pereira, M., Farinha Mendes, J., Correia de Oliveira, J., 2004. Engineering of solar photocatalytic collectors. Solar Energy 77, 513-524.

Malato, S., Fernández-Ibáñez, P., Maldonado, M.I., Blanco, J., Gernjak, W., 2009. Decontamination and disinfection of water by solar photocatalysis: Recent overview and trends. Catalysis Today 147, 1-59.

NH, O., NH, N., NH, N., Problems during drinking water treatment of cyanobacterial-loaded surface waters: Consequences for human health.

Pelaez, M., de la Cruz, A.A., Stathatos, E., Falaras, P., Dionysiou, D.D., 2009. Visible light-activated N-F-codoped TiO_2 nanoparticles for the photocatalytic degradation of microcystin-LR in water. Catalysis Today 144, 19-25.

Robertson, P., Lawton, L., Münch, B., Rouzade, J., 1997. Destruction of cyanobacterial toxins by semiconductor photocatalysis. Chemical Communications 1997, 393-394.

Rositano, J., Nicholson, B., Pieronne, P., 1998. Destruction of cyanobacterial toxins by ozone. Ozone: science & engineering 20, 223-238.

Shephard, G., Stockenström, S., De Villiers, D., Engelbrecht, W., Sydenham, E., Wessels, G., 1998. Photocatalytic degradation of cyanobacterial microcystin toxins in water. Toxicon 36, 1895-1901.

Song, W., Teshiba, T., Rein, K., Kevin, E.O.S., 2005. Ultrasonically induced degradation and detoxification of microcystin-LR (cyanobacterial toxin). Environmental science & technology 39, 6300-6305.

Tsuji, K., Watanuki, T., Kondo, F., Watanabe, M.F., Suzuki, S., Nakazawa, H., Suzuki, M., Uchida, H., Harada, K.-I., 1995. Stability of microcystins from cyanobacteria--II. Effect of UV light on decomposition and isomerization. Toxicon 33, 1619-1631.

Vilar, V.J., Gomes, A.I., Ramos, V.M., Maldonado, M.I., Boaventura, R.A., 2009. Solar photocatalysis of a recalcitrant coloured effluent from a wastewater treatment plant. Photochemical & Photobiological Sciences 8, 691-698.

Zhang, G., Zhang, P., Wang, B., Liu, H., 2006. Ultrasonic frequency effects on the removal of Microcystis aeruginosa. Ultrasonics Sonochemistry 13, 446-450.

Zhang, J.B., Zheng, Z., Yang, G.J., Zhao, Y.F., 2007. Degradation of microcystin by gamma irradiation. Nuclear Instruments and Methods in Physics Research Section A: Accelerators, Spectrometers, Detectors and Associated Equipment 580, 687-689.

5 Effect of Solar TiO_2 Photocatalysis on the Destruction of *M. aeruginosa* Cells and Inactivation of Cyanotoxins MC-LR and CYN

This chapter refers to the applicability of a solar TiO_2 photocatalytic process for the destruction of M. aeruginosa and simultaneous removal of intracellular and extracellular MC-LR. Transmission electron microcopy (TEM) was used to study the interaction between TiO_2 nanoparticles and M. aeruginosa cells. Due to the cell size, TiO_2 nanoparticles aggregates in the exterior surface of the cell, and cell lysis is mainly associated to cell wall attack by the reactive species formed in the semiconductor surface, and further release of toxins to the liquid phase. The efficiency of the TiO_2 photocatalytic process was also evaluated in the treatment of water from a Portuguese river containing cyanobacterial blooms, in which prevails the genus Microcystis. The inactivation of MC-LR, previously purified and spiked in distilled water, was assessed using a solar photocatalytic process ($[TiO_2]$ = 100 or 200 mg L^{-1}), two degradation byproducts were identified and relative abundances were evaluated during the reaction time. The best results were obtained with a catalyst concentration of 200 mg TiO_2 L^{-1}, showing a faster MC-LR and byproducts degradation. The photocatalytic process was used at the same conditions for eliminating CYN toxin, as target pollutant. CYN molecule showed a higher recalcitrant character than MC-LR, being necessary a higher solar exposure time to achieve similar inactivation efficiencies.

This Chapter is based on the research article "Pinho, L.X., Azevedo, J., Brito, A., Santos, A., Tamagnini, P., Vasconcelos, V.M., Vilar, V.J.P., Boaventura, R.A.R., 2014. Effect of Solar TiO_2 Photocatalysis on the Destruction of M. aeruginosa Cells and Inactivation of Cyanotoxins MC-LR and CYN. In submission process".

5.1 Introduction

Cyanobacteria produce a wide variety of toxins, and additionally molecules with unknown toxic potential (e.g. microviridins and aeruginosins) causing, therefore, incalculable difficulties in water treatment works, which depend on the raw surface water quality (Hoeger et al., 2005). The presence of toxic cyanobacteria in water for human consumption or recreational purposes poses a serious hazard to humans but has for too long been neglected or at most has been treated on a local level. Accumulation of cyanobacteria scum along the shores of ponds and lakes also present a hazard to wild and domestic animals. Providing the human population with safe drinking water is one of the most important issues in public health and will have more importance in the coming millennium (Hitzfeld et al., 2000a).

The most common cyanobacterial toxins found in water are the hepatotoxins microcystins (MCs) (Lawton et al., 2003a; Vilela et al., 2012). The MC-LR is a heptapeptide cyclic compound with 3-amino-9-methoxy-2,6,8-trimethyl-10-phenyldeca-4,6-dienoicacid (ADDA), containing in variable positions leucine (L) and arginine (R) (Lee et al., 2004). It acts by inhibiting protein phosphatase which leads to hyperphosphorylation of cellular proteins such as cytokeratin 8 and 18 (Hitzfeld et al., 2000b). All protein phosphatase inhibitors are harmful to humans or warm-blooded animals (Dahlmann et al., 2001). Due to chronic effects, including the high risk of primary liver cancer, WHO has recommended a 1 $\mu g\ L^{-1}$ limit for MC-LR in drinking water (Humpage and Falconer, 2003).

Cylindrospermopsin (CYN) another cyanotoxin is an alkaloid structure of sulphated and methylated tricyclic guanidine joined via a hydroxylated single carbon bridge to uracil, and contains an uracil moiety attached to a sulphated guanidine moiety, suggesting that it may have carcinogenic activity (Hummert et al., 2001). In contrast to microcystin, a toxin that is released from the cells when their rupture occurs, higher concentrations of CYN can be found in water towards the end of the bloom, when the cell are still viable (Song et al., 2012). This toxin has been associated with liver damage through mouse bioassays, with symptoms that clearly can be distinguished from those caused by other cyanobacterial hepatotoxins including MCs.

The control of cyanobacterial toxins in drinking water is a hard task and research has been focused on the upgrade of water treatment plant (WTPs) with technologies able to eliminate those toxins. Pantelic et al. (2013) reported that the elimination of cyanobacterial toxins in

drinking water can be achieved through: i) methods able to remove intracellular toxin, such as coagulation, dissolved air flotation, sand filtration and membrane processes (microfiltration, ultrafiltration, nanofiltration and reverse osmosis); ii) methods able to remove extracellular toxin, such as chlorination, activated carbon adsorption, reverse osmosis, advanced oxidation technologies (permanganate oxidation, ozonation, UV photolysis, TiO_2 photocatalysis, Fenton, photo-Fenton, sonolysis) and biological oxidation.

Special attention has been given to TiO_2 photocatalysis, in which powerful reactive oxygen species (ROS), such as hydroxyl radicals, are responsible for the inactivation of the cyanotoxin molecules into biodegradable compounds or the complete mineralization into CO_2, H_2O and inorganic ions (Andersen et al., 2014; Antoniou et al., 2009; Antoniou et al., 2008b; Bahnemann et al., 2013; Han et al., 2011; Lawton et al., 2003b; Liu et al., 2013; Pelaez et al., 2010; Robertson et al., 2011; Su et al., 2013b; Triantis et al., 2012; Vilela et al., 2012; Zhao et al., 2014).

However, there is a lack of information on the removal of cyanobacterial cells (Pinho et al., 2012), such as *M. aeruginosa*, using photocatalytic processes, regarding the elimination of intracellular and extracellular toxin, as well as on the interaction of TiO_2 nanoparticles with the cells.

The main goal of this study was to assess the performance of a solar TiO_2 photocatalytic process on the destruction of *M. aeruginosa* cells and simultaneous removal of intracellular and extracellular cyanotoxin MC-LR, using synthetic solutions and natural water from a Portuguese river containing cyanobacterial blooms. The interaction of TiO_2 nanoparticles with *M. aeruginosa* cells was evaluated by Transmission electron microcopy (TEM). The inactivation of purified MC-LR cyanotoxin spiked in distilled water was assessed using a solar photocatalytic process at different TiO_2 concentrations, and the main degradation byproducts were identified. The best photocatalyst concentration was used in the photocatalytic degradation process of CYN toxin, as target pollutant.

5.2 Material and methods and experimental procedure

The material and methods employed for the development of this work are described in Chapter 3 (sections: 3.1 – 3.5/ 3.7.2/ 3.7.3/ 3.8.1/ 3.8.3 – 3.8.6).

5.2.1 Experimental procedure

Table 5.1 summarizes the main conditions used in each experiment

Table 5.1 Summary of the experimental conditions for each experiment carried out in the present work.

Exp.	Description	Reactor	$\overline{pH}$ / $\overline{T}$	[TiO_2] mg L^{-1}	[*M. aeruginosa*] cell mL^{-1}	[MC-LR or CYN] µg L^{-1}
1	*M. aeruginosa* and MC-LR (PP and LP) destruction	Solar photoreactor	7.7-8.0 29 ºC	20	1.0×10^6	No spiked
2	Interaction between *M. aeruginosa* and TiO_2 (TEM)	Solar photoreactor	7.7-8.0 31 ºC	30	1.4×10^6	No spiked
3	*M. aeruginosa* and MC-LR (PP and LP) destruction in water naturally contaminated from a Portuguese reservoir	Solar photoreactor	8.8 30 ºC	200	*Bloom*	No spiked
4	MC-LR* inactivation	Solar photoreactor	6.5-7.0 21 ºC	100	-	~ 100
5	MC-LR* inactivation	Solar photoreactor	6.5-7.0 21 ºC	200	-	~ 100
6	CYN* inactivation	Lab-scale photoreactor SUNTEST	6.0-6.5 25 ºC	200	-	~ 70
7	MC-LR* inactivation in the presence of $OH^{\bullet}$ and $^1O_2$ scavengers	Lab-scale photoreactor SUNTEST	6.5-7.0 25 ºC	200	-	~ 100
8	CYN* inactivation in the presence of $OH^{\bullet}$ and $^1O_2$ scavengers	Lab-scale photoreactor SUNTEST	6.0-6.5 25 ºC	200	-	~ 70

Exp.: Experiment; PP: Particulate phase; LP: liquid phase; * Distillated water spiked with MC-LR and CYN previously purified.

5.2.1.1 M. aeruginosa destruction by the solar TiO_2 photocatalytic process

This experiment carried out using a pilot scale solar photoreactor (see section 3.7.3). Each of the recirculation tanks of the pilot plant was filled with 20 L of tap water. The tap water was pumped between the recirculation tank and the CPC tubes to achieve dechlorination during 24 hours before starting the experiment (the content of residual and total chlorine was < 0.002 mg Cl_2 L^{-1}(Eaton, 2005)). The pH was adjusted with NaOH (w/v = 50 %) between 7.7 and 8.0. The next day, the cyanobacteria suspension was added to each tank in order to obtain an cell suspension in the range of 10^6 cell mL^{-1} and mixed during 10 min in order to obtain a perfectly homogeneous suspension. Control samples were taken to determine the initial cell concentration in both tanks. For heterogeneous photocatalytic tests (TiO_2/UV), after taking the first sample, titanium dioxide was added up to a concentration of 20 mg L^{-1} (exp. 1) and 30 mg L^{-1} (exp. 2) and the mixture recirculated for more than 15 min. A second sample was collected just before uncovering the CPC units, in order to evaluate possible interactions between the catalyst and cells. Photolysis was carried out in the absence of TiO_2 nanoparticles.

Another experiment (exp. 3) was carried out using natural water from Torrão reservoir (Tâmega River, Portugal), collected in September 2012. Temperature (*T*), pH, conductivity and dissolved oxygen (DO) were measured *in situ* using a portable multiparameter analyzer (*Hanna Instruments 9828*). Other parameters were determined in laboratory, such as dissolved organic carbon (DOC), total dissolved nitrogen and inorganic ions. The recirculation tank of the pilot was filled with 20 L of natural water and the pH was not adjusted. Due to the high load of cyanobacteria and the presence of natural organic matter this reaction was carried out with 200 mg L^{-1} of TiO_2. It should be underlined that the catalyst concentration of 200 mg TiO_2 L^{-1} is the optimum catalyst concentration for the solar photoreactors used in this work (Malato Rodríguez et al., 2004). In all cases, samples were taken at successive time intervals to evaluate the progress of the oxidation systems, considering the cell concentration and, intracellular and extracellular cyanotoxin MC-LR concentration. The analysis of intracellular and extracellular cyanotoxin concentration carried out according to described on section 3.8.3.1 – 3.8.3.3.

5.2.1.2 Photocatalytic inactivation of MC-LR and identification of degradation by-products

The recirculation tank of the pilot plant was filled with 20 L of tap water and spiked with a MC-LR concentrated solution in order to achieve a final MC-LR concentration of approximately 100 µg L^{-1}. pH was not adjusted or controlled during experiments. The solution was homogenized by turbulent recirculation during 20 min in darkness (a first control sample was taken for further characterization).

For heterogeneous photocatalytic tests (TiO_2/UV), after taking the first sample, titanium dioxide was added 100 or 200 mg L^{-1} (exp. 4 and 5, respectively) and the mixture recirculated for more 40 min. A second sample was collected just before uncovering the CPC units, in order to evaluate possible MC-LR adsorption onto the catalyst surface. Photolysis was carried out in the absence of TiO_2 nanoparticles. In all cases, samples were taken at successive time intervals to evaluate the cyanotoxin MC-LR concentration and identification of degradation by-products (see section 3.8.3.4).

5.2.1.3 Photocatalytic inactivation of CYN

The recirculation acrylic vessel of the lab-scale photoreactor prototype was filled with 2.4 L of CYN solution (~70 µg L^{-1}), and homogenized by stirring during 15 minutes in the darkness and a first control sample was taken (exp. 6). The temperature set-point of the refrigerated thermostatic bath was set to keep the solution in the intended temperature (25ºC). Afterwards, the water was pumped to the CPC unit and recirculated in the closed system during 40 min in the darkness and a new sample was taken to observe if any adsorption occurred in the hydraulic system. Afterwards titanium dioxide was added (200 mg L^{-1}) and the mixture recirculated for more 40 min. A second sample was collected just before uncovering the CPC units, in order to evaluate possible CYN adsorption onto the catalyst surface. After that, the SUNTEST was turned on and the radiation intensity was adjusted to 500 W m^{-2}, which is equivalent to 44 W_{UV} m^{-2} measured in the wavelength range from 280 to 400 nm. Photolysis was carried out in the absence of TiO_2 nanoparticles. In all cases, samples were taken at successive time intervals to evaluate the cyanotoxin CYN concentration (see section 3.8.4).

5.2.1.4 Photocatalytic inactivation of MC-LR and CYN with addition of scavengers

These experiments were carried out in the lab-scale photoreactor in order to evaluate the effect of different reactive oxygen scavenger species (singlet oxygen; [NaN_3] = 10 mM; hydroxyl radical [D-mannitol] = 50 mM) (Hirakawa et al., 2004; Sousa et al., 2012), in the inactivation of MC-LR (~ 100 µg L^{-1}) or CYN (~ 70 µg L^{-1}) solutions (exp. 7 and 8, respectively). The scavenger species were added to water solution before the addition of 200 mg TiO_2 L^{-1}. The procedure adopted was similar to that reported in sections 5.2.1.2 and 5.2.1.3.

5.3 Results and discussion

5.3.1 *M. aeruginosa* cells disruption by a solar TiO_2 photocatalytic process

In a previous work showed at Chapter 4 (Pinho et al., 2012), a 5 log reduction in the *M. aeruginosa* concentration was obtained in less than 30 min of the solar photocatalytic process (28-32 W_{UV} m^{-2}), using TiO_2 concentrations between 30-50 mg L^{-1}. MC-LR inactivation kinetics was very fast, being not possible to detect extracellular and intracellular MC-LR after 5 minutes of reaction.

Therefore, in order to be possible to follow the extracellular and intracellular MC-LR, a lower photocatalyst concentration (20 mg L^{-1}) and a higher initial concentration of cells (~ 1.0×10^6 cell mL^{-1}) were selected for this work (exp. 1). Table 5.2 shows the evolution of the number of live cells and the extracellular and intracellular MC-LR concentration, during the photocatalytic process. The initial suspension presents high intracellular and low extracellular MC-LR concentrations, which means that up to this moment most cells were intact.

Table 5.2 Evolution of MC-LR concentration in the water (liquid phase) and in the filter (particulate phase) for the photocatalytic process with 20 mg L^{-1} of TiO_2.

Time	Q_{UV} kJ L^{-1}	MC-LR/LP µg mL^{-1}	MC-LR/PP µg mL^{-1}	Cell mL^{-1}
0	0.00	0.30	2.76	1.0×10^{6}
5	0.24	0.17	2.51	7.5×10^{5}
15	0.74	0.10	2.34	5.0×10^{5}
25	1.52	0.09	2.34	1.2×10^{4}
55	3.23	2.00	2.12	$< 10^{4}$
150	6.85	0.50	0.26	$< 10^{4}$

LP liquid phase, PP particulate phase

During the photocatalytic reaction ($\overline{T}$ = 29 ºC; $\overline{UV}$ = 29 W m^{-2}) a decrease of extracellular MC-LR concentration was observed, as well as a decrease in the number of cells, indicating cell lysis due to the attack of the reactive species formed in the surface of the semiconductor. The extracellular MC-LR concentration decreased during the initial part of the photocatalytic reaction, indicating a rapid inactivation of MC-LR toxin once released into water by cell lysis. However, after 55 minutes (Q_{UV} = 3.2 kJ L^{-1}) of photocatalytic reaction, a high increase of extracellular MC-LR concentration was observed, which is correlated to the marked decrease of live cells. Further phototreatment times led to a high reduction of extracellular and intracellular MC-LR concentration.

The applicability of the solar photocatalytic system was also tested in the treatment of natural water from Torrão reservoir (Tâmega River) presenting cyanobacteria blooms, predominantly from the genus *Microcystis* (exp.3). Table 5.3 shows the main physico-chemical parameters of the natural water. As dissolved organics are present in high concentration, they can compete for the UV photons, act as photosensitizers or compete with cells and MC-LR for the reactive species produced on the TiO_2 surface (He et al., 2012).

Table 5.3 Water quality parameters in Torrão reservoir (Tâmega River).

Parameters	Value
pH	8.8
Temperature	24 ºC
Conductivity	111 µS cm^{-1}
Dissolved oxygen	10.5 mg O_2 L^{-1}
Absorbance at 254 nm	0.07
DOC*	18.0 mg C L^{-1}
TDC*	20.6 mg C L^{-1}
DIC*	2.6 mg C L^{-1}
Total nitrogen	23.0 mg N L^{-1}
Nitrite	1.2 mg NO_2^- L^{-1}
Nitrate	< 0.01 mg NO_3^- L^{-1}
Sulphate	16.7 mg SO_4^{2-} L^{-1}
Chloride	25.3 mg Cl^- L^{-1}
Phosphate	0.5 mg PO_4^{3-} L^{-1}
Lithium	0.04 mg Li^+ L^{-1}
Sodium	0.02 mg Na^+ L^{-1}
Ammonium	< 0.01 NH_4^+ L^{-1}

*DOC-Dissolved Organic Carbon; TDC-Total Dissolved Carbon: DIC-Dissolved Inorganic Carbon

The initial intracellular MC-LR concentration was very high (~ 165 µg L^{-1}) when compared to the extracellular concentration (~ 6.5 µg L^{-1}) (Figure 3), both above the guideline value for drinking water (1 µg L^{-1}) (Hoeger et al., 2005; Svrcek and Smith, 2004). Due to the high extracellular and intracellular MC-LR concentration, a TiO_2 concentration of 200 mg L^{-1} was used, since it is the optimum catalyst concentration for the solar photoreactors used in this work (Malato Rodríguez et al., 2004).

Figure 5.1 shows a high decrease of intracellular MC-LR concentration, achieving values of 70 µg L^{-1} after 41.4 kJ_{UV} L^{-1}, which is associated with the cell lysis by the reactive species formed on the TiO_2 surface. At the same time, a slow increase of extracellular MC-LR concentration can be observed, which indicates a fast inactivation of MC-LR toxin once released into the water as a result of cell lysis. After 61.1 kJ_{UV} L^{-1}, the extracellular MC-LR concentration strongly increased, achieving values of ~ 40 µg L^{-1}. Although the solar TiO_2 photocatalytic process is efficient in the destruction of cyanobacteria and inactivation of cyanotoxins, the energy required for the complete treatment of water containing cyanobacteria

blooms makes the process uneconomic, and consequently the best treatment strategy can be the inclusion of a pre-filtration step to remove most cyanobacteria, in order to minimize the cell lysis, before the photocatalytic oxidation of the remaining cells and MC-LR present in the liquid phase.

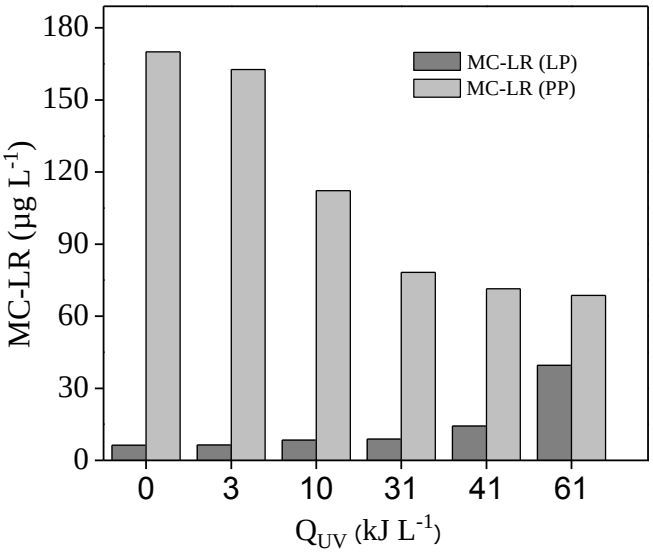

Figure 5.1 Solar TiO_2 photocatalytic oxidation of *M. aeruginosa* cells in natural water from Torrão reservoir ([TiO_2] = 200 mg L^{-1}): kinetic profile of MC-LR concentration in the liquid phase (LP) and particulate phase (PP).

5.3.2 Interaction between cyanobacterial cells and TiO_2 particles

To check the interaction between TiO_2 nanoparticles and the *M. aeruginosa* cells during the photocatalytic process, a lower amount of TiO_2 (30 mg L^{-1}) was used (exp. 2), since higher amounts cause big agglomerates, and make difficult to have a good visualization by TEM technique.

Figure 5.2 shows optical microscopy images of the cells before and after the addition of TiO_2 nanoparticles. The diameter of the cells with TiO_2 coating (Figure 5.2 b) is almost double compared to the diameter of naked cells (Figure 5.2 a), indicating that these small particles (21±5 nm) are attached around the ovoid or spherical *Microcystis* cells. The interaction between cells and TiO_2 particles was evaluated in more detail by TEM analysis.

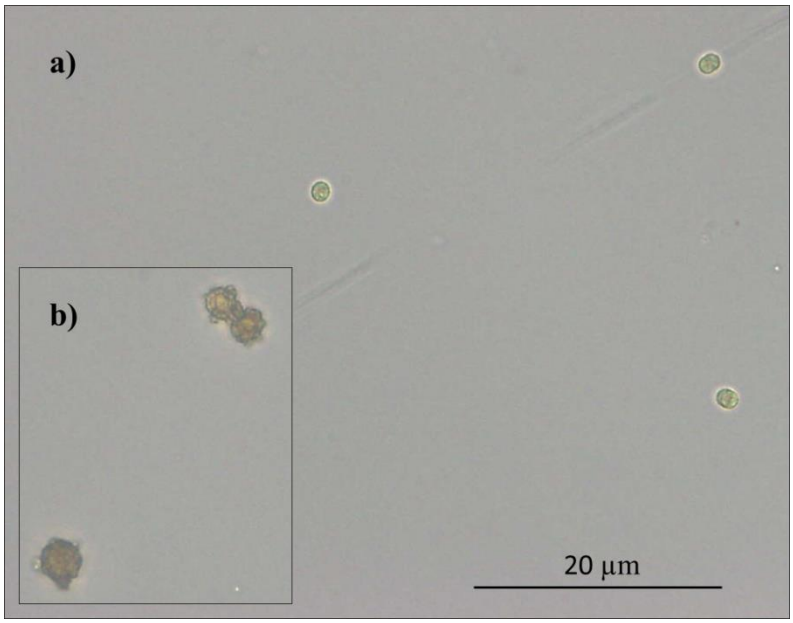

Figure 5.2 Optical microscopy images of *Microcystis aeruginosa* cells in the absence a) or in the presence b) of 30 mg TiO_2 L^{-1}.

TEM micrographs show the ovoid or spherical shape of *M. aeruginosa* cells ranging from 4.0 to 7.5 µm in diameter, as well as the presence of a thick mucilaginous capsule (Figure 5.3 a, b, c). Figure 5.3 d demonstrates that the presence of the nanoparticles in dark conditions do not affect the cells envelope. However, under UV irradiation (Figure 5.3 e-j), the mucilaginous external layer starts to be destroyed in the presence of the TiO_2 nanoparticles, which reach the surface of the cell, leading to the cell deformation (Figure 5.3 g-h). In Figure 5.3 i and j, besides the deformation, a disorganization of the cellular content is also observed. After an accumulated UV energy of 2.0 kJ L^{-1} no more live cells were detected. Planchon and collaborators (2013) reported a similar behaviour during the treatment of water contaminated with *Synechocystis* by a TiO_2 photocatalytic process.

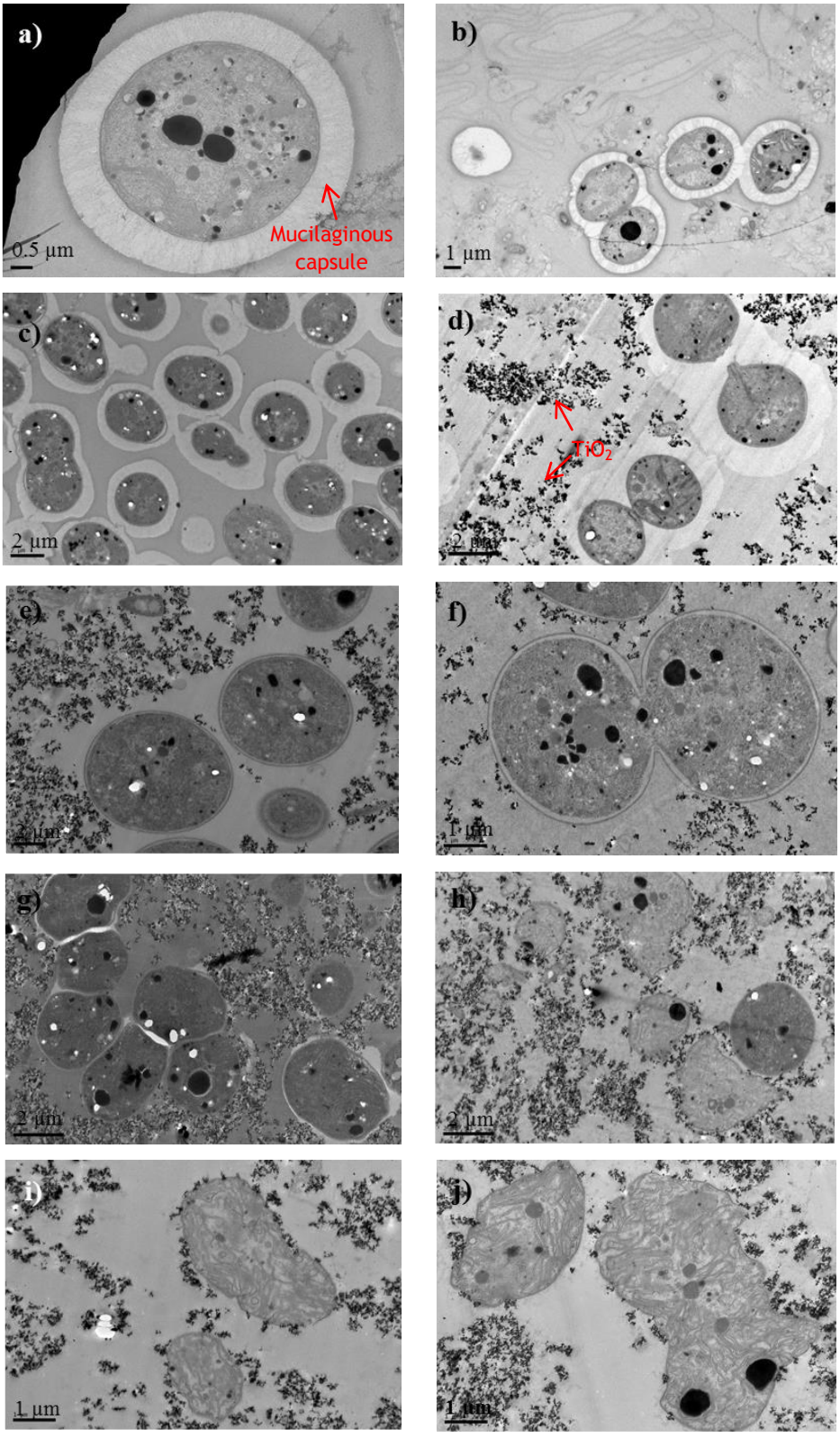

Figure 5.3 TEM images illustrating the interaction between TiO_2 and *M. aeruginosa* cells. a) and b) cells in culture medium; c) cells in tap water, d) cyanobacterial cells with of 30 mg of TiO_2 in darkness, e) to j) cyanobacterial cells with 30 mg of TiO_2 solar UV. Collected at different time exposure points: e) 5 min, f) 10 min, g) 15 min h) 20 min, i) 30 min and j) 40 min.

5.3.3 Photocatalytic inactivation of MC-LR previously purified and identification of inactivation by-products

UV alone was unsatisfactory for the MC-LR inactivation because of poor absorption of solar radiation by the molecule, even after an accumulated UV energy of 15 kJ L^{-1} (8 h) (Figure 5.4). Dark experiment performed with 100 mg L^{-1} of TiO_2 during 40 min showed no significant adsorption at pH between 6.5-7.0, which can be mainly attributed to the fact that MC-LR molecule and TiO_2 particles are negatively charged/neutral for pH values higher than 6.0 (Soares et al., 2013).

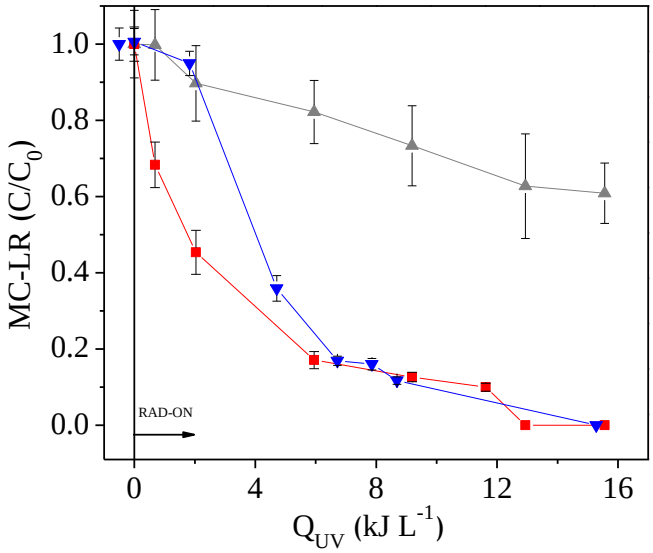

Figure 5.4 MC-LR photolysis and photocatalysis with TiO_2: (▲) Photolysis, (▼) [TiO_2] = 100 mg L^{-1}, (■) [TiO_2] = 200 mg L^{-1}.

Figure 5.4 also shows the MC-LR inactivation as a function of accumulated UV energy for two different TiO_2 concentrations. Although the optimal catalyst concentration is 200 mg TiO_2 L^{-1} (k = 0.8 ± 0.3 L kJ^{-1}; r_0 = (5 ± 2)×10 μg kJ^{-1}) similar profiles are obtained after 6 kJ_{UV} L^{-1} for the catalyst concentrations of 100 (k = 0.25 ± 0.04 L kJ^{-1}; r_0 = 19 ± 3 μg kJ^{-1}) and 200 mg L^{-1}, leading to MC-LR concentration lower than 20 μg L^{-1} , which corresponds to more than 80 % MC-LR inactivation. To achieve a MC-LR concentration below the guideline for drinking water (< 1 μg L^{-1}) it is necessary more than 12 kJ_{UV} L^{-1} (5 h exposure).

A sharp decrease of MC-LR concentration at the initial part of the reaction can be observed in Figure 5.4, which is more pronounced for the highest TiO_2 concentration used, since more hydroxyl radicals are available. After this fast initial decay of the MC-LR concentration a slow inactivation profile is attained, which can be associated to the competition for the

hydroxyl radicals between the initial intermediates generated and the MC-LR molecules, as will be discussed below.

Although the photocatalytic process is able to reduce significantly the MC-LR concentration, the formation of reaction intermediates must be evaluated in order to be known the energy dose required to achieve complete mineralization or the formation of non-toxic compounds. Although the main degradation intermediates and pathways of TiO_2 photocatalysis of MC-LR have been elucidated by several authors (Andersen et al., 2014; Antoniou et al., 2008a; Antoniou et al., 2008b; Su et al., 2013b), the relative abundance of two degradation byproducts along the reaction time was evaluated in this study. LC-MS/MS analysis revealed the presence of two main degradation byproducts with *m/z* 1029 and *m/z* 1011, eluted at 27.7 and 28.3 min, respectively.

By-product *m/z* 1029 (addition of 34 mass units) corresponds to a MC-LR molecule added of two HO- units ($C_{49}H_{76}N_{10}O_{14}$) designated as dihydroxy-microcystin by Tsuji et al. (1997). This by-product is generated by hydroxyl radical attack on the conjugated double bond of the Adda moiety, resulting in hydroxylation of MC-LR (Liu et al., 2003; Liu et al., 2002). The biological toxicity of the MC-LR is expressed by the Adda side, which is an unusual 20-carbon amino acid responsible for the PP1A and PP1B inhibition (Botes et al., 1982; Ma et al., 2012; Su et al., 2013a). *m/z* 1029 was the major MC-LR reaction intermediate found by several authors (Antoniou et al., 2008b; Lawton and Robertson, 1999; Liu et al., 2003).

LC-MS/MS revealed five fragment ions from *m/z* 1029 (1011; 928; 765; 633 and 615), which are showed in Table 5.4. Such fragmentation is consistent with the fixation of OH moieties on the conjugated diene, as reported by Lawton and Robertson (1999). Further breakdown process of MC-LR and adducts occurs through destruction of the cyclic structure of the MC-LR molecule caused by hydroxyl radicals (Ma et al., 2012).

Table 5.4 Ions composition observed for *m/z* 1029 and *m/z* 1011.

***Fragments m/z* 1029**	
m/z	**Composition and sequence**
1029	*cyclo*[$(OH)_2$Adda-Glu-Mdha-Ala-Leu-MeAsp-Arg-H]
1011	*cyclo*[$(OH)_2$Adda-Glu-Mdha-Ala-Leu-MeAsp-Arg-H] -(H_2O)
928	Ala-Leu-MeAsp-Arg-(OH)2Adda-Glu-H-(H_2O)
765	MeAsp-Arg-$(OH)_2C_{11}H_{17}NO$-Glu-Mdha-Ala-H-(NH_3)
633	Arg-$(OH)_2$Adda-Glu-H ou MeAsp-Arg-$(OH)_2$Adda-H or $(OH)_2C_{11}H_{15}O$-Glu-Mdha-Ala-Leu-H
615	Arg-$(OH)_2$Adda-Glu-H -(H_2O) or MeAsp- Arg-$(OH)_2$Adda-H-(H_2O) or $(OH)_2C_{11}H_{15}O$-Glu-Mdha-Ala-Leu-H-(H_2O)
***Fragments m/z* 1011**	
m/z	**Composition and sequence**
1011	*cyclo*[(O)Adda-Glu-Mdha-Ala-Leu-MeAsp-Arg-H]
993	*cyclo*[(O)Adda-Glu-Mdha-Ala-Leu-MeAsp-Arg-H] - (H_2O)
983	[(O)Adda-Glu-Mdha-Ala-Leu-MeAsp-Arg-H] - (CO)
615	Arg-(O)Adda-Glu-H or MeAsp- Arg-(O)Adda-H or $C_{11}H_{15}O_2$-Glu-Mdha-Ala-Leu-H

The *m/z* 1011 intermediate (MC-LR plus 16 mass units) is assigned to the addition of hydroxyl radical to unsaturated bonds and subsequent loss of H (Antoniou et al., 2008b). *m/z* 1011 and *m/z* 1029 intermediates result from hydroxyl substitution and hydroxyl addition, respectively, which are normal oxidation ways of organic compounds by hydroxyl radicals.

Although acidic pH has been found to favor the photocatalytic destruction of the microcystins, it was reported that acidic conditions can limit the available sites of the toxin for degradation to the diene bonds of Adda and the double bond of MeAsp. However, under neutral conditions, the methoxy and the aromatic groups of the Adda part of the microcystin structure can be involved (Robertson et al., 2012).

In the present work, which was carried out at neutral pH, the greatest amount of by-products *m/z* 1029 and *m/z* 1011 appears at the beginning of the reaction, achieving maximum relative abundances at 2-8 $kJ_{UV}\ L^{-1}$ (2-4 h) and decreasing for longer exposure times, being not detected at the end of the reaction time, for the experiment with 200 mg $TiO_2\ L^{-1}$ (Figure 4.5 a and b).

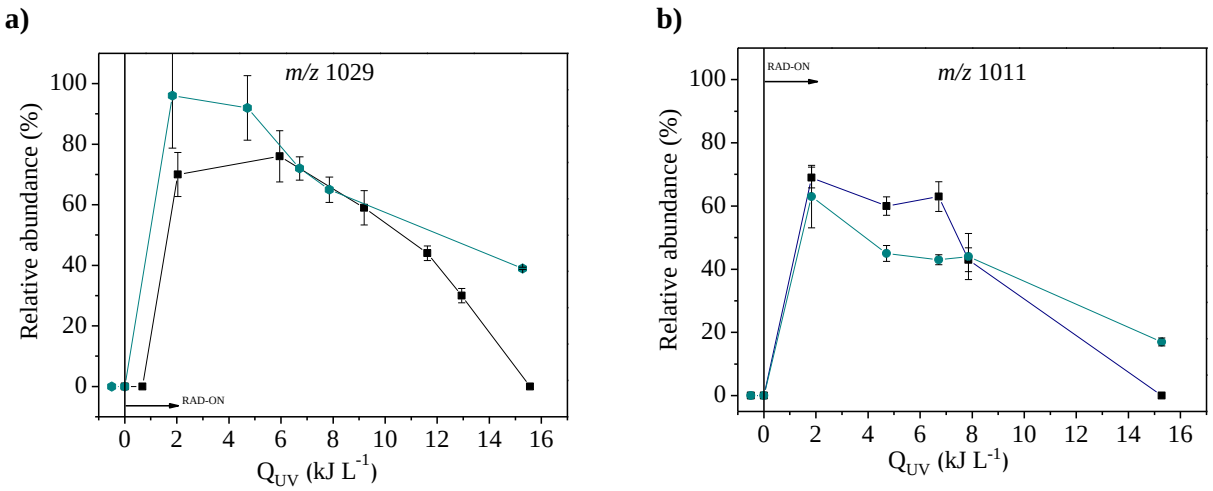

Figure 5.5 Kinetic profile of the two degradation byproducts formed during MC-LR degradation by TiO_2 photocatalysis: a) *m/z* 1029: (●) $[TiO_2]$ = 100 mg L^{-1}, (■) $[TiO_2]$ = 200 mg L^{-1} and b) *m/z* 1011: (●) $[TiO_2]$ = 100 mg L^{-1}, (■) $[TiO_2]$ = 200 mg L^{-1}.

Lawton et al. (1999), using a photocatalytic process with TiO_2 (1 % m/v) irradiated by a xenon UV lamp (280 W and spectral output 330-450 nm) in the degradation of a MC-LR solution (C_0 = 200 µg mL^{-1}) at pH 4, found seven UV detectable degradation byproducts, and six of them were not detected after prolonged irradiation times (100 min). For Antoniou et al (2008b) the majority of products appears within 2 min and reach their maximum concentration within 10 – 15 min, and all the detectable products were degraded with extended irradiation (120 min). Liu at al. (2003) using a TiO_2/H_2O_2/UV system, found at least 10 oxidation byproducts, three of them being detected after only 2 min of reaction (one was the *m/z* 1029 byproduct), with kinetic profiles similar to that reported in this work.

Considering the main results obtained, the TiO_2 photocatalytic process can be considered as an interesting process for the removal of MC-LR from water, as well as for the degradation of MC-LR degradation by-products.

5.3.4 Photocatalytic oxidation of CYN

Although cylindrospermopsin cyanotoxin has been detected in different natural waters around the world (Bouvy et al., 2000; Falconer and Humpage, 2005; Humpage and Falconer, 2003; Preußel et al., 2006), few studies reports on the application of water treatment technologies to destroy this toxin (Zhang et al., 2014), mainly due to the high costs associated with the purification process (Onstad et al., 2007; Zhao et al., 2013).

CYN is resistant and stable at varying heat, light and pH conditions because of the presence of a tricyclic sulfated guanidine zwitterion group and uracil (Chiswell et al., 1999; Hummert

et al., 2001). According to Zhao et al. (2013) the uracil moiety in CYN is critical to the toxicity of this toxin. Hydroxyl radical can react following different reaction pathways and CYN possesses a number of potential hydroxyl radical reaction sites (Song et al., 2012), being the addition of the hydroxyl radical to the uracil ring of CYN the primary reaction pathway.

Photocatalytic oxidation of CYN cyanotoxin previously purified was conducted in the lab-scale tubular photoreactor using 200 mg TiO_2 L^{-1} (exp. 7) and an initial CYN concentration of ~ 70 µg L^{-1}, which is the typical CYN concentration found in water reservoirs (Chiswell et al., 1999; Senogles et al., 2001).

Photolysis was unable to achieve CYN inactivation because of poor absorption of solar radiation by the molecule, even after an accumulated UV energy of 9 kJ L^{-1} (6 h exposure) (Figure 5.6), which is in agreement with the results reported by He et al. (2013), even using a 254 nm UV lamp. Chiswell et al (1999) also showed the high stability of CYN molecule at different values of pH, temperature and sunlight exposure. After 10 weeks at 50ºC only 57 % CYN inactivation was obtained, which was accompanied by the appearance of an intermediate compound. Additionally, boiling for 15 min does not cause a significant inactivation of CYN.

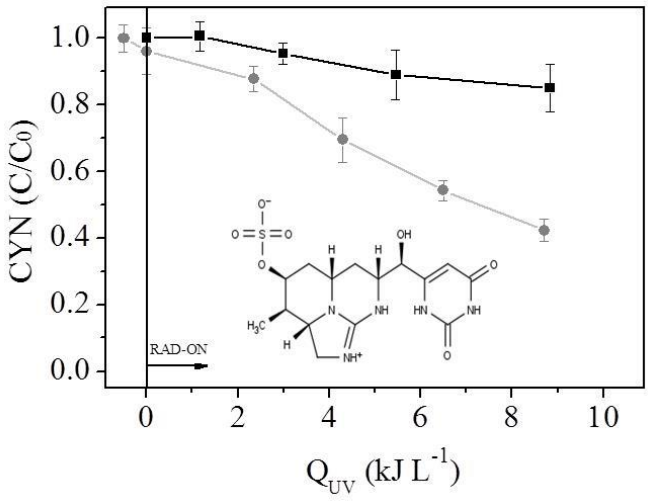

Figure 5.6 CYN solar photolysis and photocatalysis: (■) Photolysis and (●) [TiO_2] = 200 mg L^{-1}.

CYN adsorption on the surface of TiO_2 nanoparticles was also insignificant after 40 min, since CYN molecule presents an overall zero charge at pH ≤ 7.4. In a previous paper (Soares et al., 2013), using cellulose acetate monoliths coated with a P25 thin film, no adsorption was observed after 40 min in darkness, since at pH = 6, CYN molecules and TiO_2 particles are

neutral/negative species, and no attraction between them occurs. Senogles et al. (2001) also reported negligible CYN adsorption using 0.1 g L^{-1} TiO_2 at different pH values (4, 7 and 9).

Figure 5.6 shows that the CYN molecule is very stable, being necessary more than 8.7 kJ_{UV} L^{-1} to achieve approximately 50 % inactivation by the solar photocatalytic process.

Senogles et al. (2001) used P25 TiO_2 (10-100 mg L^{-1}) under UV irradiation from a UVTA™ ultraviolet disinfection system (17,500 μW cm^{-2}) to destroy CYN by photocatalysis, and observed an increasing degradation rate with the increase of the catalyst concentration. About 50 % CYN inactivation ($C_o \sim 115$ μg L^{-1}; pH ~ 7) was achieved after 20 min using 100 mg L^{-1} of TiO_2, which was considered the optimum catalyst concentration.

5.3.5 Photocatalytic inactivation of MC-LR and CYN with addition of $OH^{\bullet}$ and $^1O_2$ scavengers

To study the formation and roles of different reactive oxygen species such as hydroxyl radical and singlet oxygen, during photocatalysis, specific scavengers, D-mannitol and sodium azide (NaN_3), were employed, maintaining the same conditions of TiO_2 photocatalysis experiments with 200 mg L^{-1} of TiO_2 (exp. 8 and 9). Figure 5.7 a shows that in the absence of any scavenger the degradation rate of MC-LR was 87 % after ~ 9.5 kJ_{UV} L^{-1}. The addition D-mannitol ($OH^{\bullet}$ scavenger) decreased the MC-LR degradation to 27 %, while with the addition of NaN_3 ($^1O_2$ scavenger) the degradation was 50 %. Regarding CYN degradation, the profiles are very similar for both species (Figure 5.7 b). The addition of D-mannitol and NaN_3 led to 34 and 38 % of degradation, respectively, whereas 50 % degradation was obtained without scavengers addition. These results suggest that MC-LR degradation can be attributed to both $OH^{\bullet}$ and $^1O_2$ attack, although it may also be influenced by other reactive species not studied in this work. Even though sodium azide has been mainly described as a high selective $^1O_2$ scavenger, some authors reported its non-selectivity since it can also react with $OH^{\bullet}$ (Zhang et al., 1997), which could better justify the results obtained in this work.

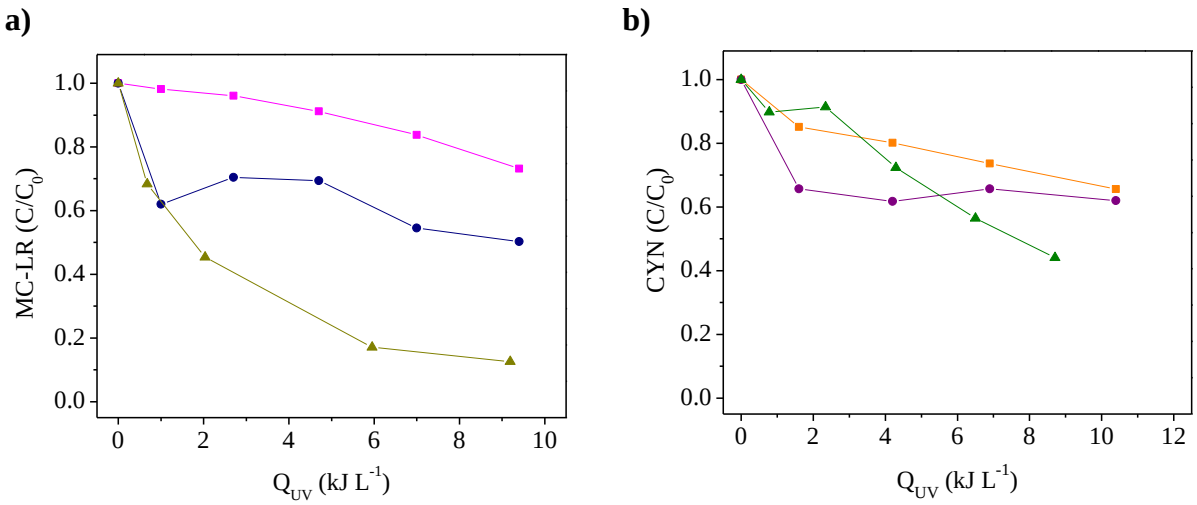

Figure 5.7 Photocatalytic inactivation of MC-LR and CYN with addition of $OH^{\bullet}$ (D-mannitol) and $^{1}O_2$ scavengers (NaN_3) ([TiO_2] = 200 mg L^{-1}). a) MC-LR: (■) D-mannitol, (●) NaN_3 and (▲) without scavengers; b) CYN: (■) D-mannitol, (●) NaN_3 and (▲) without scavengers.

Liao et al. (2013) also found in experiments of photoelectrocatalysis of MC-LR using Ag/AgCl/TiO_2, that both $OH^{\bullet}$ and $^{1}O_2$ contributed to MC-LR inactivation. In absence of any scavenger, the authors found 92 % of inactivation after 5 h, whereas the addition of NaF ($OH^{\bullet}$ scavanger) and p-benzoquinone ($^{1}O_2$ scavenger) reduced the MC-LR inactivation efficiency to 80.5 and 53.8 %, respectively, after the same reaction time. Song et al. (2012) also showed that ~65-70 % CYN inactivation was mainly associated with $OH^{\bullet}$ and singlet oxygen attack. Direct energy transfer from natural organic matter plays only a minor role.

5.4 Conclusions

A solar TiO_2 photocatalytic process was applied successfully for the destruction of *M. aeruginosa* and simultaneous removal of intracellular and extracellular cyanotoxin MC-LR, even present in natural water from a Portuguese river containing cyanobacterial blooms. Transmission electron microcopy (TEM) showed that TiO_2 nanoparticles form a layer around the cells and, under UV irradiation, the mucilaginous capsule starts to be destroyed due to the attack of reactive species formed on the TiO_2 surface, which allows the penetration of TiO_2 nanoparticles to the inner layers, leading to cells deformation and disruption.

The same photocatalytic process showed good performance in the inactivation of MC-LR and CYN cyanotoxins, previously purified and spiked in distilled water, which indicates that the best treatment strategy for cyanobacteria containing water is the inclusion of a pre-filtration step to remove most cyanobacteria to minimize cell lysis, and further photocatalytic oxidation of the remaining cells and MC-LR/CYN in the liquid phase. CYN molecule showed a higher stability than MC-LR, being necessary a higher solar exposure time to achieve similar inactivation efficiencies. The oxidation of cyanotoxins was attributed to hydroxyl radicals and singlet oxygen attack.

The photocatalytic oxidation of MC-LR in aqueous solutions is characterized by an initial fast reaction followed by a slow inactivation stage, which was attributed to the competition for the hydroxyl radicals between the MC-LR molecules and degradation byproducts. LC-MS/MS analysis revealed the presence of two main MC-LR degradation byproducts (*m/z* 1029 and *m/z* 1011) during the initial part of the reaction. MC-LR was almost completely destroyed for longer reaction times.

5.5 References

Andersen, J., Han, C., O'Shea, K., Dionysiou, D.D., 2014. Revealing the degradation intermediates and pathways of visible light-induced NF-TiO_2 photocatalysis of microcystin-LR. Applied Catalysis B: Environmental 154–155, 259-266.

Antoniou, M.G., Nicolaou, P.A., Shoemaker, J.A., de la Cruz, A.A., Dionysiou, D.D., 2009. Impact of the morphological properties of thin TiO_2 photocatalytic films on the detoxification of water contaminated with the cyanotoxin, microcystin-LR. Applied Catalysis B: Environmental 91, 165-173.

Antoniou, M.G., Shoemaker, J.A., Cruz, A.A.d.l., Dionysiou, D.D., 2008a. Unveiling New Degradation Intermediates/Pathways from the Photocatalytic Degradation of Microcystin-LR. Environmental Science & Technology 42, 8877-8883.

Antoniou, M.G., Shoemaker, J.A., de la Cruz, A.A., Dionysiou, D.D., 2008b. LC/MS/MS structure elucidation of reaction intermediates formed during the TiO_2 photocatalysis of microcystin-LR. Toxicon 51, 1103-1118.

Bahnemann, D.W., Lawton, L.A., Robertson, P.K.J., 2013. Chapter 16 - The Application of Semiconductor Photocatalysis for the Removal of Cyanotoxins from Water and Design Concepts for Solar Photocatalytic Reactors for Large Scale Water Treatment, in: Suib, S.L. (Ed.), New and Future Developments in Catalysis. Elsevier, Amsterdam, pp. 395-415.

Botes, D.P., Viljoen, C.C., Kruger, H., Wessels, P.L., Williams, D.H., 1982. Configuration assignments of the amino acid residues and the presence of N-methyldehydroalanine in toxins from the blue-green alga, Microcystis aeruginosa. Toxicon 20, 1037-1042.

Bouvy, M., Falcão, D., Marinho, M., Pagano, M., Moura, A., 2000. Occurrence of Cylindrospermopsis (Cyanobacteria) in 39 Brazilian tropical reservoirs during the 1998 drought. Aquatic Microbial Ecology 23, 13-27.

Chiswell, R.K., Shaw, G.R., Eaglesham, G., Smith, M.J., Norris, R.L., Seawright, A.A., Moore, M.R., 1999. Stability of cylindrospermopsin, the toxin from the cyanobacterium, Cylindrospermopsis raciborskii: Effect of pH, temperature, and sunlight on decomposition. Environmental Toxicology 14, 155-161.

Dahlmann, J., Rühl, A., Hummert, C., Liebezeit, G., Carlsson, P., Graneli, E., 2001. Different methods for toxin analysis in the cyanobacterium Nodularia spumigena (Cyanophyceae). Toxicon 39, 1183-1190.

Eaton, A.D., L.S. Clesceri, E.W. Rice, A.E. Greenberg, M.A.H. Franson, 2005. Standard Methods for the Examination of Water and Wastewater American Public Health Association., Washington, D.C.

Falconer, I.R., Humpage, A.R., 2005. Health Risk Assessment of Cyanobacterial(Blue-green Algal) Toxins in Drinking Water. International Journal of Environmental Research and Public Health 2, 43-50.

Han, C., Pelaez, M., Likodimos, V., Kontos, A.G., Falaras, P., O'Shea, K., Dionysiou, D.D., 2011. Innovative visible light-activated sulfur doped TiO_2 films for water treatment. Applied Catalysis B: Environmental 107, 77-87.

He, X., de la Cruz, A.A., Dionysiou, D.D., 2013. Destruction of cyanobacterial toxin cylindrospermopsin by hydroxyl radicals and sulfate radicals using UV-254 nm activation of hydrogen peroxide, persulfate and peroxymonosulfate. Journal of Photochemistry and Photobiology A: Chemistry 251, 160-166.

He, X., Pelaez, M., Westrick, J.A., O'Shea, K.E., Hiskia, A., Triantis, T., Kaloudis, T., Stefan, M.I., de la Cruz, A.A., Dionysiou, D.D., 2012. Efficient removal of microcystin-LR by UV-C/H2O2 in synthetic and natural water samples. Water Research 46, 1501-1510.

Hirakawa, K., Mori, M., Yoshida, M., Oikawa, S., Kawanishi, S., 2004. Photo-irradiated Titanium Dioxide Catalyzes Site Specific DNA Damage via Generation of Hydrogen Peroxide. Free Radical Research 38, 439-447.

Hitzfeld, B., Höger, S., Dietrich, D., 2000a. Cyanobacterial toxins: removal during drinking water treatment, and human risk assessment. Environmental health perspectives 108, 113.

Hitzfeld, B.C., Lampert, C.S., Spaeth, N., Mountfort, D., Kaspar, H., Dietrich, D.R., 2000b. Toxin production in cyanobacterial mats from ponds on the McMurdo Ice Shelf, Antarctica. Toxicon 38, 1731-1748.

Hoeger, S.J., Hitzfeld, B.C., Dietrich, D.R., 2005. Occurrence and elimination of cyanobacterial toxins in drinking water treatment plants. Toxicology and Applied Pharmacology 203, 231-242.

Hummert, C., Dahlmann, J., Reinhardt, K., Dang, H., Dang, D., Luckas, B., 2001. Liquid chromatography-mass spectrometry identification of microcystins inMicrocystis aeruginosa strain from lake Thanh Cong, Hanoi, Vietnam. Chromatographia 54, 569-575.

Humpage, A., Falconer, I., 2003. Oral toxicity of the cyanobacterial toxin cylindrospermopsin in male Swiss albino mice: Determination of no observed adverse effect level for deriving a drinking water guideline value. Environmental toxicology 18, 94-103.

Lawton, L., Robertson, P., 1999. Physico-chemical treatment methods for the removal of microcystins (cyanobacterial hepatotoxins) from potable waters. Chemical Society Reviews 28, 217-224.

Lawton, L., Robertson, P., Cornish, B., Jaspars, M., 1999. Detoxification of microcystins (cyanobacterial hepatotoxins) using TiO_2 photocatalytic oxidation. Environ. Sci. Technol 33, 771-775.

Lawton, L., Robertson, P., Cornish, B., Marr, I., Jaspars, M., 2003a. Processes influencing surface interaction and photocatalytic destruction of microcystins on titanium dioxide photocatalysts. Journal of Catalysis 213, 109-113.

Lawton, L.A., Robertson, P.K.J., Cornish, B.J.P.A., Marr, I.L., Jaspars, M., 2003b. Processes influencing surface interaction and photocatalytic destruction of microcystins on titanium dioxide photocatalysts. Journal of Catalysis 213, 109-113.

Lee, D., Kim, S., Cho, I., Kim, S., Kim, S., 2004. Photocatalytic oxidation of microcystin-LR in a fluidized bed reactor having TiO_2-coated activated carbon. Separation and Purification Technology 34, 59-66.

Liao, W., Zhang, Y., Zhang, M., Murugananthan, M., Yoshihara, S., 2013. Photoelectrocatalytic degradation of microcystin-LR using $Ag/AgCl/TiO_2$ nanotube arrays electrode under visible light irradiation. Chemical Engineering Journal 231, 455-463.

Liu, G., Han, C., Pelaez, M., Zhu, D., Liao, S., Likodimos, V., Kontos, A.G., Falaras, P., Dionysiou, D.D., 2013. Enhanced visible light photocatalytic activity of CN-codoped TiO_2 films for the degradation of microcystin-LR. Journal of Molecular Catalysis A: Chemical 372, 58-65.

Liu, I., Lawton, L., Robertson, P., 2003. Mechanistic studies of the photocatalytic oxidation of microcystin-LR: an investigation of byproducts of the decomposition process. Environ. Sci. Technol 37, 3214-3219.

Liu, I., Lawton, L.A., Cornish, B., Robertson, P.K.J., 2002. Mechanistic and toxicity studies of the photocatalytic oxidation of microcystin-LR. Journal of Photochemistry and Photobiology A: Chemistry 148, 349-354.

Ma, Q., Ren, J., Huang, H., Wang, S., Wang, X., Fan, Z., 2012. Kinetic and mechanistic study of microcystin-LR degradation by nitrous acid under ultraviolet irradiation. Journal of Hazardous Materials 215–216, 75-82.

Malato Rodríguez, S., Blanco Gálvez, J., Maldonado Rubio, M.I., Fernández Ibáñez, P., Alarcón Padilla, D., Collares Pereira, M., Farinha Mendes, J., Correia de Oliveira, J., 2004. Engineering of solar photocatalytic collectors. Solar Energy 77, 513-524.

Onstad, G.D., Strauch, S., Meriluoto, J., Codd, G.A., von Gunten, U., 2007. Selective oxidation of key functional groups in cyanotoxins during drinking water ozonation. Environmental Science & Technology 41, 4397-4404.

Pantelić, D., Svirčev, Z., Simeunović, J., Vidović, M., Trajković, I., 2013. Cyanotoxins: Characteristics, production and degradation routes in drinking water treatment with reference to the situation in Serbia. Chemosphere 91, 421-441.

Pelaez, M., Falaras, P., Likodimos, V., Kontos, A.G., de la Cruz, A.A., O'Shea, K., Dionysiou, D.D., 2010. Synthesis, structural characterization and evaluation of sol–gel-based NF-TiO_2 films with visible light-photoactivation for the removal of microcystin-LR. Applied Catalysis B: Environmental 99, 378-387.

Pinho, L.X., Azevedo, J., Vasconcelos, V.M., Vilar, V.J.P., Boaventura, R.A.R., 2012. Decomposition of Microcystis aeruginosa and Microcystin-LR by TiO_2 Oxidation Using Artificial UV Light or Natural Sunlight. Journal of Advanced Oxidation Technologies 15, 98-106.

Planchon, M., Jittawuttipoka, T., Cassier-Chauvat, C., Guyot, F., Gelabert, A., Benedetti, M.F., Chauvat, F., Spalla, O., 2013. Exopolysaccharides protect Synechocystis against the deleterious effects of Titanium dioxide nanoparticles in natural and artificial waters. Journal of Colloid and Interface Science 405, 35-43.

Preußel, K., Stüken, A., Wiedner, C., Chorus, I., Fastner, J., 2006. First report on cylindrospermopsin producing Aphanizomenon flos-aquae (Cyanobacteria) isolated from two German lakes. Toxicon 47, 156-162.

Robertson, P.K.J., Bahnemann, D.W., Lawton, L.A., Bellu, E., 2011. A study of the kinetic solvent isotope effect on the destruction of microcystin-LR and geosmin using TiO_2 photocatalysis. Applied Catalysis B: Environmental 108–109, 1-5.

Robertson, P.K.J., Robertson, J.M.C., Bahnemann, D.W., 2012. Removal of microorganisms and their chemical metabolites from water using semiconductor photocatalysis. Journal of Hazardous Materials 211–212, 161-171.

Senogles, P., Scott, J., Shaw, G., Stratton, H., 2001. Photocatalytic degradation of the cyanotoxin cylindrospermopsin, using titanium dioxide and UV irradiation. Water Research 35, 1245-1255.

Soares, P., Silva, T.C.V., Manenti, D., Souza, S.A.G.U., Boaventura, R.R., Vilar, V.P., 2013. Insights into real cotton-textile dyeing wastewater treatment using solar advanced oxidation processes. Environmental Science and Pollution Research in press, 1-14.

Song, W., Yan, S., Cooper, W.J., Dionysiou, D.D., O'Shea, K.E., 2012. Hydroxyl radical oxidation of cylindrospermopsin (cyanobacterial toxin) and its role in the photochemical transformation. Environmental Science & Technology 46, 12608-12615.

Sousa, M.A., Gonçalves, C., Vilar, V.J.P., Boaventura, R.A.R., Alpendurada, M.F., 2012. Suspended TiO_2-assisted photocatalytic degradation of emerging contaminants in a municipal WWTP effluent using a solar pilot plant with CPCs. Chemical Engineering Journal 198–199, 301-309.

Su, Y., Deng, Y., Du, Y., 2013a. Alternative pathways for photocatalytic degradation of microcystin-LR revealed by TiO_2 nanotubes. Journal of Molecular Catalysis A: Chemical 373, 18-24.

Su, Y., Deng, Y., Du, Y., 2013b. Alternative pathways for photocatalytic degradation of microcystin-LR revealed by TiO_2 nanotubes. Journal of Molecular Catalysis A: Chemical 373, 18-24.

Svrcek, C., Smith, D.W., 2004. Cyanobacteria toxins and the current state of knowledge on water treatment options: a review. Journal of Environmental Engineering & Science 3, 155-185.

Triantis, T.M., Fotiou, T., Kaloudis, T., Kontos, A.G., Falaras, P., Dionysiou, D.D., Pelaez, M., Hiskia, A., 2012. Photocatalytic degradation and mineralization of microcystin-LR under UV-A, solar and visible light using nanostructured nitrogen doped TiO_2. Journal of Hazardous Materials 211–212, 196-202.

Tsuji, K., Watanuki, T., Kondo, F., Watanabe, M.F., Nakazawa, H., Suzuki, M., Uchida, H., Harada, K.-I., 1997. Stability of Microcystins from cyanobacteria—iv. effect of chlorination on decomposition. Toxicon 35, 1033-1041.

Vilela, W.F.D., Minillo, A., Rocha, O., Vieira, E.M., Azevedo, E.B., 2012. Degradation of [D-Leu]-Microcystin-LR by solar heterogeneous photocatalysis (TiO_2). Solar Energy 86, 2746-2752.

Zhang, G., Nadagouda, M.N., O'Shea, K., El-Sheikh, S.M., Ismail, A.A., Likodimos, V., Falaras, P., Dionysiou, D.D., 2014. Degradation of cylindrospermopsin by using polymorphic titanium dioxide under UV–Vis irradiation. Catalysis Today 224, 49-55.

Zhang, X., Rosenstein, B.S., Wang, Y., Lebwohl, M., Wei, H., 1997. Identification of Possible Reactive Oxygen Species Involved in Ultraviolet Radiation-Induced Oxidative DNA Damage. Free Radical Biology and Medicine 23, 980-985.

Zhao, C., Pelaez, M., Dionysiou, D.D., Pillai, S.C., Byrne, J.A., O'Shea, K.E., 2013. UV and visible light activated TiO_2 photocatalysis of 6-hydroxymethyl uracil, a model compound for the potent cyanotoxin cylindrospermopsin. Catalysis Today.

Zhao, C., Pelaez, M., Dionysiou, D.D., Pillai, S.C., Byrne, J.A., O'Shea, K.E., 2014. UV and visible light activated TiO_2 photocatalysis of 6-hydroxymethyl uracil, a model compound for the potent cyanotoxin cylindrospermopsin. Catalysis Today 224, 70-76.

6 Oxidation of Microcystin-LR and CYN by Photocatalysis using a Tubular Photoreactor Packed with different TiO_2 Coated Supports

Photocatalytic experiments were carried out in a lab-scale tubular photoreactor with a compound parabolic collector (CPC) using artificial and natural solar radiation to promote the degradation of the cyanotoxins MC-LR and CYN in distilled and natural water. A catalytic bed of cellulose acetate transparent monoliths (CAM) coated with P25 or sol-gel TiO_2 film or with a photocatalytic 3D TiO_2-based exterior paint (PC500, VLP7000 and P25) was employed. The effect of the addition of hydrogen peroxide was also assessed. The transparent and water-permeable CAM structure offers a rugged surface, which enables a good adhesion and high surface area of the catalytic coating. Other supports, such as PVC or glass tubes and glass spheres were coated with the photocatalytic 3D TiO_2-based exterior paint. An adequate rigid material for packing the photoreactor was obtained whereas simultaneously maximizing the illuminated catalyst surface. The toxin MC-LR was purified from Microcysts aeruginosa cultures. The photocatalytic system P25-CAM/H_2O_2 can be considered the most viable process, considering the MC-LR inactivation efficiency (98 %), the cost and the simplicity of the catalyst preparation. It can be used in the treatment of natural water intended for the abstraction of drinking water, and can lower the levels of MC-LR below the guideline value of 1 µg L^{-1}. The same system was also applied to destroy CYN. CYN inactivation is also achieved by TiO_2 photocatalysis but a long exposure time is required.

This Chapter is based on the research article "Pinho, L.X., Azevedo, J., Miranda, S.M., Ângelo, J., Mendes, A., Vasconcelos, V.M., Vilar, V.J.P., Boaventura, R.A.R., 2014. Oxidation of Microcystin-LR and CYN by Photocatalysis using a Tubular Photoreactor Packed with different TiO_2 Coated Supports. In submission process".

6.1 Introduction

Blooms of cyanobacteria have been occurring largely due to the eutrophication of aquatic environments. Many rivers, lakes and reservoirs worldwide develop toxic cyanobacteria. This is especially common during the warmer months where they can appear as greenish suspensions in water. These organisms produce a wide variety of toxins and additional molecules with unknown toxic potential (e.g., microviridins, aeruginosins), and are a challenge for designers of water treatment systems, which depend on the surface raw water quality (Falconer and Humpage, 2005; Hoeger et al., 2005). Although the presence of toxic cyanobacteria/cyanotoxins in water intended for the abstraction of drinking water, agricultural or recreational purposes poses a serious hazard to humans, this situation has been neglected or at most has been treated on a local level. Accumulation of cyanobacteria scum along the shores of ponds and lakes also represents a hazard risk to wildlife and domestic animals. Providing the human population with safe drinking water is one of the most important issues as regards public health and will gain more importance in the present millennium (Hitzfeld et al., 2000).

In recent years, the use of TiO_2 as photocatalyst for water treatment has been widely reported, either as a powder in suspension or fixed to various supports (Robert and Malato, 2002). The photocatalytic reaction involving the irradiation of TiO_2 can only occur using UV light, which corresponds to 4 – 5 % of the solar light spectrum, because of the wide band gap of approximately 3.2 eV of anatase and 3.0 eV of rutile (Han et al., 2011; Pelaez et al., 2009; Yang et al., 2009). Upon absorption of suitable energy photons, electrons are injected from the valence to the conduction band of the semiconductor creating electron/hole pairs that originate mostly highly oxidizing hydroxyl and highly reduction superoxide radicals (Kaneko, 2002). These species lead to mineralization of different organic pollutants (Robert and Malato, 2002; Robertson et al., 2005; Triantis et al., 2012), including cyanotoxins (Pinho et al., 2012).

Most studies concerning water treatment using TiO_2 photocatalytic processes apply slurry suspensions of the semiconductor, showing a high efficiency on degrading and mineralizing pollutants, since the contact of the photocatalyst with the pollutants is promoted with minimal mass transfer limitations. However, heterogeneous photocatalytic processes are an interesting approach for water decontamination since a post-filtration step to retain the photocatalyst

becomes unnecessary, contrarily to what happens when slurry suspensions are used. Since mass transfer is usually the rate-limiting step in these processes applied to liquid phases, the photocatalytic reaction rate can be enhanced by incrementing the catalyst surface (Águia et al., 2011b; Gumy et al., 2006; Robert et al., 1999; van Grieken et al., 2009b).

Chemical vapor deposition, physical vapor deposition, sputtering and dip-coating are some examples of methods employed to obtain 2D TiO_2 films supported in inert surfaces (Cardona et al., 2004). Dip coating is a good option because it is simple and the equipment required is not expensive. TiO_2 concentration in the film must be taken into account and adjusted to avoid loss of the catalyst by erosion (Ávila et al., 2002). Another advantage on the application of immobilized catalyst is the fact that it can be re-used for several treatment cycles while maintaining its stability (Garcia et al., 2010; van Grieken et al., 2009b).

Mendes and co-workers (Águia et al., 2010, 2011a, b) developed a coating for immobilizing photocatalysts based on a commercial paint, which is porous (pigment volume concentration slightly above the critical value) and very resistant to photodegradation induced by the presence of the photocatalyst. The pigmentar TiO2 (rutile) was replaced by photocatalyst TiO2 and calcium carbonate (load/extender). The absence of pigmentar TiO2 (rutile) allows a greater light penetration, up to 100 µm of optical thickness. This 100-µm photoactive porous film is a 3D structure that optimises the light absorbance and has a very high specific active surface area. The main results reported by the same authors showed that the highest yields towards NO photocatalytic oxidation were obtained when incorporating in paint formulations the photocatalysts PC500 (Millennium), PC105 (Millennium), and UV100 (Sachtleben).

The type of material to be used as support is an important factor to be considered, because it directly affects activity, homogeneity, and adhesion of TiO_2 to the surface. Materials like ceramics tiles, paper, glass, fiberglass, and stainless steel have been employed (Cardona et al., 2004; Shephard et al., 2002). Borosilicate glass or quartz (Choi et al., 2006), quartz wool (Vella et al., 2010), glass reactor walls or glass flat plates, Raschig rings, glass tubes, glass cylinders (Hernández-Alonso et al., 2006; Pablos et al., 2012; Sordo et al., 2010; van Grieken et al., 2009a; van Grieken et al., 2009b), pumice stone (Subrahmanyam et al., 2008), monolithic structures (honeycomb) of ceramic (Avila et al., 1998) or metallic materials (Choi et al., 2006) have been studied as support. The thin-walled monoliths structures of polyethylene terephthalate (PET) and cellulose acetate (CA) are promising alternatives because these are inexpensive, lightweight, easily shaped polymeric materials and UV-

transparent (Portela et al., 2007).

Several commercial TiO_2 semiconductors are available in the market, showing different photocatalytic activity depending on the particle size, crystalline form and surface area, as also according to the structure of pollutants to be degraded (Gumy et al., 2006). The advances on this type of nanomaterial, which has been regarded as innovative and very efficient, can contribute to the development of insightful and proper design of nanotechnology-based photo-reactors using sunlight as a source of energy for the treatment of water contaminated with cyanotoxins and other emerging contaminants (Pelaez et al., 2012).

In heterogeneous photocatalysis, the transmittance of the supports and photocatalytic films is crucial to achieve an efficient process, maximizing the illuminated catalyst surface, considering the light path length of the tubular photoreactor. Packing the tubular photoreactor with glass spheres originates shadowed zones, principally in the center of the tube. This "shadowing effect" can be minimized employing a transparent material as support for a thin film catalyst.

Therefore, the purpose of this work was to promote the destruction of *Microcystin* (MC-LR) in natural and distilled water solutions by photocatalysis using artificial and solar UV energy and a tubular photoreactor packed with cellulose acetate transparent monoliths (CAM) coated with P25 paste or sol-gel TiO_2 films and with a photocatalytic TiO_2 loaded exterior paint (PC500, VLP7000 and P25). The effect of the addition of hydrogen peroxide was also investigated. Other supports, such as PVC or glass tubes and glass spheres were coated with the photocatalytic 3D TiO_2-based exterior paint. The best photocatalytic material was further applied to destroy *Cylindrospermopsin* (CYN).

6.2 Material and methods and experimental procedure

The general material and methods employed for the development of this work is described in the Chapter 3 (sections 3.1/ 3.2/ 3.4/ 3.5/ 3.6/ 3.7.2/ 3.8.2/ 3.8.3.1/ 3.8.3.3/ 3.8.4 - 3.8.7).

MC-LR solutions were prepared by diluting a concentrate MC-LR stock solution with distilled water. Two different stock solutions were used (Table 3.2) to eventually detect any difference related to the preparation mode and the influence of the presence of methanol in the MC-LR inactivation efficiency: (i) 50:50 % methanol:Milli-Q water equivalent to 0.2 % after dilution with distilled water in the lab-scale photoreactor, and (ii) the MC-LR stock

solution was further evaporated, allowing preparing a MC-LR solution without the presence of methanol stock solution (100 % water); the final pH of both solutions was between 6.5 and 7.0 (without any adjustment). CYN solutions were prepared by diluting a concentrate CYN stock solution with distilled water, resulting in a final pH of around 6.0.

An experiment was carried out using natural water from the Torrão reservoir (Tâmega River, (Amarante, Portugal), collected in November 2013. Temperature (*T*), pH, conductivity and Dissolved Oxygen (DO) were measured *in situ* using a portable multiparameter analyser (*Hanna Instruments 9828*). Other parameters were determined in laboratory, such as absorbance at 254 nm, dissolved organic carbon (DOC), total dissolved nitrogen and inorganic ions. The samples were previously filtered through nylon membrane filters (0.45 µm porosity and 25 mm diameter- Life Sciences). The river water was previously filtered through a GF/C filter from VWR to remove the suspended particles.

The UV spectra from MC-LR solution at pH 1.0, 3.0, 7.0 and 12.0, and CYN solution at pH 3.0, 7.0, 9.0 and 12.0, and also from the natural water and natural water spiked with MC-LR or CYN were obtained.

6.2.1 Experimental procedure

The borosilicate tube of the photoreactor was packed with different TiO_2 – coated supports: i) TiO_2-based paints (deposited on PVCT, glass tube, GS or PETM); ii) TiO_2 thin-films (sol-gel TiO_2 or P25 deposited on CAM). Prior to the experiments using TiO_2-paints, the photocatalytic paint was activated under solar UV radiation by recirculating water without toxin for 7-8 h. Afterwards the system was washed with distilled water before use.

The recirculation acrylic vessel was filled with 2.4 L of MC-LR solution (~100 µg L^{-1}) or CYN solution (~70 µg L^{-1}) and homogenized by stirring during 15 minutes in the darkness and a control sample was taken. The temperature set-point of the refrigerated thermostatic bath was set at 25 ºC. Afterwards, the water was pumped to the CPC unit and recirculated in the closed system during 40 minutes in the darkness and a new sample was taken to observe if any adsorption occurred. After that, the SUNTEST was turned on and the irradiance was set at 500 W m^{-2}, which is equivalent to 44 W_{UV} m^{-2} measured in the wavelength range 280-400 nm. When necessary, the stoichiometric amount of H_2O_2 necessary to completely mineralize the MC-LR or CYN in solution was added, and samples were taken at pre-defined times to evaluate the degradation progress.

6.3 Results and discussion

6.3.1 Photocatalytic films surface characterization

The "shadowing effect" can be minimized employing transparent monoliths as a support for the thin film catalyst, as for example PET or CAM monoliths. Figure 6.1 shows the transmittance spectra for PET and CAM monoliths with or without coating, and considering one or two sheets. Although CAM monoliths present a higher transmissibility than PET ones, both materials show more than 80 % transmissibility for wavelengths higher than 300 – 800 nm, indicating that these supports can be used for solar photocatalytic applications. The high transmissibility is also observed when the light has to cross two sheets of the monoliths, considering the path length in the tubular photoreactor.

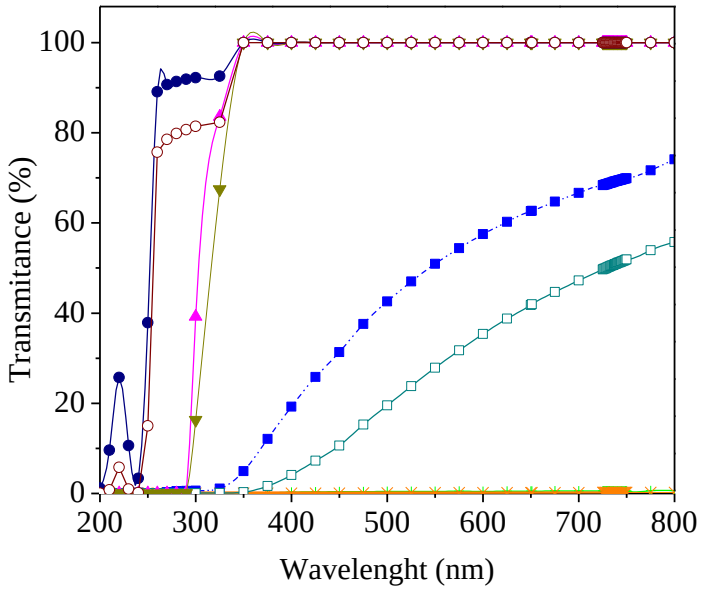

Figure 6.1 Normalized absorbance spectra of the material used in the photocatalytic reactions (see the sheets image in Fig. 3.3 d). (▲)PETM (1 sheet), (▼) PETM (2 sheets), (+) Pnt(4)-PETM (1sheet), (×) Pnt(4)-PETM (2 sheets), (♦) CAM (1 sheet), (◊) CAM (2 sheets), (■) P25-CAM (1 sheet) and (□) P25-CAM (2 sheets).

On the other hand, it can be observed a significant transmittance reduction for the coated monoliths when compared to the clean monoliths, especially in the case of Pnt(4)-PETM, revealing the presence of an opaque film. Águia et al. (2010) reported that the transmittance of a paint formulation similar to those used in this work, is negligible. However, transmittance spectra for P25-CAM and TiO_2-CAM samples show a significant increment of transmissibility mainly for wavelengths higher than 350 nm, considering the first outermost sheet (outside the hole). The transmissibility decreased considerably for the second sheet after

empty space and is even lower in the middle (after going through the two sheets) (Figure 3.3 d).

The surface morphology and chemical composition of the films Pnt(4)-PETM, Pnt(4)-GS, P25-CAM and TiO_2-CAM, before (fresh films) and after the photocatalytic process, was determined by SEM/EDX (Figure 6.2 and 6.3). All the EDX determinations showed a high amount of carbon, which can be related to the adhesive tape made of carbon, where each sample was mounted before observation (see section 3.6.2). The glass spheres painted by hand with Pnt(4) (Pnt(4)-GS) present a substantially thicker layer (144-159 µm) (Figure 6.2 a-c) than PETM coated by dip-coating (34-37 µm) (Figure 6.2 d-f). The PETM films seem to be more uniform and homogeneous than painted glass spheres (Figure 6.2 a-d). Comparing the PETM film thickness before and after the photocatalytic experiments it is possible to see that there was not significant deformation of the film structure after exposure to circulating water (Figure 6.2 e and f). According to the EDX spectra, the proportion of each element remained approximately the same after the photocatalytic experiments using the Pnt(4)-PETM samples (Figure 6.2 g and h). Similar results were reported by Monteiro et al. (2014) using a photocatalytic paint (four layers of photocatalytic paint in CAM; 9 wt. % of photo-TiO_2) for perchloroethylene degradation at gas phase.

The film thickness was determined from the cross-section images obtained for TiO2-CAM (Figure 6.3 b) and P25-CAM (Figure 6.3 e). The TiO2-CAM film thickness (always between 420-436 nm) was relatively uniform along the the whole surface of the monolith. The thickness of the layers for the monoliths, prepared with P25, is less uniform, varying from 0.867 to 1.118 µm. It is worth mentioning the amount of TiO2 deposited on each monolith: 0.0946 g for P25-CAM and 0.1632 g for TiO2-CAM. The surface of P25-CAM has the same appearance of the film obtained by Sampaio et al. (2013) from a TiO2 suspension, consisting of a granular texture due to the spheroidal shape of the TiO2 particles.

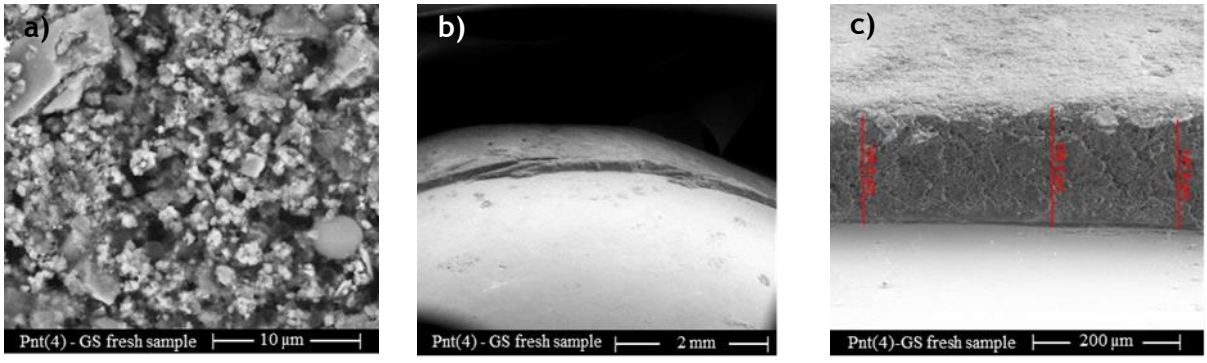

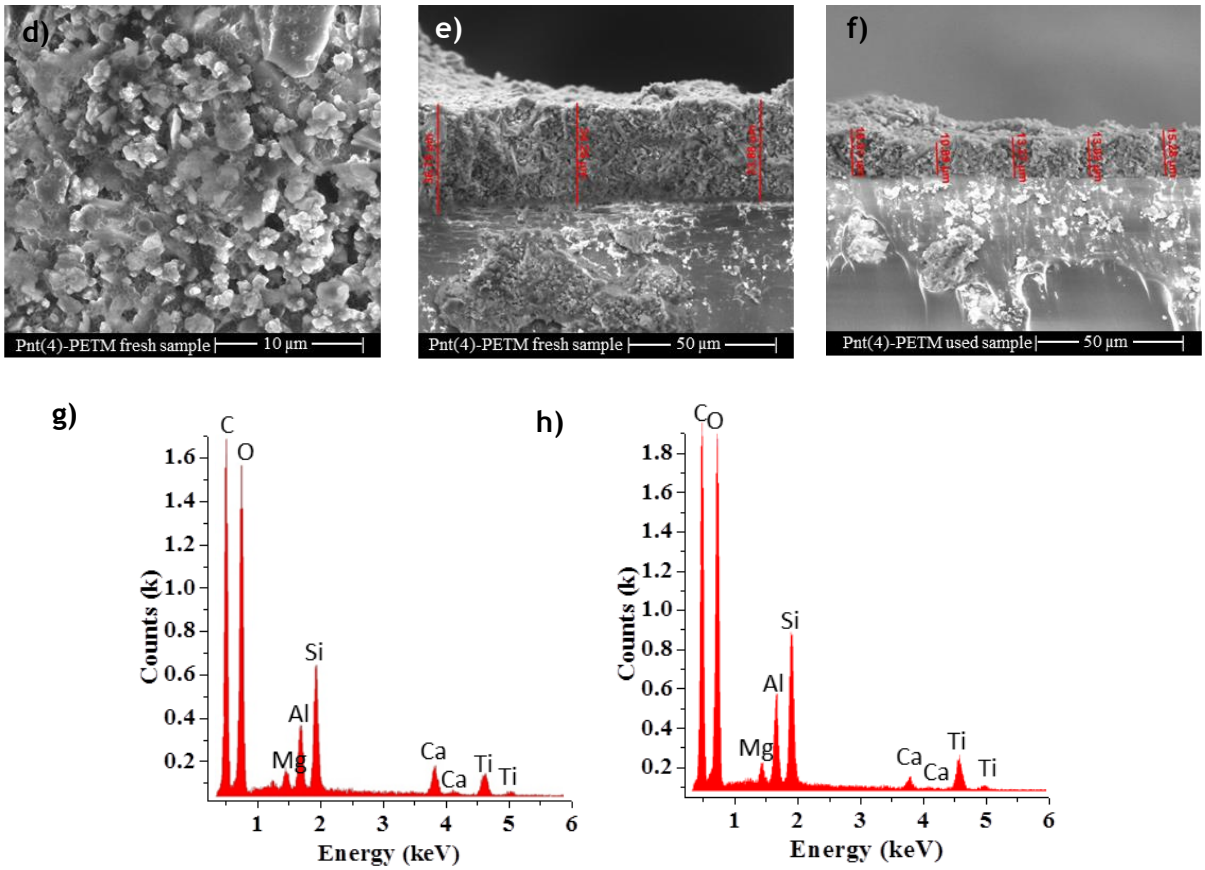

Figure 6.2 a), b) and c) SEM micrographs of the fresh sample Pnt(4)-GS; d), e) and f) SEM micrographs of the fresh and used sample Pnt(4)-PETM; g) and h) EDX spectra of the sample Pnt(4)-PETM fresh and used respectively.

Figure 6.3 d shows that the P25-CAM film structure is mainly composed of agglomerated particle, superimposed on top of each other, while the TiO_2-CAM film has a more uniform surface (Figure 6.3 a) probably due to the lower size of the TiO_2 particles. Moreover, several cracking fissures can be observed in the TiO_2-CAM film, producing a mosaic of flake-like forms, probably due to the thermal expansion coefficients of the CAM material and the TiO_2 (Narasimha Rao, 2003) produced by the sol-gel procedure (dry step); or, less probable, the fissures could be generated during the SEM analysis due to the high energy of the incident irradiation. Film delamination also occurs after the photocatalytic experiments (data not shown), where many fissures are brighter probably also due to the SEM light scattering promoted by delaminated film or, less probably, due to the partial filling of such fissures with some organics (Lopes et al., 2013a). Lopes et al. (2013a) tested the same material for gas phase photodegradation of perchloroethylene, and observed the same deformation after the photocatalytic process; however, a high photocatalytic activity was still obtained after the observed deterioration of the film. Regardless of the fissures in the surface of TiO_2-CAM, our

previous reports confirmed their stability and resistance for more than 50 h for gas phase operation (Lopes et al., 2013b).

The P25-CAM film thickness decreased substantially (0.66-0.78 µm) after the photocatalytic process, revealing a lower stability than that of TiO_2-CAM films, where it remained approximately constant. The EDX spectra showed that the proportion of each element remained approximately constant for both samples, before (Figs. 6.3 g and h) and after the photocatalytic process (data not shown).

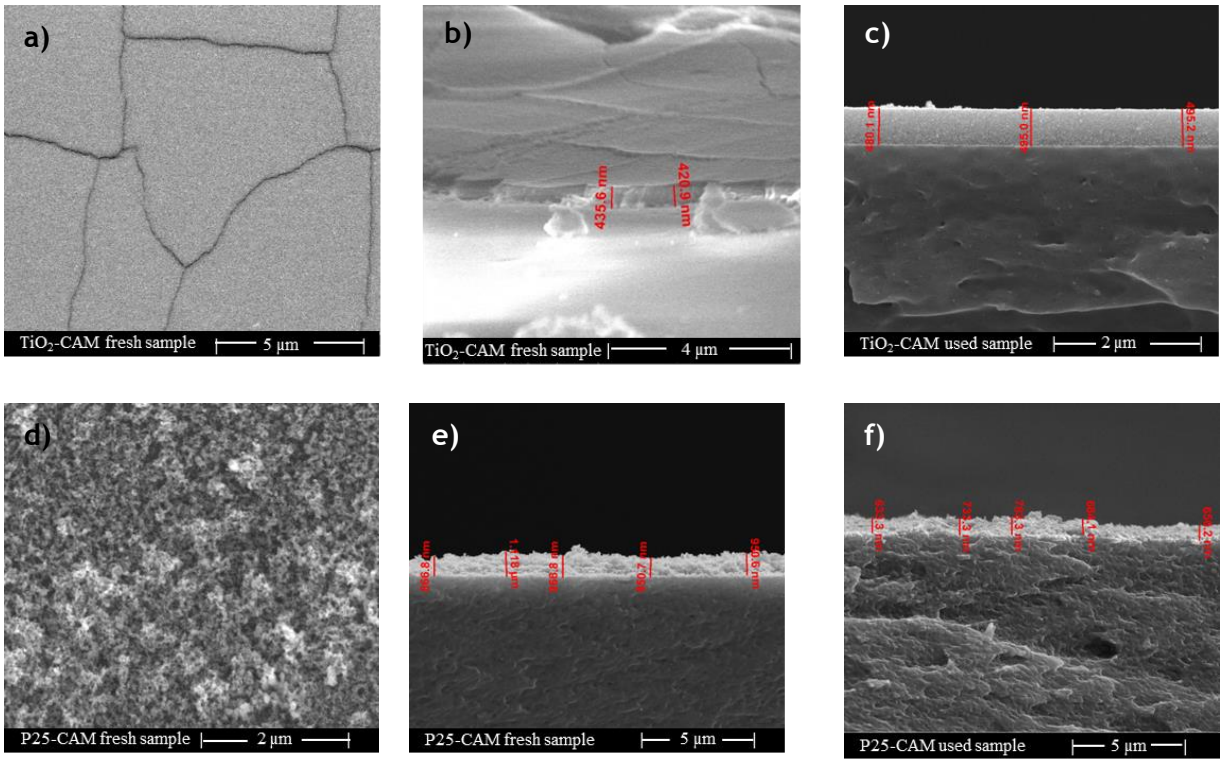

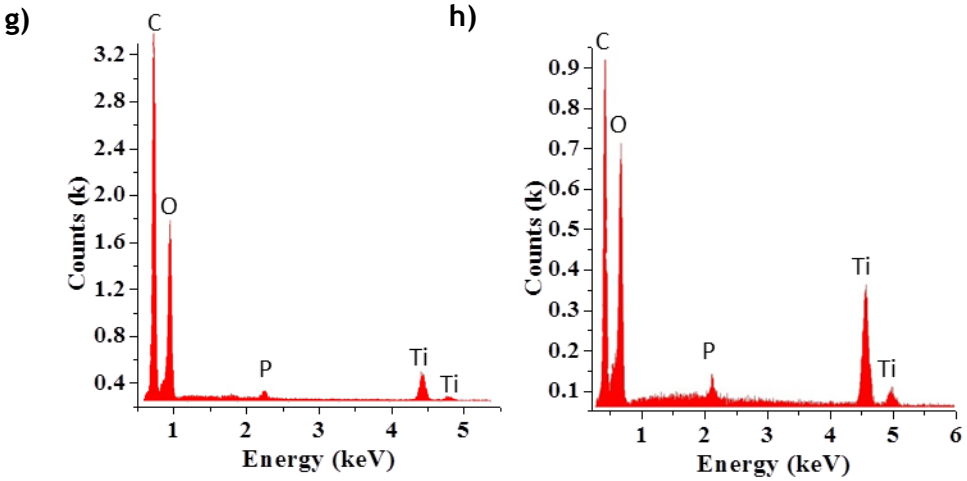

Figure 6.3 a), b) and c) SEM micrographs of the fresh and used sample TiO_2-CAM; d), e) and f) SEM micrographs of the fresh and used sample P25-CAM; g) and h) EDX spectra of TiO_2-CAM and P25-CAM respectively, both fresh sample.

6.3.2 Oxidation of MC-LR by photocatalysis using TiO_2 based paints

In this section the photocatalytic efficiency of TiO2 based paint using different types of TiO2 and immobilized in different support is evaluated. Experiments were carried out without catalyst: i) photolysis (water/MC-LR/UV) and ii) photolysis-paint (water/MC-LR/PVC tube painted with based paint/UV). MC-LR oxidation was negligible in both situations, i.e. more than 88 and 85 % of MC-LR was detected, respectively, after an accumulated UV energy of 10 kJ L^{-1} (Figure 6.4), which is in agreement with the almost negligible absorption of solar UV-visible radiation (Figure 6.5 b). In fact, several authors reported that MC-LR inactivation by UV radiation alone is not efficient (Feitz et al., 1999; Lawton et al., 2003; Pinho et al., 2012; Robertson et al., 1997; Triantis et al., 2012; Vilela et al., 2012), since the cyclic structure of the MC-LR (Figure 6.5 c) provides a high stability under sunlight and high temperatures (they can withstand after many hours of boiling) (Antoniou et al., 2009; Lawton et al., 1999; Liao et al., 2013; van Apeldoorn et al., 2007).

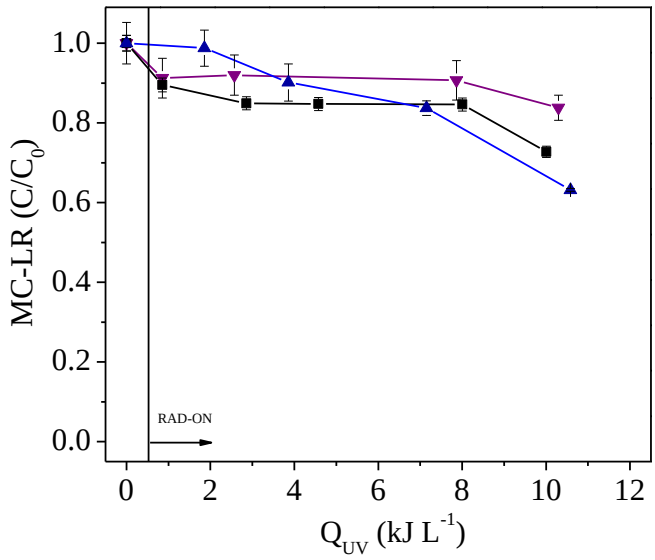

Figure 6.4 MC-LR inactivation by photolysis, photolysis with PVC tube painted with based paints without TiO_2 addiction and H_2O_2/UV: (▼) Photolysis/artificial UV, (▲) Photolysis (Pnt) and (■) H_2O_2 artificial UV.

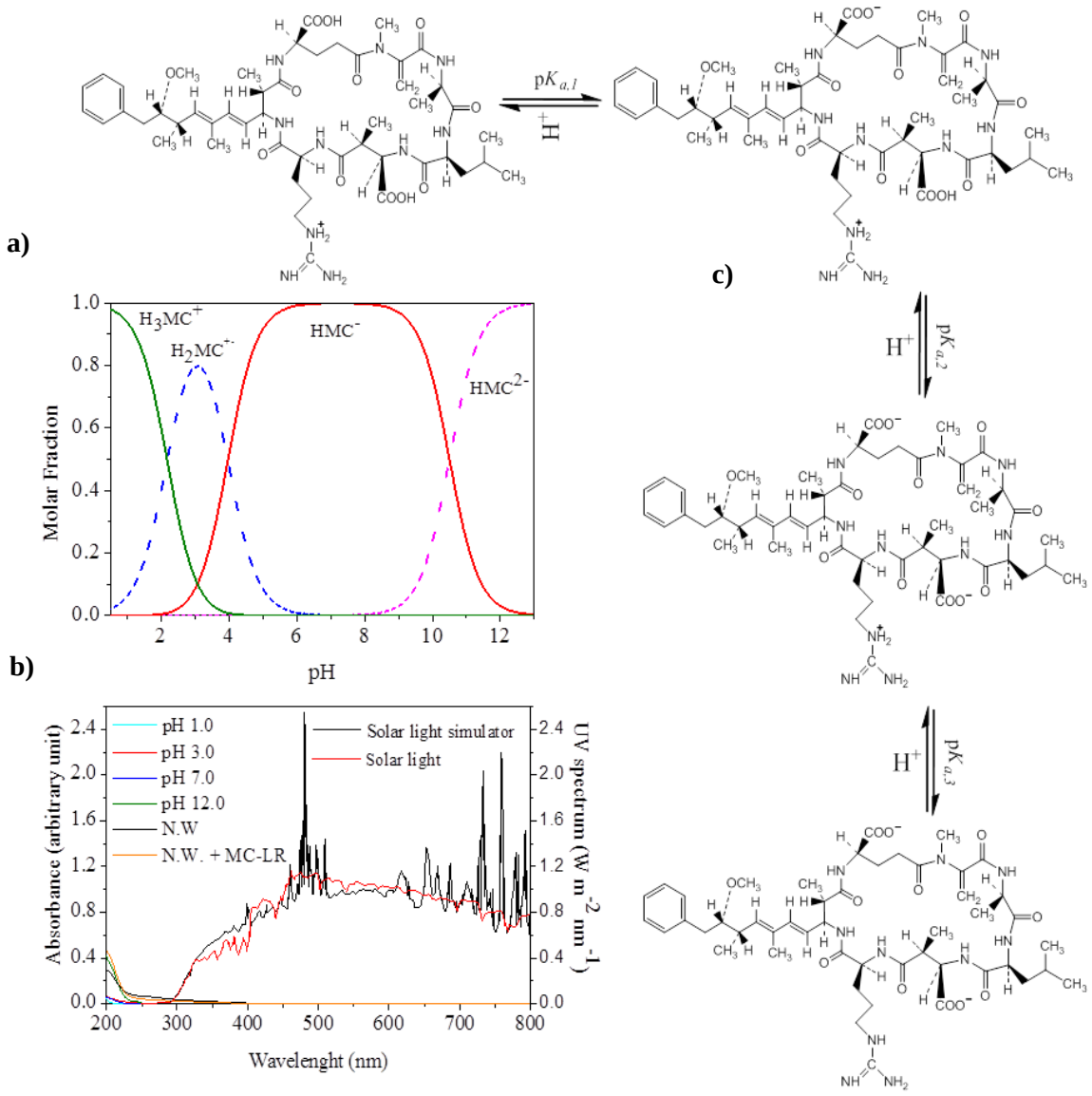

Figure 6.5 a) MC-LR speciation diagram as a function of pH; b) Normalized absorbance spectra of MC-LR at pH = 1.0, 3.0, 7.0 and 12; of natural water and natural water spiked with MC-LR; solar light simulator and natural UV spectra; and c) MC-LR dissociation equilibrium chemical structure in p$K_{a,1}$ = 2.17 (Klein et al., 2013), p$K_{a,2}$ = 3.96 (Klein et al., 2013) and p$K_{a,3}$ = 9.0 (de Maagd et al., 1999) (T = 25ºC, Ionic Strength = 0 M).

Because the purified solution of MC-LR contains MeOH as solvent, its influence in the destruction of MC-LR was studied. The obtained results are showed in the Fig. 8a for sample Pnt(4)-PVCT(M) which is compared with sample Pnt(4)-PVCT(W), without methanol. The presence of methanol inhibited the photocatalytic process efficiency in less than 10 %, acting as a scavenger of hydroxyl radicals.

Dark experiments performed with all TiO_2-based paints showed 0-10 % toxin adsorption under the operational conditions of pH between 6.5-7.0 (Figure 6.6). MC-LR contains two ionisable carboxyl groups and one ionisable amino group that are not part of peptide bonds that make up the cyclic peptide structure (Rudolph-Böhner et al., 1994) (Figure 6.5 c). The pK_a values of the carboxyl groups have been reported to be 2.17 and 3.96 (Klein et al., 2013). The intermediate species ($H_2MC^{\pm}$) is a zwitterion due to the protonated amine moiety associated with the arginine group of MC-LR (Figure 6.5 a). De Maggd et al. (1999) showed that the dissociation of this amine group likely occurs at pH > 9. For pH values higher than the point zero charge of TiO_2 (PZC = 6.7) (Ohtani, 2010), its surface becomes hydroxylated ($TiOH^-$) and the overall surface becomes negatively charged. The MC-LR molecule is also negatively charged for pH values higher than 6.0, explaining the low adsorption on the TiO_2 surface, since all the experiments were performed at pH values between 6.5 and 7.0. Pelaez et al. (2010) using films of NF-TiO_2, during 5 h of experiments in dark, concluded that the adsorption of MC-LR (initial MC-LR concentration of 500 μg L^{-1}) was approximately 39.6 % at pH 3.0, 30.1 % at pH 5.7, 9.2 % at pH 7.1 and 7.9 % at pH 8.0, which is well correlated with the charge of MC-LR molecules and TiO_2 surface according to the solution pH.

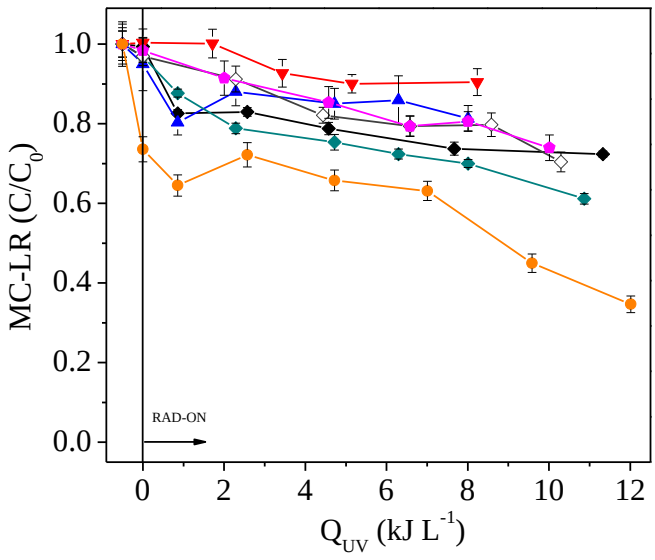

Figure 6.6 MC-LR inactivation by photocatalysis using TiO_2-based paints supported in different materials: (♦) Pnt(1)/artificial UV, (▼) Pnt(2)/artificial UV, (▲) Pnt(3)/artificial UV (♦) Pnt(4)-PVC/(W)/artificial UV, ◊) Pnt(4)-PVC/(M)/artificial UV, (●) Pnt(4)-GS/artificial UV, (●) Pnt(4)-PETM/artificial UV.

Figure 6.6 shows that the photocatalytic process using the Pnt(1), Pnt(2) and Pnt(3) TiO_2-based paints presents low MC-LR inactivation efficiencies (10-17 %). Further experiments with photocatalytic paints were performed by increasing the photoactive TiO_2 concentration

(PC500) and changing the inert support. PC500 was chosen as the photocatalyst since Águia et al. (2011b) reported a higher efficiency in the photo-oxidation of NO, using total replacement of the pigmentary TiO_2; moreover its activation step does not have to be harsher when compared to P25.

Pnt(4)-PVCT-M presents a higher efficiency in MC-LR inactivation (39 %) when compared with Pnt(1), Pnt(2) and Pnt(3) (cf. Table 3.2), which can be associated to the higher TiO_2 concentration (12 %; 100 mg L^{-1}) achieved by the total replacement of the pigmentary TiO_2 and higher light penetration. Moreover, in the Pnt(4)-PVCT-M the paint was deposited on a PVC tube with a higher diameter, when compared to the glass tube, also presenting higher resistance, practicality, low cost and, such as the glass, it is an inert material, which does not increase the organic content (DOC) of the solution.

Two others experiments were performed using the paint formulation PC500 with 12 wt. % of TiO_2 and total pigmentary TiO_2 replacement, supported in glass spheres (Pnt(4)-GS and Pnt(4)-PETM).

Despite formulation Pnt(4)-GS presents the higher TiO_2 concentration (600 mg L^{-1}) and high contact surface area, it did not lead to the best result. Probably, when the tubular photoreactor is packed with glass spheres, only a small part of the catalyst surface area is exposed to UV light, due to "shading effect", principally for the spheres that are in the center of the tube. Beyond that, the glass spheres were painted by hand, resulting in a ticker layer (± 150 μm), and probably a fraction of the TiO_2 particles were not illuminated.

The use of transparent PET monoliths coated with Pnt(4), led to a substantially increase on MC-LR inactivation efficiency, mainly attributed to the higher active contact surface, more than 7 times than using the glass or PVC cylindrical tube. A significant adsorption was also observed (25 %) for the Pnt(4)-PETM system, probably associated with the higher TiO_2 concentration and higher UV radiation penetration.

Experiments with the addition of H_2O_2 were also carried out, using Pnt(4) formulation: Pnt(4)-PVCT-W/H_2O_2 and Pnt(4)-PETM/H_2O_2. The addition of H_2O_2 had a positive effect on the prevention of the electron-hole recombination by accepting photogenerated electrons from the conduction band (Eq. 6.01) and in the production of additional $OH^{\bullet}$ radicals through reactions (Eq. 6.01) and (Eq. 6.02) (Rodríguez et al., 1996).

$$H_2O_2 + e_{CB}^- \longrightarrow OH^\bullet + OH^- \quad \text{(Eq.6.01)}$$

$$H_2O_2 + O_2^{\bullet -} \longrightarrow OH^\bullet + OH^- + O_2 \quad \text{(Eq. 6.02)}$$

The kinetic profiles show a very fast initial reaction, until 2 kJ_{UV} L^{-1}, followed by a slow inactivation process, which can be attributed to the competition of hydroxyl radicals for the initial intermediates generated and the MC-LR molecules.

The addition of H_2O_2 to Pnt(4), using the cylindrical PVC tube as support for the photocatalytic paint (Pnt(4)-PVCT-W/H_2O_2), led to an increment in the inactivation efficiency by 31 %, when compared with Pnt(4)-PVCT-W system, achieving a final MC-LR inactivation efficiency of almost 70 % after 10 kJ_{UV} L^{-1} and consuming 13 mM of H_2O_2. On the other hand, the Pnt(4)-PETM/H_2O_2 system achieved a MC-LR inactivation of 93 % after 11 kJ_{UV} L^{-1} and consuming only 2 mM of H_2O_2, which corresponds to an increment in the photocatalytic efficiency of 28 % when compared with the Pnt(4)-PETM system (Figure 6.7)

MC-LR inactivation is negligible using the H_2O_2/UV-visible system (Figure 6.4), mainly due to the low oxidant potential of H_2O_2. Moreover a negligible fraction of UVA-Vis solar radiation is absorbed by the MC-LR molecule (Figure 6.5 b) and photolysis of H_2O_2 is not significant due to the fact that radiation below 280 nm is needed for an effective H_2O_2 cleavage, and borosilicate glass tubes have a cut-off at 280 nm.

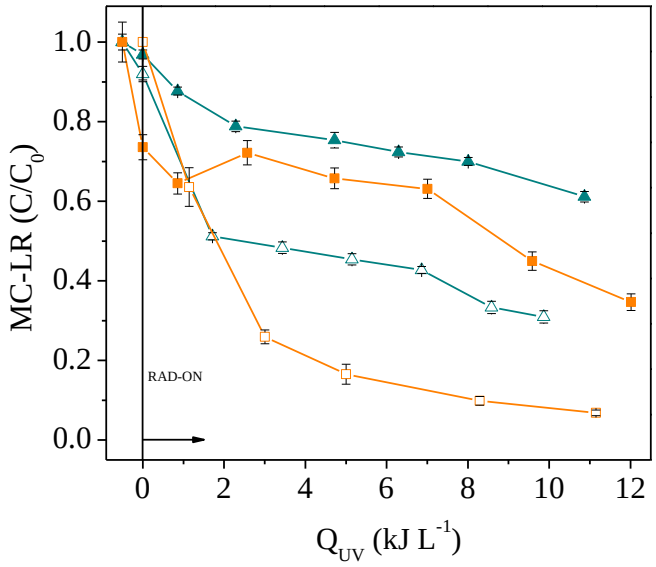

Figure 6.7 MC-LR inactivation by photocatalysis with and without H_2O_2 using TiO_2-based paint, formulation Pnt(4) supported in PVCT and PETM: (▲) Pnt(4)-PVC/(W)/artificial UV, (Δ) Pnt(4)-PVC/(W) H_2O_2/artificial UV, (■) Pnt(4)-PETM/artificial UV and (□) Pnt(4)-PETM/H_2O_2/artificial UV.

MC-LR inactivation is negligible for the H_2O_2/UV-visible system (Figure 6.4), mainly due to the low oxidant potential of H_2O_2. Moreover a negligible fraction of UVA-Vis solar radiation is absorbed by the MC-LR molecule (Figure 6.5 b) and photolysis of H_2O_2 is not significant due to the fact that radiation below 280 nm is needed for an effective H_2O_2 cleavage, and borosilicate glass tubes have a cut-off at 280 nm.

6.3.3 Oxidation of MC-LR by photocatalysis using TiO_2 thin films

In the experiments using TiO_2 thin films (P25-CAM and TiO_2-CAM), a 19 % decrease in MC-LR concentration was observed in darkness, attributed to the adsorption of MC-LR on the catalyst surface (Figure 6.8), just as happened in the system Pnt(4)-PETM, probably because of the higher TiO_2 concentration and surface area.

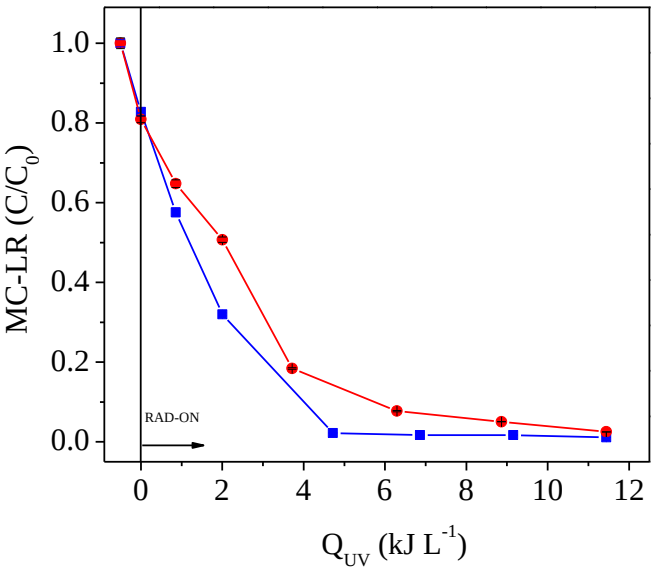

Figure 6.8 MC-LR inactivation by photocatalysis using a catalytic bed with P25-CAM and TiO_2-CAM: (■) TiO_2-CAM/artificial UV and (●) P25-CAM/artificial UV.

MC-LR inactivation by TiO_2-CAM and P25-CAM achieved ~97 % and ~90 % efficiency after 5 kJ L^{-1}, respectively (Figure 6.8). The photocatalytic inactivation process follows pseudo-first-order kinetics with k = 0.32 ± 0.03 L kJ^{-1} and k = 0.49 ± 0.03 L kJ^{-1}, respectively for P25-CAM and TiO_2-CAM systems. The slightly higher efficiency of TiO_2-CAM when compared with P25-CAM can be mainly attributed to the higher concentration of TiO_2 deposited on the surface of the CAM structure.

The higher efficiency of the P25 or sol-gel TiO_2 films when compared with the TiO_2-loaded exterior paints can be mainly associated with the mass transfer limitations inside the porous structure of the paint.

Antoniou et al. (2009) used a TiO_2-sol thin film after three dip-coatings-calcination on glass substrate to destroy MC-LR by photocatalysis, achieving ~50 % MC-LR inactivation (C_o ~ 2000 µg L^{-1}; pH ~ 6.8) after 4 h. At acidic pH (3.0) the photocatalytic efficiency increased substantially to values higher than 85 %, mainly associated with the attractive forces between the positively charged titania ($TiOH_2^+$) and negatively charged toxin ($H_2MC^{\pm}$ and HMC^-). Although low pH favours substantially the photocatalytic process efficiency, in a full-scale treatment plant, costs associated with the acidification/neutralization steps may be high, and the addition of high amounts of sodium hydroxide (NaOH) or hydrochloric acid (HCl) to water for human consumption is not possible. Feng et al. (2005) studied the photocatalytic inactivation of MC-LR (C_0 = 20 µg L^{-1}) using a nano-TiO_2 thin film, prepared

by sol-gel and dip-coating methods, and a UV 365 nm lamp, obtaining over 95 % inactivation after 120 minutes at pH 4.0. Liu et al. (2013) used a carbon-based surfactant-assisted sol-gel method to synthesize visible-light-active C-N-TiO_2 immobilized on a borosilicate glass, to destroy MC-LR (C_0 = 500 µg L^{-1} and pH 3), under visible light irradiation provided by two 15 W fluorescent lamps, and obtained between 70 and 80 % inactivation for all films tested, after 5 h exposure.

In the present work P25-CAM proved to be the best thin film formulation, because it allows a simpler and cheaper process, and the results obtained are similar to the ones obtained by TiO_2-CAM, although with a lower TiO_2 concentration. For all these reasons, P25-CAM was chosen for the photocatalytic tests with natural solar light or addition of H_2O_2.

The photocatalytic reaction using P25-CAM under natural UV radiation ($\overline{T}$ = 27 ºC; $\overline{UV}$ = 38 W m^{-2}) shows a similar MC-LR inactivation profile when compared to that obtained using artificial solar radiation with a constant UV irradiance of 44 W_{UV} m^{-2} (Figure 6.9).

The addition of H_2O_2 to the P25-CAM system under artificial UV solar light, increased substantially the initial photocatalytic reaction rate, being necessary only 1.26 mM of H_2O_2 to achieve 85 % MC-LR inactivation after 1 kJ L^{-1} accumulated energy, while when without adding H_2O_2, only 20 % of MC-LR was removed after the same reaction period. Comparing the pseudo-first-order kinetic parameters (Table 6.1) one can conclude that the best system is P25-CAM/H_2O_2 (k = 2.0 ± 0.4 L kJ^{-1} and $r_0 = (18 \pm 4) \times 10$ µg kJ^{-1}). The reaction rate decreases along the reaction, which can be attributed to the competition of hydroxyl radicals between the initial intermediates generated and the MC-LR molecules.

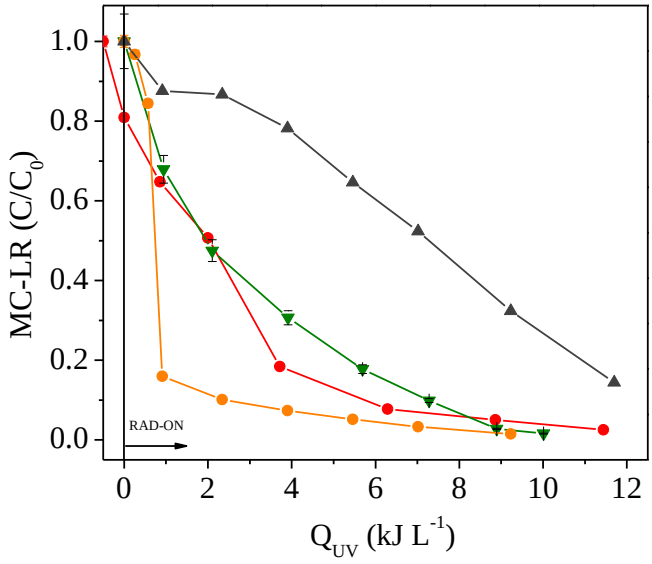

Figure 6.9 MC-LR inactivation by photocatalysis using P25-CAM with and without H_2O_2, with solar UV radiation, experiments using river water spiked with MC-LR: (●) P25-CAM/artificial UV, (▼) P25-CAM/solar UV, (●) P25-CAM/H_2O_2/artificial UV and (▲) P25-CAM/H_2O_2/artificial UV (river water).

Table 6.1 Pseudo-first-order kinetic parameters.

Run	***k* (L kJ^{-1})** [a]	***r*$_0$ (μg kJ^{-1})**[b]
P25-CAM/artificial UV	0.32 ± 0.03	25 ± 2
P25-CAM/solar UV	0.7 ± 0.3	(4 ± 1)×10
P25-CAM/H_2O_2	2.0 ± 0.4	(18 ± 4)×10
P25-CAM/H_2O_2/artificial UV (river water)	0.12 ± 0.01	11 ± 1
TiO_2-CAM/artificial UV	0.49 ± 0.03	49 ± 3

[a] Pseudo-first-order kinetic constant; [b] Initial reaction rate.

Although hydrogen peroxide can act as an alternative electro acceptor to oxygen, which can potentiate the reaction, high H_2O_2 concentrations can promote a competition between the H_2O_2 and MC-LR for active sites on the TiO_2 catalyst surface (Cornish et al., 2000; Wang and Hong, 1999), decreasing the reaction rates. According to Cornish et al. (2000) the optimum peroxide concentration is between 0.005 and 0.1 % (% v/v), considering an initial MC-LR concentration of 100 μg mL^{-1}.

A final photocatalytic experiment using natural water from the Torrão reservoir (Tâmega River, Portugal) spiked with ~ 100 μg L^{-1} MC-LR (P25-CAM-river water) was performed, in order to evaluate the influence of other inorganic and organic species present in surface

waters in degrading MC-LR. The water characteristics of the natural water are given in Table 6.2.

Table 6.2 Water quality parameters of Tâmega river water.

Parameters	Value
pH	7.3
Temperature	15 ºC
Conductivity	43 µS cm^{-1}
Dissolved oxygen	10.8 mg O_2 L^{-1}
Absorbance at 254 nm	0.063
DOC*	2.2 mg C L^{-1}
TDC*	3.7 mg C L^{-1}
DIC*	1.5 mg C L^{-1}
Total nitrogen	0.76 mg N L^{-1}
Nitrite	0.20 mg NO_2^- L^{-1}
Nitrate	3.0 mg NO_3^- L^{-1}
Sulphate	2.2 mg SO_4^{2-} L^{-1}
Chloride	4.9 mg Cl^- L^{-1}
Phosphate	< 0.05 mg PO_4^{3-} L^{-1}
Lithium	< 0.01 mg Li^+ L^{-1}
Sodium	4.3 mg Na^+ L^{-1}
Ammonium	0.02 NH_4^+ L^{-1}
Magnesium	0.36 mg Mg^{2+} L^{-1}
Calcium	1.2 mg Ca^{2+} L^{-1}

*DOC-Dissolved Organic Carbon; TDC-Total Dissolved Carbon: DIC-Dissolved Inorganic Carbon

Figure 6.9 shows a slow MC-LR degradation kinetic profile principally in the initial part of the reaction, when compared with the experiments performed with distilled water, being necessary more than 10 times UV energy and 2.75 mM of H_2O_2 to achieve 90 % MC-LR inactivation. Although the amount of dissolved organic carbon present in the natural water is low (2.2 mg C L^{-1}), which is normally attributed to the presence of recalcitrant humic substances, its concentration is several times higher than the contribution of MC-LR for DOC. Those recalcitrant organic substances can compete for the UV photons and hydroxyls radicals, as well as they can act as photosensitizers (He et al., 2012).

6.3.4 Oxidation of CYN by photocatalysis using TiO_2 thin film

Some experiments were carried out to assess the CYN inactivation efficiency of one of the materials that showed good results in MC-LR removal (P25-CAM and P25-CAM/H_2O_2). The initial CYN concentration was around 70 μg L^{-1}, a typical concentration found in water reservoirs (Chiswell et al., 1999; Senogles et al., 2001). According to Senogles et al. (2001), small variations in the concentration (50 and 120 μg L^{-1}) do not affect the TiO_2 photocatalysis of CYN.

CYN is very stable, as it was proven by Chiswell et al. (1999) in a work where they studied the effect of temperature and pH on the decomposition of CYN in darkness. The authors boiled an aqueous extract of *C. raciborskii* containing 2.5 mg L^{-1} of CYN for 15 min and no effect on the concentration was observed. Experiments were also performed at pH 4, 7 and 10. After 8 weeks at room temperature of 22 ºC, CYN maintained 75 % of the initial concentration (4 mg L^{-1}).

A negligible fraction of UVA-Vis solar radiation is absorbed by the CYN molecule at different pH values (spectra not showed), which reflects the negligible effect of photolysis in CYN concentration (see Figure 6.10). No photolysis was also observed by He and collaborators (He et al., 2013) when using a 254 nm UV lamp to destroy CYN. Beyond that, after a period of 40 min in dark, no significant adsorption was detected. Similarly, Senogles et al. (2001) did not find adsorption in the dark, using 0.1 g L^{-1} TiO_2, at pH = 4, pH = 7 and pH = 9. With a reported pK_a value of 8.8, CYN is mainly present as a zwitterion, with an overall zero charge at pH ≤ 7.4 (He et al., 2013; Onstad et al., 2007), due to the negatively charged sulfate group and the positively charged guanidine group (Máthé et al., 2013). The marginal adsorption observed in these experiments can thus be explained by the fact that at pH = 6, CYN molecules and TiO_2 particles are neutral species (Figure 6.11), so no attraction between them occurs.

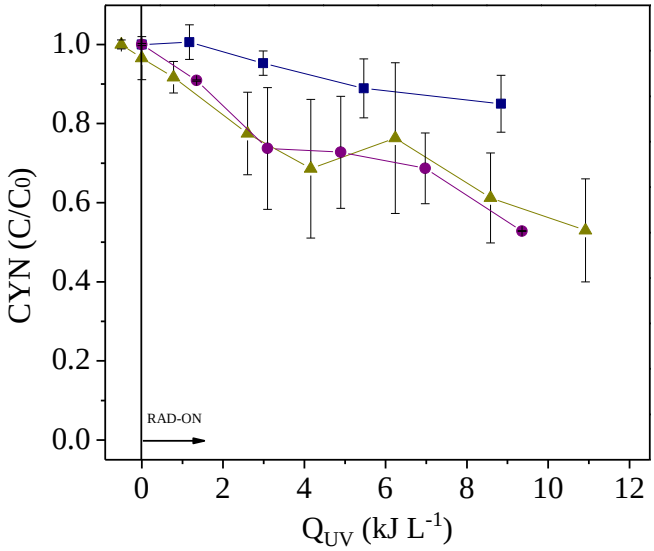

Figure 6.10 CYN inactivation by photolysis and photocatalysis using a catalytic bed with P25-CAM with artificial and solar UV radiation: (■) Photolysis-CYN/artificial UV, (▲) P25-CAM-CYN/artificial UV and (●) P25-CAM-CYN/solar UV.

a) **b)**

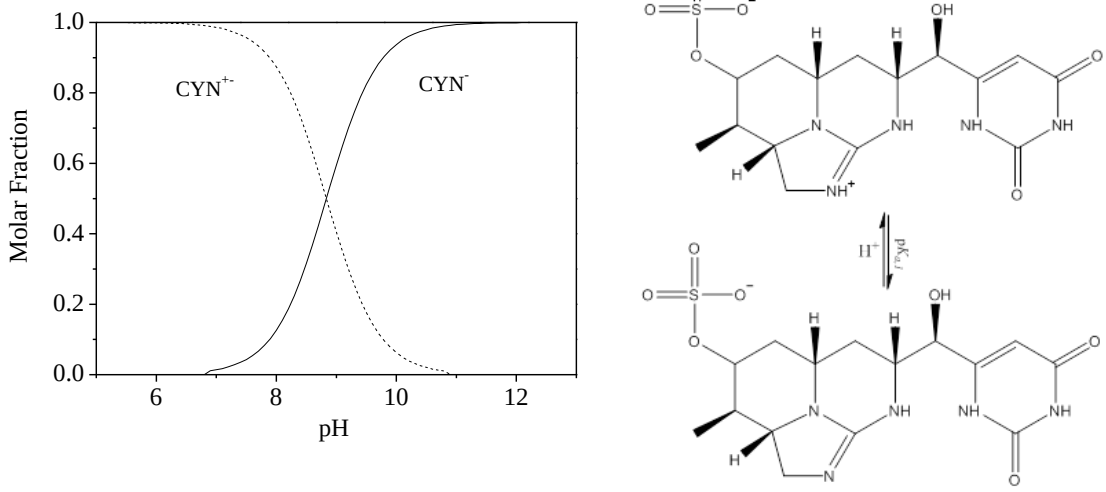

Figure 6.11 a) CYN speciation diagram as a function of pH; b) CYN dissociation equilibrium chemical structure in pK_a= 8.8 (T = 25ºC, Ionic Strength = 0 M) (He et al., 2013; Onstad et al., 2007).

No difference was observed when using P25-CAM-CYN with artificial UV and natural solar UV radiation as regards CYN inactivation: 47 % after Q_{UV} ~ 9 kJ L^{-1} in both cases (Figure 6.10). The addition of H_2O_2 (P25-CAM-CYN/H_2O_2/UV) (Figure 6.12) showed a negligible effect on the reaction rate, leading to only 40 % inactivation, a value comparable to that obtained without H_2O_2 addition and the same energy (~ 9 kJ_{UV} L^{-1}), but the result suggests

that a longer time exposure can potentiate the CYN's inactivation, because after 15.6 kJ_{UV} L^{-1} the inactivation raised to 55 %. The result from the H_2O_2/UV experiment was similar to that obtained by photolysis (Fig 6.12): ~10 % inactivation after 10 kJ_{UV} L^{-1} accumulated energy.

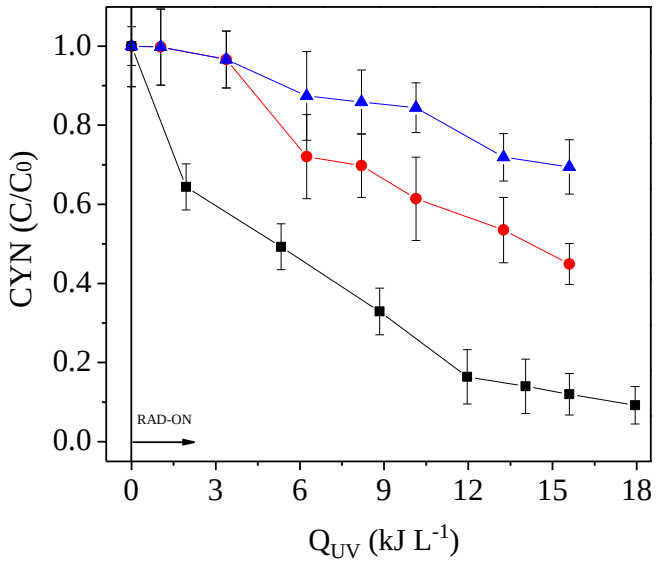

Figure 6.12 CYN inactivation by photocatalysis using P25-CAM/H_2O_2/artificial UV radiation in distilled and river water spiked with CYN, and only H_2O_2/artificial UV: (●) P25-CAM-CYN/H_2O_2/artificial UV, (■) P25-CAM-CYN/H_2O_2/artificial UV (river water) and (▲) CYN/H_2O_2/artificial UV.

To investigate the influence of the natural organic material in CYN inactivation, an experiment was carried out with river water (P25-CAM-CYN/H_2O_2/river water, Figure 6.12) from the same source of the natural water used in the MC-LR experiment (Table 6.2). In this experiment it was achieved 85 % CYN inactivation after ~ 16 kJ_{UV} L^{-1} with r_0 = 14 ± 0.9 µg kJ^{-1}, whereas when distilled water was used (P25-CAM-CYN/H_2O_2) r_0 was only 6 ± 1 µg kJ^{-1}. Senogles et al. [63] achieved a similar result corresponding to a CYN half-life of 4.4 min, against 16.1 min using Milli-Q water; the better performance was attributed to the presence of inorganic matter in the natural water. In the present work, among the elements found, Fe (0.5 mg L^{-1} of Fe at the end of the reaction), for example, possibly has contributed to induce a photo-Fenton reaction.

6.4 Conclusions

CAM or PET monoliths are a good supports for photocatalysts, when compared with cylindrical glass or PVC tubes and glass spheres. They present honeycomb three-dimensional transparent arrays, large specific photoactive surface area and consequently increased light absorption, rugged surface that enables good adhesion of the catalytic coatings, and also provide a structure rigid enough to pack homogeneously the tubular photoreactor.

The photocatalytic oxidation of MC-LR at neutral pH values was achieved successfully using different heterogeneous solar photocatalytic processes, avoiding the need of acidification/neutralization steps, as well as the post-filtration step required when slurry suspensions of the photocatalyst are used. The higher efficiency of P25 paste and sol-gel TiO_2 films deposited in CAM when compared with TiO_2 loaded exterior paints can be mainly associated with mass transfer limitations inside the porous structure of the paint.

The addition of H_2O_2 to the P25-CAM system enhanced substantially the MC-LR degradation rate, being necessary less than 1 $kJ_{UV}\ L^{-1}$ accumulated energy to achieve more than 85 % MC-LR inactivation ($C_o \sim 100\ \mu g\ L^{-1}$). The presence of H_2O_2 also enhanced significantly the efficiency of the photocatalytic system using the photocatalytic paints. The presence of organic matter in river water impairs significantly the MC-LR inactivation rate. More than 85 % inactivation of MC-LR was achieved using the P25-CAM/H_2O_2 system.

Heterogeneous photocatalysis driven by solar energy can be used for the treatment of natural water, allowing obtaining MC-LR levels below the guideline value of 1 $\mu g\ L^{-1}$. As regards CYN inactivation although TiO_2 photocatalysis seems to be a good process, a long exposure time is required.

6.5 References

Águia, C., Ângelo, J., Madeira, L.M., Mendes, A., 2010. Influence of photocatalytic paint components on the photoactivity of P25 towards NO abatement. Catalysis Today 151, 77-83.

Águia, C., Ângelo, J., Madeira, L.M., Mendes, A., 2011a. Influence of paint components on photoactivity of P25 titania toward NO abatement. Polymer Degradation and Stability 96, 898-906.

Águia, C., Ângelo, J., Madeira, L.M., Mendes, A., 2011b. Photo-oxidation of NO using an exterior paint – Screening of various commercial titania in powder pressed and paint films. Journal of Environmental Management 92, 1724-1732.

Antoniou, M.G., Nicolaou, P.A., Shoemaker, J.A., de la Cruz, A.A., Dionysiou, D.D., 2009. Impact of the morphological properties of thin TiO_2 photocatalytic films on the detoxification of water contaminated with the cyanotoxin, microcystin-LR. Applied Catalysis B: Environmental 91, 165-173.

Avila, P., Bahamonde, A., Blanco, J., Sánchez, B., Cardona, A.I., Romero, M., 1998. Gas-phase photo-assisted mineralization of volatile organic compounds by monolithic titania catalysts. Applied Catalysis B: Environmental 17, 75-88.

Ávila, P., Sánchez, B., Cardona, A.I., Rebollar, M., Candal, R., 2002. Influence of the methods of TiO_2 incorporation in monolithic catalysts for the photocatalytic destruction of chlorinated hydrocarbons in gas phase. Catalysis Today 76, 271-278.

Cardona, A.I., Candal, R., Sánchez, B., Ávila, P., Rebollar, M., 2004. TiO_2 on magnesium silicate monolith: effects of different preparation techniques on the photocatalytic oxidation of chlorinated hydrocarbons. Energy 29, 845-852.

Chiswell, R.K., Shaw, G.R., Eaglesham, G., Smith, M.J., Norris, R.L., Seawright, A.A., Moore, M.R., 1999. Stability of cylindrospermopsin, the toxin from the cyanobacterium, Cylindrospermopsis raciborskii: Effect of pH, temperature, and sunlight on decomposition. Environmental Toxicology 14, 155-161.

Choi, H., Stathatos, E., Dionysiou, D.D., 2006. Sol–gel preparation of mesoporous photocatalytic TiO_2 films and TiO_2/Al_2O_3 composite membranes for environmental applications. Applied Catalysis B: Environmental 63, 60-67.

Cornish, B., Lawton, L., Robertson, P., 2000. Hydrogen peroxide enhanced photocatalytic oxidation of microcystin-LR using titanium dioxide. Applied Catalysis B, Environmental 25, 59-67.

de Maagd, P.G.-J., Hendriks, A.J., Seinen, W., Sijm, D.T.H.M., 1999. pH-Dependent hydrophobicity of the cyanobacteria toxin microcystin-LR. Water Research 33, 677-680.

Falconer, I.R., Humpage, A.R., 2005. Health Risk Assessment of Cyanobacterial(Blue-green Algal) Toxins in Drinking Water. International Journal of Environmental Research and Public Health 2, 43-50.

Feitz, A., Waite, T., Jones, G., Boyden, B., Orr, P., 1999. Photocatalytic degradation of the blue green algal toxin microcystin-LR in a natural organic-aqueous matrix. Environ. Sci. Technol 33, 243-249.

Feng, X.G., Rong, F., Wei, T., Yuan, C.W., 2005. Studies of photocatalytic degradation of trace-level MC-LR in water on thin film of titanium dioxide, in: B, D.a.d.d.P. (Ed.), China International Conference on Nanoscience and Technology, ChinaNANO 2005. Trans Tech Publications Ltd., Beijing; China, pp. 951-954.

Garcia, A.C., Bargu, S., Dash, P., Rabalais, N.N., Sutor, M., Morrison, W., Walker, N.D., 2010. Evaluating the potential risk of microcystins to blue crab (Callinectes sapidus) fisheries and human health in a eutrophic estuary. Harmful Algae 9, 134-143.

Gumy, D., Rincon, A.G., Hajdu, R., Pulgarin, C., 2006. Solar photocatalysis for detoxification and disinfection of water: Different types of suspended and fixed TiO_2 catalysts study. Solar Energy 80, 1376-1381.

Han, C., Pelaez, M., Likodimos, V., Kontos, A.G., Falaras, P., O'Shea, K., Dionysiou, D.D., 2011. Innovative visible light-activated sulfur doped TiO_2 films for water treatment. Applied Catalysis B: Environmental 107, 77-87.

He, X., de la Cruz, A.A., Dionysiou, D.D., 2013. Destruction of cyanobacterial toxin cylindrospermopsin by hydroxyl radicals and sulfate radicals using UV-254 nm activation of hydrogen peroxide, persulfate and peroxymonosulfate. Journal of Photochemistry and Photobiology A: Chemistry 251, 160-166.

He, X., Pelaez, M., Westrick, J.A., O'Shea, K.E., Hiskia, A., Triantis, T., Kaloudis, T., Stefan, M.I., de la Cruz, A.A., Dionysiou, D.D., 2012. Efficient removal of microcystin-LR by UV-C/H_2O_2 in synthetic and natural water samples. Water Research 46, 1501-1510.

Hernández-Alonso, M.D., Tejedor-Tejedor, I., Coronado, J.M., Soria, J., Anderson, M.A., 2006. Sol–gel preparation of TiO_2–ZrO_2 thin films supported on glass rings: Influence of phase composition on photocatalytic activity. Thin Solid Films 502, 125-131.

Hitzfeld, B., Höger, S., Dietrich, D., 2000. Cyanobacterial toxins: removal during drinking water treatment, and human risk assessment. Environmental health perspectives 108, 113.

Hoeger, S.J., Hitzfeld, B.C., Dietrich, D.R., 2005. Occurrence and elimination of cyanobacterial toxins in drinking water treatment plants. Toxicology and Applied Pharmacology 203, 231-242.

Masao Kaneko I.O., Photocatalysis Science and Technology, Kodansha Springer, Tokyo, 2002

Klein, A.R., Baldwin, D.S., Silvester, E., 2013. Proton and Iron Binding by the Cyanobacterial Toxin Microcystin-LR. Environmental Science & Technology 47, 5178-5184.

Lawton, L., Robertson, P., Cornish, B., Jaspars, M., 1999. Detoxification of microcystins (cyanobacterial hepatotoxins) using TiO_2 photocatalytic oxidation. Environ. Sci. Technol 33, 771-775.

Lawton, L., Robertson, P., Cornish, B., Marr, I., Jaspars, M., 2003. Processes influencing surface interaction and photocatalytic destruction of microcystins on titanium dioxide photocatalysts. Journal of Catalysis 213, 109-113.

Liao, W., Zhang, Y., Zhang, M., Murugananthan, M., Yoshihara, S., 2013. Photoelectrocatalytic degradation of microcystin-LR using Ag/AgCl/TiO_2 nanotube arrays electrode under visible light irradiation. Chemical Engineering Journal 231, 455-463.

Liu, G., Han, C., Pelaez, M., Zhu, D., Liao, S., Likodimos, V., Kontos, A.G., Falaras, P., Dionysiou, D.D., 2013. Enhanced visible light photocatalytic activity of CN-codoped TiO 2 films for the degradation of microcystin-LR. Journal of Molecular Catalysis A: Chemical 372, 58-65.

Lopes, F.V.S., Miranda, S.M., Monteiro, R.A.R., Martins, S.D.S., Silva, A.M.T., Faria, J.L., Boaventura, R.A.R., Vilar, V.J.P., 2013a. Perchloroethylene gas-phase degradation over titania-coated transparent monoliths. Applied Catalysis B: Environmental 140-141, 444-456.

Lopes, F.V.S., Miranda, S.M., Monteiro, R.A.R., Martins, S.D.S., Silva, A.M.T., Faria, J.L., Boaventura, R.A.R., Vilar, V.J.P., 2013b. Perchloroethylene gas-phase degradation over titania-coated transparent monoliths. Applied Catalysis B: Environmental 140–141, 444-456.

Máthé, C., M-Hamvas, M., Vasas, G., 2013. Microcystin-LR and Cylindrospermopsin Induced Alterations in Chromatin Organization of Plant Cells. Marine Drugs 11, 3689-3717.

Monteiro, R.A.R., Lopes, F.V.S., Silva, A.M.T., Ângelo, J., Silva, G.V., Mendes, A.M., Boaventura, R.A.R., Vilar, V.J.P., 2014. Are TiO_2-based exterior paints useful catalysts for gas-phase photooxidation processes? A case study on n-decane abatement for air detoxification. Applied Catalysis B: Environmental 147, 988-999.

Narasimha Rao, K., 2003. Studies on thin film materials on acrylics for optical applications. Bulletin of Materials Science 26, 239-245.

Ohtani, B., 2010. Photocatalysis A to Z—What we know and what we do not know in a scientific sense. Journal of Photochemistry and Photobiology C: Photochemistry Reviews 11, 157-178.

Onstad, G.D., Strauch, S., Meriluoto, J., Codd, G.A., von Gunten, U., 2007. Selective oxidation of key functional groups in cyanotoxins during drinking water ozonation. Environmental Science & Technology 41, 4397-4404.

Pablos, C., Van Grieken, R., Marugań, J., Muñoz, A., 2012. Simultaneous photocatalytic oxidation of pharmaceuticals and inactivation of Escherichia coli in wastewater treatment plant effluents with suspended and immobilised TiO_2. Water Science and Technology 65, 2016-2023.

Pelaez, M., de la Cruz, A.A., O'Shea, K., Falaras, P., Dionysiou, D.D., 2011. Effects of water parameters on the degradation of microcystin-LR under visible light-activated TiO_2 photocatalyst. Water Research 45, 3787-3796.

Pelaez, M., de la Cruz, A.A., Stathatos, E., Falaras, P., Dionysiou, D.D., 2009. Visible light-activated N-F-codoped TiO_2 nanoparticles for the photocatalytic degradation of microcystin-LR in water. Catalysis Today 144, 19-25.

Pelaez, M., Falaras, P., Kontos, A.G., de la Cruz, A.A., O'Shea, K., Dunlop, P.S.M., Byrne, J.A., Dionysiou, D.D., 2012. A comparative study on the removal of cylindrospermopsin and microcystins from water with NF-TiO_2-P25 composite films with visible and UV–vis light photocatalytic activity. Applied Catalysis B: Environmental 121–122, 30-39.

Pinho, L.X., Azevedo, J., Vasconcelos, V.M., Vilar, V.J.P., Boaventura, R.A.R., 2012. Decomposition of Microcystis aeruginosa and Microcystin-LR by TiO_2 Oxidation Using Artificial UV Light or Natural Sunlight. Journal of Advanced Oxidation Technologies 15, 98-106.

Portela, R., Sánchez, B., Coronado, J.M., Candal, R., Suárez, S., 2007. Selection of TiO2-support: UV-transparent alternatives and long-term use limitations for H_2S removal. Catalysis Today 129, 223-230.

Robert, D., Malato, S., 2002. Solar photocatalysis: a clean process for water detoxification. The Science of The Total Environment 291, 85-97.

Robert, D., Piscopo, A., Heintz, O., Weber, J.V., 1999. Photocatalytic detoxification with TiO_2 supported on glass-fibre by using artificial and natural light. Catalysis Today 54, 291-296.

Robertson, J.M.C., J. Robertson, P.K., Lawton, L.A., 2005. A comparison of the effectiveness of TiO_2 photocatalysis and UVA photolysis for the destruction of three pathogenic micro-organisms. Journal of Photochemistry and Photobiology A: Chemistry 175, 51-56.

Robertson, P., Lawton, L., Münch, B., Rouzade, J., 1997. Destruction of cyanobacterial toxins by semiconductor photocatalysis. Chemical Communications 1997, 393-394.

Rodríguez, S.M., Richter, C., Gálvez, J.B., Vincent, M., 1996. Photocatalytic degradation of industrial residual waters. Solar Energy 56, 401-410.

Rudolph-Böhner, S., Mierke, D.F., Moroder, L., 1994. Molecular structure of the cyanobacterial tumor-promoting microcystins. FEBS Letters 349, 319-323.

Sampaio, M.J., Silva, C.G., Silva, A.M.T., Vilar, V.J.P., Boaventura, R.A.R., Faria, J.L., 2013. Photocatalytic activity of TiO_2-coated glass raschig rings on the degradation of phenolic derivatives under simulated solar light irradiation. Chemical Engineering Journal 224, 32-38.

Senogles, P., Scott, J., Shaw, G., Stratton, H., 2001. Photocatalytic degradation of the cyanotoxin cylindrospermopsin, using titanium dioxide and UV irradiation. Water Research 35, 1245-1255.

Shephard, G.S., Stockenström, S., de Villiers, D., Engelbrecht, W.J., Wessels, G.F.S., 2002. Degradation of microcystin toxins in a falling film photocatalytic reactor with immobilized titanium dioxide catalyst. Water Research 36, 140-146.

Sordo, C., Van Grieken, R., Marugán, J., Fernández-Ibáñez, P., 2010. Solar photocatalytic disinfection with immobilised TiO_2 at pilot-plant scale, pp. 507-512.

Subrahmanyam, M., Boule, P., Durga Kumari, V., Naveen Kumar, D., Sancelme, M., Rachel, A., 2008. Pumice stone supported titanium dioxide for removal of pathogen in drinking water and recalcitrant in wastewater. Solar Energy 82, 1099-1106.

Triantis, T.M., Fotiou, T., Kaloudis, T., Kontos, A.G., Falaras, P., Dionysiou, D.D., Pelaez, M., Hiskia, A., 2012. Photocatalytic degradation and mineralization of microcystin-LR under UV-A, solar and visible light using nanostructured nitrogen doped TiO_2. Journal of Hazardous Materials 211–212, 196-202.

van Apeldoorn, M.E., van Egmond, H.P., Speijers, G.J.A., Bakker, G.J.I., 2007. Toxins of cyanobacteria. Molecular Nutrition & Food Research 51, 7-60.

van Grieken, R., Marugán, J., Sordo, C., Martínez, P., Pablos, C., 2009a. Photocatalytic inactivation of bacteria in water using suspended and immobilized silver-TiO_2. Applied Catalysis B: Environmental 93, 112-118.

van Grieken, R., Marugán, J., Sordo, C., Pablos, C., 2009b. Comparison of the photocatalytic disinfection of *E. coli* suspensions in slurry, wall and fixed-bed reactors. Catalysis Today 144, 48-54.

Vella, G., Imoberdorf, G.E., Sclafani, A., Cassano, A.E., Alfano, O.M., Rizzuti, L., 2010. Modeling of a TiO_2-coated quartz wool packed bed photocatalytic reactor. Applied Catalysis B: Environmental 96, 399-407.

Vilela, W.F.D., Minillo, A., Rocha, O., Vieira, E.M., Azevedo, E.B., 2012. Degradation of [D-Leu]-Microcystin-LR by solar heterogeneous photocatalysis (TiO_2). Solar Energy 86, 2746-2752.

Wang, Y., Hong, C.-s., 1999. Effect of hydrogen peroxide, periodate and persulfate on photocatalysis of 2-chlorobiphenyl in aqueous TiO_2 suspensions. Water Research 33, 2031-2036.

Yang, X., Cao, C., Erickson, L., Hohn, K., Maghirang, R., Klabunde, K., 2009. Photo-catalytic degradation of Rhodamine B on C-, S-, N-, and Fe-doped TiO_2 under visible-light irradiation. Applied Catalysis B: Environmental 91, 657-662.

7 Main conclusions and suggestions for future work

This chapter presents the final remarks and the main conclusions from the work reported in the chapters 4, 5 and 6. Some suggestions for future work are also described.

7.1 Final remarks and conclusions

7.1.1 Photocatalytic degradation of *M. aeruginosa* using suspended TiO_2

A solar TiO_2 photocatalytic process under slurry conditions was applied successfully for the destruction of *M. aeruginosa* cells and simultaneous removal of intracellular and extracellular cyanotoxin MC-LR due to cell lysis, even in the treatment of natural water from a Portuguese river containing cyanobacterial blooms, prevailing the genera *Microcistis*.

High loads of cyanobacteria in natural waters require great amounts of energy to be destroyed by photocatalysis. The toxins already present in the water and those released by cell lysis are also high energy demanding.

Transmission electron microcopy (TEM) technique showed that TiO_2 nanoparticles form a layer around the cells and under UV irradiation, the mucilaginous external capsule starts to be destroyed due the attack of reactive species formed in the surface of TiO_2, which allows the penetration of TiO_2 nanoparticles to inner parts of the cell, leading to cell deformation and destruction.

7.1.2 Photocatalytic degradation of MC-LR and CYN using suspended TiO_2

The TiO_2 photocatalytic process under slurry conditions showed better performance in the degradation of MC-LR and CYN cyanotoxins, previously purified and spiked in distilled water, which indicates that the best treatment strategy for cyanobacteria containing water is the integration of a pre-filtration step in order to remove the majority of the cyanobacteria cells trying to avoid the cell lysis, and further photocatalytic oxidation of the remaining cells and cyanotoxins molecules present in the liquid phase.

CYN molecule showed a higher stability than MC-LR, being necessary a higher solar exposure time to achieve similar degradation efficiencies.

The photocatalytic oxidation of MC-LR in aqueous solutions is characterized by an initial fast reaction rate followed by a slow degradation profile, which was attributed to the competition for the hydroxyl radicals between the MC-LR molecules and degradation byproducts. LC-MS/MS analysis revealed the presence of two main degradation byproducts with *m/z* 1029

and *m/z* 1011 during the initial part of the MC-LR photocatalytic oxidation, which was almost complete destroyed for higher reaction times.

7.1.3 Photocatalytic degradation of MC-LR and CYN using immobilized TiO_2

CAM or PET monoliths proved to be a good support for TiO_2-based photocatalysts, as they present honeycomb three-dimensional transparent arrays, large photoactive surface area and rugged surface allowing for a suitable adhesion of the catalytic coating. The photocatalytic oxidation of MC-LR at neutral pH values was achieved successfully using different heterogeneous solar photocatalytic processes, avoiding the need of acidification/neutralization steps, as well as a post-filtration step when slurry suspensions of the photocatalyst are used. P25 or sol-gel TiO_2 films deposited in CAM showed to be more efficient than TiO_2-loaded exterior paints. The addition of H_2O_2 to the P25-CAM system improved the MC-LR degradation efficiency and also enhanced significantly the efficiency of the photocatalytic system using photocatalytic paints. TiO_2 heterogeneous photocatalysis also proved to be a good process for CYN degradation but a longer exposure time is required.

Photocatalytic experiments carried out using natural water from Tâmega River spiked with MC-LR or CYN were performed, aiming at evaluating the influence of the natural organic matter on the photocatalytic destruction of cyanotoxins, using the monoliths of cellulose acetate with P25 and H_2O_2 addition (P25-CAM/H_2O_2/UV). Although the degradation of MC-LR was slower when compared to the degradation in distilled water, heterogeneous photocatalysis driven by solar energy can be used for the treatment of natural water, allowing obtaining MC-LR levels below the guideline value of 1 $\mu g\, L^{-1}$. The presence of organic matter, as happens in natural water, impairs the MC-LR degradation rate.

Oppositely, the CYN degradation rate using the same system was higher in natural water than in distilled water containing this toxin, which suggests that the presence of Fe species in the river water probably promoted the photo-Fenton reaction.

7.1.4 Photocatalytic reactors

Three different types of reactors were used in the present work: i) Lab-scale glass immersion photoreactor; ii) Lab scale photoreactor prototype – SUNTEST and iii) Pilot scale solar photoreactor. The energy source in the first photoreactor is a medium pressure mercury lamp,

whereas SUNTEST uses solar artificial radiation and the photoreactor at pilot scale uses natural solar energy.

The experiments were performed in the three reactors and the obtained results were similar. The treatment process optimization can start at laboratory scale and then proceed in a pilot scale reactor using solar energy as UV source.

7.1.5 General conclusion

TiO_2 photocatalysis is a very efficient treatment to destroy cyaonobacteria and cyanotoxins in a pilot plant designed to treat a large volume of water. The sun is a promising energy source for photocatalysis, in order to produce drinking water from natural water contaminated by cyanobacteria and cyanotoxins. This technology can be implemented in remote areas not reached by the drinking water network, and where qualified experts are not available. There is no need of chemicals addition and only the photocatalyst and sunlight are required. Photocatalysis can lower the level of toxins below the value of 1 $\mu g\ L^{-1}$.

7.2 Suggestions for future Work

New research work can be carried out employing different catalysts and supports such as TiO_2 nanotubes and TiO_2 doped with metals. Fenton reaction, photo-Fenton reaction, ferrioxalate-based Fenton reaction and electrochemical processes can also be optimized for degradation of cyanobacteria and cyanotoxins.

The application of photocatalytic processes downstream from membrane filtration of water contaminated with cyanobacteria should be also evaluated.

A limited number of works concerning cyanotoxin CYN degradation is available. So, more attention should be given to the development of effective methods for its elimination, considering the degree of toxicity of CYN. The photocatalytic degradation of other cyanotoxins can also be studied.

Further studies regarding the interaction of MC-LR and CYN with organic and inorganic compounds naturally found in water can be performed. The identification of degradation byproducts, mainly from CYN, and their toxicity assessment, is also a matter of concern.